

Application of UHPC in Long Span Bridge Design

Tam Ngo
Master Thesis
4/21/16

Assessment Committee:

- Prof. Dr. Ir. D. A. Hordijk
- Dr. Ir. C. van der Veen
- Ir. A. D. Reitsema
- Dr. Ir. R. Abspoel
- Ir. H. de Waardt

Preface

In this rapport I present the final results of my master thesis titled “Application of Ultra-High Performance Concrete in Long Span Bridge Design”. It also represents the completion of my educational program Structural Engineering at the faculty of Civil Engineering and Geosciences at the Delft University of Technology. Although the master thesis is an individual project that I have been working on for the past few months, the results could not have been as they are without the help of the people around me.

First of all I want to express my gratitude towards Huig de Waardt, my supervisor at Witteveen+Bos, for his enthusiasm and inspiring ideas contributing to my research. Secondly I want to thank Cor van der Veen, for taking the time to read all of my work and making valuable comments on my work. Also special thanks to Albert Reitsema for helping me through the complex processes of research and design. Furthermore a word of gratitude for Prof. Hordijk for staying critical making sure I got the most out of myself and making sure this thesis became is good as can be. Last but certainly not least I want to thank my family for supporting me every step of the way.

Tam Ngo

Delft, March 2016

Abstract

In the last few decades great progression has been made in the research and development of a fairly new type of concrete called ultra-high performance concrete (UHPC). This high-tech material has excellent material properties compared to conventional concrete and has the potential to make more slender and lighter structures. However the material is still very expensive and requires designers to minimize material usage in order to make an economic structure.

Up to today only few structures are built using UHPC, despite that it seems that the application of UHPC has plenty of potential. Especially in long span bridges it can be a very viable solution. Because the self-weight of the structure makes up a significant part of the total loading on the structure, the material saving ability of the material has a double effect. On the one hand the material saving reduces material costs, on the other hand the material saving causes a considerable reduction of the total loading on the structure. To fully benefit from these effects, the material use should be kept to a minimum. This can be achieved by finding a structural concept that utilizes the excellent material properties of UHPC as much as possible.

UHPC has a very high compressive strength combined with excellent shear capacity. Besides that it is suitable for very high levels of prestress to resist tensile forces. A study using design calculations for rectangular cross-sections have shown that the application of UHPC instead of conventional concrete leads to a significant reduction of the required volume of concrete. This holds especially for shear elements and tensile elements with a high level of prestress. Since box beams has webs as shear elements and a bottom flange as a prestressed tensile member, UHPC box beams are chosen as the best solution for long span UHPC bridges.

The application of UHPC can optimize the box-shaped cross-section in several ways. Very slender beams can be made by applying a high level of prestress. Also wider beams with very thin webs can be made thanks to the high shear capacity. For this master thesis five different types of UHPC box beams are developed. These optimized box beams are designed for bridges spanning 60m, 70m, 80m, 85m and 90m. The most important advantages of these UHPC box beams over box beams made of conventional concrete are:

- The beams are more slender:
- The beams are wider:
 - Less beams have to be manufactured, transported and assembled, decreasing the amount of time and labor required to build the bridge.
- The beams are lighter:
 - The total loading of the bridge is decreased by the lower self-weight.
 - They are easier to transport and to hoist.
 - Longer beams up to 90m can be made without exceeding the 170t weight-limit for transport by road.

These benefits allow the UHPC box beams to be a fit solution for spans that are too long for conventional box beam solutions, without having to build an intermediate pier or to switch to segmented or cast in-situ solutions. Moreover they can replace old bridges with a stronger one without having to replace the substructure. Therefore it can be concluded that UHPC beams provide build new bridges and replace old bridges with minimal traffic hindrance.

Contents

Preface.....	II
Abstract	IV
1 Introduction.....	1
1.1 Problem Description.....	1
1.2 Research Objectives	1
1.3 Research Question	1
1.4 Research Method	2
2 Literature study	4
2.1 Purpose.....	4
2.2 Introduction.....	4
2.3 State of the Art	4
2.4 Physical and Mechanical Properties.....	9
2.5 Cost and Sustainability Aspects.....	15
2.6 Summary.....	19
2.7 Conclusion	20
3 NSC Design vs. UHPC Design	21
3.1 Purpose.....	21
3.2 Cost and Material Efficiency of UHPC	21
3.3 Conclusion	46
4 Architectural Design	47
4.1 Purpose.....	47
4.2 Conclusion	48
5 Topology Optimization	50
5.1 Purpose.....	50
5.2 Conclusion	50
6 Concept Analysis.....	51
6.1 Purpose.....	51
6.2 UHPC Slab Bridge.....	51
6.3 UHPC Box Bridge	51
6.4 UHPC Double-T girder/Pi-girder Bridge.....	53
6.5 UHPC Arch Bridge	54
6.6 Conclusion	55
7 UHPC Box Bridge Variants	57
7.1 Purpose.....	57
7.2 Beams vs. Segments	57

7.3	Internal Prestressing vs. External Prestressing.....	57
7.4	Box Beams vs. H-beams.....	58
7.5	Conclusion	58
8	Transport.....	59
8.1	Purpose.....	59
8.2	Transportation Method.....	59
8.3	Challenges	60
8.4	Conclusion	61
9	UHPC Box Beam Bridge Design 60m	62
9.1	Purpose.....	62
9.2	Cross-Section Properties	62
9.3	Cross Section Properties of a 60m UHPC Beam	66
9.4	Loads.....	66
9.5	Prestress	73
9.6	Moment Capacity	76
9.7	Shear and Torsion Capacity	79
9.8	Moment Capacity Transverse Direction.....	83
9.9	Deflection	85
9.10	Crack Width	87
9.11	Fatigue.....	87
9.12	Unity Check Summary	88
10	UHPC Box Beam Bridge Design >60m	89
10.1	Purpose.....	89
10.2	70m Box Beam Design.....	89
10.3	80m Box Beam Design.....	90
10.4	85m Box Beam Design.....	92
10.5	90m Box Beam Design.....	93
10.6	Overview of the Designs.....	95
11	Comparison with Existing Box Beam Solutions	96
12	Optimization Variant: Strands in Web (SIW).....	99
12.1	Purpose.....	99
12.2	Optimization Challenges.....	99
12.3	Overview Designs	101
12.4	Comparison with Other Box Beam Solutions	103
13	Optimization Variant: Kinked Strands in Web (KSIW)	105
13.1	Purpose.....	105

13.2	Overview of the Designs.....	105
13.3	Comparison with Other Box Beam Solutions	106
14	Application of the Designed UHPC Box Beams	108
14.1	New Bridges.....	108
14.2	Replacing Old Bridge	108
15	Conclusion	113
16	Recommendations.....	115
17	References.....	116
18	Appendix.....	117
	Appendix A: Architectural Design.....	118
	Appendix B: Topology Optimization.....	134
	Appendix C: SCIA Engineering Reports.....	145

1 Introduction

1.1 Problem Description

With the ever increasing traffic intensity on highways, demands for new bridges grow. Moreover many existing bridges reach their service life and/or do not have the capacity to carry the increased traffic intensities and many of them might have to be replaced or strengthened. When a new bridge should cross a highway with high traffic intensity, there is often a demand for a bridge that can be built with minimum traffic hindrance. The same holds for old bridges that have to be replaced. It is desired that these can be replaced with minimum traffic hindrance. By taking away the need for an intermediate pier the traffic hindrance can be reduced significantly. However, at the same time the span increases with a considerable amount. So in order to reduce traffic hindrance, road bridges that can span longer distances are needed. Moreover it is also desirable that when a bridge is replaced, the existing substructure would still be able to resist the increased traffic loading. This can only be achieved if the replacing superstructure is considerably lighter.

In the last decades a new material, called Ultra-High Performance Concrete (UHPC), is being developed and has shown promising results in both experiments and in practice. This material that is characterized by very high compressive strength, shear capacity and favorable cracking behavior, has the potential to make very durable bridges that have the possibility to span long distances without intermediate piers. In addition these bridges can also be considerably lighter. Therefore this material seems to be the ideal candidate to be applied in road bridges that require minimum traffic hindrance during construction.

However the high costs of the material, which is more than eight times the costs of conventional concrete, poses a serious challenge for the designer of the bridge. In order to make an economic design, the material use should be kept to a minimum. This can be achieved by finding a structural concept that utilizes the excellent material properties of UHPC as much as possible.

1.2 Research Objectives

The objective of this report is to find an economic design for UHPC in long span ($\geq 60\text{m}$) road bridges. Different design concepts will be investigated to find the one that is most suitable. This concept will be optimized and ultimately a design of an optimized UHPC bridge will be presented.

1.3 Research Question

Main research question:

How can UHPC be applied in long span road bridge design, while utilizing its excellent material properties as much as possible and being cost-efficient?

Sub questions:

- *What are the physical and mechanical properties of UHPC?*
- *What are the costs of application of UHPC?*
- *How does UHPC perform regarding material and cost efficiency under different types of loading compared to conventional concrete?*
- *What is the optimal structural concept/solution for UHPC bridges?*
- *How can this concept be optimized?*
- *How can this concept be implemented into a practical design?*

1.4 Research Method

The research can be roughly divided into six phases:

1. Literature Study
2. Comparison Study
3. Concept Analysis
4. Design
5. Design Optimization
6. Conclusion

1.1.1 Literature Study

During the literature study all the knowledge and information, which are necessary to achieve the research objectives and answer the research question, are collected and reported. This means all relevant physical and mechanical properties of UHPC are collected and summarized. This will also be done for cost indications of the production and maintenance of UHPC structures. To obtain a feel for the possibilities of UHPC bridges, relevant reference projects should be studied. Finally relevant norms, regulations, recommendations and calculation methods should be collected and summarized. From the collected recommendations a selection is made of which ones will be used.

1.1.2 Comparison Study

To demonstrate and also investigate the difference between conventional concrete and UHPC, simple design calculations are carried out for both materials. The results of these calculations will show how UHPC performs in different types of loading in comparison to conventional concrete. The level of performance will be based on material and cost savings and can therefore determine the rate of efficiency of different designs.

1.1.3 Concept Analysis

All the information from the literature study and comparison study, can now be utilized to make a selection for the bridge concept. Different types of bridges will be analyzed for their compatibility with the requirements and also to investigate to which extent they are optimal. To generate ideas for the ideal bridge concept, topology optimization software will also be used. This phase will be called the design study.

1.1.4 Design

Once a decision is made on the concept of the bridge, a preliminary design can be made by means of a spreadsheet. A spreadsheet is used to be able to easily change parameters, during the design optimization phase. The input of the spreadsheet should contain cross sectional properties, material properties, loads, internal forces, prestress and reinforcement. The internal forces can be obtained from the FEM model, which will also be made in this phase. The output of the spreadsheet will contain unity checks in ULS and SLS. Also the amount of used material, construction weight and cost indication will result from the sheet.

1.1.5 Optimization Study

The main objective of the optimization study is to investigate how parameters can be changed to achieve a more efficient design with more favorable properties. To achieve this, the UHPC design, parameters of for example the cross sectional size and shape, level of prestress or reinforcement are varied, until the most favorable output is found. The result of the optimization study will show an optimized design of a UHPC bridge design.

1.1.6 Conclusion

Based on the found results of the entire thesis a conclusion will be drawn and recommendations are given.

2 Literature study

2.1 Purpose

The purpose of this chapter is to gain knowledge and understanding of UHPC. By understanding the benefits and disadvantages of the material, design concepts can be developed, that have the potential to be very efficient. Moreover information about current developments in the application of the material demonstrate the possibilities and help to generate ideas for new concepts. At the end of this chapter a conclusion will be drawn on the opportunities that application of UHPC offers and how these can be used to make efficient designs.

2.2 Introduction

In current concrete technology a fairly new type of concrete called “Ultra High Performance Concrete” (UHPC), which is supposed to have superior properties compared to conventional concrete, is on the verge of a breakthrough. This material differs from conventional concrete by having:

- smaller maximum grain size;
- higher packing density;
- lower water cement ratio;
- fine steel fibres added to the concrete mix.

These measures result in excellent mechanical properties and durability, when compared to conventional concrete by specifically having:

- significantly increased compressive/tensile strength;
- very low permeability leading to great durability;
- ductile behaviour.

In the last few decades tremendous progression has been made in the research and development of UHPC.

2.3 State of the Art

Due to its exceptionally high characteristic strength and great durability, it has a lot of potential in structural applications, especially in the use of prestressed concrete structures such as bridges. Examples of successful applications of this new high-tech material have shown great results by decreasing the cross sectional area as well as the amount of prestressing steel and even leaving out reinforcement bars. Therefore it is a very fit solution for designing bridges that require slenderness and/or complex shapes. Moreover examples of life cycle assessments comparing UHPC with conventional concrete were made. These resulted in a more favorable carbon footprint for UHPC, when looking at the production and maintenance over the total life time. So UHPC is superior to conventional concrete not only regarding structural performance but also with respect to durability and sustainability.

However, still very few bridges are built using UHPC for various reasons. The lack of standardized norms and regulations is an important factor. Standardization for mix design and design rules can greatly reduce engineering costs. Only in France and Japan design recommendations have been published in resp. 2002 and 2004 [3]. Therefore in these countries the application of this material is by far more numerous than in other countries. Also the high production costs play a role in the limited use of UHPC. The price per cubic meter of UHPC ranges from four to five times the price of

conventional concrete [3]. In short, the current situation still limits application of UHPC due to high engineering and production costs.

Although a lot of research is done on the characteristics of UHPC and plenty of knowledge and information is available, there is still little experience with UHPC bridge design. To encourage the application of this material, more research needs to be done on when it is best to apply UHPC and how to use it to its fullest potential.

2.3.1 Completed UHPC Bridges

Since the first UHPC bridge was built in Sherbrooke, Canada in 1997 many other projects followed. Especially in France and Japan numerous pedestrian and heavy traffic bridges were constructed in UHPC. They come in different types and shapes. Examples exist of UHPC slab bridges, arch bridges and cable-stayed bridges. The bridges mostly have unconventional innovative shapes. This shows that there are many possibilities to develop new shapes for even further optimized use of UHPC. The Netherlands however are still behind on the application of UHPC with only a few new bridges built with the new material. As for Dutch reference projects relevant for this research, footbridges with a span of 60m, there are none. This means that reference projects from other countries shall be considered [3].

2.3.1.1 *Sherbrooke (footbridge), Canada*

For example the first UHPC bridge in Sherbrooke, Canada was a pedestrian bridge with a span of 60m. It consisted of six precast segments, which were each 10m and had a rather unconventional shape. These truss-shaped segments had a UHPFRC ribbed deck acting as a top chord, the bottom chord consisted of two UHPFRC prestressed beams and the braces were stainless steel tubes filled with UHPFRC [3].

2.3.1.2 *Calgary (footbridge), Canada*

Another relevant reference project is the Glenmore/Legsby footbridge in Calgary, Canada built in 2007. This bridge consisted of a 33,6m long UHPC drop-in element in the shape of a T-beam. The total bridge spans 53m and crosses an eight-lane highway without intermediate piers. At midspan the precast beam is 1,1m deep and 3,6m wide. The beam weighs 100t and contains 2% steel fibres [3].

2.3.1.3 *Pont du Diable (footbridge), France*

In France in 2005 a very long span footbridge without intermediate piers of 69m is built using UHPC. It consists of 15 segments of 4,6m. The segments are 1,8m deep and about 2m wide. The webs of the segments are 120mm wide and the deck is 30mm deep [3].

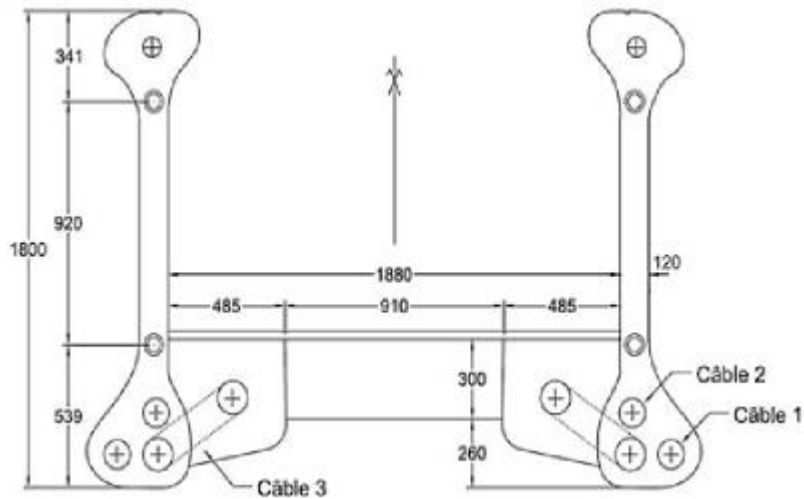


Figure 2-1: Cross-section Pont du Diable [3]

2.3.1.4 Sakata-Mirai (footbridge), Japan

In Japan the Sakata-Mirai UHPC footbridge spans 50,2m and weighs just 56t. The six precast segments contain no steel reinforcing bars and are externally prestressed [3].

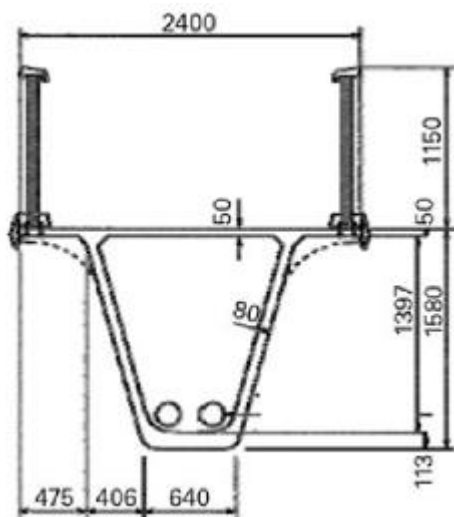


Figure 2-2: Cross-section Sakata-Mirai [3]

2.3.1.5 Bridge of Peace (footbridge), South-Korea

The “Bridge of Peace” in Seoul is a UHPC arch bridge for pedestrians spanning 120m. It consists of 6 precast prestressed segments shaped as double-T beams that are 4,3m wide and 1,3m deep. The deck is 30mm deep and has transverse ribs every 1,225m [3].

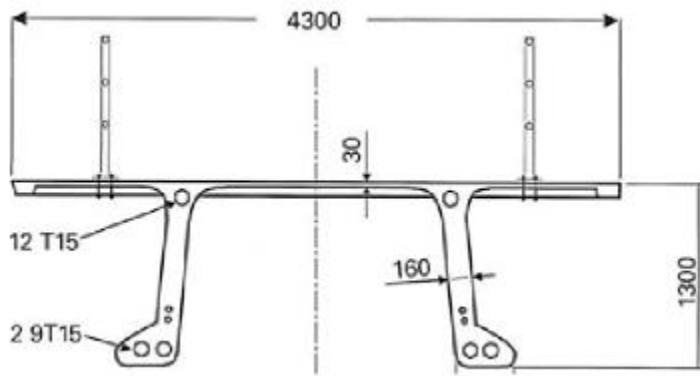


Figure 2-3: Cross-section Bridge of Peace [3]

2.3.1.6 KICT cable-stayed footbridge, South Korea

The Korean Institute of Construction Technology (KICT) cable-stayed footbridge is a full scale research project for long-span cable-stayed UHPC bridges. The bridge segments are precast, prestressed and fibre reinforced [3].

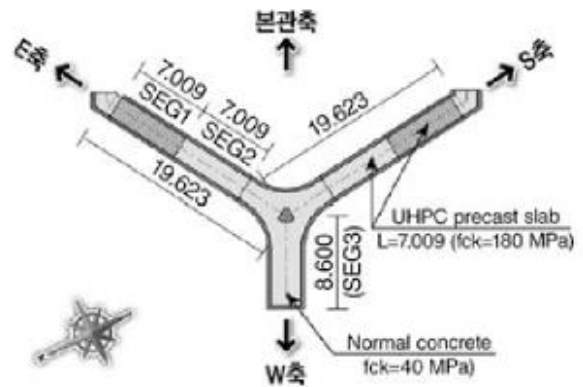


Figure 2-4: Overview KICT cable-stayed footbridge [3]

2.3.1.7 Bourg-les-Valence (road bridge), France

This bridge, which was the first UHPC bridge in France, has spans of 20,5 and 22m and is composed out of double-T beams. The beams have a depth of 900mm. The top flange is 2200mm wide and has a thickness of 150mm. Passive reinforcement is only applied in the joints between the segments [3].



Figure 2-5: Bourg-les-Valence road bridge (left) and the double T-beams (right) [3]



Figure 2-8: Picture of the Mars Hill Bridge [8]

2.3.1.11 Jakway Park Bridge (road bridge), United States

The bridge consists of three pi-girders that span 15,6m. The girders is 838mm deep and 2540mm wide.

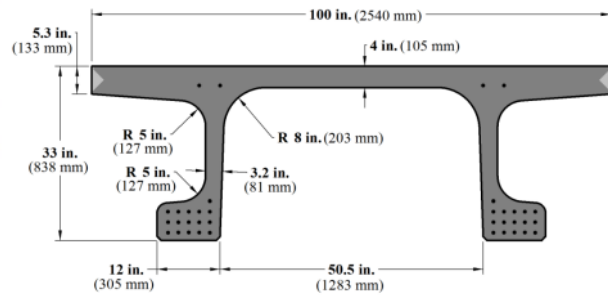


Figure 2-9: Picture of the Jakway Park bridge (left) and the cross-section of the pi-girders (right) [8]

2.3.2 Overview Road Bridges in UHPC

Name	Type	Span (m)	Depth (mm)
Bourg-les-Valence	Double T-girders	22,0	900
Pont de la Chabotte	Segmented Box Girder	47,4	1600
Pont Pinel	Inverted T-Girders	27,0	620
Mars Hill Bridge	Bulb-tee Girders	33,5	1140
Jakway Park Bridge	Pi-girders	15,6	838

Table 2-1: Overview of completed road bridges executed in UHPC

2.4 Physical and Mechanical Properties

In order to determine when it's best to apply UHPC and how to use it to its fullest potential, a good understanding of the material and its behavior is required. Therefore in this chapter the physical and mechanical properties of UHPC are summarized. In order to be able to design with the material, recommendations regarding characteristic and design values are also provided. These are taken from the "Recommendations on Ultra High Performance Fiber-Reinforced Concretes" developed by the AFGC [1]. This is basically the French design code for UHPC.

2.4.1 Density

UHPC is slightly denser than conventional concrete, due to reduced pore volume and increased aggregate packing density. Different mixes of UHPC are available with different values for the density. The values range from 2500 to 2800 kg/m³. The characteristic density of UHPC from Ductal is about 2500 kg/m³ [1]. This value will be used throughout this thesis for all design calculations.

2.4.2 Compressive Strength

Depending on the concrete mix and whether heat treatment is performed UHPC can reach a very high characteristic compressive strength (f_{ck}) as compared to conventional concrete ranging from 150 to 250 MPa [1]. Especially the water/cement ratio is an important factor. According to the French recommendations on UHPC, the design value for the compressive strength (f_{cd}) is determined by the following formula that is based on the Eurocode [1].

$$f_{cd} = \alpha_{cc} * \frac{f_{ck}}{\gamma_c}$$

In preliminary design an f_{cm} of 180MPa and an f_{ck} of 150MPa is recommended [1]. For conventional concrete an α_{cc} of 1 is recommended by the Eurocode and the Dutch national annex (NEN-EN1992-1-1). The French recommendations on UHPC recommends an α_{cc} of 0,85 for UHPC[1]. α_{cc} is a reduction factor that takes into account long term effects unfavorable effects due to load positioning. However the material properties given in [2] for C170/200. The values for the compressive strength in [2] are shown below.

$$f_{ck} = 170MPa$$

$$\alpha_{cc} = 1,00$$

$$f_{cd} = \alpha_{cc} * \frac{f_{ck}}{\gamma_c} = 1,00 * \frac{170}{1,5} = 113,3MPa$$

The elastic strain limit for compression

$$\varepsilon_{c0} = \frac{f_{ck}}{E_{cm}}$$

The design value for elastic strain limit for compression

$$\varepsilon_{c0d} = \frac{f_{cd}}{E_{cm}} = \frac{113,3}{50000} = 0,0023$$

The concrete strain limit for compression according to [1]

$$\varepsilon_{cud} = \left(1 + 14 \left(\frac{f_{ctfm}}{f_{cm}} \right) \right) \varepsilon_{c0d} [1]$$

In the case of preliminary design [1] recommends $\varepsilon_{cud} = 2,7 * 10^{-3}$ taking $f_{ctfm} = 9MPa$.

However $\varepsilon_{cud} = 2,6 * 10^{-3}$ is chosen according to [2].

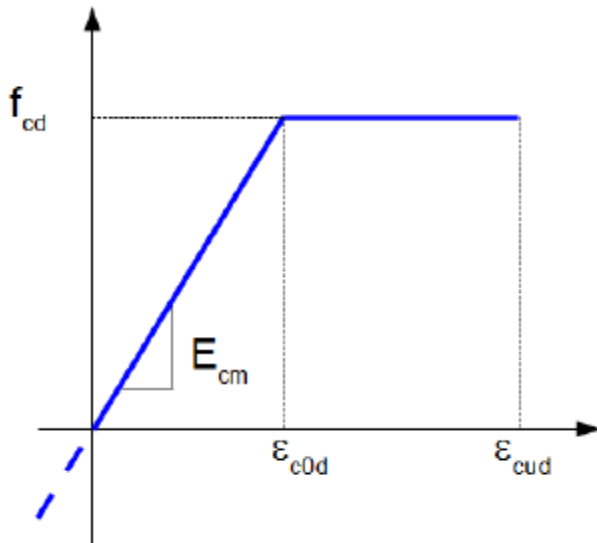


Figure 2-10: Compressive Stress-Strain Diagram for UHPC Design [3]

2.4.3 Tensile Strength

Similar to compression, UHPC also shows a considerable increase in characteristic tensile strength (f_{ctk}), which can range from 7 to 11 MPa [3]. However unlike conventional concrete UHPC retains tensile strength after cracking. Due to the fibers either strain hardening or softening occurs depending on the fiber content, geometry and orientation [3]. For preliminary design assumptions should be made for these aspects. The assumptions differ for thick and thin elements [1]. The fact that UHPC retains its strength, also means that for design calculations the tensile strength of concrete does not have to be neglected.

For thick elements low strain-hardening behavior is assumed with a characteristic elastic tensile stress ($f_{ctk,el}$) of 9MPa and a characteristic post-cracking strength (f_{ctfk}) of 9MPa. The fiber orientation factor K will be 1,25 for global effects and 1,75 for local effects [1].

The design stress-strain curve for low strain-hardening is shown in the following graph.

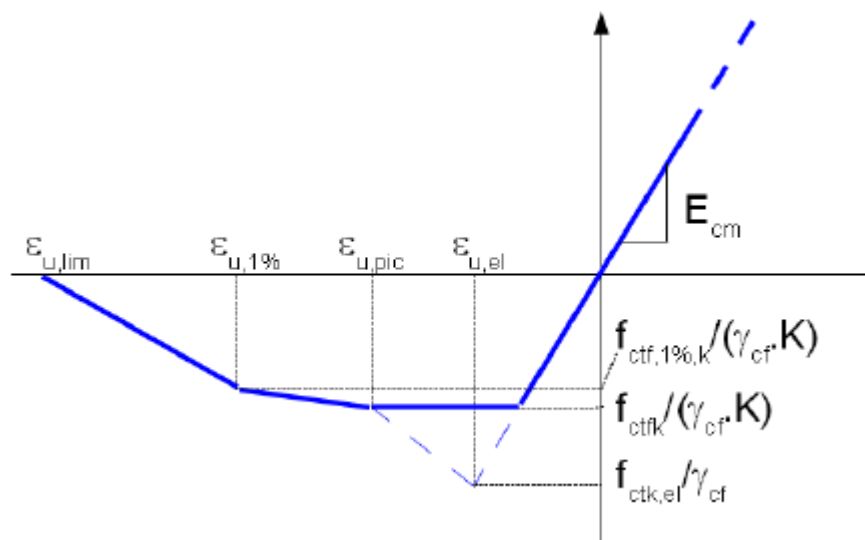


Figure 2-11: Tensile Stress-Strain Diagram for UHPC Design of thick elements [3]

This design curve was found by truncating the real stress-strain curve:

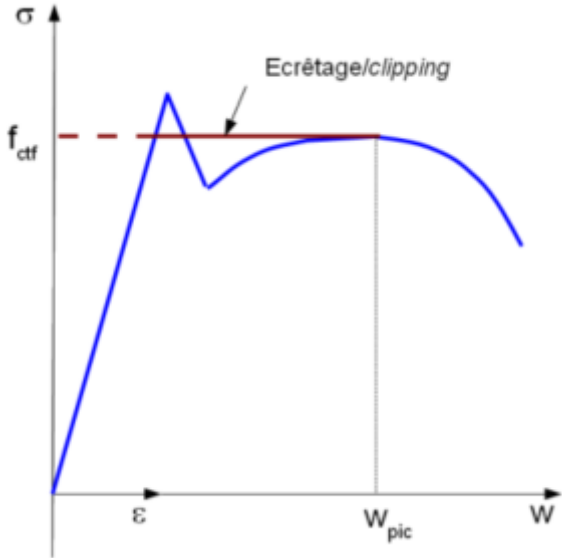


Figure 2-12: Example on how a real stress-strain diagram can be transformed in a design diagram for low strain-hardening

In case of strain-softening the design curve can be found by truncating at the stress level that corresponds with a crack width of 0,3mm:

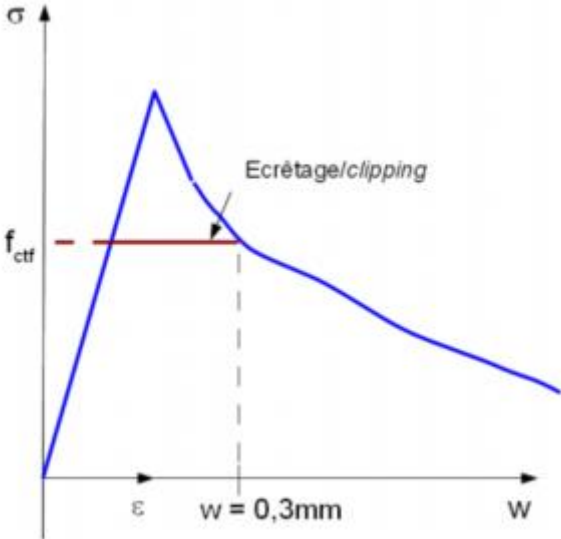


Figure 2-13: Example on how a real stress-strain diagram can be transformed in a design diagram for strain-softening

The strain values can be found with the following formulas:

$$\varepsilon_{peak} = \frac{w_{peak}}{l_c} + \frac{f_{ctk,el}}{E_{c,eff}} \text{ at SLS}$$

$$\varepsilon_{u,peak} = \frac{w_{peak}}{l_c} + \frac{f_{ctk,el}}{\gamma_{ef} E_{c,eff}} \text{ at ULS}$$

Where w_{peak} = crack opening corresponding to the local peak or 0.3 mm if there is no peak.

$$l_c = \frac{2}{3}h$$

Figure 2-14: Formulas to calculate the strain values from the tensile stress-strain diagram for UHPC

Thin elements are characterized by having a thickness (e) equal to or smaller than 3 times the fiber length (l_f). For these type of elements we assume during preliminary design a f_{ctk} of 9 MPa and a strain limit ($\varepsilon_{u,lim}$) of $2,5 \cdot 10^{-3}$. The values for K are taken the same as for thick elements [1].

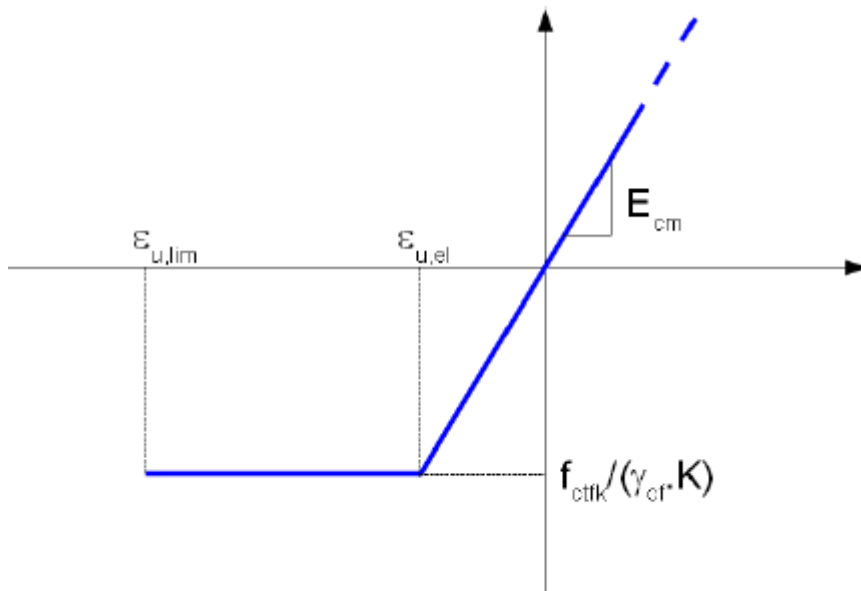


Figure 2-15: Tensile Stress-Strain Diagram for UHPC Design of thin elements [3]

2.4.4 Flexural Strength

Due to the ductile behavior in tension induced by the fibers, UHPC has a more favorable stress distribution over the height of the construction height regarding flexural behavior than conventional concrete. Tensile strength of the concrete is no more neglected, when calculating bending strength. The stress distribution for a thick element loaded in bending is shown below. This stress distribution is based on the constitutive law shown in Figure 2-11.

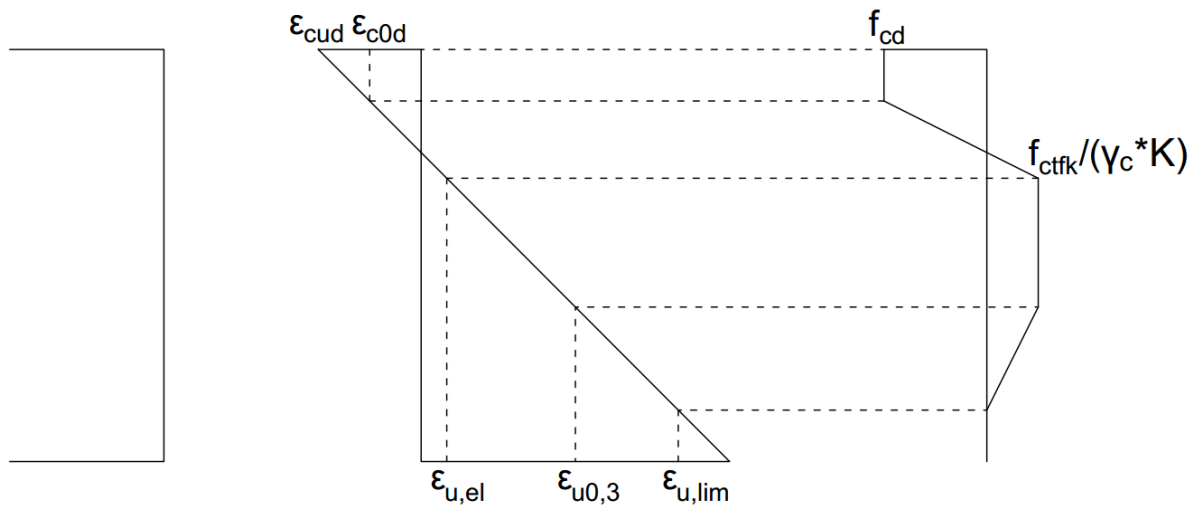


Figure 2-16: A cross-section of a thick element, its strain distribution and stress distribution (f.l.t.r.)

2.4.5 Modulus of Elasticity

The mean value for the modulus of elasticity (E_{cm}) for UHPC is also increased compared to conventional concrete. This means much stiffer structures can be designed. An E_{cm} of 50.000 MPa should be taken as guideline during design calculations [1].

2.4.6 Shrinkage

Naturally UHPC is susceptible to shrinkage. In case of wet curing, shrinkage is mainly caused by autogenous¹ shrinkage. When heat treatment is applied, shrinkage will occur during this process. This will reduce or even prevent further shrinkage after treatment depending on whether heat treatment is carried out during curing or when the concrete is already hardened. During preliminary design the following can be assumed about the shrinkage deformation:

- No heat treatment: 550 $\mu\text{m}/\text{m}$ for autogenous shrinkage and 150 $\mu\text{m}/\text{m}$ for drying shrinkage for an outdoor environment with an average relative humidity of about 50 to 70%²
- Heat treatment during curing: 550 $\mu\text{m}/\text{m}$ total shrinkage, for an outdoor environment with a relative humidity of 50 to 70%
- Heat treatment when concrete is hardened: total shrinkage of 550 $\mu\text{m}/\text{m}$ before the end of the heat treatment, after which the total shrinkage is nil [1]

2.4.7 Creep

Creep deformation of UHPC can be significantly reduced by means of heat treatment. During preliminary design the following can be assumed about the creep coefficient:

- $\Phi = 0.8$ if there is no treatment;
- $\Phi = 0.4$ with treatment during curing;
- $\Phi = 0.2$ with treatment when concrete is hardened [1].

¹ The paragraph about shrinkage makes reference to [1]. This reference states endogenous shrinkage instead of autogenous. However it is highly likely that autogenous shrinkage is meant.

² The average humidity of the outside environment in the Netherlands is approximately 80%, which is likely to lead to less shrinkage

2.4.8 Fatigue

Many studies have been done on the fatigue behavior of UHPC. They mostly show similar or slightly better performance in comparison to conventional concrete. Whether UHPC has a fatigue limit is still up for discussion.

To determine the fatigue strength for UHPFRC the following formula is proposed:

$$f_{cd,fat} = 0,85 * \beta_{cc}(t) * \frac{f_{ck}}{\gamma_c} * \left(1 - \frac{f_{ck}}{400}\right) =$$

This is a modification to the Eurocode which is necessary to prevent a large underestimation of the fatigue strength for UHPFRC [3].

2.4.9 Summary mechanical properties

Density	ρ	2.500	kg/m ³
Characteristic compressive strength	f_{ck}	150	N/mm ²
Characteristic elastic tensile strength	$f_{ctk,el}$	9	N/mm ²
Characteristic post-cracking tensile strength	f_{ctfk}	9	N/mm ²
Mean modulus of elasticity	E_{cm}	50.000	N/mm ²
Fibre orientation factor for global effects	K_{global}	1,25	-
Fibre orientation factor for local effects	K_{local}	1,75	-
Material factor UHPC	γ_c	1,5	-
Shrinkage - heat treatment hardened concrete	$\epsilon_{cs,hht}$	550 ³	$\mu\text{m}/\text{m}$
Shrinkage - heat treatment during curing	$\epsilon_{cs,cht}$	550	$\mu\text{m}/\text{m}$
Shrinkage - no heat treatment	$\epsilon_{cs,nht}$	700	$\mu\text{m}/\text{m}$
Creep factor - heat treatment hardened concrete	Φ_{hht}	0,2	-
Creep factor - heat treatment during curing	Φ_{cht}	0,4	-
Creep factor - no heat treatment	Φ_{nht}	0,8	-

Table 2-2: Mechanical Properties of UHPC

2.5 Cost and Sustainability Aspects

2.5.1 Current Price Level

The price of conventional concrete is usually around the €100/m³. The price for the US market of components for UHPC mixes sold by Ductal ranges from \$750 to \$1000/yd³ (approx. €750 to €1000/m³), which can be almost ten times the price for conventional concrete. Therefore a research was done in the US to develop alternative mixes, which were less expensive, but with similar qualities. This research resulted in promising new mixes that had material costs of approximately \$250/yd³ [4]. Another source reports that the price for UHPC is four to five times the price of conventional concrete [3]. For cost estimation in this thesis 830 €/m³ is chosen as an assumption for the price of UHPC [5]. This price is calculated according to Figure 2-19 and Figure 2-20. Other costs will be calculated by estimation based on current price levels.

Conventional Concrete	100,00	€/m ³
Ultra-High Performance Concrete	830,00	€/m ³
Reinforcement Steel	0,95	€/kg
Post-tensioned Prestressing Steel	7,30	€/kg
Pre-tensioned Prestressing Steel	3,00	€/kg

Table 2-3: Estimation of Material Costs

³ This value of the shrinkage will only take place during the heat treatment. After heat treatment no further shrinkage will be found.

2.5.2 Material Costs

But why is UHPC so expensive compared to conventional concrete? To answer this question the mix components and production method should be investigated. The tables below show mix proportions of typical UHPC mixes [3] [4] [5].

	UHPC fine (0/0.5 mm) M2Q [45]	UHPC fine (0/0.5 mm) M3Q [46]	UHPC coarse (0/8 mm) B5Q [47]	UHPC roadbuilding [16]	UHPC no- slump [18]
	[kg/m ³]				
Water	166	183	158	107	49
Cement	832	775	650	404	186
Ultrafine granulated blast furnace slag	—	—	—	24	—
Silica fume	135	164	177	54	51
Superplasticizer dosage FMW/b [% by mass] ^{a)}	1.1	1.1	1.2	0.6	1.2
Quartz powder, fine	207	193	325	—	93
Quartz powder, coarse	—	—	131	32	38
Quartz sand 0.125/0.5	975	946	354	541	101
Quartz sand 0/2	—	—	—	—	616
Quartz sand 0.6/2	—	—	—	283	—
Gravel 2/8	—	—	—	—	821
Gravel 8/16	—	—	—	—	616
Basalt 2/8	—	—	597	1123	—
Micro-wire fibres	2.5% by vol.	2.5% by vol.	2.5% by vol.	1.0% by vol.	—

^{a)} Superplasticizer with respect to binder

Figure 2-17: Examples of UHPC mix compositions [3]

Material	lbs/yd ³	% by wt.
Portland Cement (15 µm)	1200	28.7
Silica Fume (-1 µm)	390	9.3
Quartz Flour (10 µm)	355	8.4
Sand (150 to 600 µm)	1720	40.8
Steel Fibers (0.5" long, 8 mm Ø)	263	6.2
High-Range Water Reducer	51.8	1.2
Accelerator/Corrosion Inhibitor	50.5	1.2
Water	184	4.4

Figure 2-18: Typical UHPC mix composition (Greybeal, 2003) [4]

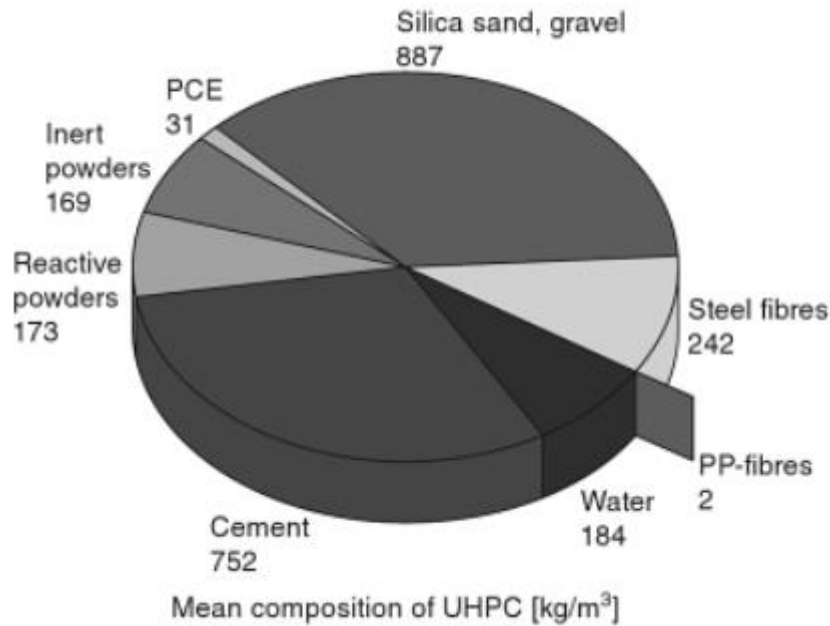


Figure 2-19: Mean composition of UHPC (Stengel & Schiessl, 2008) [5]

The main differences between conventional concrete and UHPC that can be seen immediately from these figures are that UHPC contains fibers and significantly more cement. The effects on the costs of these differences can be determined by the individual component prices and their contribution to the total price. These prices of the components are provided in the table below [5].

Raw material	Market price (€/1000 kg)
Well cement	110
Portland cement	70
Silica fume	500
Quartz powder fine	55
Quartz powder very fine	75
Limestone powder fine	30
Limestone powder very fine	40
Silica sand	26
Superplasticizer (PCE)	1,500
Micro steel fibres (0.15 mm)	2,500
Steel fibres (0.40 mm)	1,800

Figure 2-20: Market price of raw materials used for UHPC [5]

Steel fibres and superplasticizers are by far the most expensive components. However they make up only a small part of the total mix. Their relative contribution to the total price is far more interesting. Price contribution of the components is shown in the figure below [5].

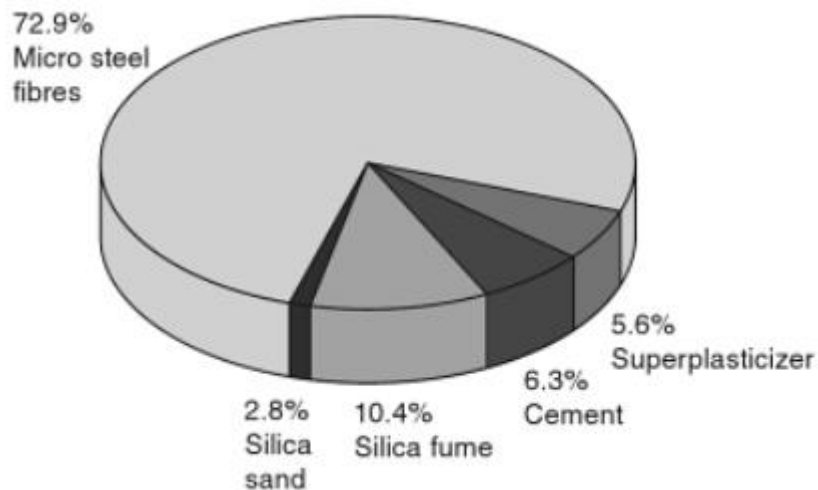


Figure 2-21: Contribution of raw materials to the overall cost of UHPC [5]

It seems that despite the fact that fibers make up just a small part of the volume and mass of UHPC, it is still the largest contributor to the production material costs. In the future there should be lots of opportunity to develop technologies to use these fibers more efficiently to achieve a considerable reduction of the costs of this component. Some examples are by optimizing fiber orientation magnetically or by only applying fibers locally.

2.5.3 Cost benefits

Although the application of UHPC leads to a significant increase in initial costs, it can still be profitable. First of all the high production costs can partly be compensated for by the reducing the amount of concrete, which in turn can also reduce the self-weight, leading to less foundation costs. The reduced amount of concrete will also reduce transportation costs. The excellent shear capacity of UHPC takes away the need for shear reinforcement, which reduces steel costs. Moreover the absence of reinforcement steel eliminates the need for concrete cover, resulting in decreased amount of required concrete. Finally the excellent durability leads to practically maintenance free structures, which reduces life-cycle costs. All these costs benefits do not automatically apply and are only potential benefits. A smart design has to be made to benefit from these. The main mechanism that determines the cost benefits is that UHPC can reduce required amount of material with its increased strength, but on the other hand the increased strength is achieved by applying more expensive material. This is a trade-off that really depends on the design of the structure.

2.5.4 Sustainability Aspects

Application of UHPC has the potential to make sustainable structures. As stated before, the reduction of transportation mass and maintenance costs will reduce energy consumption and emission of greenhouse gasses such as CO₂. However this can only be achieved with a proper design. Due to the energy intensive production process of the material, which is caused by fiber content, heat treatment and high cement content among others, the material use should be kept to a minimum. This is a similar trade-off to the one mentioned in the previous paragraph about cost benefits.

According to [5] the environmental impact of a UHPC precast single span bridge girder equals 1,5 to 2,4 times the impact of conventional concrete depending on the impact category. So despite the 50% reduction of required concrete, this study shows that it can still have a larger ecological footprint. However because UHPC has better durability, service life should be taken into account. UHPC is expected to have at least twice the service life of conventional concrete. This could compensate the environmental impact for the overall life time. An example of proper sustainable design with UHPC

can be found in Germany. A research on the sustainability of the Gärtnerplatz Bridge in Kassel has shown by means of a life-cycle assessment that the total CO₂ emission was only 40% of the emission of the variant in conventional concrete in its overall life time [3]. However this bridge was not exclusively built with UHPC, for it also contained some steel. Also a service life twice as long as for conventional concrete was assumed.

2.6 Summary

UHPC is a type of concrete with physical and mechanical properties that are superior to conventional concrete. The increased strength, stiffness and ductile behavior of the material opens up new possibilities, like more slender structures, higher prestress and absence of passive steel reinforcement, but also asks for another approach to the design. To design with UHPC the possibilities and limitations of the material must be known.

First of all the design values for mechanical properties can provide insight in the material behavior on forehand. Later these values can be used to make calculations. The mechanical properties are summarized in the table below.

Density	ρ	2.500	kg/m ³
Characteristic compressive strength	f_{ck}	150	N/mm ²
Characteristic elastic tensile strength	$f_{ctk,el}$	9	N/mm ²
Characteristic post-cracking tensile strength	f_{ctfk}	9	N/mm ²
Mean modulus of elasticity	E_{cm}	50.000	N/mm ²
Fiber orientation factor for global effects	K_{global}	1,25	-
Fiber orientation factor for local effects	K_{local}	1,75	-
Material factor UHPC	γ_c	1,5	-
Shrinkage - heat treatment hardened concrete	$\epsilon_{cs,hht}$	550	$\mu\text{m}/\text{m}$
Shrinkage - heat treatment during curing	$\epsilon_{cs,cht}$	550	$\mu\text{m}/\text{m}$
Shrinkage - no heat treatment	$\epsilon_{cs,nht}$	700	$\mu\text{m}/\text{m}$
Creep factor heat treatment hardened concrete	Φ_{hht}	0,2	-
Creep factor heat treatment during curing	Φ_{cht}	0,4	-
Creep factor no heat treatment	Φ_{nht}	0,8	-

Table 2-4: Mechanical Properties of UHPC

Secondly, costs aspects play a large role in designing with UHPC. Due to high costs of especially steel fibers the price is significantly higher than conventional concrete. The high production costs are seen as a considerable limitation factor and should be kept in mind when designing. In order to make the use of UHPC beneficial, the design must utilize UHPC's qualities as much as possible. This can be achieved by various measures like making smaller and lighter cross-sections and leaving out reinforcement bars. The more the UHPC design is optimized, the more the use of UHPC becomes economically attractive compared to conventional concrete. In addition UHPC can become significantly cheaper by reducing the required fiber content. Technologies to optimize fibre content or distributing fibers strategically are needed to achieve this. To compare the costs of design with conventional concrete and UHPC the following prices are used.

Conventional Concrete	100,00	€/m ³
Ultra-High Performance Concrete	830,00	€/m ³
Reinforcement Steel	0,95	€/kg
Post-tensioned Prestressing Steel	7,30	€/kg
Pre-tensioned Prestressing Steel	3,00	€/kg

Table 2-5: Estimation of Material Costs

Similar to costs the significantly higher environmental impact of UHPC environmental should also be kept to a minimum by minimizing material use. However the great durability of UHPC can compensate the environmental impact over its longer service life. The service life is expected to be at least twice the life span of conventional concrete.

In conclusion there are lots of possibilities that application of UHPC can offer bridge design. However, the use of this material can only be beneficial when economical designs are made. Since the application of UHPC is still in infancy lots of progress can be made, when it comes to optimizing design.

2.7 Conclusion

In order to find an optimized design the major advantages should be exploited and major disadvantages should be avoided. From the literature study can be concluded that the following properties offer the most opportunities, namely:

- Excellent compressive strength
- Excellent shear resistance

The major disadvantages are:

- Very high material costs
- Low tensile strength

Since cost-efficiency is crucial to achieve a successful design, material use should be minimized, to mitigate the high material costs. This will be the main objective. Naturally material can be saved by utilizing the excellent material properties of UHPC. Thus the following design philosophy can be implemented to find an optimized design:

The structure will be made (entirely) out of UHPC, while minimizing the material use, by utilizing the excellent properties of UHPC to its fullest potential.

The word “entirely” is in brackets, because although the application of UHPC is the main focus of this thesis, the possibility remains that there are structural elements that are simply not effective or economic enough, when executed in UHPC. In that case a “hybrid” structure will be designed.

Since UHPC has such a high compressive strength and only limited tensile strength, it is obvious that prestressing can be an effective way to save material. The high compressive strength will allow high prestressing forces, thus allowing very slender bridges. The high shear resistance of UHPC can be utilized in different ways. Omitting shear reinforcement is an option. Reducing web thicknesses is also a possibility.

3 NSC Design vs. UHPC Design

3.1 Purpose

Before different concepts for a UHPC bridge are analyzed, the main differences between designing with NSC and UHPC are demonstrated. This is done by means of design calculations for a simple rectangular cross-section. These cross-sections will be checked for different types of loading. Not only will this show the differences in calculation methods, but also the difference between the required amounts of material and behavior under different types of loading. The results can be interpreted for concept development and optimization of different designs.

3.2 Cost and Material Efficiency of UHPC

UHPC has many structural properties that are superior to conventional concrete classes. On the other hand UHPC is more than 8 times as expensive. The superior properties give several benefits, with concrete volume reduction as primary selling point. In addition volume reduction also means material cost reduction. As a consequence UHPC can be more cost efficient and competitive in certain cases. Cost efficiency will be determined by designing some basic elements for different types of loading. The table below shows an overview of which cases will be investigated:

	ULS	SLS
Compression member	Compressive resistance	
Tensile member	Tensile resistance	Crack width
Bending/Shear member	Bending resistance	
	Shear resistance	

Table 3-1: List of checks that are performed for different type of elements to determine their material and cost efficiency

To determine the economy for each case a UHPC and a C45 with the same resistance are calculated for their dimensions and costs. C45 is chosen for its frequent use in bridge structures and good price/quality ratio⁴. The result is an overview of the required volume and costs, which will give insight on how UHPC members perform compared to C45 members. Moreover these results can give insight on how UHPC performs under different types of loading in general.

In order to express the competitiveness of the different concrete variants, the strength, cost and volume ratio are determined.

$$SR = \frac{UHPC \text{ resistance}}{Conventional \text{ concrete resistance}}$$

$$CR = \frac{UHPC \text{ costs}}{Conventional \text{ concrete costs}}$$

$$VR = \frac{UHPC \text{ volume}}{Conventional \text{ concrete volume}}$$

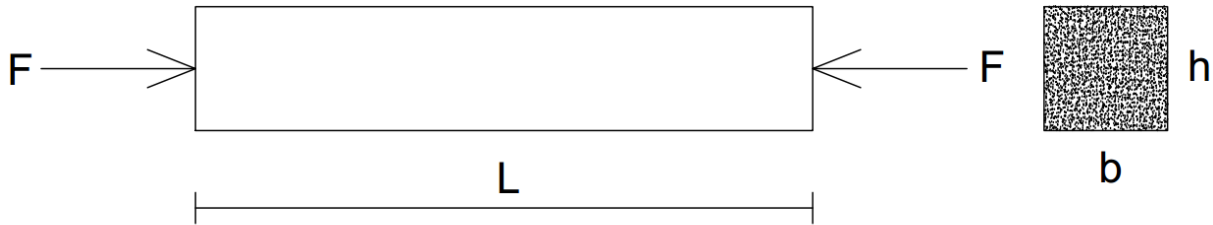
The strength ratio (SR) is kept at one to compare different variants with the same resistances. A cost ratio (CR) that is larger than one represents a higher cost for UHPC. A volume ratio (VR) that is lower than one represents a volume reduction for UHPC. The lower these two values are, the more attractive it will be to apply UHPC. Furthermore to measure the overall performance taking into account both cost efficiency and volume efficiency the cost-volume efficiency (CVE) is introduced:

$$CVE = CR \times VR$$

⁴ Nowadays concrete class C60 is used more frequently in prefab elements.

As the CVE becomes lower for a certain comparison, the application of UHPC becomes more attractive than the conventional concrete.

3.2.1 Compression



To investigate how UHPC performs in compression compared to C45/55, compressive members loaded in longitudinal direction with a square cross-section and an undetermined length are calculated. The compressive resistance is determined by using a simple formula:

$$N_c = f_{cd} * A_c$$

For different values of the compressive resistance the required cross-sectional area and costs are determined. Since the compressive strength is constant, the cross-section should increase in order to increase the resistance. As a consequence the material costs also increase. As expected the required cross-sectional area and costs increase linearly with the required compressive resistance.

The tables and graphs below show how the required cross-sections and material costs change for different values of the compressive resistance.

Compressive Force (kN)	Required Area (m ²)	
	C45/55	UHPC
1875	0,062	0,022
2700	0,090	0,031
3675	0,122	0,043
4800	0,160	0,056
6075	0,202	0,071
7500	0,250	0,088

Table 3-2: Required cross-section area for different values of compressive force

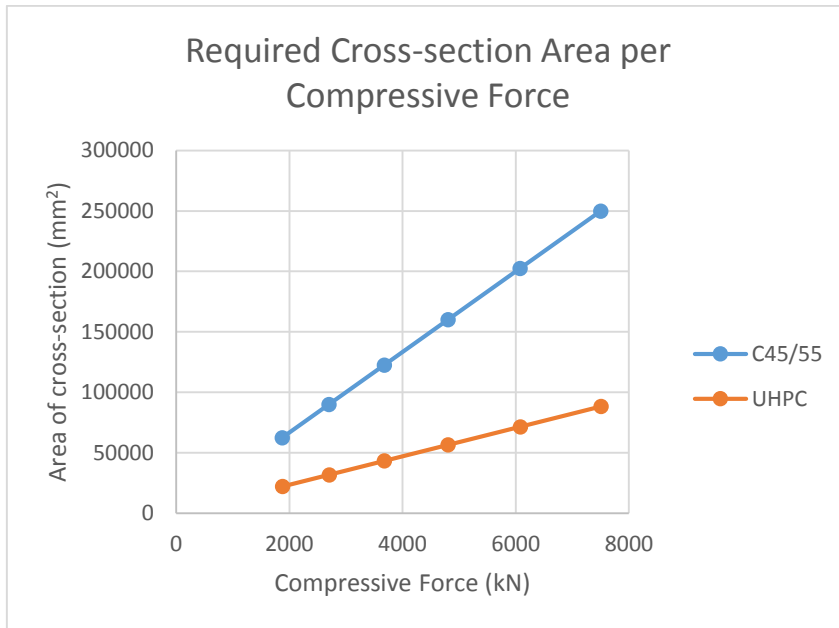


Figure 3-1: Required cross-section area for different values of compressive force

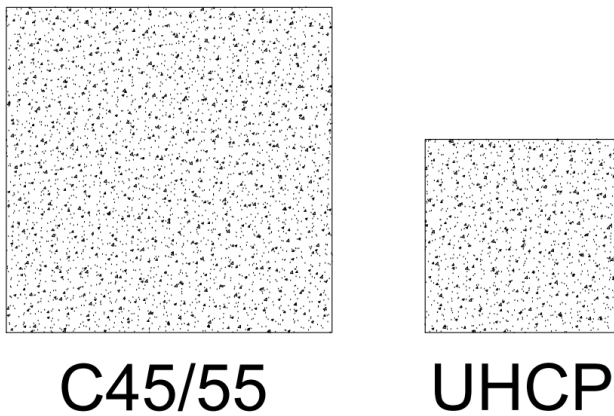


Figure 3-2: Required cross-sections (on scale) for any compressive resistance

Compressive Force (kN)	Concrete costs (€/m²)	
	C45/55	UHPC
1875	6,25	18,33
2700	9,00	26,39
3675	12,25	35,91
4800	16,00	46,90
6075	20,25	59,35
7500	25,00	73,26

Table 3-3: Concrete costs for different values of the compressive force

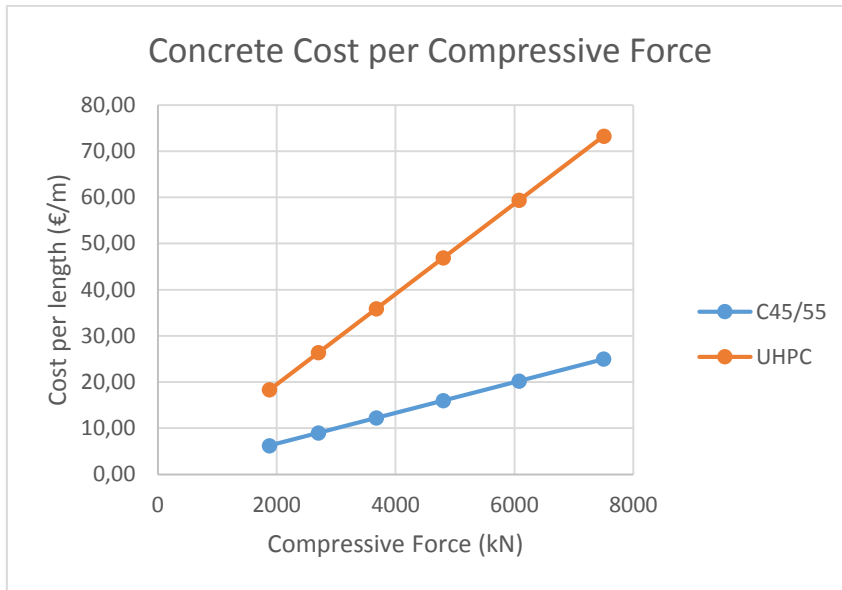


Figure 3-3: Concrete costs for different values of the compressive force

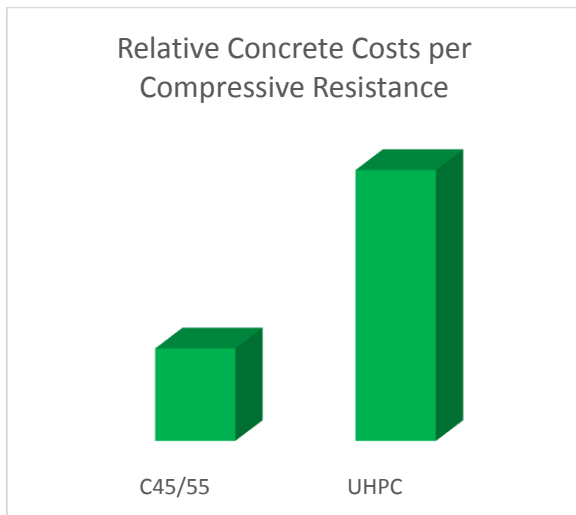
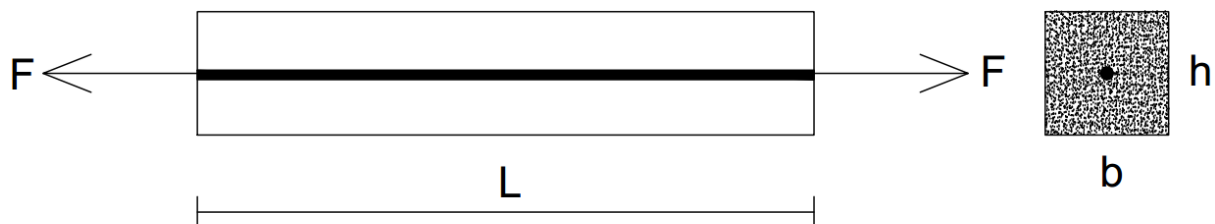


Figure 3-4: Relative concrete costs (on scale) for any compressive resistance

For this case a CR of 2,93 and a VR of 0,35 was found, which gives a CVE of 1,04. So when UHPC is applied instead of C45/55, a price increase of 193% can be expected. However the volume can be decreased with 65%. This holds for all resistances because of the linearity of the formula. Note that buckling is not taken into account.

3.2.2 Tension



To investigate how UHPC performs in tension compared to C45/55, tensile members loaded in longitudinal direction with a square cross-section and an undetermined length are designed based on

the cracking force. By the “cracking force” the force in the concrete right before cracking of the concrete is meant. The cracking force is calculated with the following formula:

$$N_{cr} = f_{ct}A_c(1 + \alpha_e\rho)$$

Note that tensile members that have bar reinforcement still retains its capacity after cracking, especially in case of high reinforcement ratios. In that case crack width will also play a role. This will be discussed in the crack width paragraph.

In addition prestressed tensile members will also be designed to demonstrate the benefits of using prestress in UHPC. For these prestressed members the cracking force is determined with the following formula:

$$N_{cr} = f_{ct}A_c + E_pA_p \frac{f_{ct}}{E_c} + P$$

For different values of the cracking force the required concrete volume and costs are determined. C45/55 and UHPC with different bar reinforcement ratios are investigated:

- C45/55 with minimum bar reinforcement (C45/55 0,42%)
- UHPC without bar reinforcement (all tension carried by fibers) (UHPC 0%)
- UHPC with minimum bar reinforcement (UHPC 1,35%)
- UHPC with a high amount of bar reinforcement (UHPC 3,00%)
- C45/55 with prestressing (C45/55 P 1,45%)
- UHPC with prestressing (UHPC P 4,84%)

These six concrete variants will be referred to by their abbreviations in the brackets. Minimum passive reinforcement is approximated with the following formula:

$$\rho_{min} \geq \frac{f_{ct}}{f_{yd}}$$

The minimum reinforcement prevents brittle failure by making sure the bar reinforcement yields after the concrete cracks.

The reinforcement ratios for the prestressed variants are determined as follows:

$$A_{p,req} = \frac{P_{max}}{\sigma_{pm\infty}} = \frac{A_c * \sigma_{c,max}}{\sigma_{pm\infty}} = \frac{A_c * 0,45f_{ck}}{\sigma_{pm\infty}}$$

$$\rho_p = \frac{A_{p,req}}{A_c}$$

The maximum concrete compressive stress $\sigma_{c,max}$ is chosen based on NEN-EN 1992-1-1 §5.10.2.2, which allows to neglect non-linearity of creep if the concrete compressive stress is not permanently above $0,45 * f_{ck}$. Note that the Eurocode allows an even higher concrete compressive stress of up to $0,7 * f_{ck}$.

The table and graph below show an overview of the required cross-section area for different cracking force values.

Cracking Force (kN)	Required Area (m ²)					
	C45/55 (0,42%)	UHPC (0%)	UHPC (1,35%)	UHPC (3,00%)	C45/55 (P 1,45%)	UHPC (P 4,84%)
100	0,055	0,025	0,017	0,016	0,005	0,001
500	0,275	0,126	0,085	0,080	0,023	0,007
1000	0,551	0,252	0,171	0,161	0,045	0,014
2000	1,102	0,505	0,342	0,322	0,090	0,028

Table 3-4: Required cross-section areas for different values of the cracking force

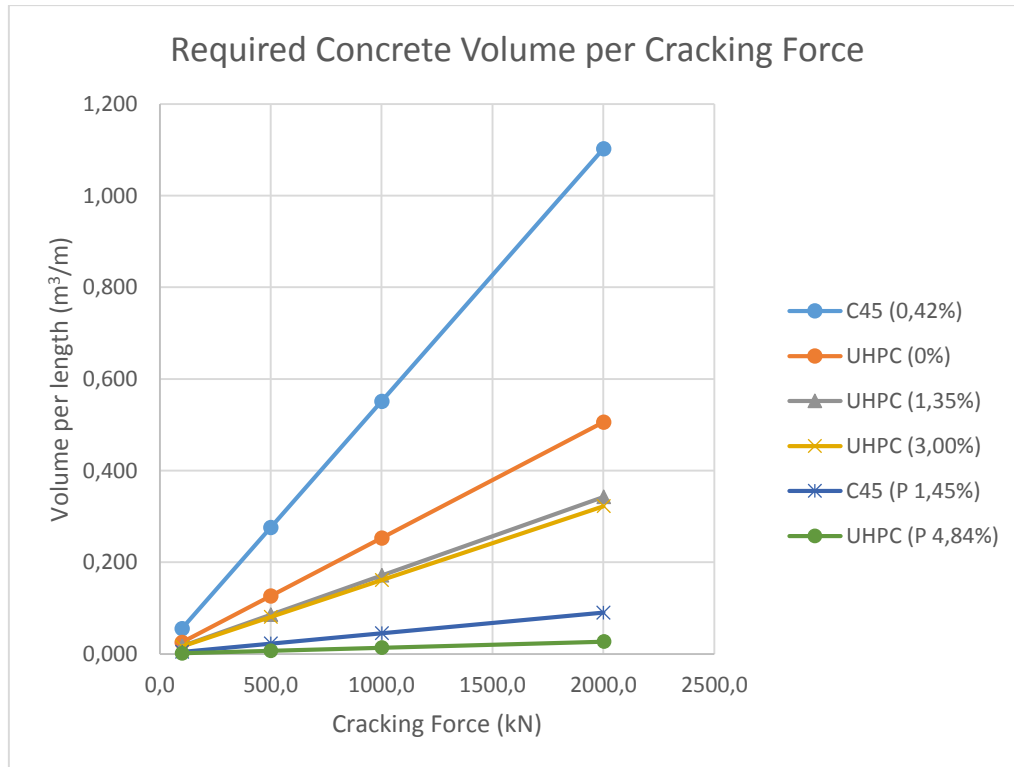


Figure 3-5: Required cross-section areas for different values of the cracking force

For a single concrete strength and reinforcement ratio, the required cross-sectional area and costs increase linearly with the cracking force. For a single cracking force the cross-sections differ significantly. As shown in the figure below, C45/55 requires a much larger cross-section than UHPC and prestress leads to a significant decrease in required concrete volume for both C45/55 and UHPC.

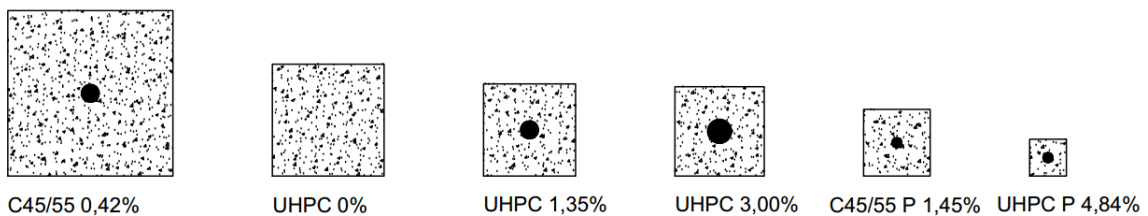


Figure 3-6: Required cross-sections (on scale) for any cracking force

This figure also shows that increasing the amount of steel does not have a significant positive influence on the cracking force, since the cross-section with more steel is not much smaller.

From the required cross-sectional areas the material costs can be calculated. The table and graph below show an overview of the concrete costs for different cracking force values.

Cracking Force (kN)	Material costs (€/m)					
	C45/55 (0,42%)	UHPC (0%)	UHPC (1,35%)	UHPC (3,00%)	C45/55 (P 1,45%)	UHPC (P 4,84%)
100	7,23	21,01	15,49	16,97	1,99	2,66
500	36,14	104,95	79,73	84,87	9,93	13,26
1000	72,27	209,91	159,40	169,72	19,85	26,50
2000	144,53	419,70	318,72	339,38	39,68	53,03

Table 3-5: Material costs for different values of the cracking force

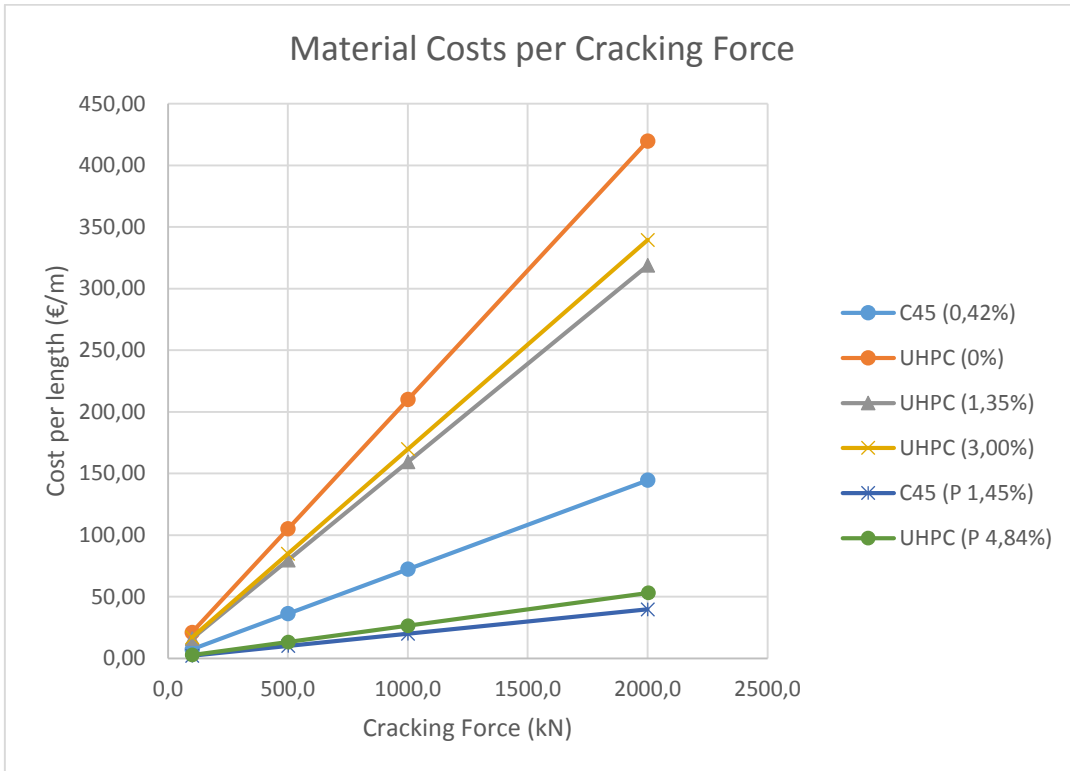


Figure 3-7: Material costs for different values of the cracking force

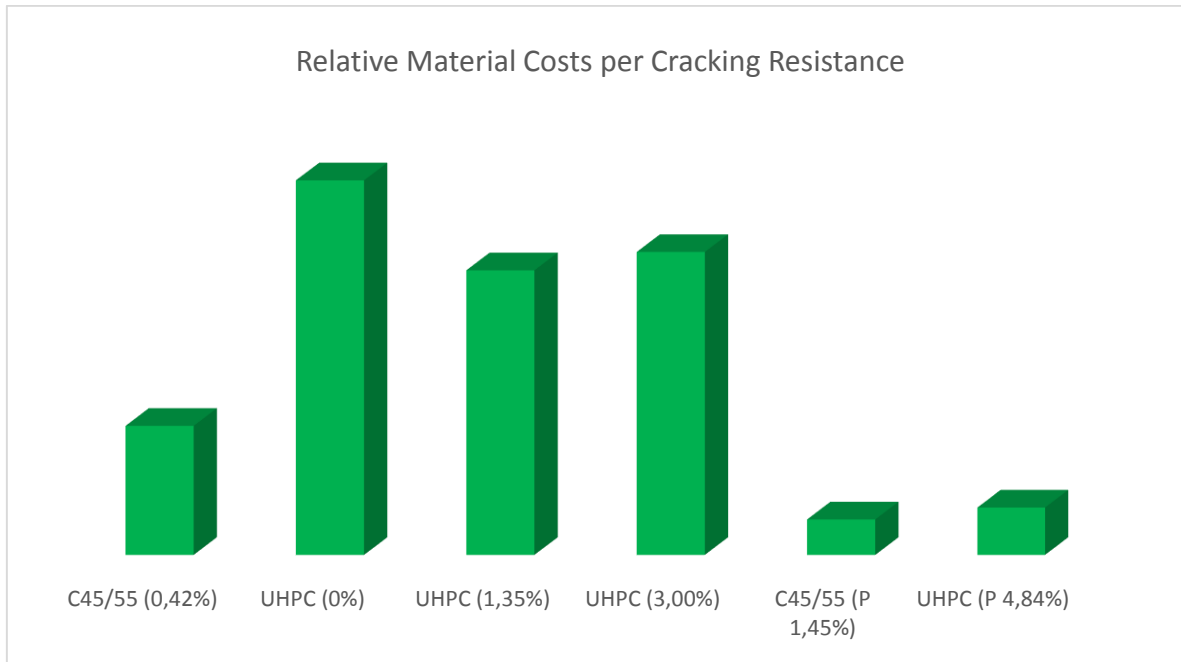


Figure 3-8: Relative material costs (on scale) for any cracking force

At first glance it can already be concluded that, when designing based on cracking force, applying UHPC without bar reinforcement for tensile members does not pay off. Both the volume curve and the cost curve are significantly higher than the curves for UHPC with bar reinforcement. This has to do with the fact that AFGC recommendations on UHPC applies an increased fibre orientation factor for tensile members, namely $K_{local}=1,75$ instead of $K_{global}=1,25$.

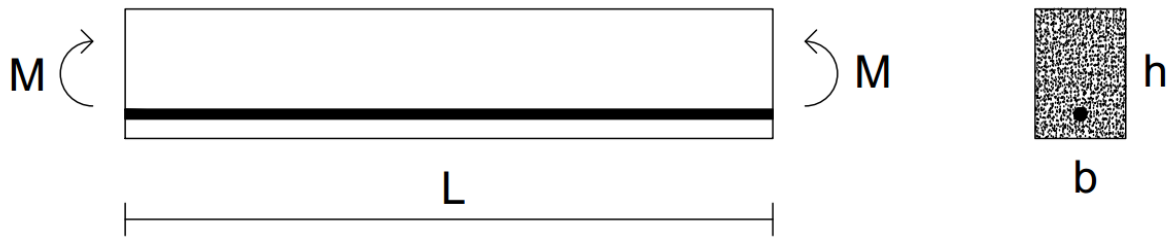
The CR, VR and CVE are determined for specific pairs of concrete variants to compare their material and cost efficiency:

- C45/55 (0,42%) vs. UHPC (0%)
- C45/55 (0,42%) vs. UHPC (1,35%)
- C45/55 (0,42%) vs. UHPC (3,00%)
- C45/55 (P 1,45%) vs. UHPC (P 4,84%)

As stated before UHPC without bar reinforcement is not quite efficient. Compared to C45/55 this material will give a cost increase of 190% and only a volume reduction of 64%. When minimum bar reinforcement is applied in UHPC, it becomes more attractive to use UHPC. The cost increase is now reduced to 120% and the volume can be reduced with almost 70%. This gives a CVE value of 0,686. By increasing the amount of bar reinforcement to 3% UHPC volume can be reduced even more. But at the same time the cost increases. The CVE rises to 0,687, which means that the costs increases faster than the volume decreases. From this can be concluded that high amounts of reinforcement is not very rewarding in terms of volume reduction. However higher amounts of bar reinforcement is necessary for higher resistances and maintaining proportional dimensions.

The prestressed variants both lead to significant material volume and material cost reduction. But when comparing prestressed conventional concrete with prestressed UHPC, UHPC gives significant volume reduction. The VR is 0,30. The costs slightly increase, leading to a CR of 1,34. The CVE is 0,40.

3.2.3 Bending



To investigate how UHPC performs in bending compared to C45/55, bending beams with a constant h/b ratio of $3/2$, a constant concrete cover of 60mm and an undetermined length are calculated for their bending resistance. The moment resistance for UHPC is calculated with the strain-distribution method:

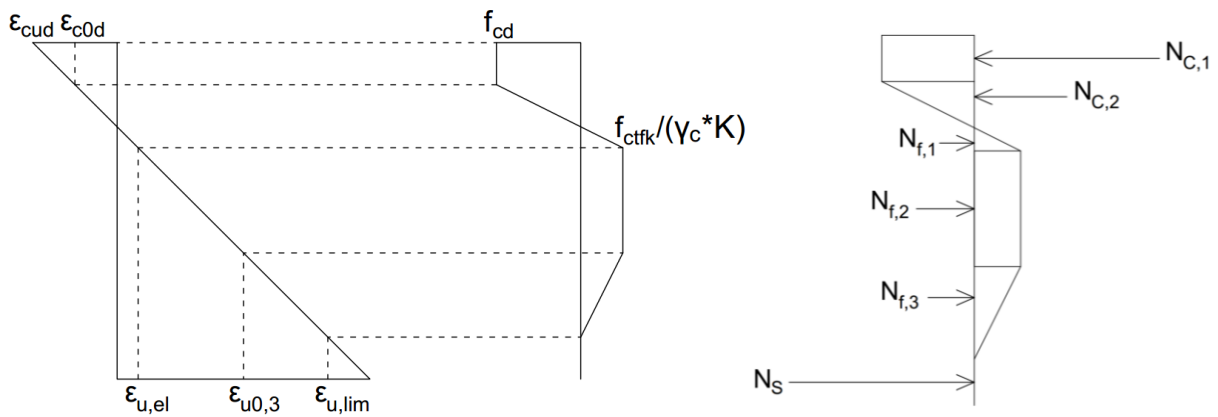


Figure 3-9: Stress-strain distribution used to determine moment capacity of a cross-section

The internal forces are described with the following formulas:

$$N_{C,1} = k_1 * x_u * f_{cd} * b$$

$$N_{C,2} = k_2 * x_u * f_{cd} * \frac{1}{2} * b$$

$$N_{f,1} = x_1 * f_{ctd} * \frac{1}{2} * b$$

$$N_{f,2} = x_2 * f_{ctd} * b$$

$$N_{f,3} = x_3 * f_{ctd} * \frac{1}{2} * b$$

$$N_S = A_s * f_{yd}$$

$$k_2 = \frac{\epsilon_{c3}}{\epsilon_{cu3}}$$

$$k_1 = 1 - k_2$$

$$x_1 = \frac{\epsilon_{u,el}}{\epsilon_{cud}} * x_u$$

$$x_2 = \frac{\varepsilon_{u0,3} - \varepsilon_{u,el}}{\varepsilon_{cud}} * x_u$$

$$x_3 = \frac{\varepsilon_{u,lim} - \varepsilon_{u0,3}}{\varepsilon_{cud}} * x_u$$

All values are known except for x_u . This value can be found with horizontal equilibrium:

$$N_{C,1} + N_{C,2} = N_{f,1} + N_{f,2} + N_{f,3} + N_S$$

Now with the values of the internal forces the moment capacity can be calculated with moment equilibrium.

For different values of the bending moment resistance the required concrete volume and costs are determined by means of a spreadsheet. C45/55 and UHPC with different bar reinforcement ratios are investigated:

- C45/55 with low amount of bar reinforcement (C45/55 0,21%)
- UHPC with low amount of bar reinforcement (UHPC 0,45%)
- C45/55 with high amount of bar reinforcement (C45/55 1,58%)
- UHPC with high amount of bar reinforcement (UHPC 3,00%)⁵

The table and graph below show an overview of the required cross-section area for different values of the moment resistance.

Moment Resistance (kNm)	Required Area (m ²)			
	C45/55 (0,21%)	UHPC (0,45%)	C45/55 (1,58%)	UHPC (3,00%)
50	0,140	0,086	0,044	0,028
100	0,218	0,133	0,067	0,043
200	0,341	0,208	0,104	0,066
500	0,620	0,376	0,184	0,116
1000	0,978	0,591	0,287	0,181
2000	-	-	0,449	0,282

Table 3-6: Required cross-section area for different values of the moment resistance

⁵ The reinforcement ratio of 3,00% is checked for both failure of the concrete compression zone and whether all reinforcement bars will fit.

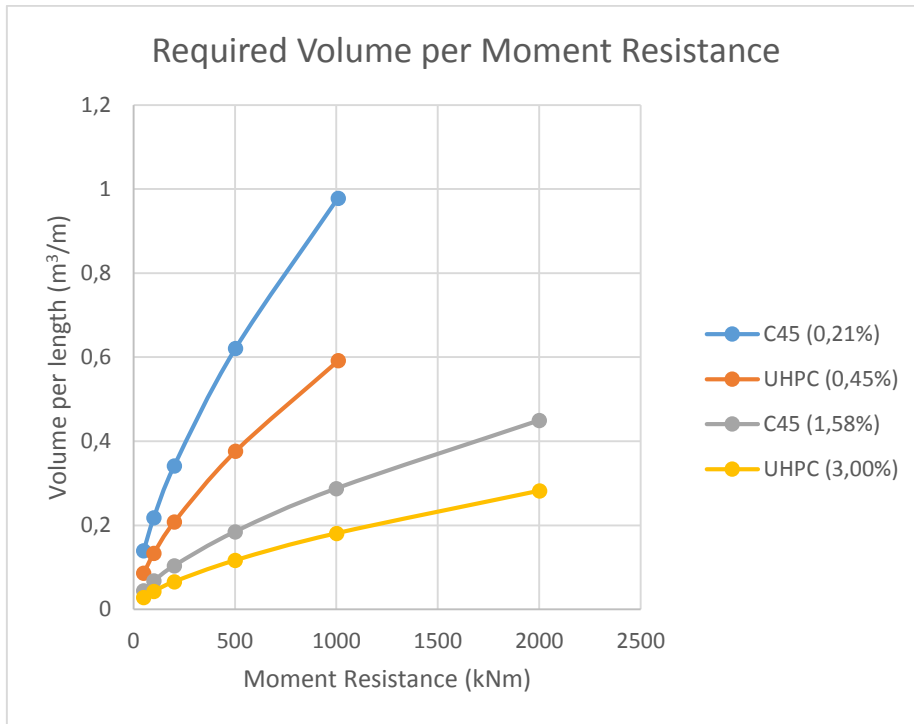


Figure 3-10: Required concrete volume for different values of the moment resistance

The figure below shows the required cross-sections of the four different cases on scale. Since the reinforcement bars still carry most of the tensile force and the fibers only a small part, the application of UHPC does not decrease the cross-section as much as applying additional steel reinforcement.

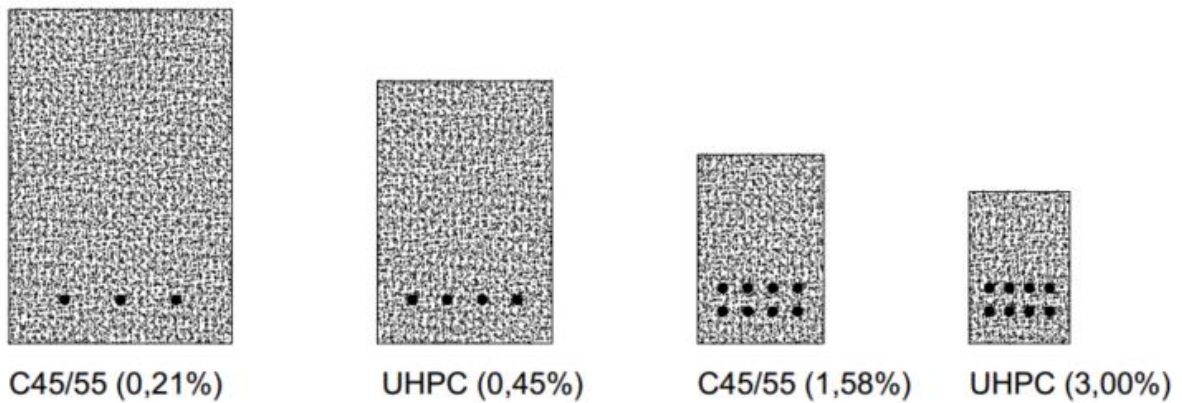


Figure 3-11: Required cross-sections (on scale) for a bending moment capacity of 50 kNm

With the required cross-sections areas the costs can be determined for these cross-sections. These are show in the table and graph below:

Moment Resistance (kNm)	Material Costs (€/m)			
	C45/55 (0,21%)	UHPC (0,45%)	C45/55 (1,58%)	UHPC (3,00%)
50	16,18	74,39	9,71	30,21
100	25,22	115,31	14,73	45,55
200	39,48	179,66	22,58	69,48
500	71,76	324,96	40,13	122,81
1000	113,06	510,84	62,45	190,57
2000	-	-	97,59	297,13

Table 3-7: Concrete costs for different values of the moment resistance

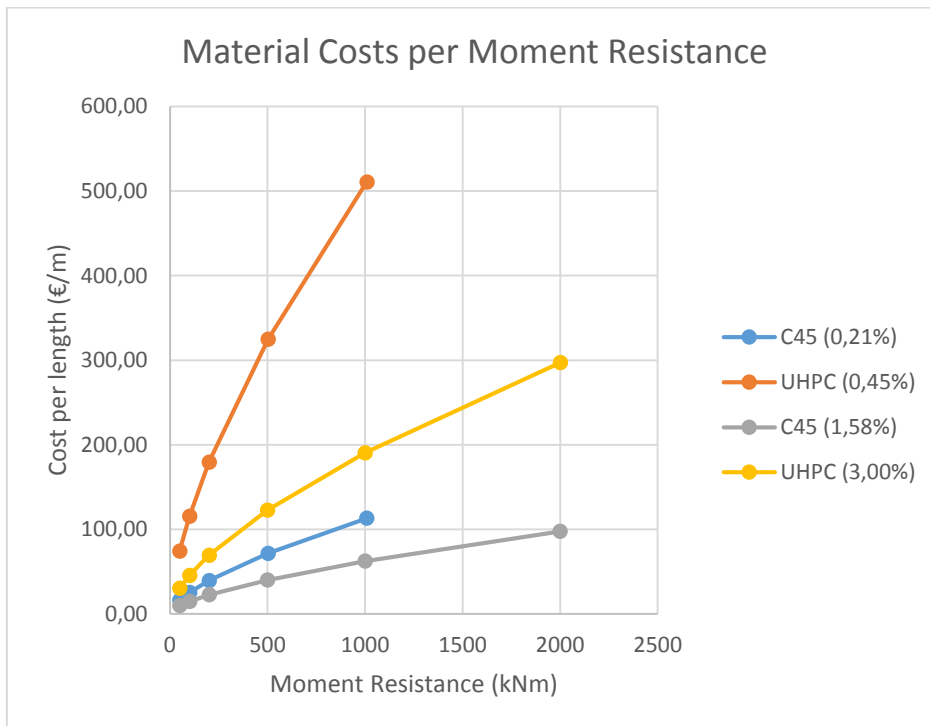


Figure 3-12: Material costs for different values of the moment resistance

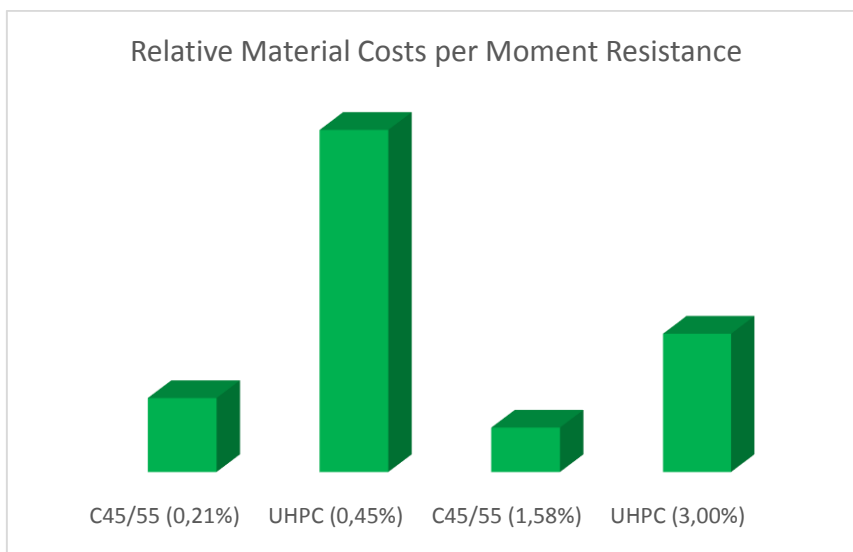


Figure 3-13: Relative material costs (on scale) for a bending moment capacity of 50 kNm

In contrast to axial strength the volume and costs are not linear for bending moment resistance. Both required volume and costs decrease as the required bending moment resistance increases.

To determine competitiveness the CR, VR and CVE are determined for the following pairs:

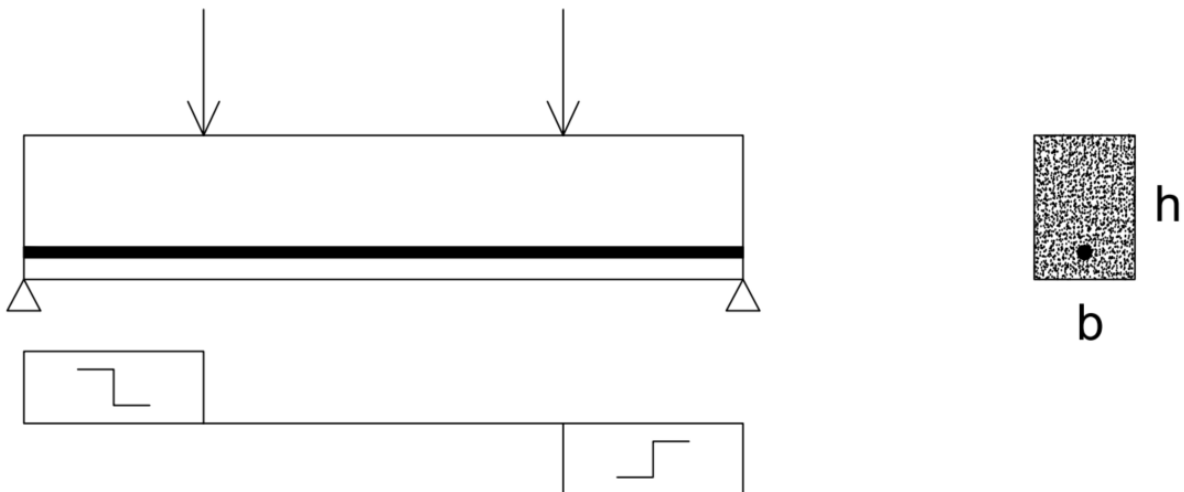
- C45/55 (0,21%) vs. UHPC (0,45%)
- C45/55 (1,58%) vs. UHPC (3,00%)

In general a high cost increase can be expected in combination with a limited volume reduction. However the CVE decreases at higher bending moment resistances, due to both decreasing costs and volume. This means that UHPC does not perform well in bending resistance, but becomes increasingly attractive at higher bending loads.

When the amount of bar reinforcement is increased UHPC becomes more interesting. The CVE drops significantly. Furthermore UHPC can handle larger amounts of bar reinforcement without failure of the compression zone, thanks to its excellent compressive strength. The positive effect of the increase of reinforcement is of course limited by the maximum reinforcement, which is determined by failure of the concrete compression zone and the number of reinforcement bars that can fit in the cross-section.

Note that CVE only takes into account volume and costs. Not only does volume reduction leads to cost reduction, but also reduction of the self-weight. With a fixed total moment capacity and a reduced self-weight the residual moment capacity increases. So an additional aspect that favors application of UHPC is not accounted for by CVE.

3.2.4 Shear



To investigate how UHPC performs in shear compared to C45/55, shear beams with a constant d/b ratio of 17/15, a constant concrete cover of 30mm and an undetermined length are calculated for their shear resistance. The UHPC shear resistance is calculated with the following formulas taken from the AFGC recommendations on UHPC

Concrete contribution to shear resistance:

$$V_{RD,c} = \frac{0,21}{\gamma_{cf} * \gamma_E} * k * f_{ck}^{\frac{1}{2}} * b_w * h$$

$$\gamma_{cf} * \gamma_E = 1,5$$

$$k = \begin{cases} 1 + 3 * \frac{\sigma_{cp}}{f_{ck}} & \sigma_{cp} \geq 0 \text{ (compression)} \\ 1 + 0,7 * \frac{\sigma_{cp}}{f_{ctk,0.05}} & \sigma_{cp} < 0 \text{ (tension)} \end{cases}$$

Fiber contribution to shear resistance:

$$V_{Rd,f} = \frac{A_{fv} * \sigma_{Rd,f}}{\tan \theta}$$

$$A_{fv} = b_w * z$$

$$z = 0,9 * d$$

$$\sigma_{Rd,f} = \frac{1}{K * \gamma_{cf} * w_{lim}} \int_0^{w_{lim}} \sigma_f(w) dw$$

The residual tensile strength of the fiber-reinforced cross-section $\sigma_{Rd,f}$ can be found using the stress-strain diagram for the tensile constitutive law. By taken the average value of the stress over the red-filled region $\sigma_{Rd,f}$ is found.

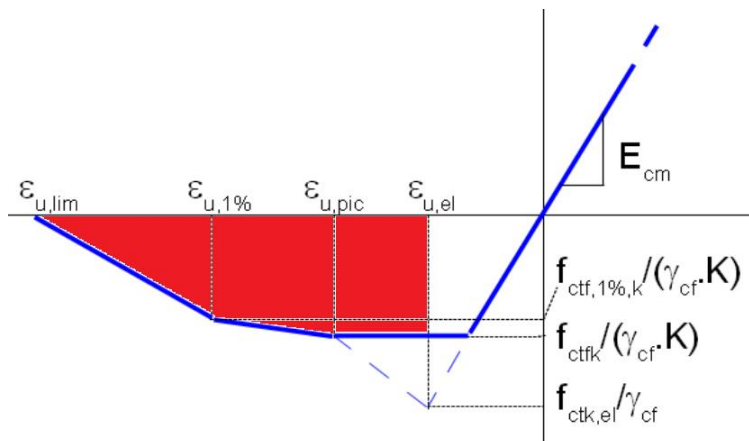


Figure 3-14: Method for finding the residual tensile strength of the fiber-reinforced cross-section $\sigma_{Rd,f}$ using the stress-stain diagram

To simplify the calculation only the region up to the 0,3mm crack is taken into account, assuming no larger cracks will occur.

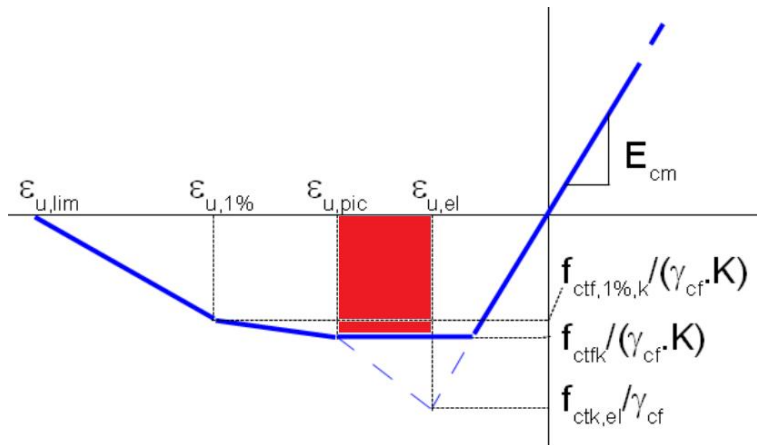


Figure 3-15: Simplified method for finding the residual tensile strength of the fiber-reinforced cross-section $\sigma_{Rd,f}$ using the stress-strain diagram

$$\sigma_{Rd,f} = \frac{9}{1,25 * 1,3} = 5,54 \text{ MPa}$$

Stirrups contribution to shear resistance:

$$V_{Rd,s} = \frac{A_{sw}}{s} * z * f_{ywd} * \cot \theta$$

$$\theta = 30^\circ$$

The total shear resistance is found by adding the contributions of the concrete, fibers and steel:

$$V_{Rd} = V_{Rd,c} + V_{Rd,f} + V_{Rd,s}$$

The shear resistance is limited by the strength of the compressive struts:

$$V_{Rd,max} = \frac{2 * 1,14 * \frac{\alpha_{cc}}{\gamma_c} * b_w * z * f_{ck}^{\frac{2}{3}}}{(\cot \theta + \tan \theta)}$$

Noteworthy about calculation method for shear resistance is that there is a fundamental difference between C45 and UHPC. For C45 $V_{Rd,c}$ and $V_{Rd,s}$ cannot be added as a total shear resistance as stated in NEN-EN 1992-1-1. When calculating UHPC according to the AFGC recommendations the contribution of concrete, steel and fibers are added as a total shear resistance. So initially it seems that the AFGC is overestimating shear resistance. However, the Eurocode allows a very small compressive strut angle θ of approximately $21,8^\circ$, while the AFGC recommends a larger θ of 30° , which compensates the additional shear capacity. On the other hand the addition of the contributions of concrete, steel and fibers, might not even be an overestimation, since fibers have a positive influence on the rotation capacity of the compressive struts. Tests at the Delft University of Technology in 2004 have found that the strut inclination can even be extended to $1 \leq \cot(\theta) \leq 3$, which allows a minimum strut inclination of approximately $18,4^\circ$.

For different values of the shear resistance the required concrete volume and costs are determined by means of a spreadsheet. C45/55 and UHPC with different shear reinforcement ratios are investigated:

- C45/55 without shear reinforcement (C45/55 0 %)

- UHPC without shear reinforcement (UHPC 0%)
- C45/55 with shear reinforcement (C45/55 2%)
- UHPC with shear reinforcement (UHPC 2%)

All these variants include longitudinal bar reinforcement of 0,21%.

The table and graph below show the required cross-section area for different values of the shear resistance.

Shear Resistance (kNm)	Required Area (m ²)			
	C45/55 (0%)	UHPC (0%)	C45/55 (2%)	UHPC (2%)
50	0,122	0,006	0,021	0,006
100	0,257	0,012	0,033	0,011
200	0,542	0,023	0,051	0,019
400	-	0,044	0,079	0,036

Table 3-8: Required cross-section area for different values of the shear resistance

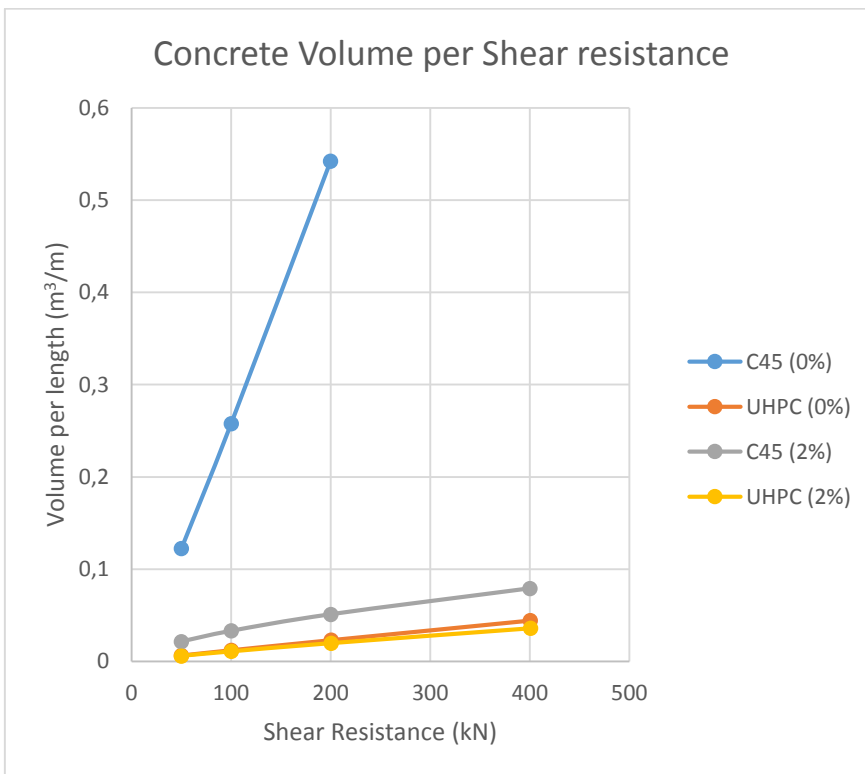


Figure 3-16: Required cross-section area for different values of the shear resistance

The required cross-sections of the four different variants for $V_{Rd} = 50\text{kN}$ and $V_{Rd} = 400\text{kN}$ are shown on scale in the figure below.

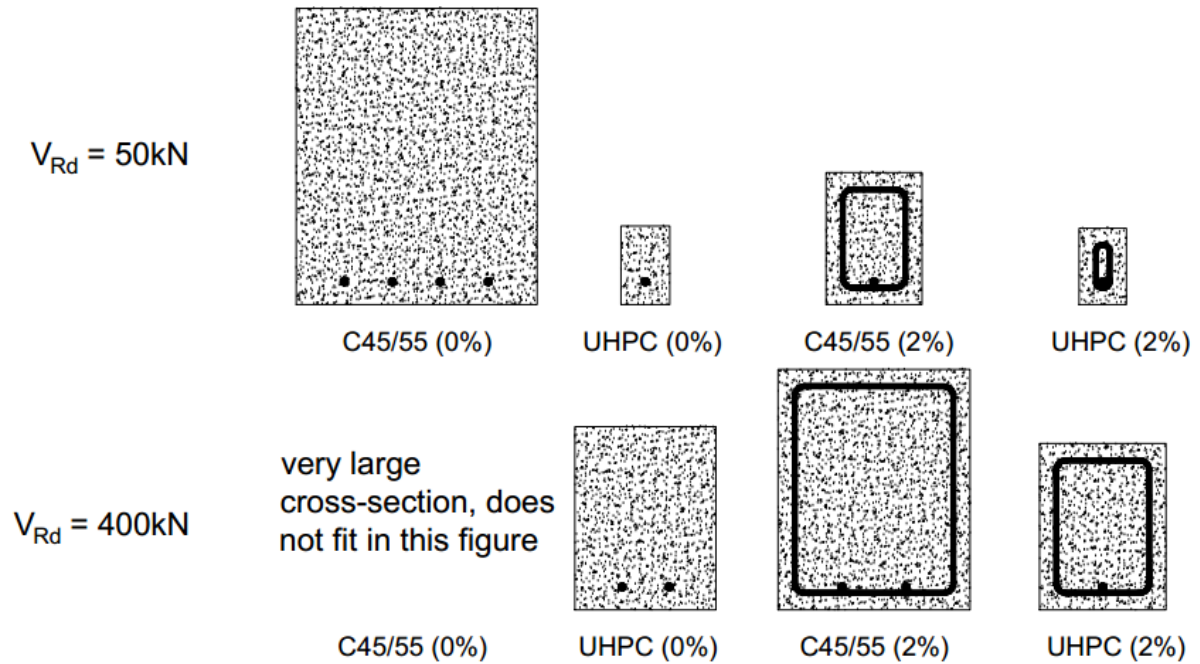


Figure 3-17: Required cross-sections (on scale) for a shear capacity of 50kN and 400kN

With the required cross-sections the costs can be calculated. These are shown in the following table and graph.

Shear Resistance (kNm)	Material Costs (€/m)			
	C45/55 (0%)	UHPC (0%)	C45/55 (2%)	UHPC (2%)
50	13,99	5,48	5,10	5,79
100	29,58	10,17	7,98	10,51
200	62,33	19,22	12,51	19,20
400	-	36,81	19,67	35,01

Table 3-9: Material costs for different values of the shear resistance

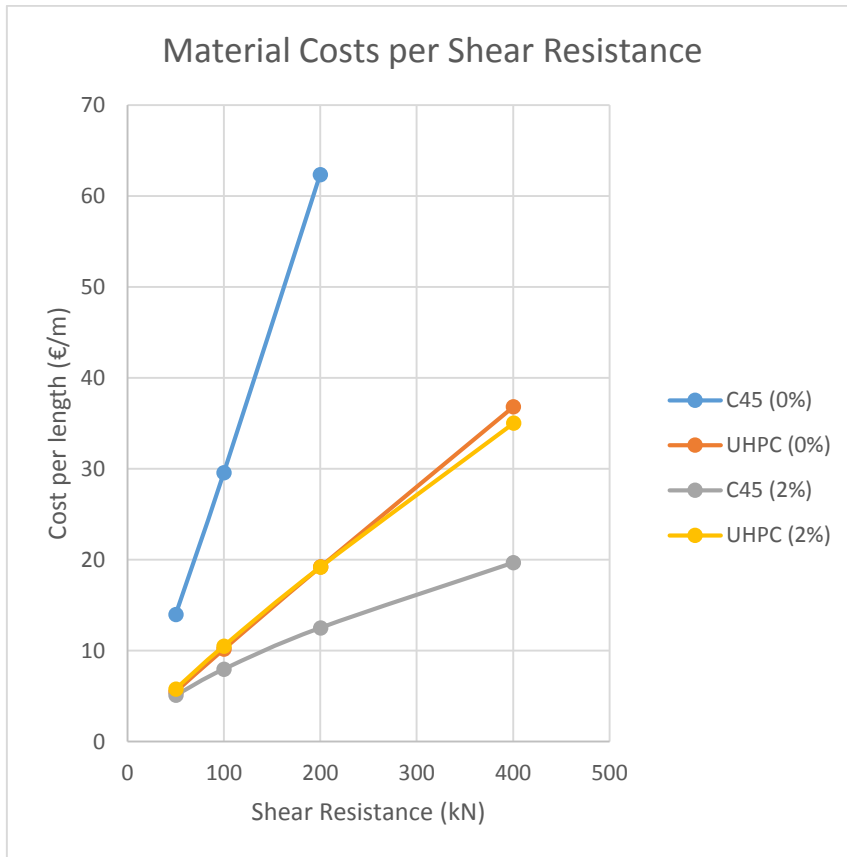


Figure 3-18: Material costs for different values of the shear resistance

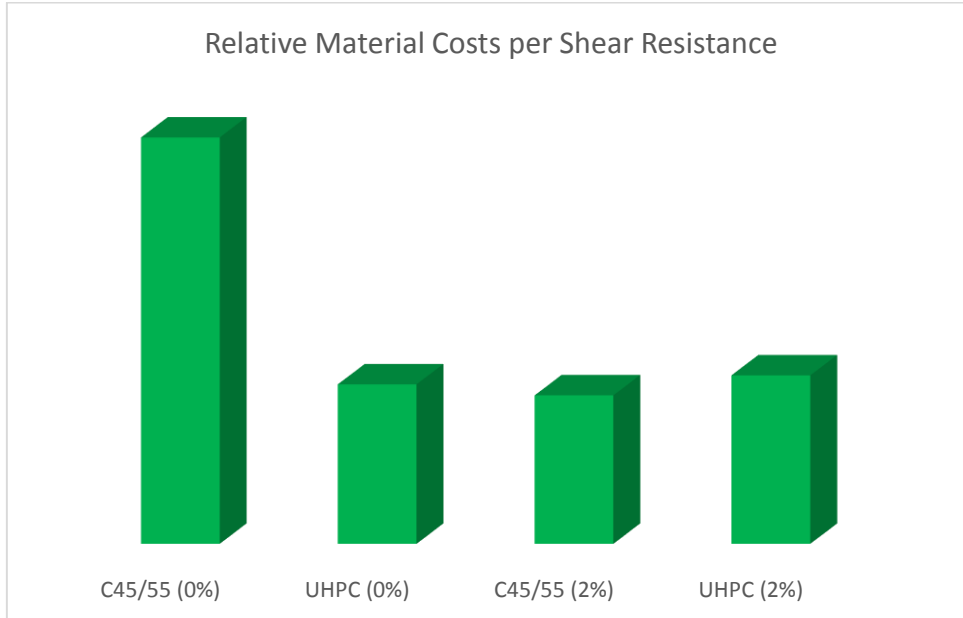


Figure 3-19: Relative material costs (on scale) for a shear capacity of 50 kN

Immediately can be seen that C45/55 without shear reinforcement has very poor shear resistance, since a huge volume of concrete is required compared to the other concrete variants. UHPC has exceptional shear capacity. Even without shear reinforcement it is still more volume efficient than C45 with shear reinforcement. Furthermore, when regarding shear capacity, application of UHPC is both costs and volume saving compared to C45/55 without shear reinforcement. This effect

increases for higher shear strengths. When comparing C45/55 with shear reinforcement with UHPC, C45/55 is still cheaper than UHPC, whether there is shear reinforcement applied or not.

To determine competitiveness the CR, VR and CVE are determined for the following pairs:

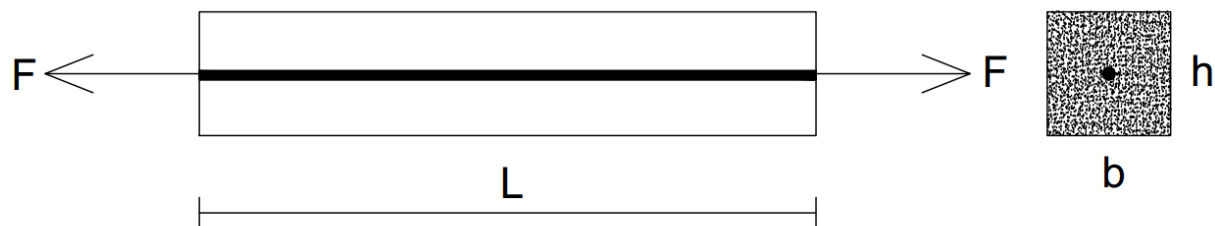
- C45/55 (0%) vs. UHPC (0%)
- C45/55 (2%) vs. UHPC (0%)
- C45/55 (2%) vs. UHPC (2%)
- UHPC (0%) vs. UHPC (2%)

When comparing C45/55 (2%) with UHPC (0%) we can find that the application of UHPC (0%) is very effective in volume saving and only lead to a small cost increase. Therefore a very low CVE can be found. The CVE increases as the shear capacity increases. The costs increase and the volume reduction decreases as shear capacity increase. So UHPC (0%) becomes less efficient in shear, when shear forces increase.

When comparing C45/55 (2%) with UHPC (2%) we can find similar results as with UHPC (0%). However, the CVE values are relatively lower. The CVE still increases as the shear capacity increases.

When comparing UHPC (0%) with UHPC (2%) we can find that CVE values decreases for higher shear strengths. So UHPC (0%) might be attractive for low shear strengths, but as the shear strength increases, UHPC (2%) becomes a better option. Also noteworthy is that UHPC is very resistance to compressive strut failure, which allows high shear reinforcement ratios.

3.2.5 Crack Width



To investigate how UHPC performs in crack control compared to C45/55, tensile members loaded in longitudinal direction with a square cross-section and an undetermined length are designed. Crack widths of C45 are calculated with the following method taken from the AFGC recommendations on UHPC in §7.3.4 [1]:

The crack width at the position of the reinforcement bar is calculated with the following formula.

$$w_s = s_{r,max,f} * (\varepsilon_{sm,f} - \varepsilon_{cm,f})$$

The $s_{r,max,f}$ is the maximum crack spacing calculated with:

$$s_{r,max,f} = 2,55 * (l_0 + l_t)$$

This formula consist of a concrete cover term:

$$l_0 = \frac{1,33 * c}{\delta}$$

And a transfer length term that depends on the bond strength of the reinforcement bars:

$$l_t = \frac{0,3 * k_2 * \left(1 - \frac{f_{ctfm}}{f_{ctm,el}}\right)}{\delta * \eta} * \frac{\phi}{\rho_{eff}} \geq \frac{l_f}{2}$$

In case of strain-hardening ($f_{ctfm} \geq f_{ctm,el}$) the transfer length would become zero, if there was no lower bound determined by half of the fiber length.

Parameter δ expresses the positive influence that fibers have on the contribution of the cover zone and the bond strength of the reinforcement bars.

$$\delta = 1 + 0,5 \frac{f_{ctfm}}{f_{ctm,el}}$$

Factor η is a bond factor that depends on the type of reinforcement. Table 7.2 in [1] states that for reinforced concrete with ribbed bars:

$$\eta = 2,25$$

The value $\varepsilon_{sm,f} - \varepsilon_{cm,f}$ is the difference between the mean strain of the steel and the concrete, while taking into account the contribution of fibers.

$$\varepsilon_{sm,f} - \varepsilon_{cm,f} = \frac{\sigma_s}{E_s} - \frac{f_{ctfm}}{E_{cm}} - \frac{k_t \left(\frac{f_{ctm,el} - f_{ctfm}}{\rho_{eff}} \right) (1 + \alpha_e * \rho_{eff})}{E_s}$$

The first term of the formula $\frac{\sigma_s}{E_s}$ is the strain in the reinforcement steel.

The steel stress in the crack σ_s can be calculated using horizontal equilibrium:

$$N_E = \sigma_s * A_s + \sigma_f * A_c$$

The horizontal equilibrium formula yields the following expression for the steel stress.

$$\sigma_s = \frac{N_E - \sigma_f * A_c}{A_s}$$

In case of prestressing, the steel stress σ_s will be replaced by the stress differential of the tendon $\Delta\sigma_p$, which can be found using horizontal equilibrium:

$$N_E = \sigma_s * A_s + \sigma_f * A_c + P$$

$$\Delta\sigma_p = \frac{N_E - \sigma_f * A_c - P}{A_p}$$

The fiber stress σ_f can be found from the strain-strain diagram. Since in this case pure tensile members will be designed for a pre-determined crack width, a single value over the whole cross-section will be found for fiber stress. The fiber stress is likely to be f_{ctfk}/K , since this stress level is found for all crack widths between ε_{el} and $\varepsilon_{u0,3}$. So crack widths between 0mm and 3mm always give a fiber stress of f_{ctfk}/K .

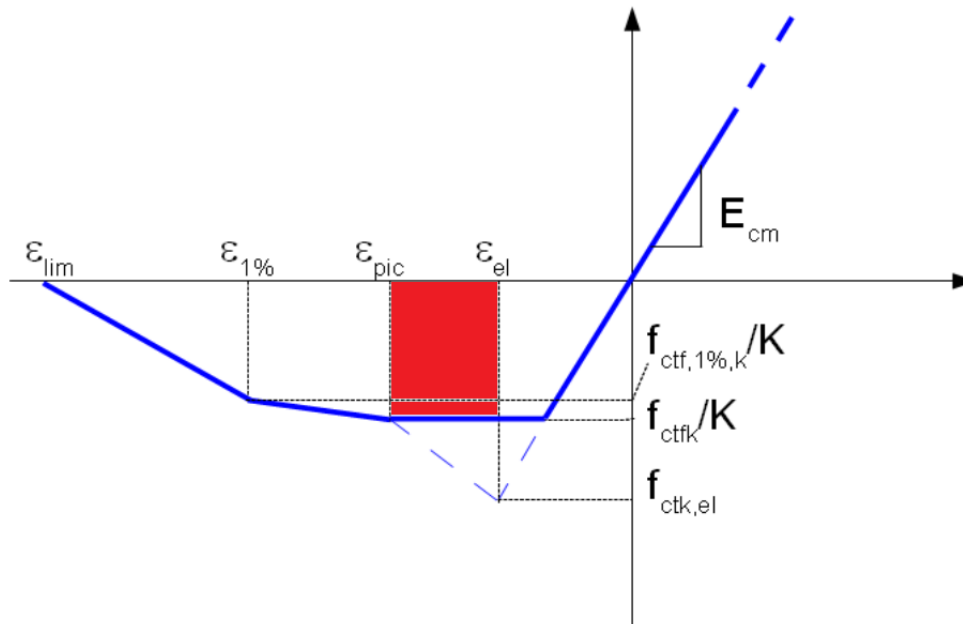


Figure 3-20: The red-filled region shows the range of crack widths that give a constant fiber stress

The required amount of prestress is determined as follows:

$$A_{p,req} = \frac{P_{max}}{\sigma_{pm\infty}} = \frac{A_c * \sigma_{c,max}}{\sigma_{pm\infty}} = \frac{A_c * 0,45 f_{ck}}{\sigma_{pm\infty}}$$

$$\rho_p = \frac{A_{p,req}}{A_c}$$

The maximum concrete compressive stress $\sigma_{c,max}$ is chosen based on NEN-EN 1992-1-1 §5.10.2.2, which allows to neglect non-linearity of creep if the concrete compressive stress is not permanently above $0,45 * f_{ck}$. Note that the Eurocode allows an even higher concrete compressive stress of up to $0,7 * f_{ck}$.

The second term $\frac{f_{ctfm}}{E_{cm}}$ is the strain in the cracked concrete, in which fibers are activated.

The last term is the strain residual in the concrete that is still in the elastic phase. Since a simplified design curve with truncation is used, $f_{ctm,el} - f_{ctfm}$ equals zero. The additional strength of the concrete in elastic phase above the fiber strength is neglected, so no residual strain is found. Naturally if the additional elastic strength is taken into account, a smaller difference between mean steel strain and mean concrete strain, thus a smaller crack width is found.

With the crack width at the position of the reinforcement w_s the crack width at the outer fiber w_t can be found using the following formula:

$$w_t = w_s * \frac{h - x - x'}{d - x - x'}$$

In this formula h is the total height, d is the effective depth, x is the height of the compression zone and x' is the height of the uncracked zone under tension. Since the member in question is a pure tensile member without bending, w_t will equal w_s .

In the SLS the w_t should not be wider than the maximum crack width w_{max} .

$$w_t \leq w_{max}$$

According to table 7.1 from [1] the w_{max} for reinforced UHPC in exposure class XC4 is 0,2mm. Prestressed UHPC has a stricter maximum crack width of 0,1mm for XC4. Exposure class XC4 is chosen based on the statement in [1] that this exposure class is for superstructures of bridges, which are not protected from rain. The same exposure class will be used later on to make a design for a long span UHPC road bridge.

Different concrete variants are investigated namely:

- C45/55 (3%)
- UHPC (3%)
- C45/55 (4%)
- UHPC (4%)
- C45/55 (P 1,45%)
- UHPC (P 4,84%)

For these variants the minimum required dimensions and costs are calculated while constraining the maximum crack width under different tension loads by means of a spreadsheet. For both reinforcement bars and prestressing strands a diameter of 12mm is chosen. Note that this diameter can give problems fitting the strands in the cross-section of variant UHPC (P 4,84%), so for this variant a larger diameter will be chosen. The table and graph below show an overview of the required cross-section area for different cracking force values.

Tensile Force (kN)	Required Area (m ²) for exposure class XC4					
	C45/55 (3%)	UHPC (3%)	C45/55 (4%)	UHPC (4%)	C45/55 (P 1,45%)	UHPC (P 4,84%)
500	0,064	0,026	0,047	0,022	0,021	0,006
1000	0,129	0,053	0,094	0,044	0,043	0,012
2000	0,259	0,106	0,188	0,088	0,085	0,024
4000	0,519	0,212	0,376	0,176	0,171	0,047

Table 3-10: Required cross-section areas for exposure class XC4 under different tensile loads

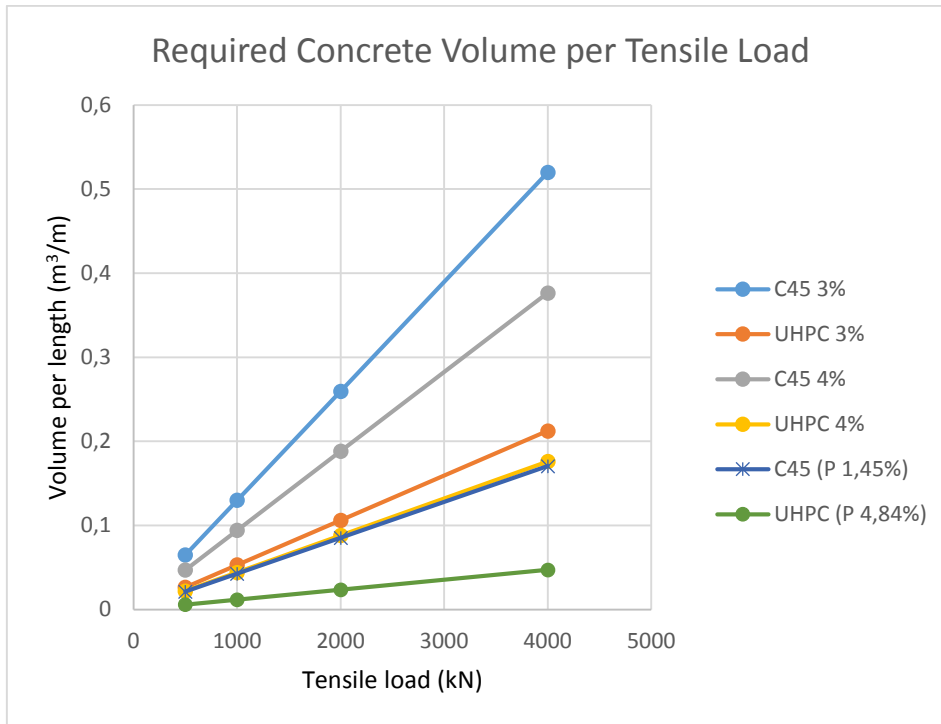


Figure 3-21: Required cross-section areas for exposure class XC4 under different tensile loads

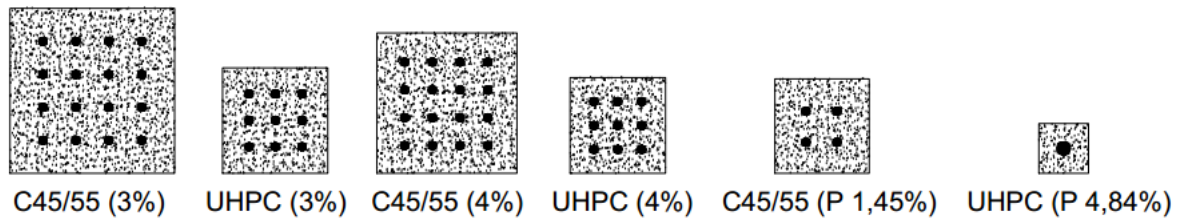


Figure 3-22: Required cross-sections (on scale) for exposure class XC4 for any tensile load

From the required cross-section areas the costs can be calculated. These are shown in the following table:

Tensile Force (kN)	Material costs (€/m) for exposure class XC3					
	C45/55 (3%)	UHPC (3%)	C45/55 (4%)	UHPC (4%)	C45/55 (P 1,45%)	UHPC (P 4,84%)
500	20,94	27,95	18,66	24,80	9,38	11,59
1000	41,88	55,90	37,33	49,62	18,75	23,17
2000	83,69	111,76	74,66	99,22	37,50	46,36
4000	167,54	223,53	149,19	198,41	75,01	92,69

Table 3-11: Material costs for exposure class XC4 under different tensile loads

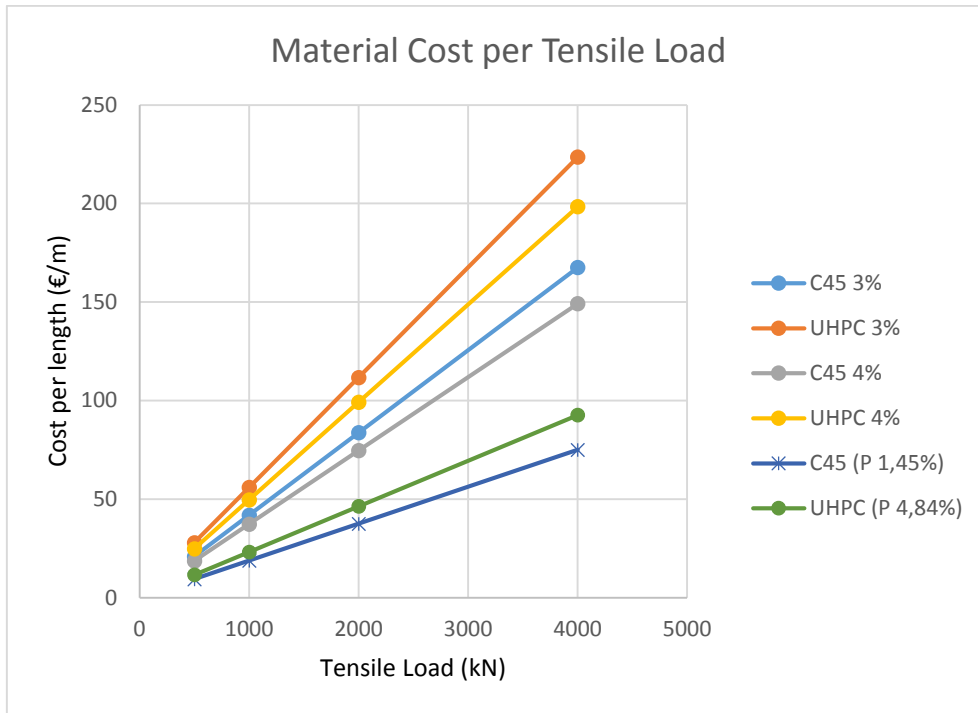


Figure 3-23: Material costs for exposure class XC4 under different tensile loads

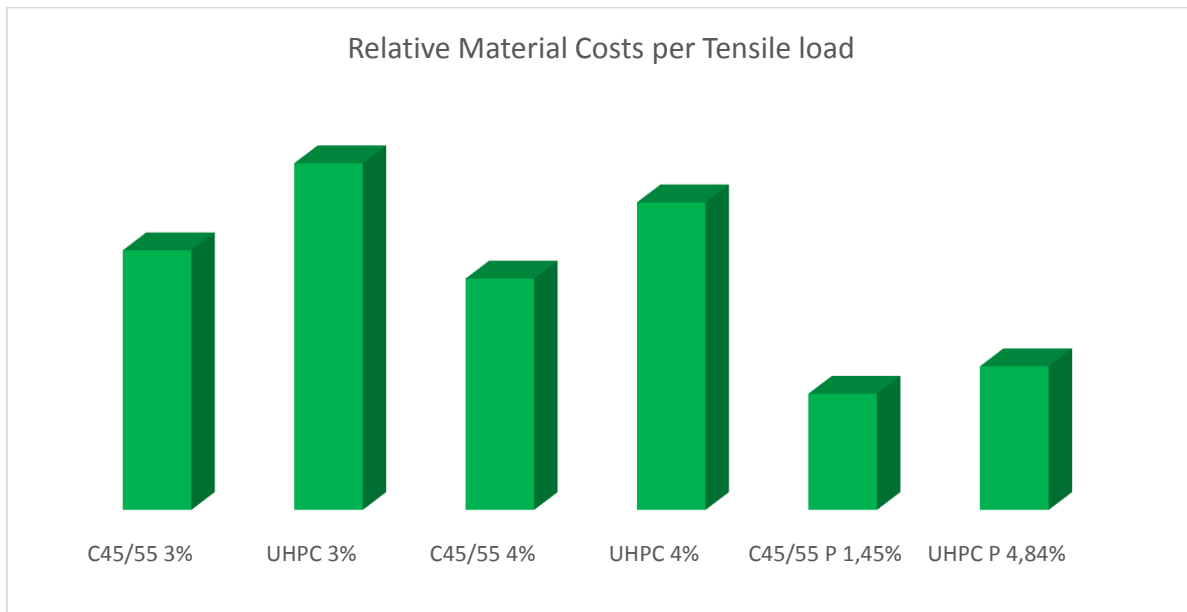


Figure 3-24: Relative material costs for exposure class XC4 under any tensile load

As can be seen in the graphs, increasing the reinforcement ratio in UHPC can increase cost reduction and volume reduction. However up to a certain point the reinforcement would not fit in the cross-section anymore, so there is a limit to increasing this.

The CR, VR and CVE are determined for specific pairs of concrete variants.

- C45/55 (3%) vs. UHPC (3%)
- C45/55 (4%) vs. UHPC (4%)
- C45/55 (P 1,45%) vs. UHPC (P 4,84%)

For the 3% variants the CR is 1,34 and the VR is 0,41. The CVE therefore is 0,54. Increased reinforcement ratio of 4% gives slightly less favorable results for UHPC. Namely a CR of 1,33 and a VR of 0,47. The CVE is increased to 0,62. When comparing UHPC 3% with UHPC 4%, a higher reinforcement ratio is preferred, because applying more reinforcement is both costs and volume saving.

The comparison of prestressed variants favor the application of UHPC more than the reinforced variants. Both the CR and VR are lower, resp. 1,24 and 0,28. The CVE decreases to 0,34.

3.2.6 Summary

As expected compressive members are the most effective in UHPC. They can resist high compressive forces with only small dimensions. They have a low CVE value of 1,04. This indicates they require relatively low cost with small dimensions. However, cost would still increase when chosen over C45.

Tensile members are significantly less effective in UHPC, because large dimensions are required for relatively small loads. When comparing reinforced UHPC with reinforced C45 the CVE's are quite low, namely around 0,69. These values hold only, when assuming that they fail when the cracking force is reached. However, when we assume the members fail at cracking force, very low resistances are found.

More realistic (and higher) tensile resistances are found when higher reinforcement ratios are applied and the extra capacity after cracking is taken into account. In that case crack width becomes governing and we will see CVE's around 0,54. Compared to tension members designed for the cracking there is a decrease in CVE, because the application of UHPC has more favourable effect on post-cracking behaviour than on pre-cracking behaviour.

To further increase tensile resistance tensile members can be prestressed. Prestressed conventional concrete is both cost and volume saving compared to reinforced UHPC. However the application of prestressed UHPC compared to prestressed conventional concrete, when designing for cracking force, is more favourable (CVE=0,40) than reinforced UHPC compared to reinforced concrete (CVE=0,69). This also holds for designing for the crack width, which give a CVE of 0,54 for reinforced UHPC compared to conventional concrete and a CVE of 0,34 for prestressed UHPC compared to prestressed conventional concrete.

This has to do with the higher compression strength of UHPC, which allows a higher prestressing force.

Bending resistance can hardly benefit from the application of UHPC. CVE's are generally very high for reinforced bending members. However they decrease with higher reinforcement ratios and higher bending moment capacities. Since the CVE is still 1,91 even at very high bending moment capacities (2000kNm) and reinforcement ratios (UHPC 3,00% and C45 1,58%), reinforced UHPC does not benefit bending capacity enough to be considered.

The increased shear resistance as a consequence of the application of UHPC is quite significant. It shows that it can easily resist the shear forces without shear reinforcement, since it has low CVE's for UHPC 0% vs. C45 2%. The CVE decreases even more, when shear reinforcement is added to the UHPC. Therefore it is very effective to apply UHPC to omit shear reinforcement.

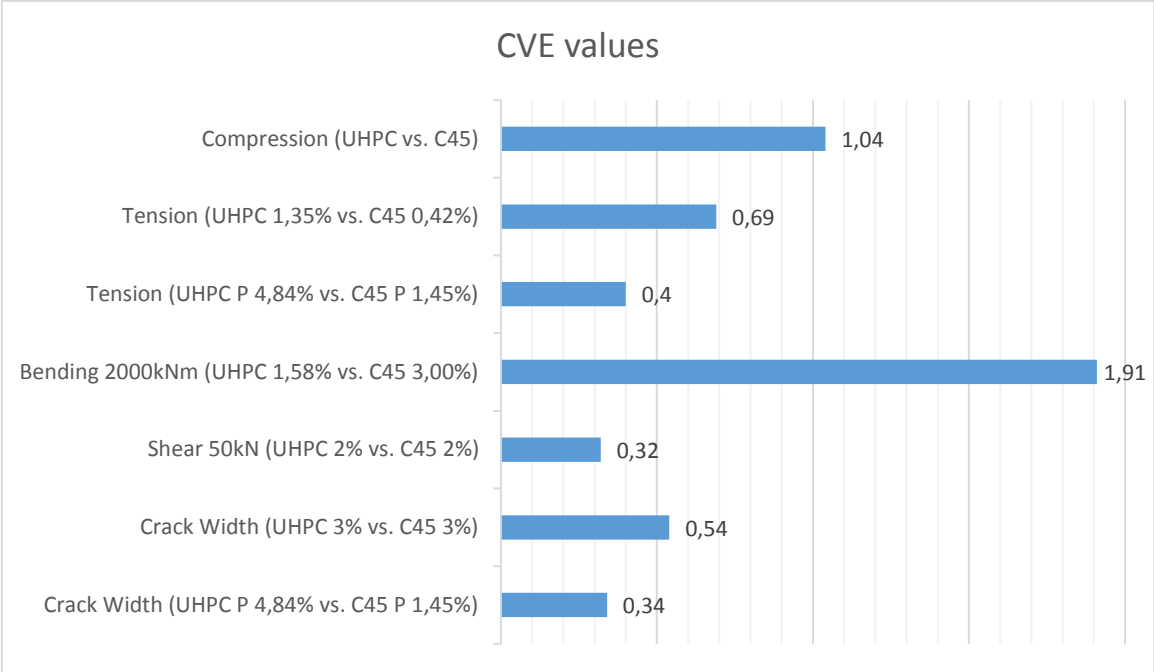


Figure 3-25: Overview of some CVE values

3.3 Conclusion

The application of UHPC in bridges would be the most viable in structures that are mainly loaded in compression, since these would be more economically competitive due to the high rate of material savings. UHPC in tension and also bending do not have this high rate of material savings and are therefore less effective. The application of prestress can increase the tensile and bending resistance. This is especially effective for UHPC, since it allows a high level of prestress. Also since the fibers in UHPC have a positive influence on post cracking behavior, it is advised to allow cracking during design in order to utilize this positive characteristic of the material. Application of UHPC can increase shear resistance significantly, so members, in which shear resistance is governing, can benefit from the use of UHPC.

4 Architectural Design

4.1 Purpose

This part of the report does not necessarily tie in with the research objectives and is therefore included in the appendix as a side study. The results are briefly discussed in this chapter. The complete study is found in the appendix A.

In the early stages of this master thesis the application of UHPC in footbridges was investigated instead of road bridges. A case study was chosen, namely a new footbridge that would cross the A9 (highway) at Amstelveen. The intention was to start off with an architectural design, which means making an aesthetic design, while not taking structural solutions into consideration. This would give freedom to develop new out-of-the-box shapes and forms. Seven different designs were drafted and three of them were analyzed further. The application of UHPC on these designs would be investigated. The philosophy was *to apply UHPC only when it's needed to carry the stresses, while maintaining the shape and slenderness of the architectural design*. The architectural designs that were studied are shown in the figure below.

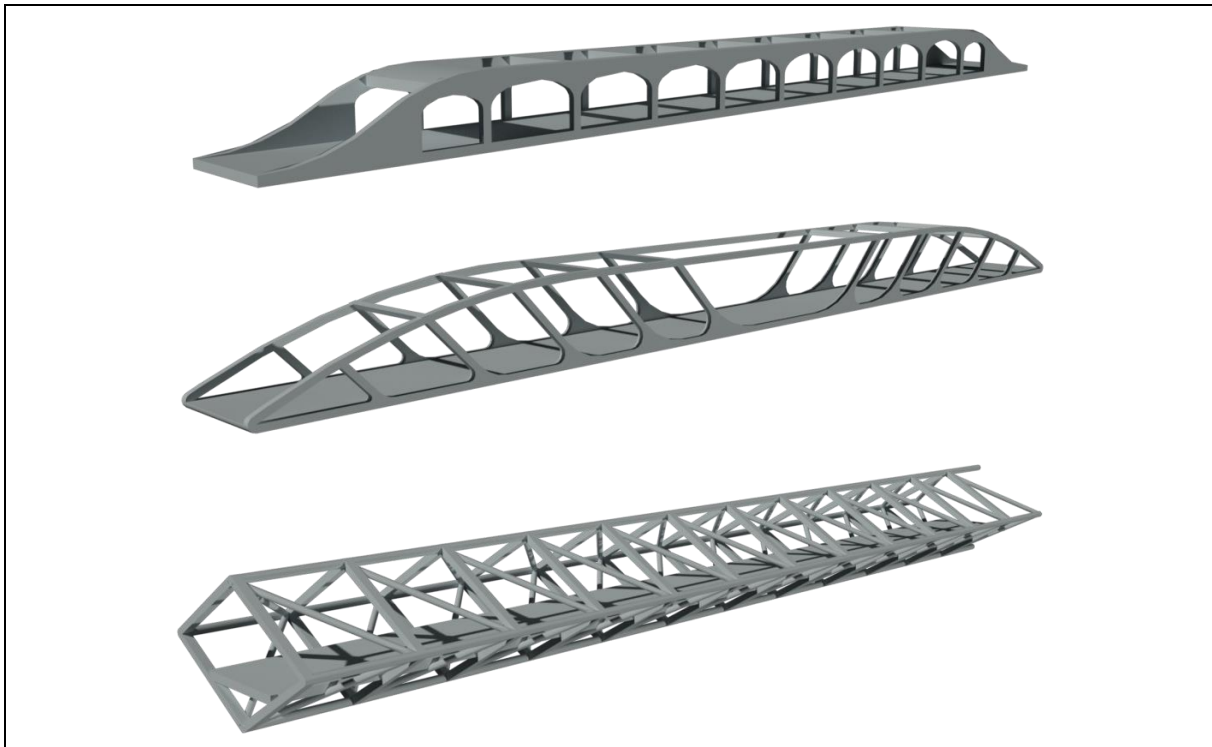


Figure 4-1: Selected Concepts (from top to bottom) "Voided Box Girder", "ESO-Inspired Truss" and "Diamond Portal"

Design that did not make the cut are show in the following figure.

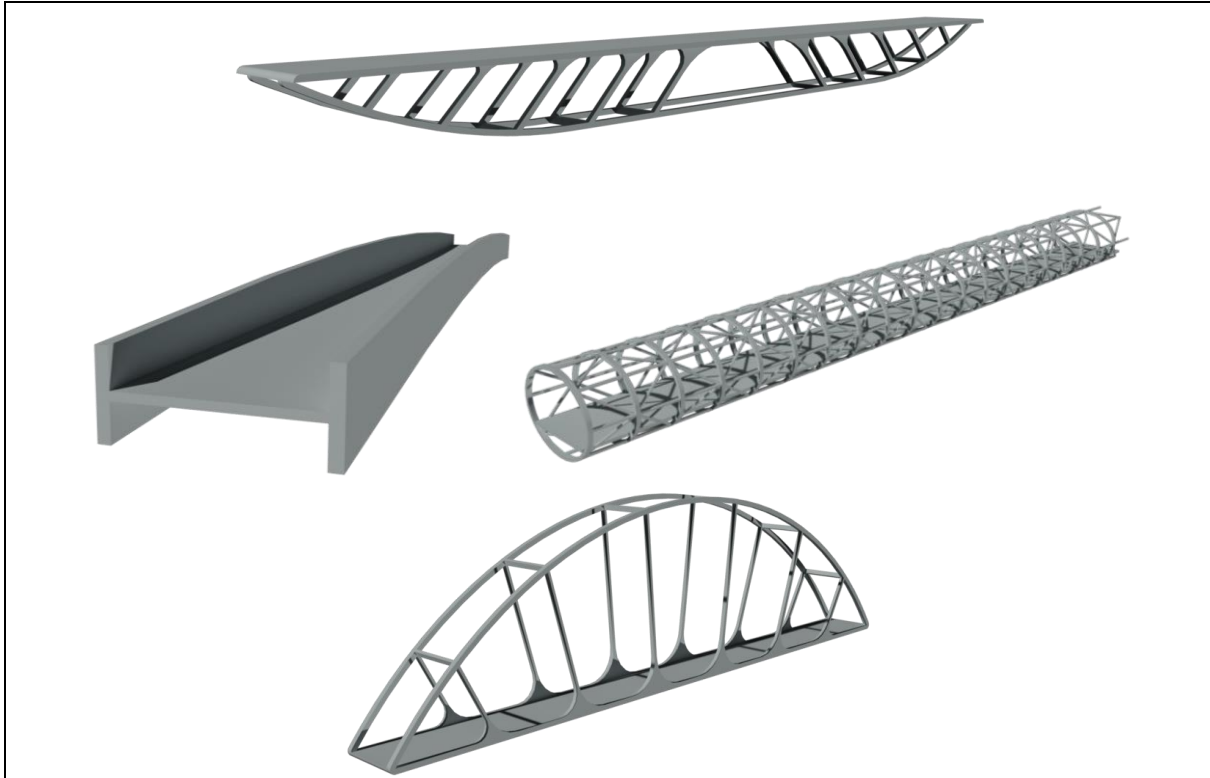


Figure 4-2: Fallen Concepts “Π-truss” (t.l.), “H-girder” (t.r.), “Ellipse Portal” (b.l.) and “Organic Arch” (b.r.)

4.2 Conclusion

As the master thesis progressed this research was discontinued. The reason for the discontinuation was because the developed this approach method was unable to successfully find optimized designs for UHPC. Another reason was because UHPC road bridges were preferred over UHPC footbridges, since they are in higher demand. Nonetheless some conclusions can be drawn from the study.

4.2.1 Implementation and results of the design philosophy

In this chapter designs were developed by first designing with a solely “architectural approach”, not considering structural solutions, but only aesthetic purposes. Consecutively structural solutions were developed with the following philosophy:

Apply UHPC only when it is needed to carry the stresses, while maintaining the shape and slenderness of the architectural design.

This philosophy was implemented by preferably applying UHPC in members that were loaded by a high compressive stress, because this is the most effective way of utilizing UHPC’s excellent mechanical properties. Furthermore members that have to resist high bending stresses, would also be applied in UHPC, as this can also decrease required amount of concrete volume.

This philosophy resulted in designs that required UHPC in just a few members. These member mostly also had to resist tensile stresses, so reinforcement bars were still required. However in many cases shear reinforcement could be omitted, thanks to the excellent shear capacity of UHPC.

4.2.2 Limitations of the design philosophy

As innovative and aesthetic shapes are designed by an architect and structural solutions are provided by a structural engineer, the question arises whether this method will really optimize the use of the material UHPC. In the preceding paragraphs, design concepts developed according to this method, did not result in very effective UHPC structures. Applying a material according to a fixed shape seems

more like treatment of symptoms, than providing an optimized solution for the material. The solutions provided in the preceding paragraphs show optimized solutions for a specific shape, not an optimized solution in general.

So in order to find this general optimized solution for UHPC another design philosophy will be used. Instead of holding on to a certain design and applying UHPC where needed, the application of UHPC will be the basic principle for the development of new shapes and designs. In addition the knowledge and experience from investigating the application of UHPC with the architectural approach will be taken in mind in this new method. Ultimately this method should yield a design that utilizes the strengths of UHPC, such as excellent compression and shear strength as much as possible.

5 Topology Optimization

5.1 Purpose

The results in this part of the report do not necessarily tie in with the research objectives and is therefore included in the appendix as a side study. The results are briefly discussed in this chapter. The complete study is found in the appendix B.

In the early stages of the master thesis the possibility of using topology optimization to find an optimized design is investigated. Topology optimization can be a useful tool to find possible optimized structures, provided that the model and boundary condition input is proper and simulates the reality. The outcome of the optimization will be a single solution that is optimized exactly and only for what is put in. If the input is not valid or incomplete, the outcome will be as such. Since it is very hard to make a perfectly realistic model for the boundary conditions and material properties, the results should not be assumed as an optimal solution automatically, but should be carefully evaluated for their validity. Due to these limitations, the main purpose of the topology optimization is to develop ideas for solutions.

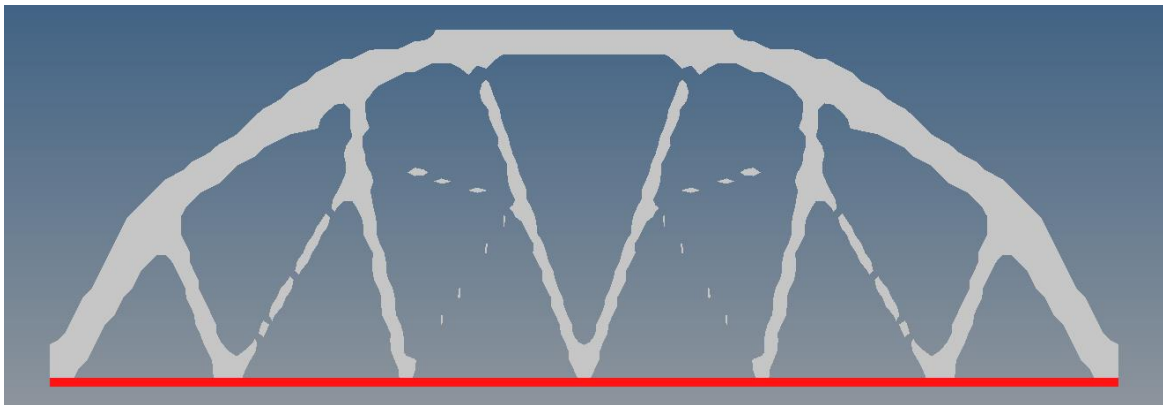


Figure 5-1: Figure 5-2: Minimum compliance optimization without height restriction with five points that either carry a downward vertical force or not, leading to an optimization problem with 32 load combinations

5.2 Conclusion

The results of the optimization do not show an optimal structure for UHPC specifically, but more for a general linear-elastic material. It also does not show an optimal configuration of the ties, since it is only optimized for a specific configuration of nodal loads. It does however provide some insight for possible solutions. First of all, the arch is a very effective way to transfer self-weight to the supports under compression only, which is very favourable for UHPC. Moreover the diagonal configurations of the ties can decrease bending moments in the arch. These results inspire to investigate the possibility of an arch bridge in UHPC. More on this concept will be discussed in §6.5.

6 Concept Analysis

6.1 Purpose

The purpose of this chapter is to find the most suitable concept to implement in a long span UHPC bridge design. This can be achieved by analyzing several concepts. The following concepts will be analyzed:

- UHPC (Voided) Slab Bridge
- UHPC Box Bridge
- UHPC Double T-girder/Pi-girder Bridge
- UHPC Arch Bridge

Pros and cons will be evaluated to determine to which extent the concept is an optimal solution. Moreover adaptations of conventional concepts can be proposed to find this. Ultimately a concept will be chosen that is believed to be optimal and this concept will be investigated further.

6.2 UHPC Slab Bridge

The prestressed concrete slab bridge is a conventional concept for cast in-situ concrete bridges that span up to 50m.

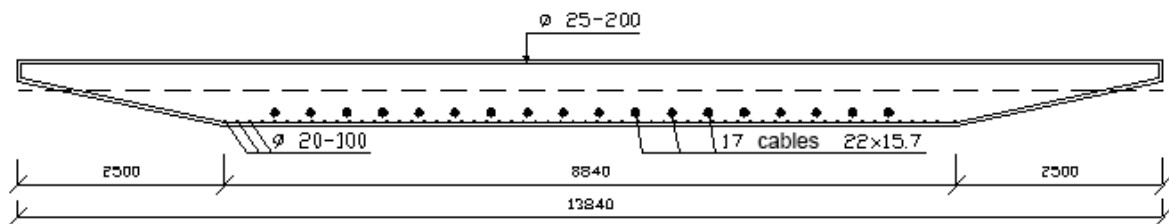


Figure 6-1: Typical cross-section for a cast in-situ concrete slab bridge with post-tensioned and passive steel reinforcement

6.2.1 Benefits

Slab bridges have the potential to make slender bridges that are easily fabricated. The simplicity and low production costs are characteristic for this concept. Massive slabs leave plenty of room for the ducts that are required for post-tensioning. Post-tensioning is a good method to couple several precast slab segments in case the bridge becomes too long.

6.2.2 Disadvantages

Slab bridges are massive structures that are quite heavy. That makes them less suitable for long spans, since self-weight becomes increasingly dominant in that case.

6.2.3 Optimization

To decrease the self-weight, thus also decreasing the required prestress, voided slabs can be applied. This will also decrease the amount of required concrete and steel and increase the slenderness ratio. Larger voids will increase this effect. However the size of the voids is limited to minimum cover and required space for prestressing strands/tendons.

6.3 UHPC Box Bridge

The box bridge is a conventional concept for both concrete and steel. Box bridges in conventional concrete can span up to 90m and steel box bridges can span over a 100m. Conventionally different configurations of box bridges are applied for different span ranges. Up to 68m multiple precast concrete box beams placed side by side has been applied many times. For larger spans up to 90m a single box girder, mostly segmented due to the large span, is applied. This type of bridge is lighter,

because of the lighter webs. Whether the bridge is made up from segments or separate beams has a large influence how the bridge can be designed, optimized and executed.

To clearly indicate the difference between the two types of box bridges we define the following:

- *The box bridge: a general term for bridges with one or more box-shaped cross-sections.*
- *The box beam bridge: a bridge consisting out of multiple beams spanning the whole bridge.*

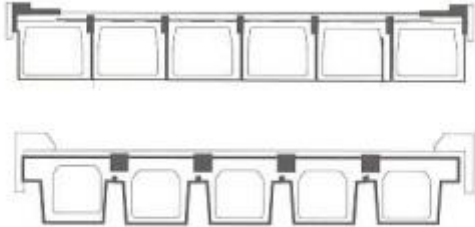


Figure 6-2: Examples of cross-sections for box beam bridges

- *The box girder bridge: a bridge consisting out of box-shaped longitudinal segments.*



Figure 6-3: Example of a box girder bridge segment

In addition H-beams can be considered, which are very similar to box beams. They have the advantage that they do not need an EPS formwork to create the void. They however have significantly lower torsional stiffness.

6.3.1 Benefits

Box bridges allow a light structure by reducing the required amount of concrete and steel. This reduces material costs and makes them considerably lighter than other bridge types such as (voided) slab bridges and inverted T-beam bridges. In addition the reduced weight can reduce foundation costs. Besides its weight-saving ability box girders are also known to have high torsional stiffness.

6.3.2 Disadvantages

The box bridge is more complex to design and to fabricate compared to the slab bridge.

6.3.3 Optimization

Optimization of the box bridge can be carried out in many different ways. The thickness of the flanges or the webs can be reduced. Besides varying thicknesses there are other ways to optimize the box bridge, such as varying web spacing or cantilever length. In case of a wide bridge, the number of webs should be optimized.

6.4 UHPC Double-T girder/Pi-girder Bridge

The double-T girder and pi-girder have already been applied for short span road bridges UHPC bridges and long span footbridges. They are somewhat similar to I-beam bridges or U-beam bridges with the main difference that the deck is already attached during precasting. U-beams and I-beams are applied for conventional concrete bridges up to 55m.



Figure 6-4: UHPC double T-beams for short span road bridge

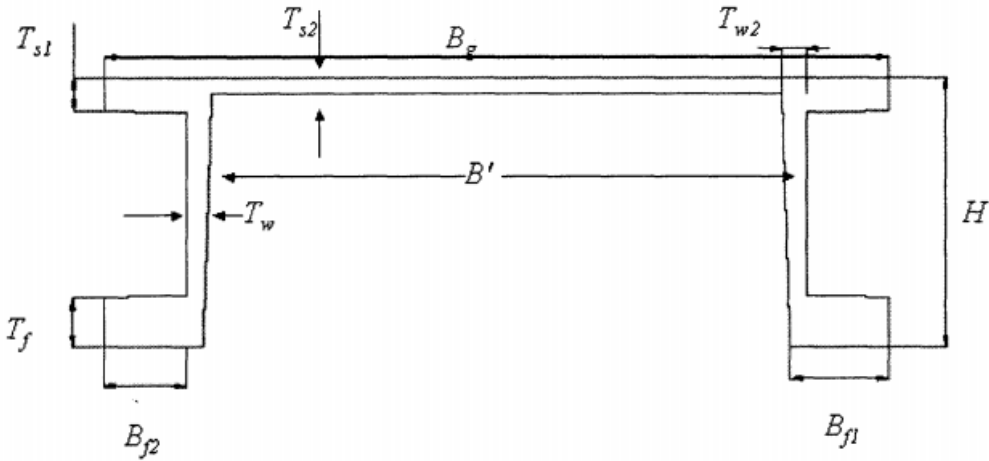


Figure 6-5: Cross-section of a UHPC pi-girder

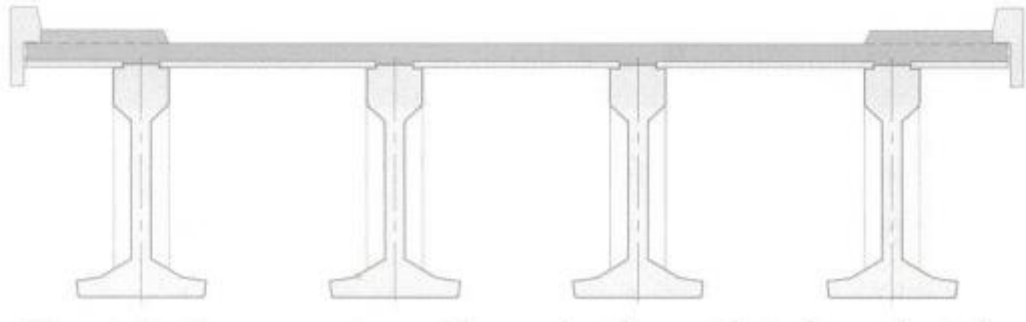


Figure 6-6: Typical lay-out for I-beam bridge, which has some similarities with the double T-girder bridge

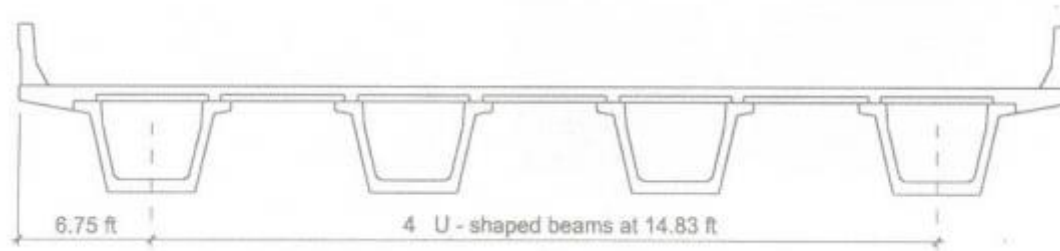


Figure 6-7: Typical lay-out for a U-beam bridge, which has some similarities with a pi-girder bridge

6.4.1 Benefits

Double-T girder and pi-girder bridges make considerably lighter bridges compared to a slab bridge, while still maintaining simplicity of fabrication.

6.4.2 Disadvantages

Double-T girder and Pi-girder Bridges do not provide much space for prestressing strands and/or tendons. So when a high level of prestress is required, which is the case for long spans, these concepts are not viable.

6.4.3 Optimization

There are many parameters that can optimize these concepts. Increasing beam spacing and width can reduce the required amount of concrete. Also flange and web thicknesses and the depth of the beam can be varied.

6.5 UHPC Arch Bridge

Concrete arch bridges in the Netherlands are quite rare, because most of them are made of steel. Spans of steel arch bridges range from 50 to 500m. The application of UHPC in arch bridges has already been researched and even executed.

6.5.1 Benefits

Since an arch bridge is mainly loaded in compression, the application of UHPC fits well because of its excellent compressive strength and relatively small tensile strength. The high compressive strength of the material gives the opportunity to make a very light and slender arch. Moreover the permanent compressive loading due to self-weight, allows a reduction of required prestressing steel. Finally aesthetics often plays a role in the decision whether an arch bridge is chosen or not. Since the arch bridge is an aesthetically pleasing structure, this concept is chosen in case aesthetics is in high demand.

6.5.2 Disadvantages

At the supports of an arch bridge large horizontal thrust forces are present. Since the soil in the Netherlands is soft, this has to be resolved by either a massive substructure or by a tie connected to the support. The last solution is known as a tied-arch bridge. The massive substructure can be costly and requires sufficient space, which might not be available. The tied-arch bridge requires a tie that has to resist very high tensile forces. Applying UHPC in such a construction element requires a high amount of prestressing steel.

6.5.3 Optimization

An important parameter for design and optimization of an arch bridge is the span-to-rise ratio. A higher arch decreases stresses in compression arch and tensile tie, but also decreases lateral stability due to wind loads. In addition the height of the arch can be limited by the available space at the

construction site and crane capacity. A low arch has high stresses in arch and tie, but has better lateral stability and decreases the length of the arch. Since UHPC has a very high compressive strength, possibilities for a very low arch as a way of optimization can be investigated.

6.6 Conclusion

Since the objective is to find solutions for long span (>60m) road bridges, the box bridge has the preference over the slab, double T-girder and pi-girder. The box bridge is a conventional solution for such spans mainly because of the ability to reduce self-weight, which becomes increasingly dominant for longer spans. Moreover the concept offer a wide range of possibilities for optimization and provides many ways to apply a high level of prestress.

To demonstrate the effectivity of the box bridge the box-shaped cross-section is linked to the results of chapter 3. In this chapter the effectivity of rectangular cross-sections in UHPC are compared to rectangular cross-sections in C45 and expressed in a single efficiency value called CVE. A lower efficiency value means more cost and volume efficiency for UHPC compared to C45. The figure below shows the found CVE's.

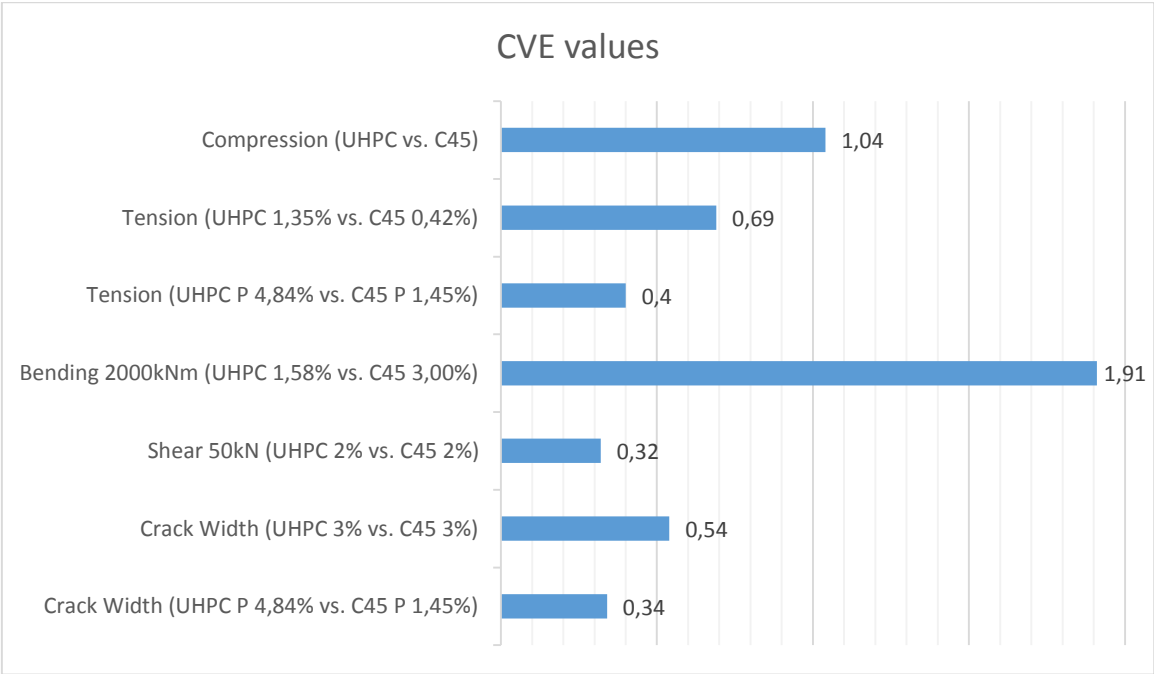


Figure 6-8: Overview of some CVE values

A rectangular reinforced bending member in UHPC clearly performs poorly in CVE. A box-shaped cross-section solves this by having a compressive member at the top and a prestressed tensile member at the bottom (flanges). Both these type of members perform very well in CVE and combined with a significant height spacing they can resist a high bending moment. In a box-shaped cross-section shear is resisted by the webs. Because UHPC also performs very well in shear, the cross-section area of the webs can be reduced and/or shear reinforced can be omitted.

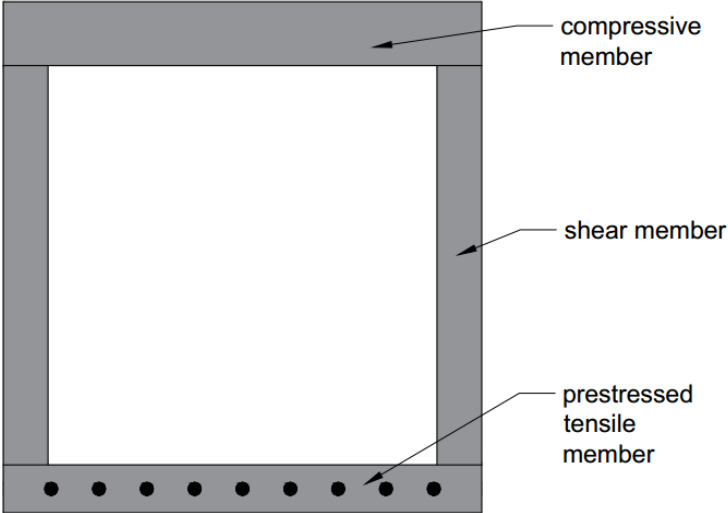


Figure 6-9: Distribution of internal forces in a box-shaped cross-section

The rejection of double-T and pi-girders is also supported by [7], stating that double-T and pi-girders are only suitable for short spans mostly due to shortage of space for prestressing strands. Longer spans would require segmental post-tensioned systems.

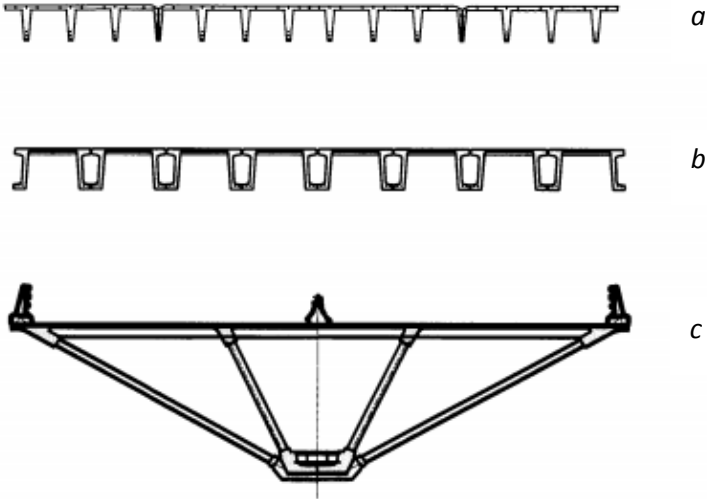


Figure 6-10: Examples of UHPC girders for (a) short spans ($L < 21m$); (b) medium spans ($L < 36m$); and (c) long spans ($L < 36m$) [7]

The arch bridge is, like the box girder bridge, suitable for long spans. However the arch bridge is not suitable as a general solution, but more of a special case due to complex execution. Plenty of space is required for both transportation and assembly. Since this cannot be guaranteed the arch bridge concept is rejected.

A prestressed box bridge would be an appropriate solution and shall be investigated further.

7 UHPC Box Bridge Variants

7.1 Purpose

The purpose of this chapter is to specify design choices and design parameters for the box bridge. Design parameters will be explained on how these can optimize the design. The following aspects/parameters are discussed:

- Box beam bridge vs. Box girder bridge (Beams vs. Segments)
- Internal/External prestressing
- H-girders vs. box girders

7.2 Beams vs. Segments

Since UHPC has to be fabricated in precasting plants, the bridge has to be assembled from multiple elements to avoid transportation problems. The choice between multiple beams or segments has significant consequences for both execution method and design. When regarding solely execution method, beams are always preferred over segments, if crane and transportation capacity allows it. In that case the beams can simply be hoisted into position. This is a fast execution method that requires little time and labor on the building site. If beams are too long or too heavy to be transported practically, segmented bridges should be considered. More on the possibilities and limitations of transportation can be found in the next chapter.

Segmented bridges usually require more complex execution methods. Segments have to be coupled using post-tensioning. A method to execute precast segmented bridges, which is conventional outside of the Netherlands, is by means of an assembly truss. All segments are placed in position on top of an assembly truss, which will temporarily support the segments. When the segments are coupled through prestressing the assembly truss can be removed and placed onto the next span if applicable. This method is often time-consuming and requires intensive labor on site and is therefore costly.

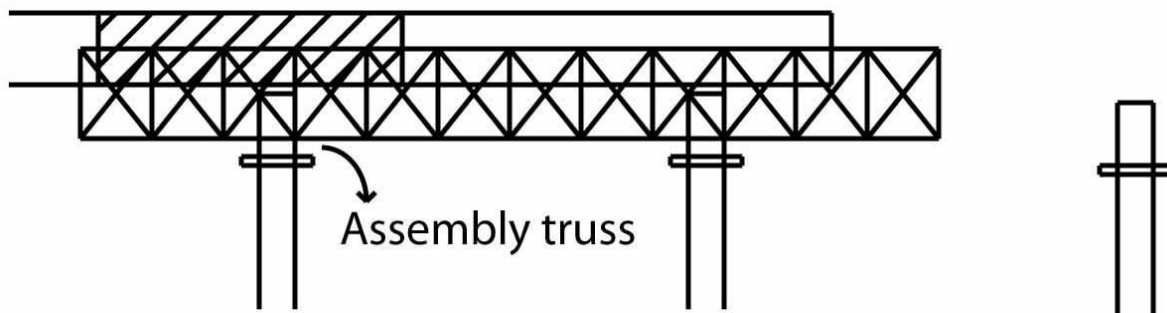


Figure 7-1: Execution method for precast segmental bridges by means of assembly truss [Lecture slides "Concrete Bridges" course by C. van der Veen at Delft University of Technology]

7.3 Internal Prestressing vs. External Prestressing

As stated before an important design parameter is flange and web thickness. In case of internal prestressing the bottom flange or web thickness is often governed by the amount of strands/tendons that should fit. When a high level of prestress is applied, one can expect that fitting the tendons/strands in the cross-section can result in very thick and therefore heavy flanges/webs.

In order to save material, external prestressing can be applied. External prestressing offers additional benefits besides material savings such as easier casting due to absence of pre-tensioning strands or post-tensioning ducts and less prestressing losses due to friction. A master thesis [Ten Voorde, 2004]

has shown that an externally prestressed segmented box girder bridge in UHPC with a span of 100m was technically and economically feasible.

However the use of external prestressing also has some drawbacks. External prestressing hardly contributes to the moment capacity, so if moment capacity becomes governing, then external prestressing is not advisable. Other drawbacks are that the tendons are susceptible to fatigue and subject to vibrations.

An interesting option is the combination of internal and external prestressing. The internal prestress is applied by means of pre-tensioning, which is limited because the 28 day strength is not yet reached. The external prestressing is applied later as an additional prestressing load, when the concrete is at full strength.

7.4 Box Beams vs. H-beams

Box beams have a relatively complex shape to cast. Especially the void poses a challenge for the formwork. In order to cast the box shape in a single pour, an EPS filling is used to create the void. After demoulding the filling cannot be reused. Since EPS is relatively expensive, “Lodewikus Voorgespannen Beton” has developed the LOD H-girder [6]. This beam is very similar to the traditional box girder, as can be seen in the figure below.

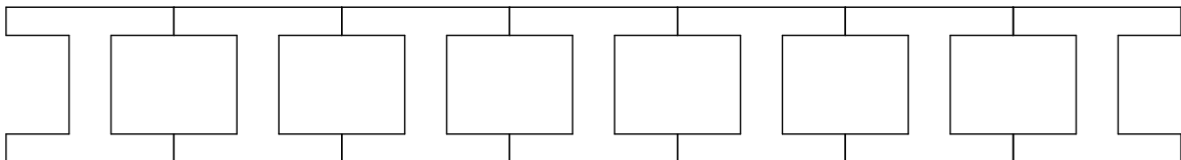


Figure 7-2: Schematization of an H-beam bridge cross-section, resembling a box beam bridge with the box-shaped voids

The open shape of the H-beam allows single pour casting without the need for EPS filling, providing a cost advantage over traditional box beams. However the open shape also reduces the torsional stiffness, which is detrimental for the load spread in transverse direction.

The H-beam should have the preference over traditional box beams as long as torsional stiffness is not governing.

7.5 Conclusion

There are many different ways to execute a box bridge. A bridge can be made either out of segments or beams. Beams are preferred over segments, as they require little construction time and labor on site and is therefore cheaper. An important limitation on these beams is that they should be able to be transported. Since UHPC can make lighter beams than conventional concrete, the transport can be lighter and longer beams can be made for the same weight limitation. Therefore UHPC box beams can be a useful standard product for long span bridges. “Haitsma Beton” currently manufactures box beams up to 68m out of conventional concrete. UHPC beams can extend this maximum length to become a competitive general solution for long span bridges. How long these beams can practically become regarding transportation, will be investigated in the next chapter.

In addition the box beam can be optimized further by applying external prestressing in addition to internal prestressing, which allows less material use and self-weight. By applying the H-beam concept the production process can become cheaper, which can be very beneficial for standard elements with a high production volume.

8 Transport

8.1 Purpose

Since UHPC elements have to be manufactured in precasting plants, transportation is always an important factor, when it comes to realizing a UHPC bridge. This is especially the case when the elements that have to be transported become very large and heavy. As stated before a bridge made out of beams is always preferred over segments, because of the shorter execution time on site. Longer span bridges require longer beams, which can provide a challenge for transportation. Not only because the weight increases, but also the geometry requires more space to maneuver.

In this thesis only transportation by road will be regarded, because the main focus is long span bridges that cross roads. Transport by water, which can offer additional possibilities and benefits, cannot always be guaranteed in that case, but transport by road can.

In order to find out to which extent beams can be applied with regard to transportation by road, the geometry and weight that can be practically and economically transported has to be investigated. By means of interviews with transport company “Van Der Meijden”, heavy lifting company “Mammoet” and the RDW, a public authority responsible for mobility, the challenges and limitations of transportation are collected and reported in the following paragraphs.

8.2 Transportation Method

The most conventional method to transport bridge beams by road is with a combination of a heavy-duty truck pulling heavy-duty trailers. The required number of trailers is determined by the required number of axles. Conventional trailers of Mammoet have either three or five axles. Since beams are very long but not very heavy, two trailers normally suffice. One trailer at each end will support the beam. The beam can be supported by bearings that allow rotations in any direction and make vertical translations to be able to make turns and keep the beam level on inclined roads. The trailers are connected only by the beam, so axial forces will occur in the beam during transport. These forces can become quite large during high acceleration and deceleration, so the beam must be able to resist them.



Figure 8-1: Transportation by road of a 61,75m box beam with a combination of a heavy-duty truck pulling heavy-duty trailers [From: <http://www.wvandermeijden.nl/>]

8.3 Challenges

8.3.1 Road capacity

The most important challenge of the transportation of bridge beams from precasting plant to building site is the capacity of the roads. This is almost always governing for the limitation of size and weight. The following factors often determine these limitations:

- Maximum weight capacity of a road/bridge (maximum axle loads)
- Obstacles along and above the road
- Sharp turns

Solutions to cope with these limitations are among others:

- Temporary pontoon placement to spare a bridge
- Temporary blocking of the road to maintain sufficient space and safety
- Temporary removal of obstacles along the road (such as traffic signs, gantries are rarely allowed to be removed)
- Go off-road (often requires placement of steel/composite plates to support the vehicle)

In order to make sure the existing infrastructure can facilitate the transportation, cooperation with the RDW is required, which is responsible for permits of exceptional transport. Since there are no general regulations on exceptional transport, the RDW facilitates the negotiations between the transportation company and road authorities to determine whether a permit is granted for a certain route. They also have a consulting function.

To find an upper limit for geometry and weight in general is nearly impossible, because then all the considered road authorities should be approached and negotiated with. However a general rule of 10t per axle, which is common in exceptional transport, can be applied. In some cases this value is increased to 12t per axle. This is often not a real challenge since axles can be added easily by the

transportation company. Note that for the crossing of some bridges a lower maximum axle load applies. To maintain a practical upper limit for the total axle loads 240t is chosen. This number is based on practical number of axles and self-weight of the vehicle. When assuming a self-weight of 70t, the beam can weigh up to 170t.

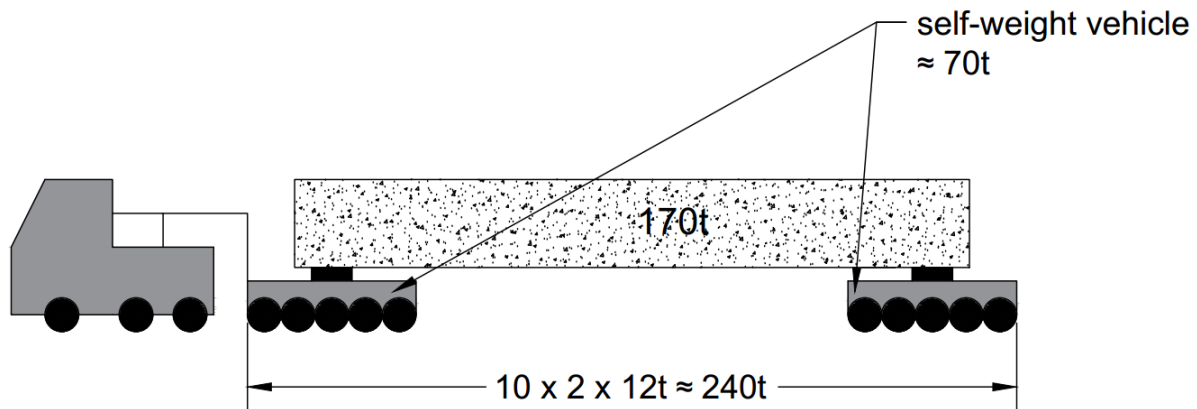


Figure 8-2: Schematization to determine the maximum weight of the transportation vehicle based on maximum axle loads

The biggest challenge is the length of the vehicle, which is most probably the governing upper limit for the beam. It becomes a problem in sharp turns, because of its swept path, which may not cross obstacles along the road. The current record for longest bridge beam transported by road is 61,75m. This length is achieved with intensive negotiations with many different parties and according to the RDW it seems like this is the upper limit. However depending on the start and destination of transport there is a possibility of a greater length. The best way to determine this length is to choose a route and analyze this route for the swept path.

8.3.2 Equipment capacity

Capacity of cranes and trucks is rarely a governing factor. Modern equipment is able to transport beams of almost any size and weight. Length is the most significant size parameter, which is not much of a problem for truck and trailer combinations. The length of these combinations can be adjusted according to the required length. The current record for heaviest bridge beam transported by road is 158t. Van Der Meijden believes that there is still some room for extension. A truck and trailer combination of Van Der Meijden can carry around 250t. Mammoet has the equipment for even heavier transport by combining multiple trailers with that can carry a total of 36t per axle. The self-weight of the trailer is approximately 3,5t per axle. So the load can weigh 32,5t per axle. However this is far more than the allowed axle load for the roads. So the governing number of axles will be determined by the road capacity, which allows only 12t per axle, not the equipment.

8.4 Conclusion

The limits of exceptional transport by road is more often based upon negotiation than on regulation. The weight limit of the beam can be taken as 170t based on a general rule of thumb of 12t per axle. Exceptions exist however, for example when the transport has to cross a bridge that has lower load limits. This will not be taken into account. The length limit of the beam depends on the route of transport. To find a realistic limit a swept path analysis of the route should be executed.

9 UHPC Box Beam Bridge Design 60m

9.1 Purpose

As a starting point a design will be made for a 60m x 15m internally prestressed box beam bridge. The concrete class will be C170, so the characteristic compression strength will be 170MPa. The design process is carried out by means of a spreadsheet, which allows parameter optimization. Parameters can be changed in order to optimize the output. Unity checks can quickly show, where there is still room for optimization. For example a beam width of 1200mm and web thickness of 155mm lead to a UC of 0,49 for the shear capacity. From this result can be concluded that beam width can be increased and/or the web thickness can be decreased in order to optimize the shear capacity. Optimization of the parameters are discussed in the following paragraphs. After that the optimized design is presented and method of design calculation is discussed. Ultimately the structural performance is shown by means of a collection of unity checks.

9.2 Cross-Section Properties

9.2.1 Concrete cover

The concrete cover is taken from the AFGC Recommendations and based on environmental class XD3 (exposed to frequent splashing of water containing chlorides) and structural class S5 (service life of 100 years with concrete class \geq C45/55). The minimum cover for passive reinforcement steel c_s is 25mm and for prestressing steel c_p is 30mm. In order to take into account manufacturing tolerances 5mm is added to the minimum concrete cover to determine the minimum thickness. This value is according to Δc_{dev} from the Dutch National Annex of NEN-EN 1992-1-1. Ultimately the minimum concrete cover becomes $c_s = 30\text{mm}$ and $c_p = 35\text{mm}$.

9.2.2 Beam Height Optimization

A limited height for a beam is desirable for several reasons. A limited height is favorable for maintaining sufficient headroom with only a small elevation of the bridge. By limiting the required elevation, costs of soil transport can be reduced significantly. Another reason to limit the height is because this makes manufacturing easier. Less formwork is required. Limiting the geometry is also favorable for transportation, since maintaining a limited swept path is often a challenge during transportation.

When reducing the height a number of challenges arise. The first problem that is encountered is related to the reduced eccentricity of the prestressing steel. As a result the prestressing force increases significantly and more strands are required. To accommodate the additional strands the height of the bottom flange can be adjusted accordingly.

Another problem that arises, when decreasing the height, is the increased compressive force leading to a high concrete stress. This leads to high prestressing losses, but can also lead to an exceedance of the maximum compressive stress of the concrete. This stress is limited to 60% of the characteristic strength of the concrete for pre-tensioned systems in the SLS and 70% of the $f_{ck}(t)$ right after demoulding. However fatigue in the compression zone is mostly governing for the height.

9.2.3 Beam Width Optimization

To limit the required number of beams the beam width can be increased, which is favorable because production time and transportation time can be reduced. Of course the beam width is limited by the required web area, which is responsible for the shear resistance. The beam width can be increased as long as there is overcapacity in shear resistance. Because of the high shear strength of UHPC, it is expected that a relatively large beam width is possible.

However a beam width that is too large will lead to high transverse moments due to local effects. Initially a beam width of 2500mm was designed, but this width causes the slender web without transverse reinforcement to fail under the transverse moment. To mitigate the local effects on the transverse moment the beam width was decreased to 1500mm. This led to a more favorable transverse moment distribution and allowed the web to be slender and without transverse reinforcement.

Another limitation to the width is caused by transportation. An increased width increases the swept path of the transportation vehicle and can prevent the vehicle from accessing certain roads and making certain sharp turns.

9.2.4 Top Flange Thickness Optimization

The top flange thickness is determined mainly by the axle loads, causing bending stresses in the top flange. The self-weight of the top flange and other uniformly distributed loads also cause bending stress, but to a lesser degree. The top flange should be thick enough to facilitate both post-tensioning ducts for transverse prestressing and transverse passive reinforcement in the top and the bottom. Moreover the internal lever arm should be large enough to provide sufficient moment resistance. The main function of the transverse prestressing to couple the box beams, but it also has a positive influence on the moment resistance of the top flange.

$$d_{top,min} = 2c_s + 2\phi_s + c_p + \phi_{duct} = 2 * 30 + 2 * 10 + 35 + 55 = 170mm$$

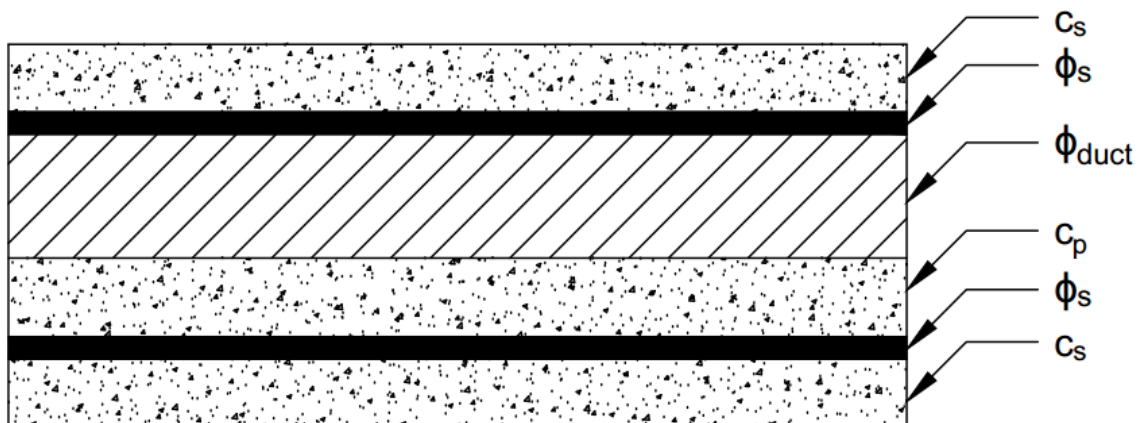


Figure 9-1: Cross-section of the top flange showing the minimum thickness

Note that in this case the duct for post-tensioning is in the top flange coupled to the top reinforcement bar. The minimum thickness of the top flange could be decreased by placing ducts below the top flange in transverse ribs for a more optimized thickness. However it was chosen not to apply this method, to enable the use of less complex formwork.

Although a very thin top flange is favorable for the self-weight of the bridge, it can be necessary to increase top flange thickness, for instance when the compression zone is susceptible to fatigue failure. Another reason to thicken the top flange is to limit the height of the compression zone. In case a high level of prestress is applied, the compression zone increases considerably. NEN-EN1992-1-1 §6.1(5) states that the average compressive strain in flanges of box beams should be limited to the elastic limit. However, since the elastic limit of the compressive strain of UHPC is only slightly smaller than the ultimate compressive strain, it is very unlikely that this limit will be reached.

Note that the height of the compressive zone can also be limited by the rotational capacity, given by the formula below.

$$x_u \leq \frac{500 * d}{500 + f_{yd}}$$

However it is not necessary to take this into account, since the structure is statically determinate.

9.2.5 Bottom Flange Thickness Optimization

The governing factor for the bottom flange thickness is the amount of prestressing strands that has to be applied. As the required number of strands increases additional layers of strands are needed. The minimum bottom flange thickness is determined by the number of layers, minimum concrete cover and minimum strand spacing. The strand spacing according to AFGC Recommendations is the same as with conventional concrete in Eurocode. The minimum concrete cover for prestressing steel is 30mm (including manufacturing tolerance 35mm). Note that when minimum cover and strand spacing are complied with the values stated in the AFGC recommendations, the splitting stresses are sufficiently accounted for.

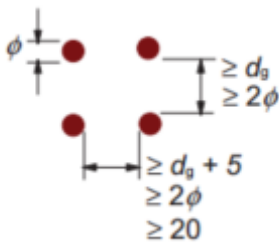


Figure 9-2: Minimum strand spacing according to Eurocode

$$d_{bot,min} = \phi \left(1 + 3(n_{layers} - 1) \right) + 2c = 15,7(1 + 3(3 - 1)) + 2 * 35 \approx 175mm$$

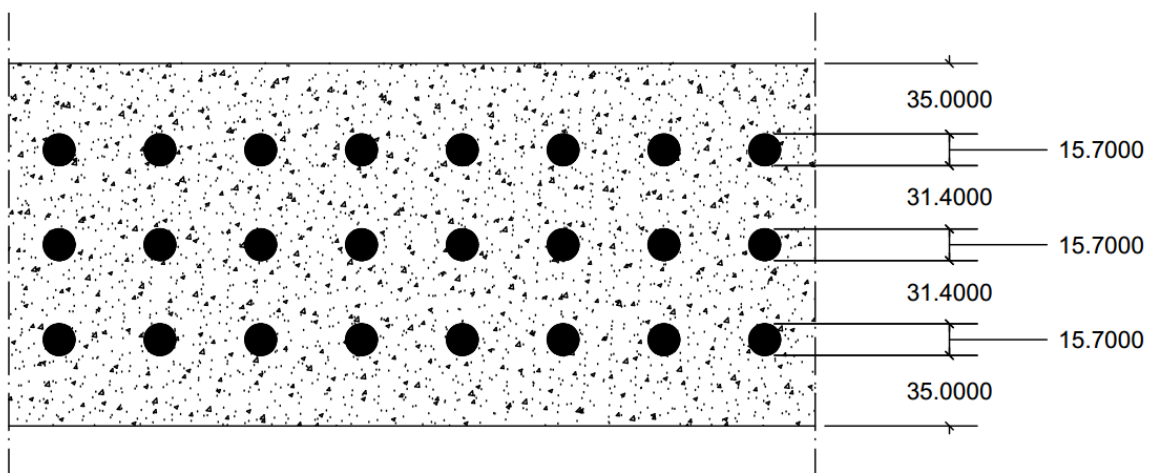


Figure 9-3: Cross-section of the bottom flange showing the minimum thickness for three layers of strands

9.2.6 Web Thickness Optimization

The minimum web thickness is influenced by two factors: the shear capacity and the number of kinked strands. Since it is not expected that the shear resistance will become governing, the

minimum web thickness will be based on the number of layers of kinked strands, concrete cover and minimum strand spacing:

$$d_{w,min} = \phi \left(1 + 3(n_{layers} - 1) \right) + 2c = 15,7(1 + 3(1 - 1)) + 2 * 35 \approx 85mm$$

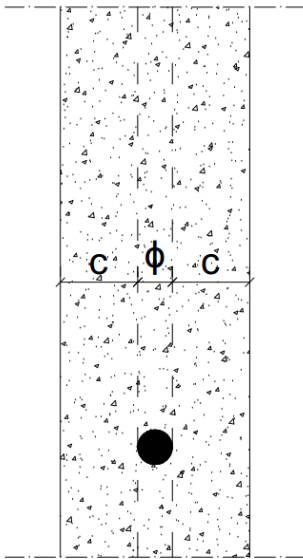


Figure 9-4: Cross-section of the web showing the minimum thickness

During calculations on the transverse moment due to local effects it was found that the web could not resist the transverse moment with the thickness of 85mm in case the beam width was 2500mm. The transverse moment capacity of the web could have been increased by increasing the thickness of the web and applying transverse reinforcement, which results in another minimum thickness.

$$d_{w,min} = 5\phi_p + 2\phi_s + 2c = 5 * 15,7 + 2 * 10 + 2 * 30 \approx 160mm$$

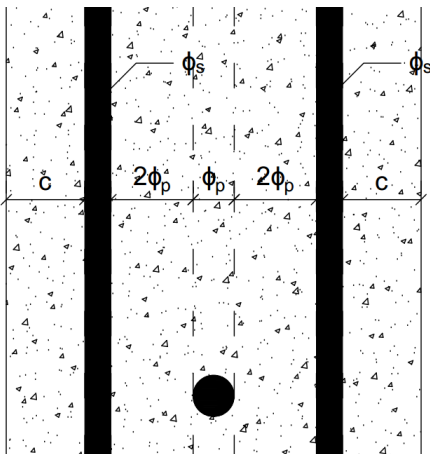


Figure 9-5: Cross-section of a web showing the minimum thickness needed, when stirrups are applied

However it was chosen to decrease the beam width to increase the transverse moment capacity of the web to prevent that the thicker webs will also attract additional moments due to the increased stiffness of the webs.

9.3 Cross Section Properties of a 60m UHPC Beam

Height	h		1300	mm
Width	b		1500	mm
Top flange thickness	d_{top}		170	mm
Bottom flange thickness	d_{bot}		225	mm
Web thickness	d_w		90	mm
Cross-section area	A_c		$0,755 \times 10^6$	mm^2
Top fiber distance to neutral axis	z_t		693	mm
Bottom fiber distance to neutral axis	z_b		607	mm
Moment of inertia	I_c		$1,908 \times 10^{11}$	mm^4
Section modulus top fiber	W_t		$2,75 \times 10^8$	mm^3
Section modulus bottom fiber	W_b		$3,15 \times 10^8$	mm^3
Amount of prestressing steel	A_p		156000	mm^2
Drape of prestressing strands	f_p		493	mm
Mass	G		115,5	t

Table 9-1: Cross-section properties of a 60m UHPC box beam

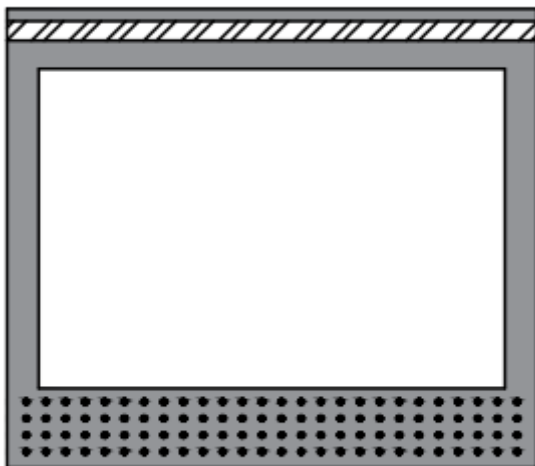


Figure 9-6: Cross-section of a 60m box beam showing the duct for transverse post-tensioning and pre-tensioned strands

9.4 Loads

To determine the internal forces of the bridge is modelled in SCIA Engineer as an orthotropic plate with a length of 60m and a width of 15m. The plate is simply supported by modelling line supports at the ends of the plate. Since the design of the beams is an iterative process, the self-weight of the beams is not modelled and will be added later on. The same holds for the prestressing. All other loads, which are already known, can be modelled in SCIA. The following loads will act on the bridge.

- Permanent Loads
 - Self-weight (beam)
 - Super-imposed dead load (asphalt, curb, safety barrier etc.)
 - Prestressing load
- Variable Loads
 - Traffic loads (Load Model 1 conform NEN-EN 1991-2)

The orthotropic parameters are determined using the method as described below.

Determine the longitudinal bending stiffness of the deck:

$$I_{y,deck} = \frac{n_{girders} * I_{y,girder}}{b_{deck}}$$

$$D_{11} = E * I_{y,deck}$$

Determine the transverse bending stiffness of the deck by applying a unit load M_0 at each end of the top flange of a beam and determining the bending moment M_1 at the middle of the top flange by means of a FEM-model.

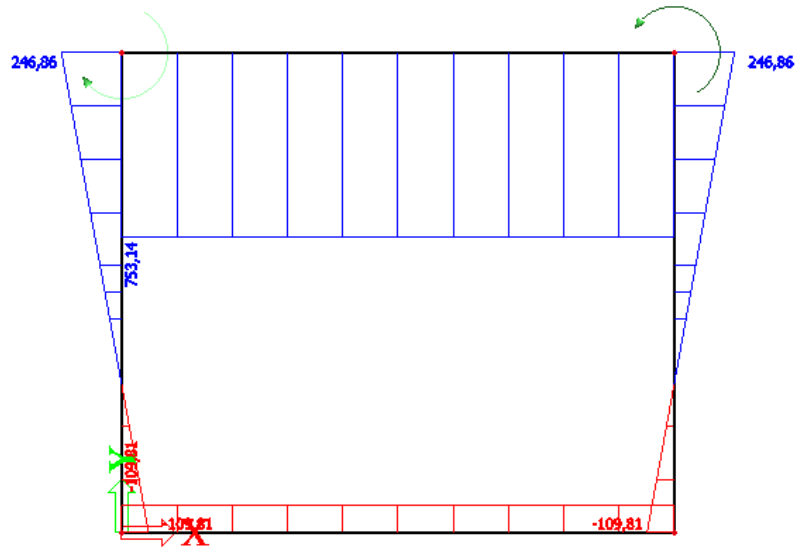


Figure 9-7: Transverse moment distribution under a unit load of 1000kNm used to determine transverse bending stiffness

$$I_{x,deck} = \frac{M_0 * b_{girder}}{M_0 * d_w + M_1 * b_0} * K$$

$$M_0 = 1000 \text{ kNm}$$

$$M_1 = 753,14 \text{ kNm}$$

$$K = \frac{1}{12} * d_{top}^3$$

$$b_0 = b_{girder} - d_w$$

$$D_{22} = E * I_{x,deck}$$

With the longitudinal and transverse bending stiffness D_{12} can be found:

$$\nu_{12} = 0,2$$

$$\nu_{21} = \frac{I_{x,deck}}{I_{y,deck}} \nu_{12}$$

$$D_{12} = \nu_{12} * D_{22} = D_{21} = \nu_{21} * D_{11}$$

Determine the longitudinal torsion stiffness of the deck:

$$I_{y,torsion,girder} = \frac{4A_0^2}{\frac{2h_0}{d_w} + \frac{b_0}{d_{top}} + \frac{b_0}{d_{bot}}} + \frac{2 * h_0 * d_w^3 + b_0 * d_{top}^3 + b_0 * d_{bot}^3}{3}$$

$$A_0 = h_0 * b_0$$

$$I_{y,torsion,deck} = \frac{n_{girders} * I_{y,torsion,girder}}{b_{deck}}$$

Determine the transverse torsion stiffness of the deck:

$$I_{x,torsion,girder} = \frac{1}{6}(d_{top}^3 + d_{bot}^3)$$

$$I_{x,torsion,joint} = \frac{1}{6}h_{joint}^3$$

$$I_{x,torsion,deck} = \frac{\frac{1}{2} * d_w * I_{x,torsion,joint} + \frac{1}{2} * b_0 * I_{x,torsion,girder}}{\frac{1}{2} * b_{girder}}$$

With the torsional stiffness in longitudinal and transverse direction D_{33} can be found:

$$\frac{E(I_{y,torsion,deck} + I_{x,torsion,deck})}{4(1 + \nu_{12})(1 + \nu_{21})}$$

Determine the shear stiffness with:

$$D_{44} = \frac{E}{2(1 + \nu_{12})} * h_{girder}$$

$$D_{55} = \frac{E}{2(1 + \nu_{12})} * h_{joint}$$

Ultimately the following orthotropic parameters are applied in SCIA Engineer:

D11	6,37E+06
D22	2,67E+04
D12	5,33E+03
D33	3,91E+06
D44	2,71E+07
D55	6,25E+06

Table 9-2: Orthotropic parameters for a 60m long box beam bridge

9.4.1 Self-weight

For the self-weight of the beam the distributed load can be found with the cross-section area:

$$q_{G,k} = A_c * 25 \frac{kN}{m^3}$$

The moment caused by the self-weight of the beam is calculated with:

$$M_{G,k} = \frac{q_{G,k}L^2}{8}$$

9.4.2 Super-Imposed Dead Loads

The super-imposed dead loads are permanent loads, which are not caused by the self-weight of the beam. They are caused by a 150mm thick asphalt layer covering the bridge deck and loads on the edge caused by the safety barrier, inspection path and curb. A width of 1,5m is assumed for the safety barrier, railing, inspection path and curb.

The load from the asphalt layer is calculated with:

$$0,150m * 24 \frac{kN}{m^3} = 3,6 \frac{kN}{m^2}$$

The curb is assumed to give the same loading as the asphalt. Therefore the load for both asphalt and curb is modelled as a surface load in SCIA. The results in SCIA show a $m_{dl,k}$ of 1620 kNm/m.

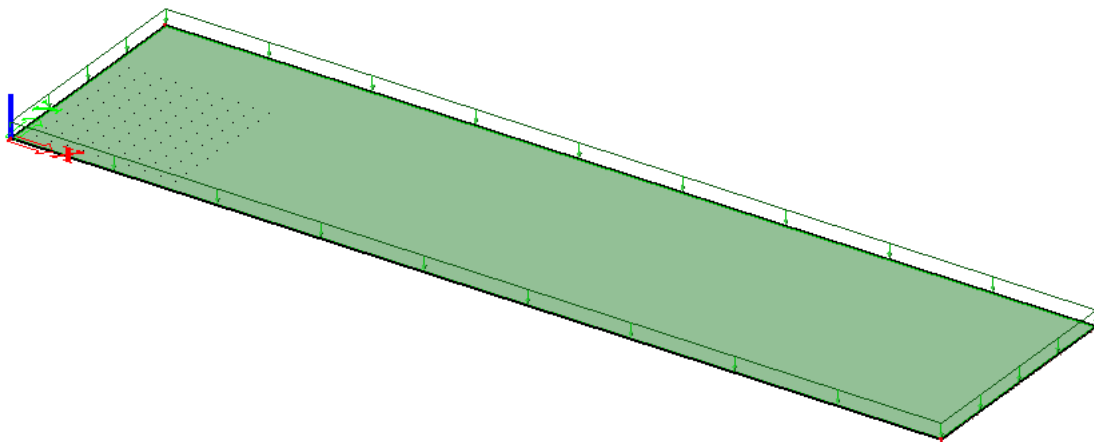


Figure 9-8: Positioning of the uniformly distributed super-imposed dead load (both asphalt and curb)

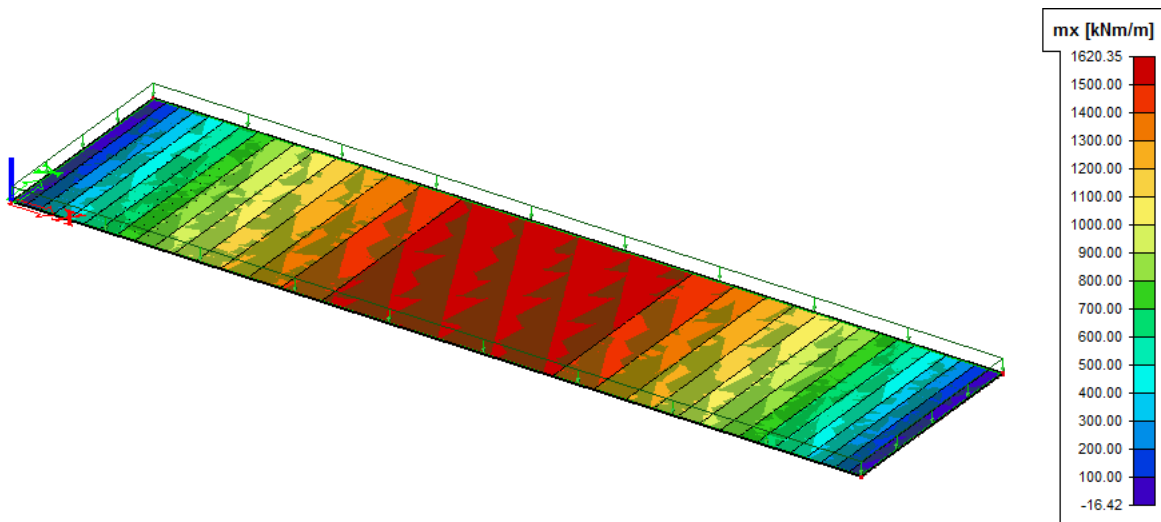


Figure 9-9: Moment distribution in longitudinal direction caused by the super-imposed dead load (asphalt and curb)

The safety barriers, railing and edging elements at the edge of the bridge are modelled as line loads of 3,65 kN/m.

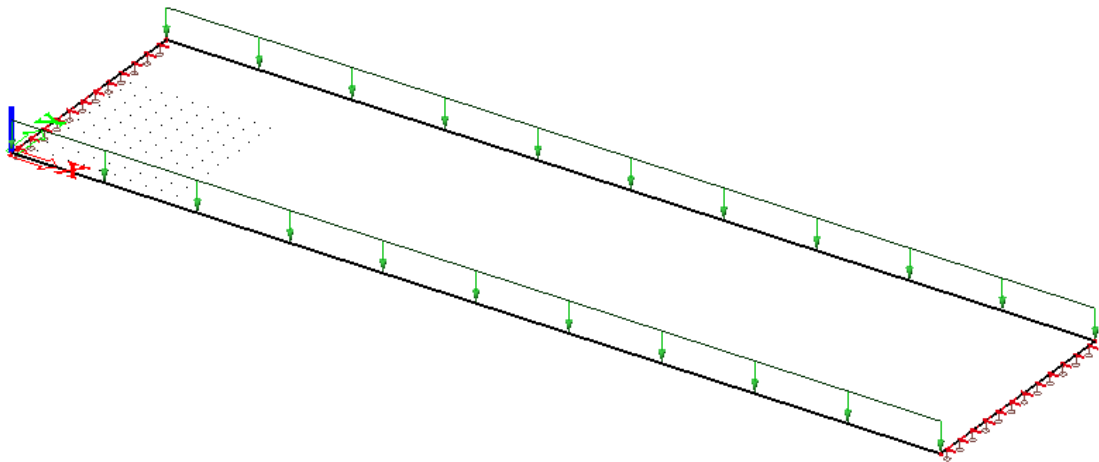


Figure 9-10: Positioning of the line loads representing the safety barriers, railing and edging elements

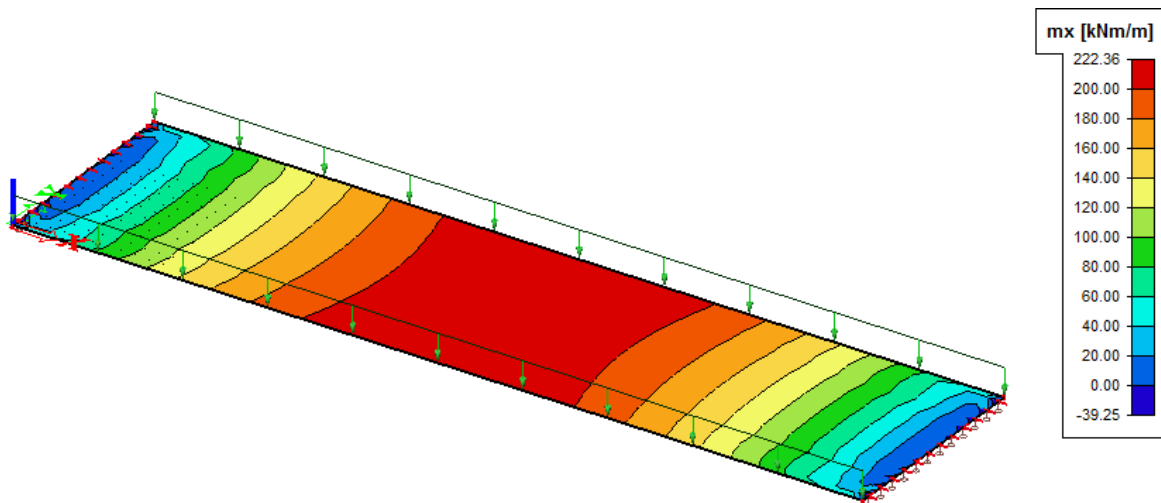


Figure 9-11: Moment distribution in longitudinal direction caused by the super-imposed dead load (edging elements etc.)

Total moment due to the super-imposed dead loads is the sum of the values of m_x . Since the width of the beam is 1,25m, this value has to be multiplied by 1,25 to find the moment in the beam. Equivalent distributed loads are determined with the following formula:

$$q_{i,k} = \frac{8 * M_{i,k}}{L^2}$$

The equivalent distributed load for the super-imposed dead load $q_{dl,k}$ is 4,10 kN/m.

9.4.3 Prestressing loads

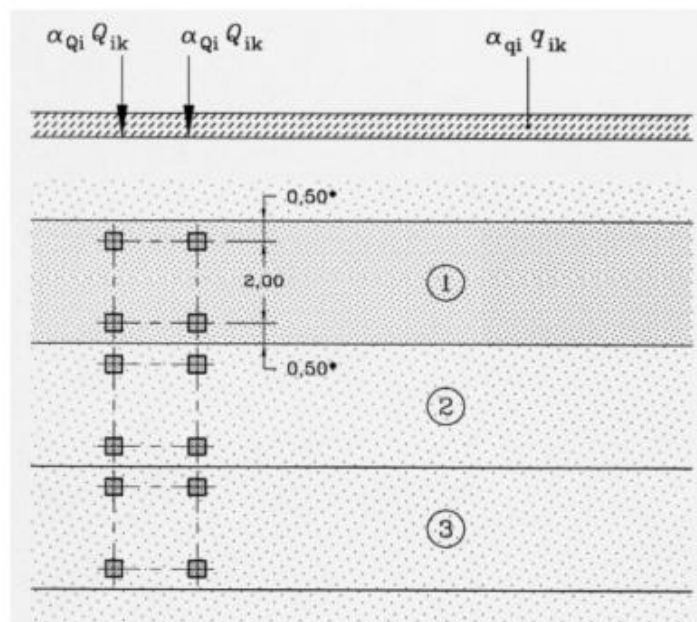
Prestressing loads are determined in §9.5

9.4.4 Traffic loads

Load model 1 conform Eurocode contains a combination of three tandem systems (TS) uniformly distributed loads (UDL). Values and positioning of these loads are stated below.

Positie	Tandemstelsel TS	Gelijkmatig verdeelde belasting (GVB)
	Aslast Q_{ik} (kN)	q_{ik} (of q_{rk}) (kN/m ²)
Rijstrook nummer 1	300	9
Rijstrook nummer 2	200	2,5
Rijstrook nummer 3	100	2,5
Overige rijstroken	0	2,5
Resterende oppervlakte (q_{rk})	0	2,5

Figure 9-12: Table indicating values of the TS and UDL taken from the NEN 1991-2



Verklaring

- (1) rijstrook nummer 1 : $Q_{1k} = 300 \text{ kN}$; $q_{1k} = 9 \text{ kN/m}^2$
 - (2) rijstrook nummer 2 : $Q_{2k} = 200 \text{ kN}$; $q_{2k} = 2,5 \text{ kN/m}^2$
 - (3) rijstrook nummer 3 : $Q_{3k} = 100 \text{ kN}$; $q_{3k} = 2,5 \text{ kN/m}^2$; tussenafstand assen in tandemstelsel = 1,2 m
- * Voor $w_l = 3,00 \text{ m}$

Figure 9-13: Table indicating the placement of loads on the notional lanes taken from the NEN 1991-2

The positioning of the notional lanes takes 1,5m of width at each side into account for the safety barrier, inspection path and curb.

Note that the loads are multiplied by an α -factor. Factor α_{q1} is taken as 1,15 as stated in the Dutch national annex. This factor leads to a uniformly distributed load of 10,35 kN/m². Factors α_{qi} with $i > 1$ are taken as 1,40, which leads to a uniformly distributed load of 3,5 kN/m²

In order to find the maximum moment in a beam, which is needed to determine the required prestress, the heaviest lane (10,35 kN/m²) is positioned at the edge (the beam at the edge is governing due to transverse action) and the heaviest tandem system is placed at midspan (the governing cross-section for bending moment is at midspan). The results in SCIA show a maximum moment for traffic loads of $m_{Q,k} = 3143$ kNm/m. The moment in the beam has to be multiplied with the width of the beam. The equivalent distributed load for traffic loads $q_{Q,k}$ is 8,73 kN/m.

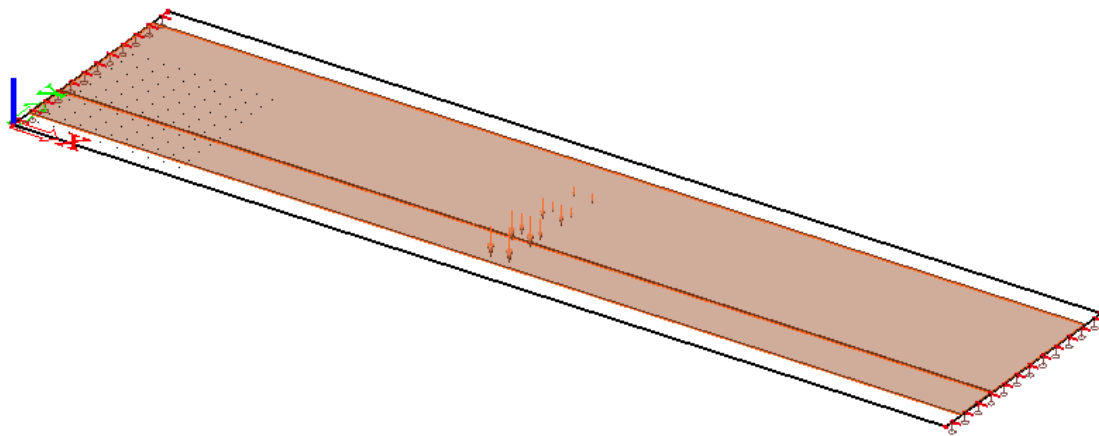


Figure 9-14: Positioning of the tandem systems and UDL's to find the governing moment

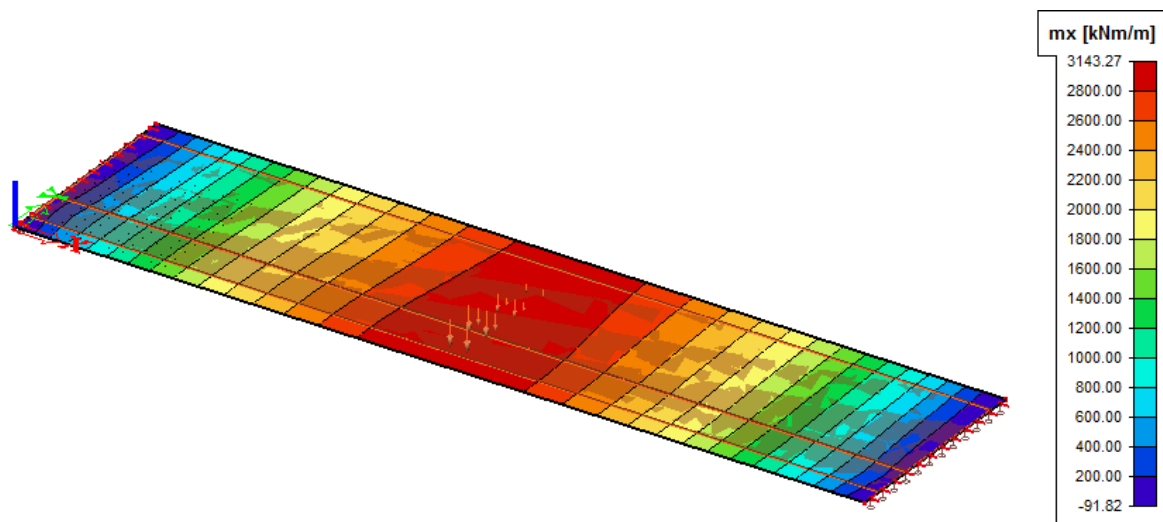


Figure 9-15: Moment distribution in longitudinal direction caused by LM1

The first requirement gives a lower bound for the prestressing force $P_{m\infty}$. The others give upper bounds for the prestressing force P_{m0} . The required P_{m0} can be found by estimating the prestressing losses at 20%. P_{m0} can then be calculated with the required $P_{m\infty}$ with the following formula.

$$P_0 = \frac{P_{\infty}}{0,8}$$

With the required initial prestressing force the required amount of prestressing strands can be found.

$$A_{p,tot} = \frac{P_0}{\sigma_{p0}}$$

$$\text{required number of strands} = \frac{A_{p,tot}}{A_{p,strand}}$$

When a number of strands is chosen this should be calculated back to a prestressing force P_0 and be checked for the upper bound that was found earlier.

$$A_p = \text{number of strands} * A_{p,strand}$$

$$P_0 = A_p * \sigma_{p0}$$

9.5.1 Prestressing losses

Then the losses should be checked to see whether the estimation of the losses is safe. Elastic losses are calculated with the following formula:

$$\Delta\sigma_{el} = A_p * E_p * \frac{n-1}{2 * n} * \frac{\Delta\sigma_c}{E_{cm}}$$

$$\Delta\sigma_c = \frac{P_{m0}}{A_c} + \frac{P_{m0} * f_p^2}{I_c}$$

$$\sigma_{p,max} = \sigma_{p0} + \Delta\sigma_{el} \leq 1488 \frac{N}{mm^2}$$

The extra stress to compensate for the elastic loss does not exceed the maximum allowed stress in the prestressing steel. In case it does exceed the maximum allowed stress of 1488MPa, a lower prestress σ_{p0} should be assumed to determine the prestress.

Time-dependent losses are calculated with a single formula provided by the Eurocode.

$$\Delta P_{c+s+r} = A_p \Delta\sigma_{p,c+s+r} = A_p \frac{\varepsilon_{cs} E_p + 0,8 \Delta\sigma_{pr} + \frac{E_p}{E_{cm}} \varphi(t, t_0) \cdot \sigma_{c,QP}}{1 + \frac{E_p}{E_{cm}} \frac{A_p}{A_c} \left(1 + \frac{A_c}{I_c} z_{cp}^2\right) [1 + 0,8 \varphi(t, t_0)]}$$

The losses are calculated and compared to the estimated losses. These are below the estimated losses, so the estimation is safe.

9.5.2 Fitting of the strands

A total of 92 prestressing strands with diameter of 15,7mm are applied. When applying the minimum spacing of the Eurocode, the strands can only fit, if they are placed in four layers. As a consequence

the bottom flange thickness increases. The minimum thickness of the bottom flange is calculated with:

$$d_{bot,min} = 2 * c + \phi(3 * (\text{number of layers} - 1) + 1)$$

With a concrete cover of 30mm and a strand diameter of 15,7mm the minimum thickness of the bottom flange becomes:

$$d_{bot,min} = 2 * 35 + 15,7(3 * (4 - 1) + 1) \approx 225mm$$

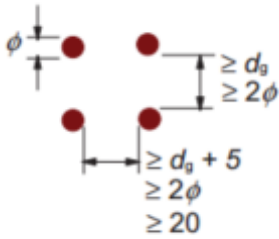


Figure 9-18: Minimum spacing of pre-tensioned strands according to the Eurocode

9.6 Moment Capacity

The moment resistance is determined using the stress-strain diagram for compression to determine the compressive internal forces and the stress-strain diagram for tension to determine the tensile internal forces.

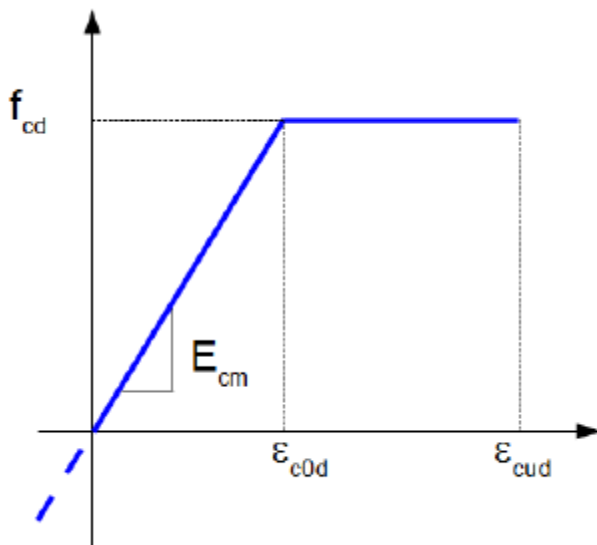


Figure 9-19: Compressive Stress-Strain Diagram for UHPC Design [3]

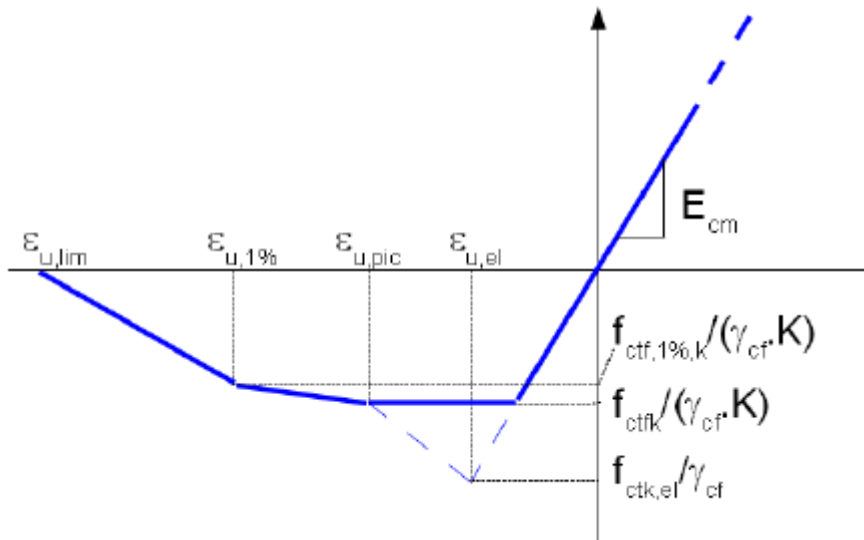


Figure 9-20: Tensile Stress-Strain Diagram for UHPC Design of thick elements [3]

As a first guess the height of the compressive zone x_u can be approximated by assuming a rectangular cross-section.

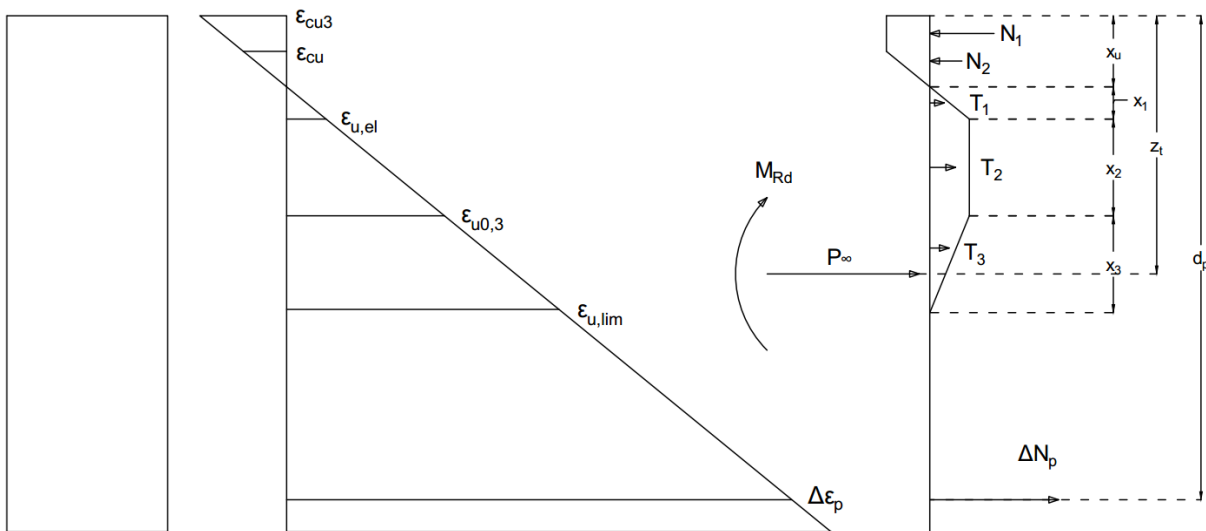


Figure 9-21: Schematization of internal forces used to determine bending moment capacity of rectangular cross-sections

The x_u can be found using horizontal equilibrium of the internal forces and expressing these internal forces in x_u .

$$P_{\infty} + \Delta N_p = N_1 + N_2 + T_1 + T_2 + T_3$$

$$P_{\infty} = A_p * \sigma_{p\infty}$$

$$\Delta N_p = A_p (f_{pd} - \sigma_{p\infty})$$

$$N_1 = \left(1 - \frac{\varepsilon_{c3}}{\varepsilon_{cu3}}\right) * x_u * f_{cd} * b$$

$$N_2 = \frac{\varepsilon_{c3}}{\varepsilon_{cu3}} * x_u * f_{cd} * \frac{1}{2} * b$$

$$T_1 = x_1 * f_{ctd} * \frac{1}{2} * b$$

$$T_2 = x_2 * f_{ctd} * b$$

$$T_3 = x_3 * f_{ctd} * \frac{1}{2} * b$$

$$x_1 = \frac{\varepsilon_{u,el}}{\varepsilon_{cud}} * x_u$$

$$x_2 = \frac{\varepsilon_{u0,3} - \varepsilon_{u,el}}{\varepsilon_{cud}} * x_u$$

$$x_3 = \frac{\varepsilon_{u,lim} - \varepsilon_{u0,3}}{\varepsilon_{cud}} * x_u$$

The approximated x_u and the height of the tensile zone where fibers are activated turns out to be larger than the top flange so the assumption of a rectangular cross-section is an underestimation of the x_u . The void of the box beam that is partly included in the x_u has to be taken into account. So as a second guess x_u is assumed to be larger than the top flange and the top flange is assumed to end somewhere in the compressive elastic zone.

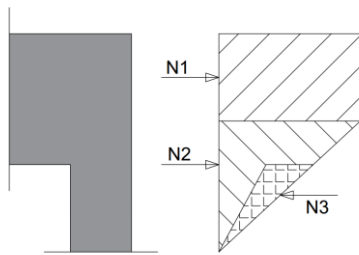


Figure 9-22: Method to take into account the void, when determining the contribution of the compression zone

The x_u is now assumed at a certain value and the internal forces that follow from this value should make horizontal equilibrium. However the equations should be modified to take into account the void of the box and an extra internal force N_3 is introduced. This force compensates for the void in the compressive zone.

$$P_\infty + \Delta N_p = N_1 + N_2 - N_3 + T_1 + T_2 + T_3$$

$$P_\infty = A_p * \sigma_{p\infty}$$

$$\Delta N_p = A_p (f_{pd} - \sigma_{p\infty})$$

$$N_s = 0$$

$$N_1 = \left(1 - \frac{\varepsilon_{c3}}{\varepsilon_{cu3}}\right) * x_u * f_{cd} * b$$

$$N_2 = \frac{\varepsilon_{c3}}{\varepsilon_{cu3}} * x_u * f_{cd} * \frac{1}{2} * 2 * d_w$$

$$N_3 = \frac{1}{2} * f_{cd} * (b - 2d_w) * (x_u - d_{top})$$

$$T_1 = x_1 * f_{ctd} * \frac{1}{2} * 2 * d_w$$

$$T_2 = x_2 * f_{ctd} * 2 * d_w$$

$$T_3 = x_3 * f_{ctd} * \frac{1}{2} * 2 * d_w$$

$$x_1 = \frac{\varepsilon_{u,el}}{\varepsilon_{cud}} * x_u$$

$$x_2 = \frac{\varepsilon_{u0,3} - \varepsilon_{u,el}}{\varepsilon_{cud}} * x_u$$

$$x_3 = \frac{\varepsilon_{u,lim} - \varepsilon_{u0,3}}{\varepsilon_{cud}} * x_u$$

By means of a spreadsheet different values of x_u can be evaluated, until horizontal equilibrium is found. Then the assumption made earlier should be checked (top flange ends in the compressive elastic zone).

$$x_u - d_{top} \leq \frac{\varepsilon_{c3}}{\varepsilon_{cu3}} * x_u$$

The found x_u is used to calculate the correct internal forces, which are used to find the moment resistance by means of moment equilibrium.

$$M_{Rd} = N_1 \left(x_u - \frac{x_{u1}}{2} \right) + N_2 \left(\frac{2}{3} x_{u2} \right) - N_3 \left(\frac{2}{3} (x_{u2} - d_{top}) \right) + T_1 \left(\frac{2}{3} x_1 \right) + T_2 \left(x_1 + \frac{x_2}{2} \right) + T_3 \left(x_1 + x_2 + \frac{x_3}{3} \right) + \Delta N_p (d_p - x_u) + P_\infty (z_t - x_u) = 14365 \text{ kNm}$$

The M_{Ed} is determined with the following formula:

$$M_{Ed} = M_{G,d} + M_{dl,d} + M_{Q,d} - P_\infty * f_p = 9029 \text{ kNm}$$

Then the unity check for moment capacity can be carried out:

$$\frac{M_{Ed}}{M_{Rd}} = \frac{10848 \text{ kNm}}{16517 \text{ kNm}} = 0,66 \leq 1$$

9.7 Shear and Torsion Capacity

The total shear resistance is found by adding the contributions of the concrete, fibers and steel:

$$V_{Rd} = V_{Rd,c} + V_{Rd,f} + V_{Rd,s} \leq V_{Rd,max}$$

Concrete contribution of a prestressed section to shear resistance:

$$V_{Rd,c} = \frac{0,24}{\gamma_{cf} * \gamma_E} * k * f_{ck}^{\frac{1}{2}} * b_w * z$$

$$\gamma_{cf} * \gamma_E = 1,5$$

$$k = \begin{cases} 1 + 3 * \frac{\sigma_{cp}}{f_{ck}} & \sigma_{cp} \geq 0 \text{ (compression)} \\ 1 + 0,7 * \frac{\sigma_{cp}}{f_{ctk,0.05}} & \sigma_{cp} < 0 \text{ (tension)} \end{cases}$$

$$\sigma_{cp} = \frac{P_\infty}{A_c}$$

Fiber contribution to shear resistance:

$$V_{Rd,f} = \frac{A_{fv} * \sigma_{Rd,f}}{\tan \theta}$$

$$A_{fv} = b_w * z$$

$$z = 0,9 * d$$

$$\sigma_{Rd,f} = \frac{1}{K * \gamma_{cf} * w_{lim}} \int_0^{w_{lim}} \sigma_f(w) dw$$

$$\theta = 30^\circ$$

Stirrups contribution to shear resistance:

$$V_{Rd,s} = \frac{A_{sw}}{s} * z * f_{ywd} * \cot \theta$$

The sum of all contributions equals:

$$V_{Rd} = V_{Rd,c} + V_{Rd,f} + V_{Rd,s} = 2414 \text{ kN}$$

The shear resistance is limited by the strength of the compressive struts:

$$V_{Rd,max} = \frac{2 * 1,14 * \frac{\alpha_{cc}}{\gamma_c} * b_w * z * f_{ck}^{\frac{2}{3}}}{(\cot \theta + \tan \theta)} = 1650 \text{ kN}$$

The shear force is calculated with:

$$V_{Ed} = \frac{L * (q_{G,d} + q_{dl,d}) - \frac{P_\infty * f_0}{L/3}}{2} + V_{Ed,Q} = 1601 \text{ kN}$$

Note that the negative term is caused by the upward force at the kinks of the prestressing strands.

The value of $V_{Ed,Q}$ is determined using the plate model in SCIA. The axle loads are placed at a small distance from the supports taking into account direct load ... to find the governing shear force. The distance from the supports is chosen as $2,5 * d$. The found value $q_{max,b}$ multiplied by the beam width gives the shear force contribution of LM1.

$$V_{Ed,Q} = q_{max,b} * B_{girder} = 509 * 1,250 = 636 \text{ kN}$$

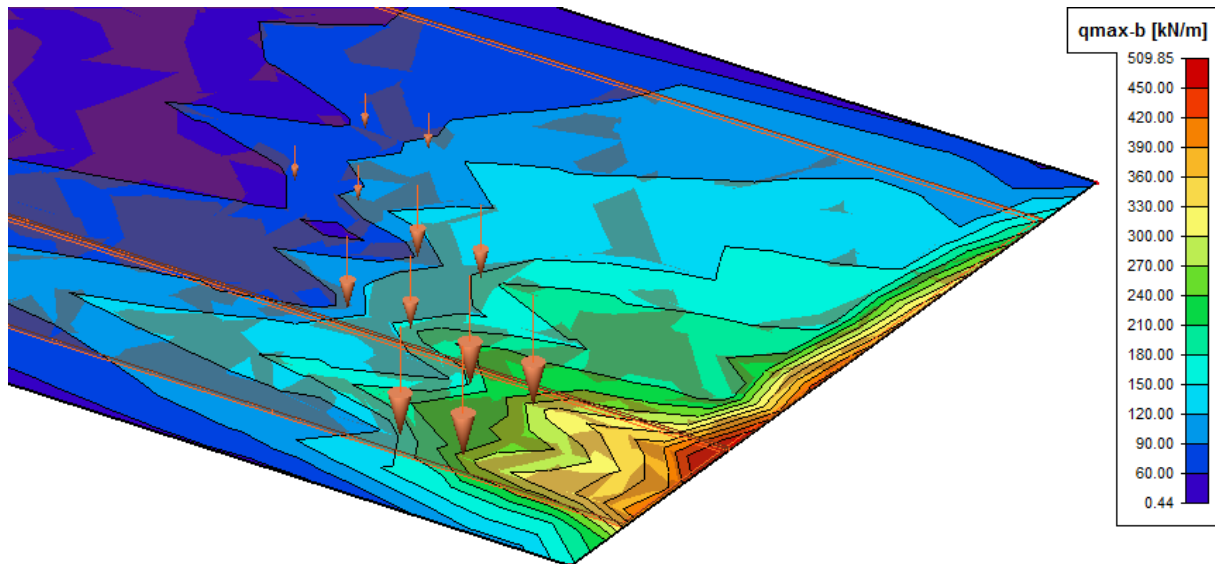


Figure 9-23: SCIA model determining the governing shear force contribution of LM1 with rigid line support

A more realistic value is found when an elastic support is modelled, since the bearings are not rigid, but have a certain stiffness. The stiffness of the support is chosen as such that the bearing will allow a vertical displacement of 1mm under the self-weight of the girder. Therefore the stiffness can be determined as follows:

$$K = \frac{0,5 * G}{w * B} = \frac{0,5 * 115500kg * 9,81 \frac{N}{kg}}{0,001m * 1,5m} = 377,7 \frac{MN}{m^2}$$

The elastic support leads to a more uniformly distributed shear distribution and a lower peak value.

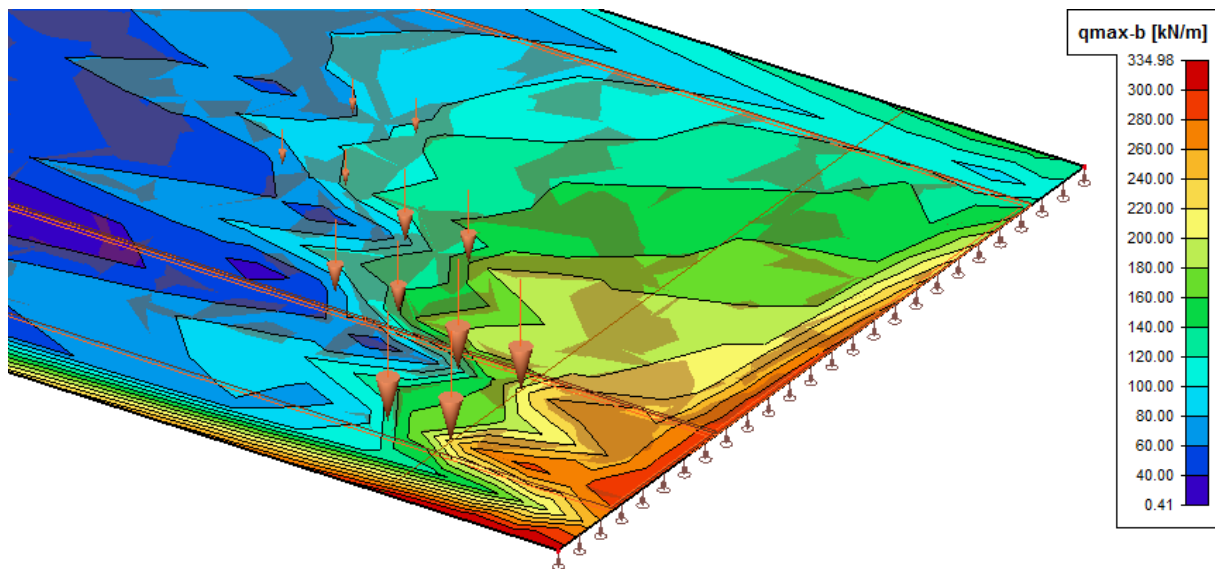


Figure 9-24: SCIA model determining the governing shear force contribution of LM1 with elastic line support

Since the rigid support gives an overestimation of the shear force. The shear force with elastic supports is used for the design.

$$V_{Ed,Q} = q_{max,b} * B_{girder} = 335 * 1,5 = 503kN$$

The torsion resistance can be found with the following formula:

$$T_{Rd,max} = 2 * 1,14 * \frac{\alpha_{cc}}{\gamma_c} * f_{ck} * 2 * A_k * t_{ef,i} * \sin \theta * \cos \theta$$

$$A_k = \left(h - \frac{d_{top} + d_{bot}}{2} \right) * (b - d_w)$$

$$t_{ef,i} = \frac{A_c}{u}$$

$$\theta = 30^\circ$$

The contribution of torsion is already included in the shear capacity.

Ultimately the resistance for combined shear and torsion can be checked with the unity check:

$$\frac{T_{Ed}}{T_{Rd,max}} + \frac{V_{Ed}}{V_{Rd}} = 0,97 \leq 1$$

In a later phase of the research the plate model for the determination of shear force was refined. A finer mesh was chosen and for the axle loads, at first modelled as nodal loads, were changed to surface loads. This showed a significantly changed force distribution, which is far more realistic.

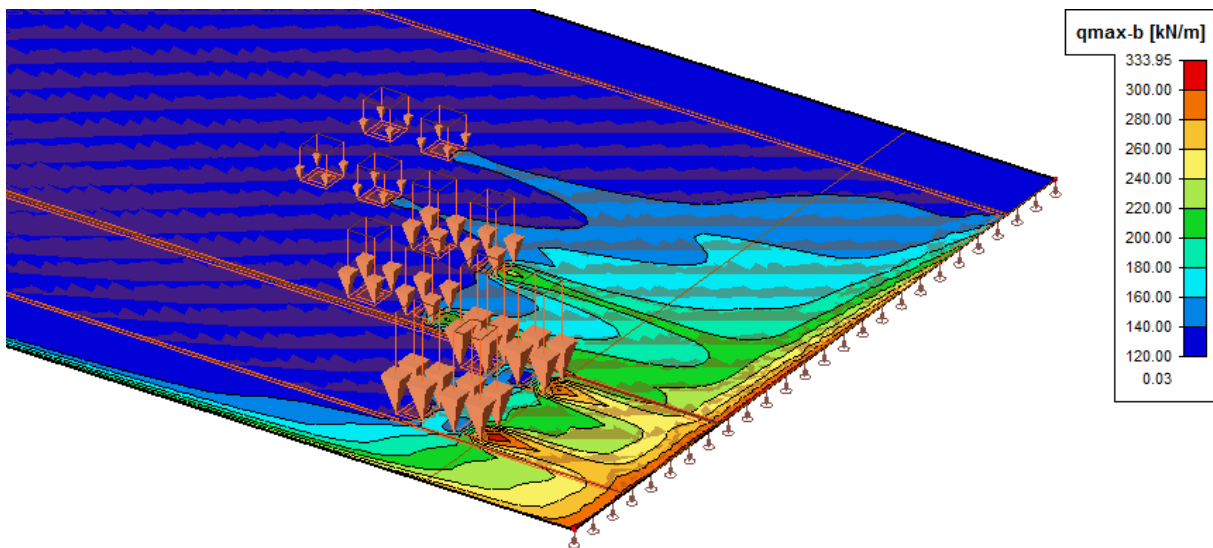


Figure 9-25: Refined SCIA plate model to determine shear force

In order to find an even more realistic value the average value of the shear force per beam should be taken instead of the peak value.

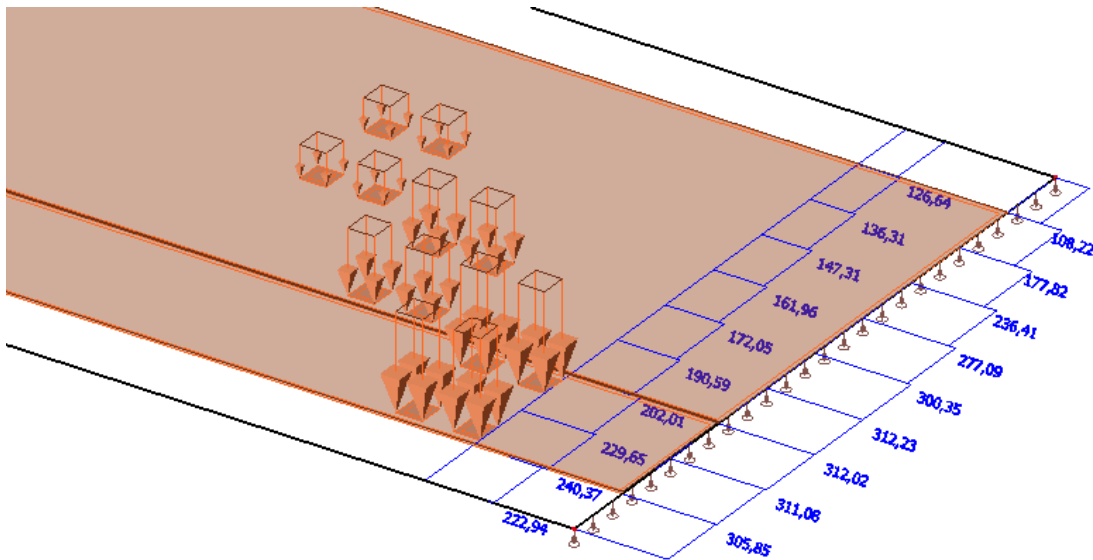


Figure 9-26: Refined SCIA plate model for determination of average shear force per beam

However for the design of the beams the coarse model with peak value is used to stay on the safe side of designing, since this value is conservative.

9.8 Moment Capacity Transverse Direction

In order to check the moment capacity in transverse direction both global and local effects have to be taken into account.

The global effect is found by taking $m_y + K_y * m_{xy}$ from the orthotropic plate model. The maximum value for $m_y = 9,09$ kNm/m is found at midspan at the edge of the slow lane. The contribution of torsion is determined by the torsional stiffness in transverse direction. The torsion m_{xy} given in SCIA has a very high value, but this is not the torsional moment in transverse direction. The given m_{xy} has to be multiplied by the torsional stiffness in transverse direction K_y . The K_y is found by the following formula:

$$K_y = \frac{2 * I_{y,torsion,girder}}{I_{y,torsion,girder} + I_{x,torsion,girder}} = 0,0000213$$

This is a very low stiffness, which means that torsion will be taken up mostly in longitudinal direction. The maximum m_{xy} is 347 kNm/m. When multiplying this with K_y a very small transverse torsion contribution is found. Ultimately the global effect can be taken as $M_{E,global} = 9,09 + 0,0000213 * 347 = 9,09$ kNm/m.

The local effect is found by placing tandem systems at the most unfavorable position for a single beam, which is a single wheel load of 150kN placed at the middle of a beam. Since this situation does not always coincide with the situation of the global effect, the local effect can be reduced. A reduction factor of 0,75 is assumed.

Both these effects are modelled in a 1D beam model. Note that the wheel load is distributed over the asphalt layer causing a spread of 45° over the height of the asphalt layer. The results show significant bending moments in both top flange and web, namely $M_{E,local,tf} = 36,64$ kNm and $M_{E,local,web} = 6,43$ kNm for local effects and $M_{E,global,tf} = 5,98$ kNm and $M_{E,global,web} = 1,96$ kNm for global effects.

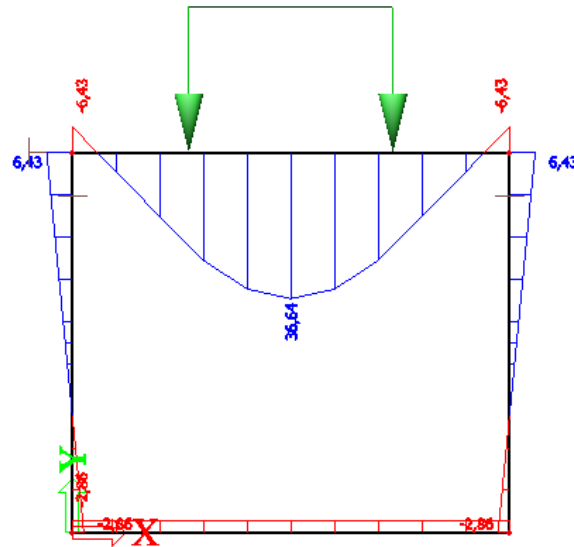


Figure 9-27: Moments in transverse direction caused by local effects

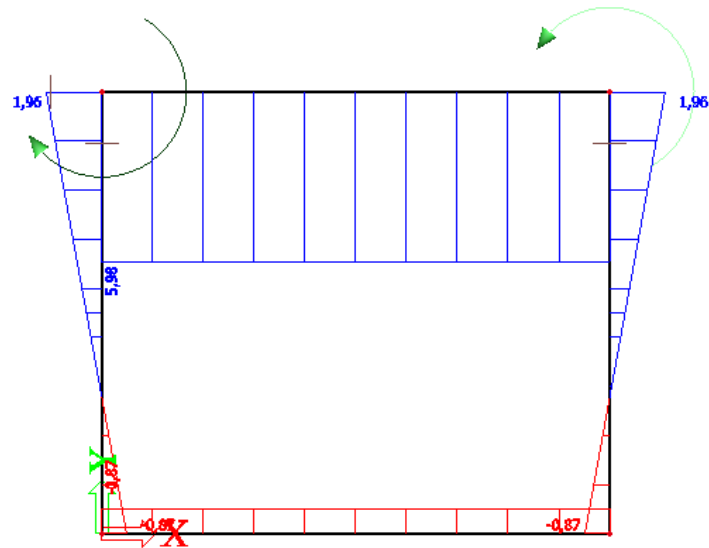


Figure 9-28: Moments in transverse direction caused by global effects

These values for the moments are in the SLS. To find the values in the ULS a load factor of 1,5 is applied. The ULS moments have to be checked for the top flange and web.

The total load on the top flange is given by $M_{Ed} = 1,5 * (0,75 * 36,64 \text{ kNm} + 5,98 \text{ kNm}) = 50,19 \text{ kNm}$. The moment capacity is determined by calculating the resistance of the cross-section shown below.

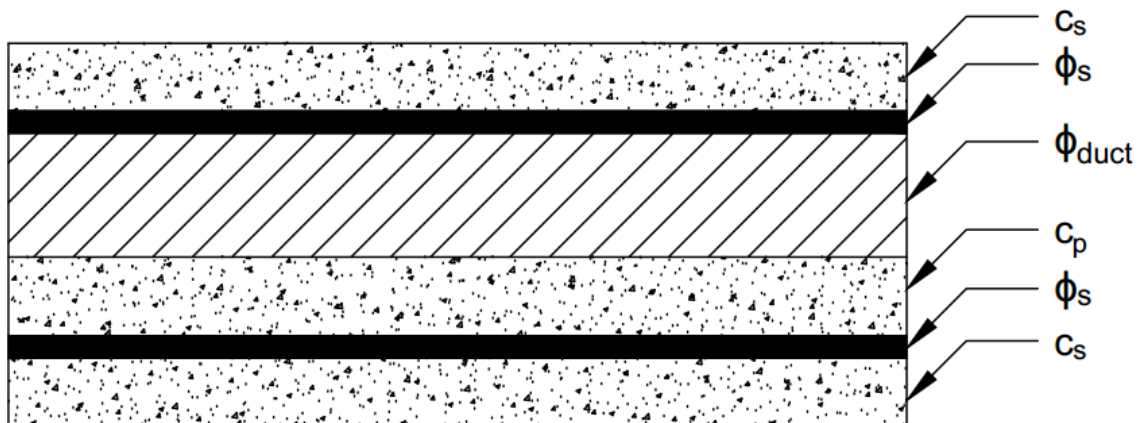


Figure 9-29: Cross-section of the top flange showing the positions of reinforcement bars and duct

A method similar to the one in §9.6 is used with the exception that the constitutive law for thin elements (stated in §2.4.3) is used to determine the stress-strain distribution. The c.t.c. spacing of the reinforcement bars and ducts is chosen to be 250mm. The reinforcement bars have a diameter of 10mm and the tendons consist of 3 strands with a cross-section area of 150mm² each and a $\sigma_{p\infty} = 1395\text{MPa}$. This configuration of reinforcement and prestressing results in a $M_{cr} = 114,5 \text{ kNm}$, a $M_{Rd} = 359,2 \text{ kNm}$. These values are well above M_{Ed} . When no reinforcement bars are applied there is still enough moment capacity, namely $M_{cr} = 114,5 \text{ kNm}$ and $M_{Rd} = 336,9 \text{ kNm}$. So the top flange can be even more slender.

The total load on the web is given by $M_{Ed} = 1,5 * (0,75 * 6,43 \text{ kNm} + 1,96 \text{ kNm}) = 10,17 \text{ kNm}$. The moment capacity is determined by calculating the resistance of the cross-section shown below.

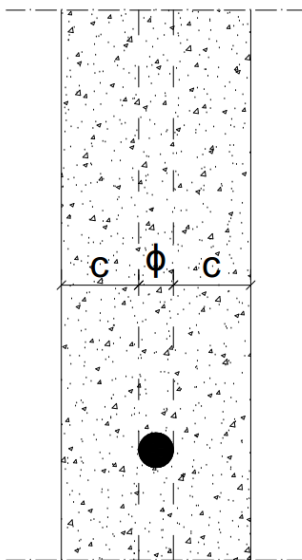


Figure 9-30: Cross-section of the web showing the minimum thickness for a single prestressing strand

The M_{cr} of this cross section is 12,2 kNm. The M_{Ed} is 10,17 kNm, which means the web will not crack in the ULS and has sufficient transverse moment capacity.

9.9 Deflection

According to ROK 1.3 by “Rijkswaterstaat” the deflection of the structure under frequent traffic loads should be limited to $L/300$. This limit is to prevent excessive vibrations in the structure. There is also

a requirement for the permanent camber. This should be at least $L/1000$. A permanent camber is applied for a number of reasons:

- For aesthetics, because a straight alignment of the bridge would appear like it sags.
- To guarantee sufficient headroom under deflection due to traffic loads.
- To take into account deviations between theory and practice.

The permanent camber is determined by calculating the total deflection under permanent loads including the prestressing, while also taking into account the time-dependent effects, such as creep and prestressing losses.

So there are two cases to be checked, namely the maximum deflection under frequent traffic loads and the minimum permanent camber. The load combination to determine the deflection under frequent traffic loads is as follows:

$$q = \psi_2 q_{Q,TS,k} + \psi_2 q_{Q,UDL,k}$$

The ψ_2 is found in table NB.9 – A2.1 of the Dutch National Annex of NEN-EN 1990 and is for both the tandem system (TS) and uniformly distributed load (UDL) equal to 0,4.

The SCIA plate model is used to determine the deflection:

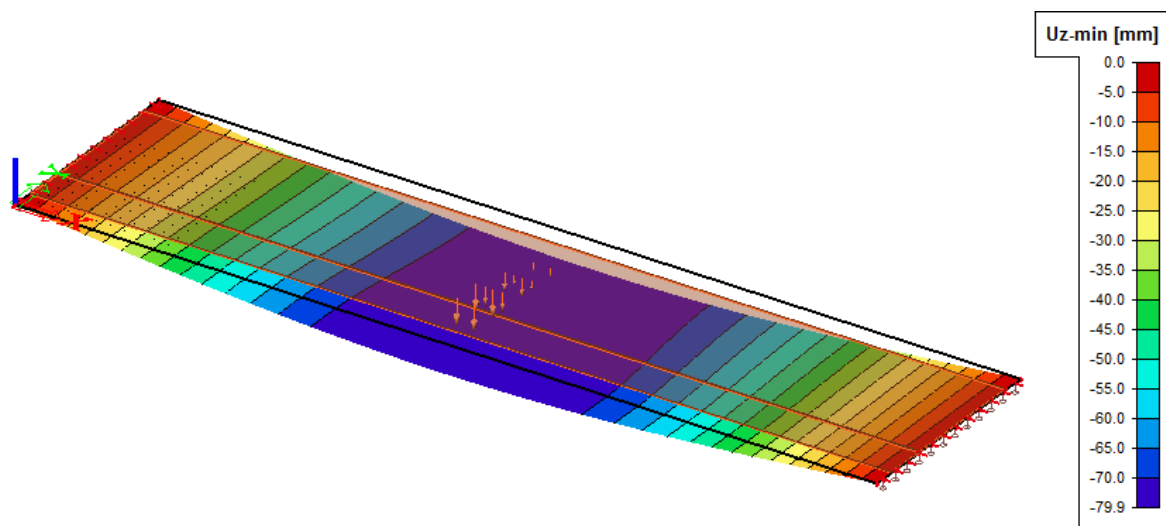


Figure 9-31: SCIA plate model showing results for the deflection under frequent traffic loads

The load combination to calculate the minimum camber is:

$$u_{camber} = u_p - u_G$$

The deflection under the prestressing load is calculated with the following formula:

$$u_p = \frac{1}{8} \frac{M_p L^2}{EI}$$

$$M_p = P_\infty * f_{p,average}$$

The deflection under self-weight is calculated with the following formula:

$$u_G = \frac{5}{384} \frac{q_G L^4}{EI}$$

Creep deformation is taken into account by using the effective Young's modulus:

$$E_{c,eff} = \frac{E_{cm}}{1 + \varphi(\infty, t_0)}$$

9.10 Crack Width

Crack width calculation is not necessary if the cracking moment (M_{cr}) is not reached in the SLS. The M_{cr} is found with the following formula:

$$M_{cr} = W_{cb} * f_{ctk,el} + W_{cb} * \frac{P_{\infty}}{A_c} = 11762 \text{ kNm}$$

The moment in the SLS is determined by:

$$M_{Ek} = M_{G,k} + M_{dl,k} + M_{Q,k} - M_p = 5401 \text{ kNm}$$

Since the beam is fully prestressed, it is expected that the cracking moment will not be reached. To check this a unity check can be executed.

$$\frac{M_{Ek}}{M_{cr}} = \frac{5401 \text{ kNm}}{11762 \text{ kNm}} = 0,46 \leq 1$$

9.11 Fatigue

In order to determine the fatigue resistance of the concrete and prestressing steel the fatigue load has to be determined. The fatigue load for LM 1 is found by multiplying the characteristic TS load with 0,7 and the characteristic UDL load with 0,3.

9.11.1 Concrete Fatigue in Compression Zone

The governing section for the fatigue resistance of the concrete is at the top of the beam at midspan. This section should be checked whether it can resist the number of loading cycles over its service life. For traffic category 1 NEN-EN 1991-2 states that $2,0 \cdot 10^6$ cycles per year act on the bridge. So for a service life of 100 years, the fatigue resistance should be at least $2,0 \cdot 10^8$ cycles.

The number of cycles that can be resisted by the concrete is determined by using the calculation method stated in NEN-EN 1992-2. This method uses the following formula:

$$N_j = 10^{\left(14 \frac{1 - E_{cd,max,i}}{\sqrt{1 - R_j}}\right)}$$

$$R_j = \frac{E_{cd,min,i}}{E_{cd,max,i}}$$

$$E_{cd,min,i} = \frac{\sigma_{cd,min,i}}{f_{cd, fat}}$$

$$E_{cd,max,i} = \frac{\sigma_{cd,max,i}}{f_{cd, fat}}$$

The fatigue strength of concrete is calculated with the formula stated in §2.4.8. The fatigue resistance turns out to be $7,26 \cdot 10^8$, which is considerably larger than the number of cycles over the service life of the structure.

9.11.2 Prestressing Steel Fatigue

According to NEN-EN 1992-1-1 it is allowed to assume sufficient fatigue resistance of prestressing strands in case the stress range $\Delta\sigma_s$ does not exceed 70MPa. The stress range of the steel can be calculated by converting the concrete stress at the height of the prestressing steel to a steel stress:

$$\Delta\sigma_s = \sigma_{s,max} - \sigma_{s,min} = \Delta\sigma_c \frac{E_p}{E_c}$$

The minimum concrete stress at the height of the prestressing steel is found with:

$$\sigma_{s,min} = -\frac{P_\infty}{A_c} - \frac{M_p * f_p}{I_c} + \frac{M_G * f_p}{I_c} + \frac{M_{dl} * f_p}{I_c}$$

The maximum concrete stress at the height of the prestressing steel is found with:

$$\sigma_{s,max} = -\frac{P_\infty}{A_c} - \frac{M_p * f_p}{I_c} + \frac{M_G * f_p}{I_c} + \frac{M_{dl} * f_p}{I_c} + \frac{M_{Q,fat} * f_p}{I_c}$$

The maximum stress range turns out to be 7,27MPa, which is far below the 70MPa limit, so it can be concluded that the structure has sufficient fatigue resistance.

9.11.3 Concrete Fatigue in Transverse Direction

Since there is no transverse reinforcement, the concrete has to resist all the tensile stresses in transverse direction and can therefore be subject to fatigue failure. [1] states that no irreversible damage will occur, if the tensile stresses remain below the elastic limit strength. So fatigue failure is prevented, in case the tensile stresses remain below $f_{ctk,el}$. In section 9.8 it is shown that no cracking occurs in transverse direction in the ULS. Since the fatigue loading is always lower than the loading in the ULS, fatigue failure is always prevented in case the beam can resist the transverse moments in the ULS.

9.12 Unity Check Summary

In the table below all the unity checks performed in the previous paragraphs are summarized. All unity checks are all equal to or less than 1, proving the soundness of the design.

Moment	0,66
Shear	0,97
Transverse moment top flange (cracking)	0,44
Transverse moment web (cracking)	0,84
Deflection (traffic)	0,34
Deflection (camber)	0,16
Cracking	0,46
Concrete fatigue	0,28
Steel fatigue	0,10

Table 9-4: Summary of performed unity checks for a 60m long box beam

10 UHPC Box Beam Bridge Design >60m

10.1 Purpose

In addition to the design of the 60m long box beam, box beams of 70m, 80m, 85m and 90m are made. These designs are made with the same method as stated in chapter 9. The purpose of this chapter was to investigate how UHPC box beams perform, when spans are pushed to the limits. Since it is expected that at some point the beams will reach the 170t weight limit, spans were increased until a span was found that could not be transported by road anymore. The findings and results of each design are discussed in the following paragraphs.

10.2 70m Box Beam Design

Height	h	1600	mm
Width	b	1500	mm
Top flange thickness	d_{top}	170	mm
Bottom flange thickness	d_{bot}	225	mm
Web thickness	d_w	85	mm
Cross-section area	A_c	$0,797 \times 10^6$	mm^2
Top fiber distance to neutral axis	z_t	855	mm
Bottom fiber distance to neutral axis	z_b	745	mm
Moment of inertia	I_c	$3,144 \times 10^{11}$	mm^4
Section modulus top fiber	W_t	$3,68 \times 10^8$	mm^3
Section modulus bottom fiber	W_b	$4,22 \times 10^8$	mm^3
Amount of prestressing steel	A_p	174000	mm^2
Drape of prestressing strands	f_p	631	mm
Mass	G	142,2	t

Table 10-1: Cross-section properties of a 70m long fully prestressed box beam

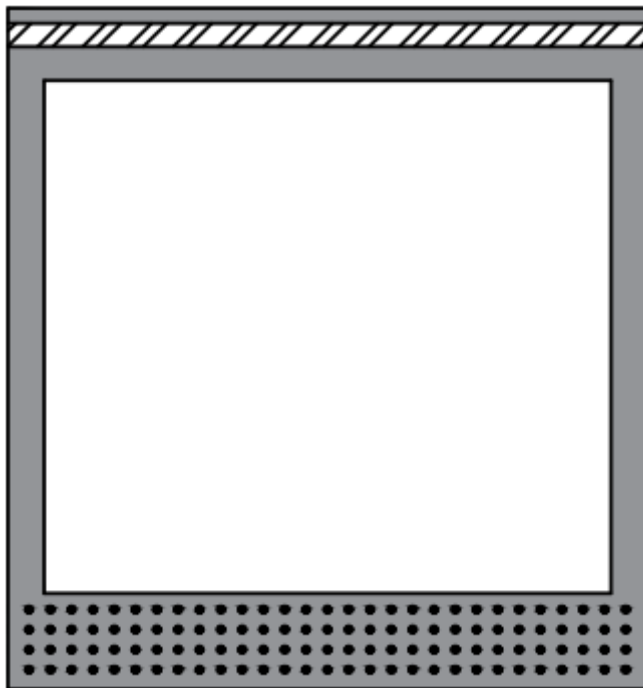


Figure 10-1: Cross-section of a 70m box beam showing the duct for transverse post-tensioning and pre-tensioned strands

Moment	0,58
Shear	0,95
Transverse moment top flange (cracking)	0,47
Transverse moment web (cracking)	0,74
Deflection (traffic)	0,31
Deflection (camber)	0,17
Cracking	0,43
Concrete fatigue	0,42
Steel fatigue	0,17

Table 10-2: Summary of performed unity checks for a 70m long box beam

The design of the 70m long box beam is quite similar to the 60m design. With a height of 1600mm the slenderness ratio is slightly decreased. The web thickness can be decreased slightly to optimize the shear capacity. The beam width, top and bottom flange thickness are the same. As a result the unity checks are quite similar for the most part.

10.3 80m Box Beam Design

Height	h	2000	mm
Width	b	1250	mm
Top flange thickness	d_{top}	170	mm
Bottom flange thickness	d_{bot}	225	mm
Web thickness	d_w	85	mm
Cross-section area	A_c	$0,77 \times 10^6$	mm^2
Top fiber distance to neutral axis	z_t	1062	mm
Bottom fiber distance to neutral axis	z_b	938	mm
Moment of inertia	I_c	$4,570 \times 10^{11}$	mm^4
Section modulus top fiber	W_t	$4,30 \times 10^8$	mm^3
Section modulus bottom fiber	W_b	$4,87 \times 10^8$	mm^3
Amount of prestressing steel	A_p	180000	mm^2
Drape of prestressing strands	f_p	824	mm
Mass	G	156,3	t

Table 10-3: Cross-section properties of an 80m long fully prestressed box beam

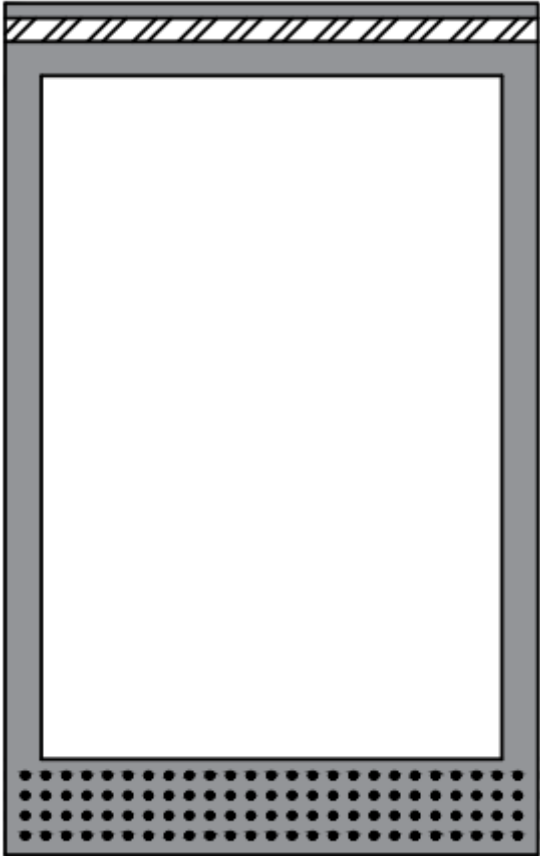


Figure 10-2: Cross-section of an 80m box beam showing the duct for transverse post-tensioning and pre-tensioned strands

Moment	0,64
Shear	0,74
Transverse moment top flange (cracking)	0,41
Transverse moment web (cracking)	0,46
Deflection (traffic)	0,23
Deflection (camber)	0,28
Cracking	0,50
Concrete fatigue	0,04
Steel fatigue	0,22

Table 10-4: Summary of performed unity checks for an 80m long box beam

As the span increases to 80m the slenderness ratio slightly decreases once again. The top flange thickness remains the same. The beam width is decreased to 1250mm to comply with the 170t weight limit. Therefore there is some overcapacity in shear.

10.4 85m Box Beam Design

Height	h	2200	mm
Width	b	1000	mm
Top flange thickness	d_{top}	170	mm
Bottom flange thickness	d_{bot}	270	mm
Web thickness	d_w	85	mm
Cross-section area	A_c	$0,74 \times 10^6$	mm^2
Top fiber distance to neutral axis	z_t	1199	mm
Bottom fiber distance to neutral axis	z_b	1001	mm
Moment of inertia	I_c	$4,99 \times 10^{11}$	mm^4
Section modulus top fiber	W_t	$4,17 \times 10^8$	mm^3
Section modulus bottom fiber	W_b	$4,99 \times 10^8$	mm^3
Amount of prestressing steel	A_p	225000	mm^2
Drape of prestressing strands	f_p	864	mm
Mass	G	160,1	t

Table 10-5: Cross-section properties of an 85m long fully prestressed box beam

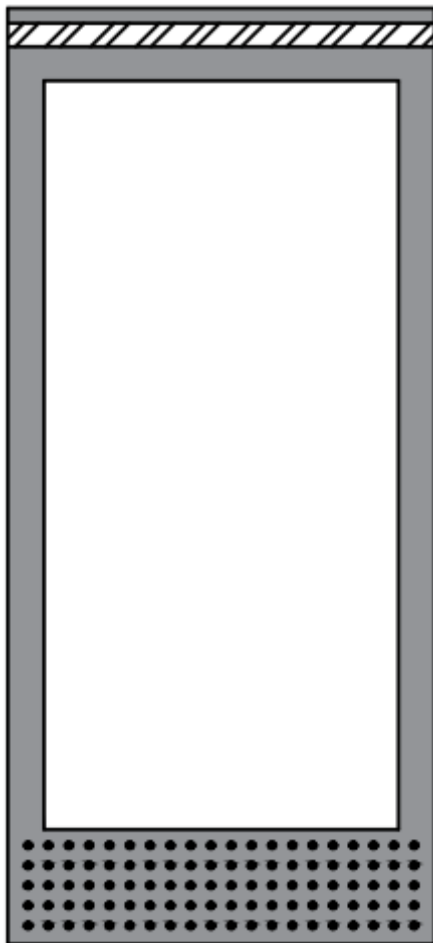


Figure 10-3: Cross-section of an 85m box beam showing the duct for transverse post-tensioning and pre-tensioned strands

Moment	0,57
Shear	0,61
Transverse moment top flange (cracking)	0,33
Transverse moment web (cracking)	0,30
Deflection (traffic)	0,22
Deflection (camber)	0,34
Cracking	0,45
Concrete fatigue	0,15
Steel fatigue	0,22

Table 10-6: Summary of performed unity checks for an 85m long box beam

Due to the increased loading an extra layer of prestressing strands is required. As a result the bottom flange thickness is increased. The width of the beam is decreased to 1000mm to comply with the weight limit. This resulted in a less optimized shear capacity, which is shown in the relatively low unity check of 0,61 for shear resistance compared to the 60m and 70m beams (both at least 0,95). It also resulted in a less optimized transverse moment capacity. Note that the beam widths are chosen to build up to a total deck width of exactly 15m, so the beam width can be given by $W=15/n$, with n is any integer.

10.5 90m Box Beam Design

Height	h	2450	mm
Width	b	1000	mm
Top flange thickness	d_{top}	170	mm
Bottom flange thickness	d_{bot}	270	mm
Web thickness	d_w	85	mm
Cross-section area	A_c	$0,78 \times 10^6$	mm^2
Top fiber distance to neutral axis	z_t	1332	mm
Bottom fiber distance to neutral axis	z_b	1118	mm
Moment of inertia	I_c	$6,51 \times 10^{11}$	mm^4
Section modulus top fiber	W_t	$4,89 \times 10^8$	mm^3
Section modulus bottom fiber	W_b	$5,82 \times 10^8$	mm^3
Amount of prestressing steel	A_p	225000	mm^2
Drape of prestressing strands	f_p	981	mm
Mass	G	179,3	t

Table 10-7: Cross-section properties of a 90m long fully prestressed box beam

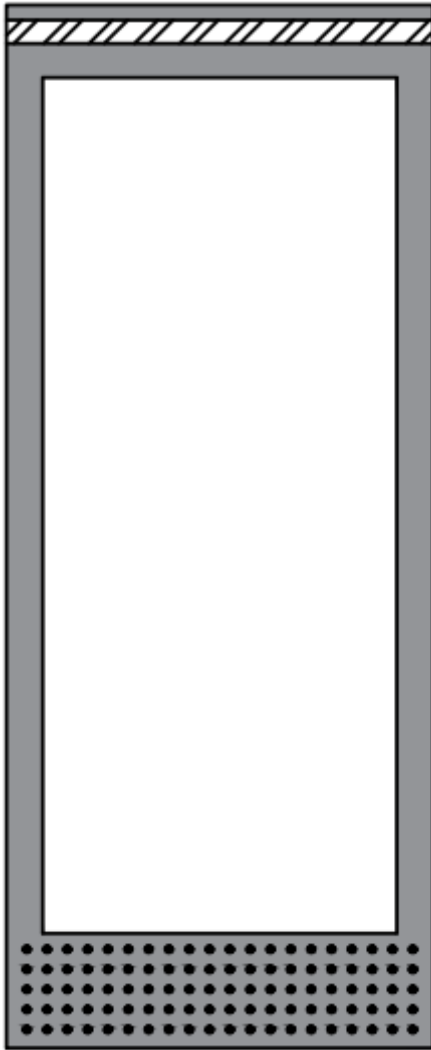


Figure 10-4: Cross-section of a 90m box beam showing the duct for transverse post-tensioning and pre-tensioned strands

Moment	0,60
Shear	0,59
Transverse moment top flange (cracking)	0,34
Transverse moment web (cracking)	0,27
Deflection (traffic)	0,21
Deflection (camber)	0,49
Cracking	0,48
Concrete fatigue	0,03
Steel fatigue	0,27

Table 10-8: Summary of performed unity checks for a 90m long box beam

A 90m long box beam can only comply with the 170t weight limit, if a beam width smaller than 1000mm is chosen. However it was chosen not to make such a design for two reasons. First of all a smaller width would lead to an even larger overcapacity for shear, due to a large number of webs in the bridge. The main benefit of the application of UHPC is its high shear capacity, so it is contradictory to apply a large number of webs in a UHPC bridge. The second reason not to make box beams with a small width is, because of the many times a beam has to be manufactured and

transported to form a complete bridge. Making beams with a width under 1000mm is both impractical and inefficient.

Instead a 90m long box beam is designed with a more optimized width disregard of the weight limit of 170t to demonstrate its technical feasibility and level of performance. These beams with optimized width are quite heavy and can only be transported by water. However with a length of 90m and a weight of 179,3t, they are still considerably lighter and longer than the longest beams ever made in the Netherlands. These beams were made by “Haitsma Beton” and are 68m long and weigh 240t each.

10.6 Overview of the Designs

Beam and Bridge Properties					
Span	60	70	80	85	90
Concrete Class	C170	C170	C170	C170	C170
Slenderness ratio	46,2	43,8	40,0	38,6	36,7
Height	1300	1600	2000	2200	2450
Width	1500	1500	1250	1000	1000
Top flange thickness	170	170	170	170	170
Bottom flange thickness	225	225	225	270	270
Web thickness	90	85	85	85	85
Beam mass	115,5	142,2	156,3	160,1	179,3
Total cross-section area	7,55	7,97	9,20	11,09	11,73
Total amount of p-steel	156000	174000	180000	225000	225000
Unity Checks					
Moment	0,66	0,58	0,64	0,57	0,60
Shear	0,97	0,95	0,74	0,61	0,59
Transverse moment top flange (cracking)	0,44	0,47	0,41	0,33	0,34
Transverse moment web (cracking)	0,84	0,74	0,46	0,30	0,27
Deflection (traffic)	0,34	0,31	0,23	0,22	0,21
Deflection (camber)	0,16	0,17	0,28	0,34	0,49
Cracking	0,46	0,43	0,50	0,45	0,48
Concrete fatigue	0,28	0,42	0,04	0,15	0,03
Steel fatigue	0,10	0,17	0,22	0,22	0,27

Table 10-9: Overview of properties and unity checks of the UHPC box beam designs (KS-beams)

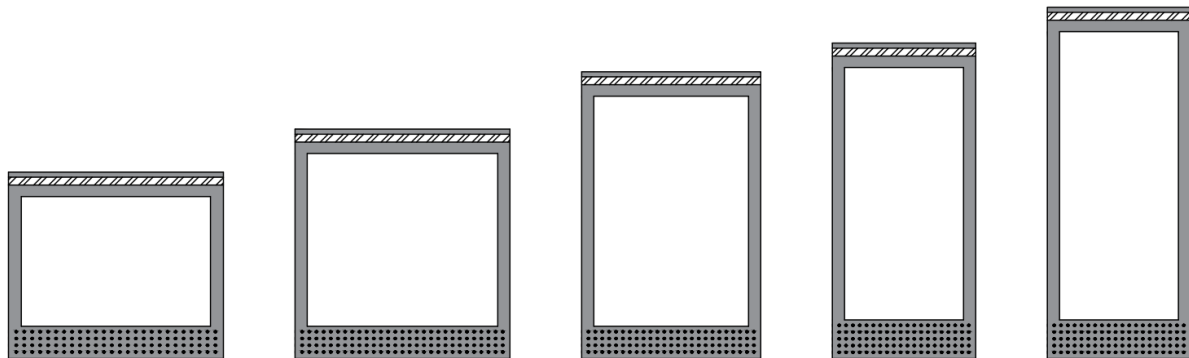


Figure 10-5: Overview of box beams for 60m, 70m, 80m, 85m and 90m (f.l.t.r)

11 Comparison with Existing Box Beam Solutions

To investigate how the designed UHPC box beams perform on a structural level, the box beams are compared to existing box beam solutions. The brochures of SKK-beams by “Spanbeton” and the HKP-beams by “Haitsma Beton” are used as a reference. The cross-sections of the beams are shown in the figure below.

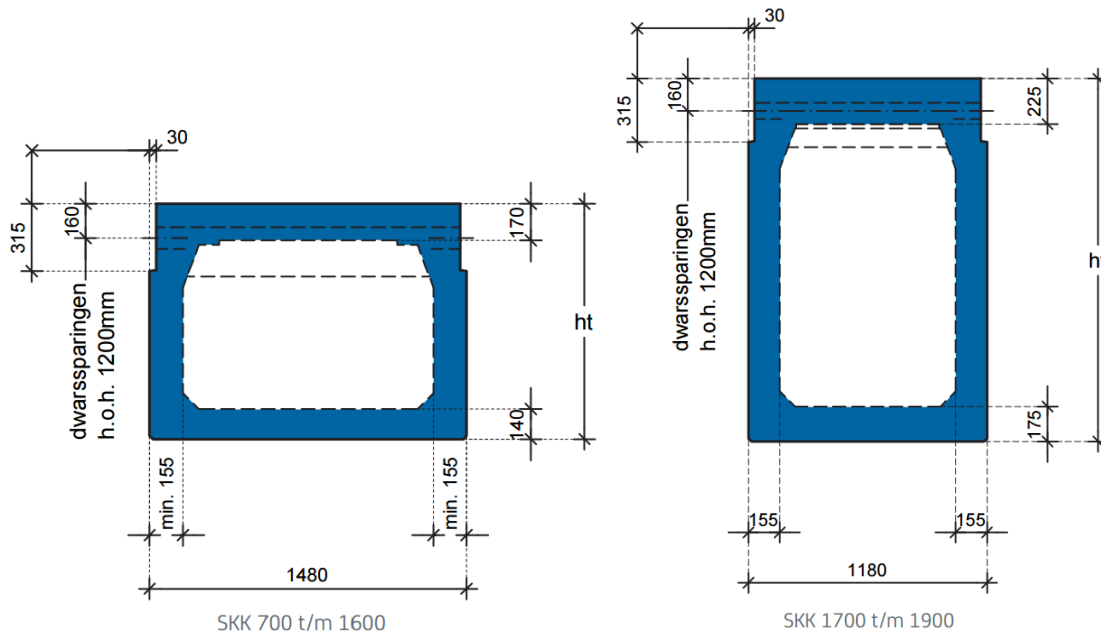


Figure 11-1: Cross-sections of SKK-beams [Brochure of SKK/PIQ box beam structures by Spanbeton]

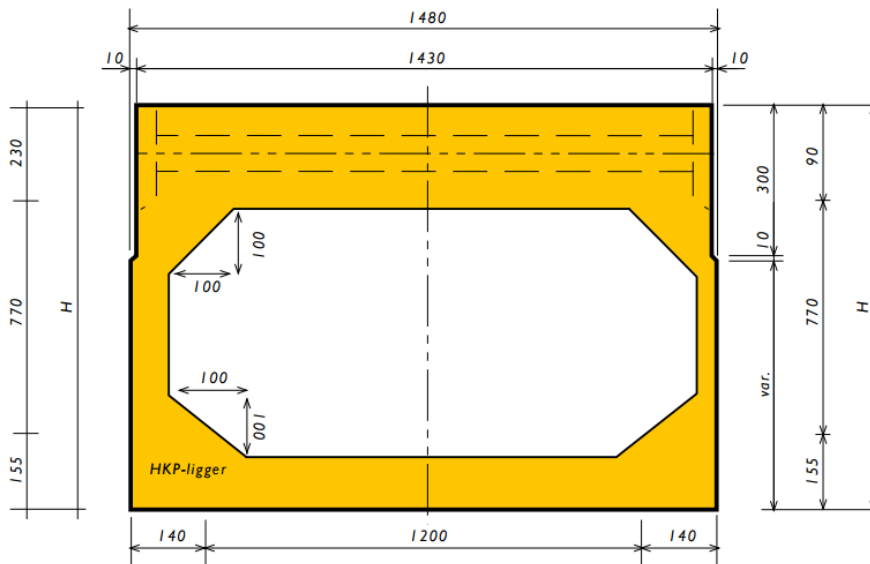


Figure 11-2: Cross-section of HKP-beam [Brochure of HKP box beam structures by Haitsma Beton]

SKK-beams and HKP-beams are characterized by their height. Naturally as the height increases, so does the load bearing capacity of the beams. SKK-beams come in heights from 700mm to 1900mm. HKP-beams from 800mm to 1800mm. The brochures contain graphs that show the load bearing capacity of the beams. These load bearing capacity graphs can be used to determine, which beam height is required for different spans and loadings. The data from these brochures are collected together with the data from the UHPC box beams designed for this master thesis and shown in a

graph that shows the required height for different spans under the traffic loads based on NEN-EN 1991-2. The graph contains three different beam types:

- UHPC beams (C170)
- SKK-beams (C60)
- HKP-beams (C55)

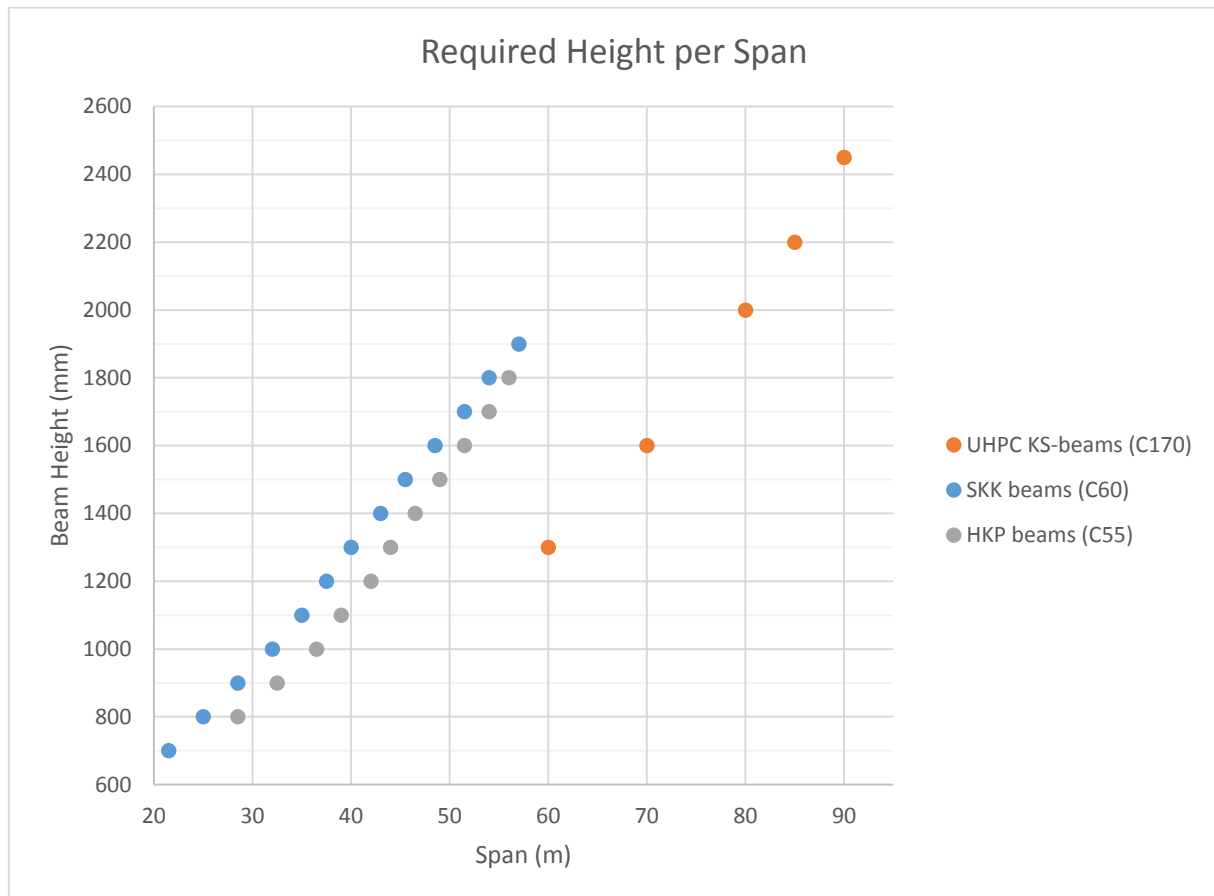


Figure 11-3: Required beam height of several beam types for different spans under traffic loads according to Eurocode

This graphs shows the benefits of the UHPC beams for slenderness. For example an SKK-beam of 1600mm can only span up to 48,5m. A UHPC beam with the same height can span 70m. Moreover it shows that the UHPC beams can cover a much greater range of spans. The SKK-beam with the greatest height (1900mm) can span up to 57m. With that height a UHPC beam can span almost 80m.

In addition to slenderness benefits UHPC beams also provide weight benefits. The weight of the beams can be greatly reduced. A small weight is beneficial for the total loading on the bridge, transportation and also translates to material cost savings. The graph below shows the self-weight of the bridge for different spans of UHPC beams and SKK-beams.

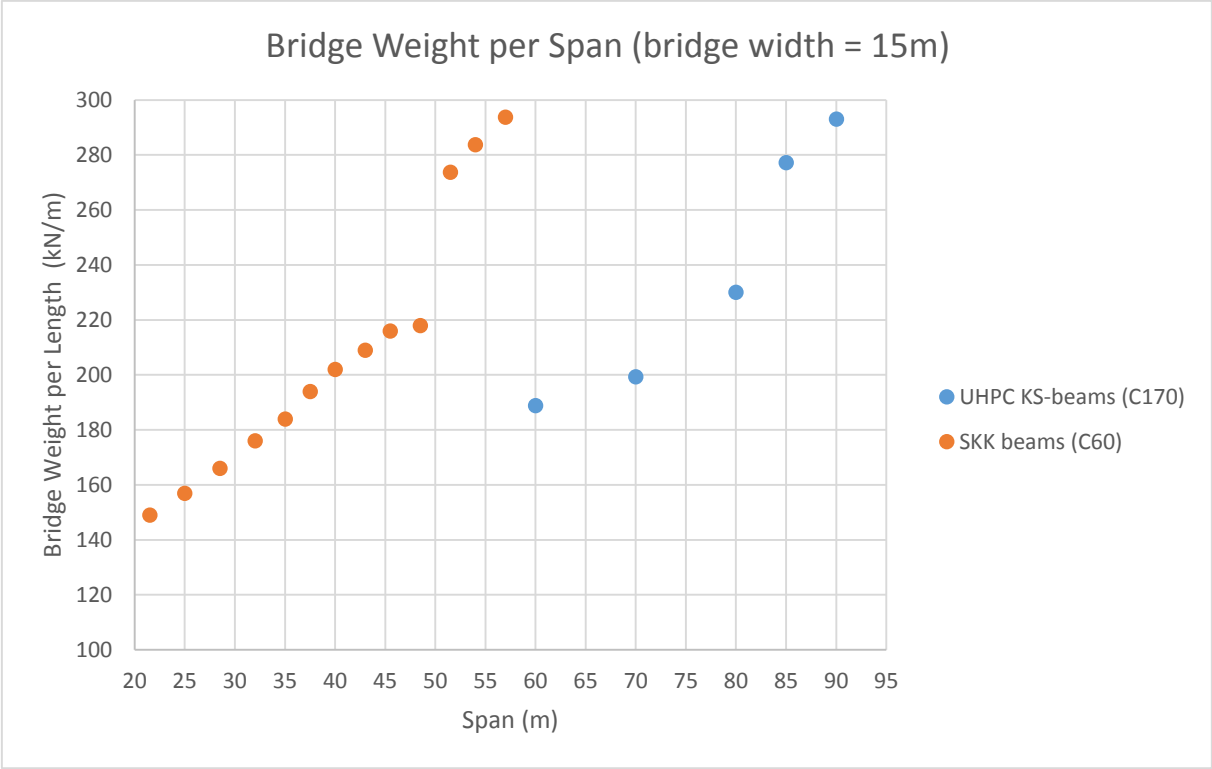


Figure 11-4: Self-weight of UHPC and SKK bridges for different spans under traffic loads according to Eurocode

The UHPC bridge is significantly lighter than the SKK-bridge. For example a 60m long UHPC bridge has about the same self-weight as an SKK-bridge that spans only 35m. Moreover a SKK-bridge that should span 60m would be at least 55% heavier. In other words, when applying UHPC beams instead of SKK beams, the same bridge can be made with only 64% of the original weight.

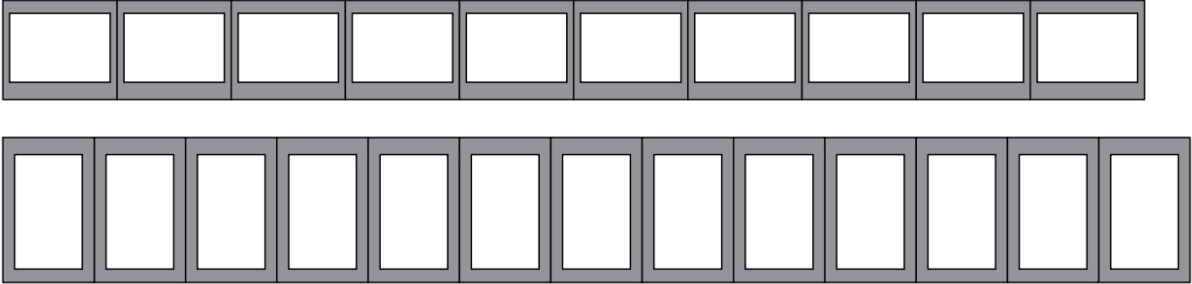


Figure 11-5: Cross-section of a 60m UHPC box beam bridge (above) and 57m SKK-beam bridge (below) on scale

As a result of both the slenderness and weight benefits it can be concluded that UHPC box beams can be a competitive alternative for existing box beam solutions that use more conventional concrete classes such as C60. This alternative becomes more attractive as spans increase, because at some point the C60 beams becomes very large and heavy. As a result they cannot meet with slenderness requirements or cannot be practically transported anymore. The UHPC beams are still slender and light enough to transport by road up to spans of 85m. Therefore UHPC beams provide a fit solution for spans that are too long for conventional box beam solutions, without having to switch to segmented or cast in-situ solutions.

12 Optimization Variant: Strands in Web (SIW)

12.1 Purpose

The box beams as designed in chapter 9 and chapter 10 require thick bottom flanges in order to fit all the prestressing strands. An effective way to apply even more prestress without having to increase the bottom flange thickness is to place strands in the web. Especially as beams increase in height more strands can fit in the cross-section. This way an even more optimized UHPC box beam can be designed. Designs of this variant are made for bridges of 60m, 70m, 80m, 85m and 90m. These designs are expected to be even more slender and lighter.

12.2 Optimization Challenges

Note that the kinked strands in the previous designs cannot be applied anymore. This means that the favorable effect on the shear capacity caused by the upward forces from the kinks will no longer apply. This may affect the required web thickness and/or beam width in a negative way.

Furthermore applying high level of prestress requires a longer period of time before demoulding can take place. Right after demoulding the concrete stress is limited to $0,7 \cdot f_{ck}(t)$. Since a higher prestress is applied a longer period of time is needed for the concrete to reach sufficient strength to be demoulded. So although the higher prestress is favorable for the slenderness and weight of the bridge, it can be more time-consuming, which can be costly.

Also tensile stresses at the supports at the top of the beam will become very high, if no measures are taken to prevent this. To prevent these high tensile stresses the strands should be unbonded from the concrete up to a certain distance to the support. The distance should be such that the bending moment caused by self-weight of the beam causes enough compression at the top to limit the tensile stresses caused by the eccentricity of the prestressing force. The strands can be unbonded by covering the strands over a certain distance with ducts before pouring the concrete, so no bond stresses can be transferred between the strands and the concrete in that area. The required bending moment $M_{G,x}$ is determined with the following formula:

$$-\frac{1,2P_0}{A_c} + \frac{1,2P_0 \cdot f_p}{W_t} - \frac{0,9M_{G,x}}{W_t} \leq f_{ctd}$$

Note that a load factor of 1,2 is taken for local effects of the unfavorable of prestressing force and a reduction factor of 0,9 for the favorable self-weight. The distance x to the supports, where bending moment $M_{G,x}$ is reached, can be found with the following formula:

$$M_{G,x} = \frac{1}{2} q_G x (L - x)$$

In addition these measures also limit the spalling stresses and therefore no splitting reinforcement will be necessary.

To give an example of the order of magnitude for the distance the value x is calculated for a 60m SIW-beam.

$$-\frac{1,2 \cdot 17748 \text{ kNm}}{0,612 \text{ m}^2} + \frac{1,2 \cdot 17748 \text{ kNm} \cdot 0,52 \text{ m}}{0,22 \text{ m}^3} - \frac{0,9 \cdot M_{G,x}}{0,22 \text{ m}^3} \leq 4,0$$

$$M_{G,x} = 2438 \text{ kNm}$$

$$2805 = \frac{1}{2} \cdot 15,3 \cdot x (60 - x)$$

$$x = 6,91m$$

The figure below shows the total moment distribution in the ULS in case of strands bonded over the whole span and strands that are unbonded around the supports. Note that the maximum moment in the unbonded area is smaller than the maximum moment at midspan, proving that this area also suffices in the ULS. Note that in reality the bending moment does not jump with a straight line as seen in the curve, but changes linearly over the transmission length of the strand.

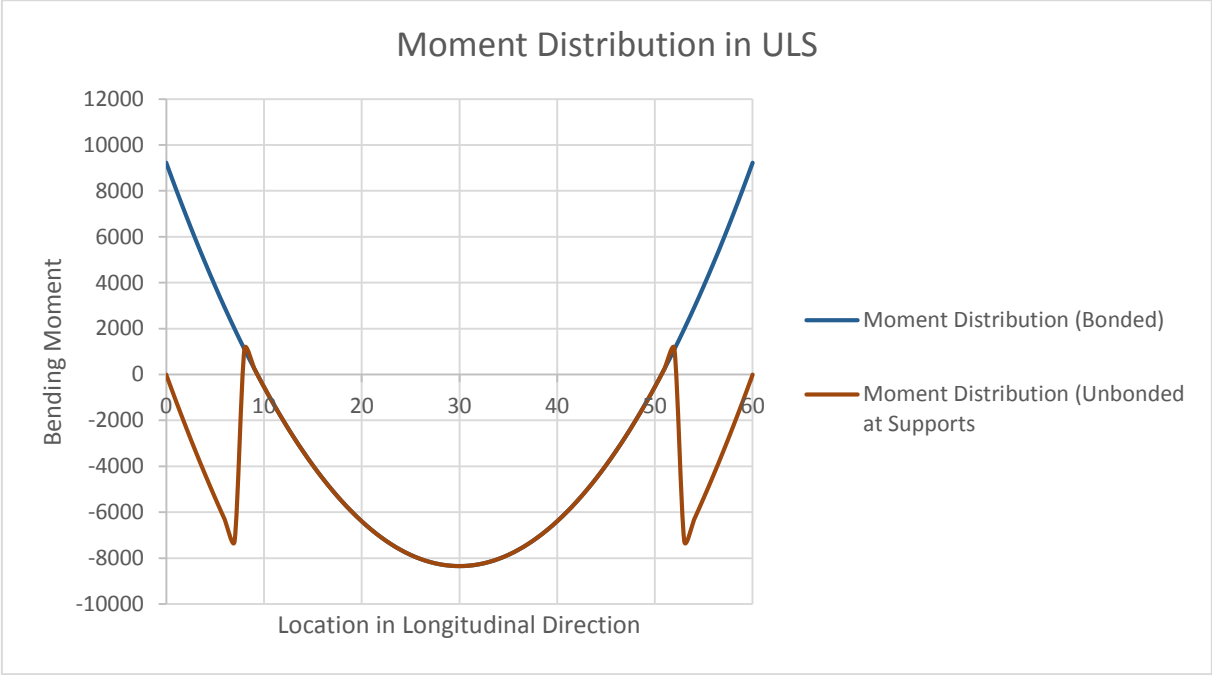


Figure 12-1: Moment distribution in the ULS showing the difference between bonded and partly unbonded strands

12.3 Overview Designs

Beam and Bridge Properties					
Span	60	70	80	85	90
Concrete Class	C170	C170	C170	C170	C170
Slenderness ratio	48,0	46,7	41,0	38,6	37,5
Height	1250	1500	1950	2200	2400
Width	1500	1500	1500	1250	1000
Top flange thickness	170	170	170	170	170
Bottom flange thickness	175	175	175	175	225
Web thickness	95	85	85	85	85
Beam mass	105,4	127,3	161,1	161,7	168,8
Total cross-section area	6,89	7,14	7,90	8,96	11,04
Total amount of p-steel	150000	153000	162000	181800	234000
Unity Checks					
Moment	0,68	0,71	0,71	0,67	0,57
Shear	0,96	0,96	0,89	0,88	0,74
Transverse moment top flange (cracking)	0,42	0,48	0,49	0,41	0,34
Transverse moment web (cracking)	0,84	0,72	0,62	0,42	0,28
Deflection (traffic)	0,40	0,33	0,30	0,26	0,23
Deflection (camber)	0,12	0,16	0,21	0,27	0,32
Cracking	0,47	0,49	0,55	0,54	0,46
Concrete fatigue	0,71	0,58	0,66	0,19	0,27
Steel fatigue	0,11	0,18	0,28	0,28	0,26

Table 12-1: Overview of properties and unity checks of the UHPC box beam designs (SIW-beams)

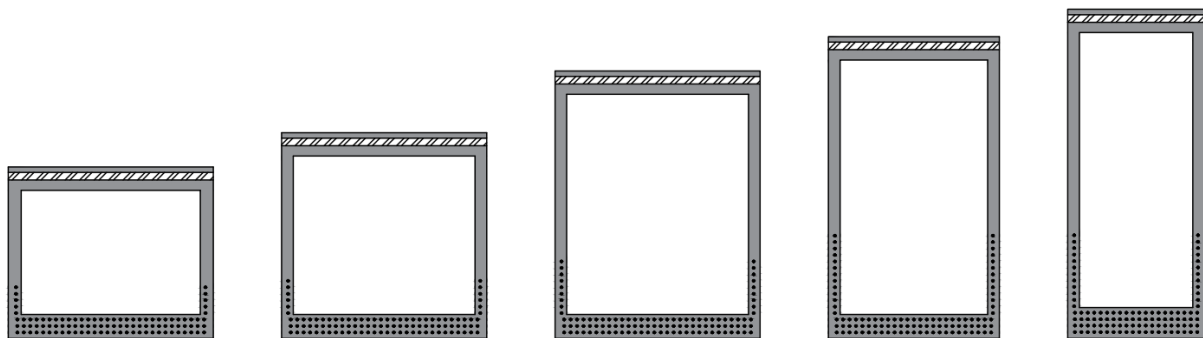


Figure 12-2: Overview of SIW box beams for 60m, 70m, 80m, 85m and 90m (f.l.t.r)

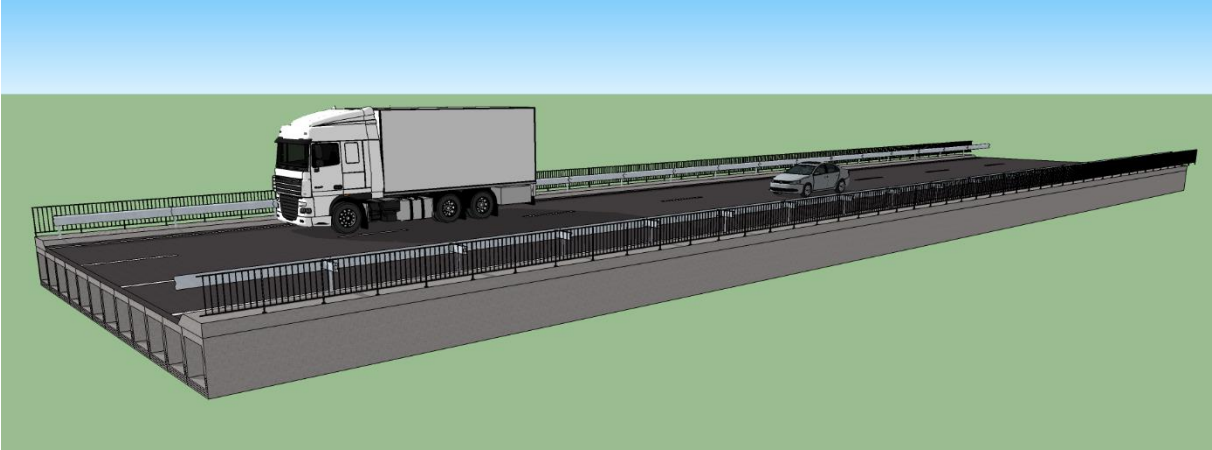


Figure 12-3: Impression of a 60m long UHPC bridge consisting of the SIW-beams showing the slenderness

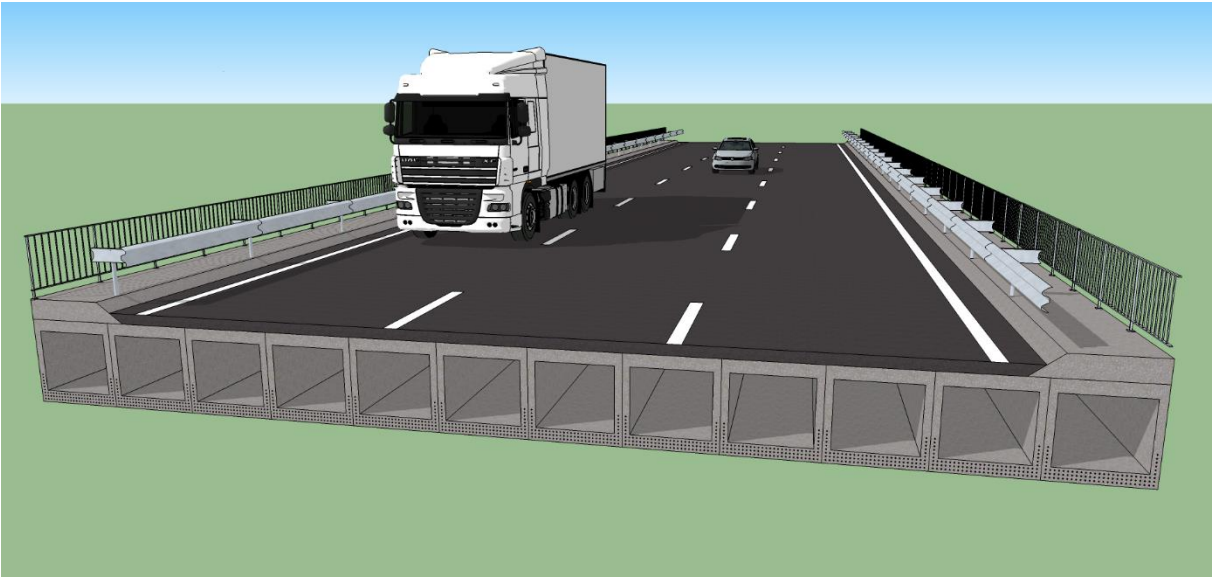


Figure 12-4: Impression of a 60m long UHPC bridge consisting of the SIW-beams showing the cross-section

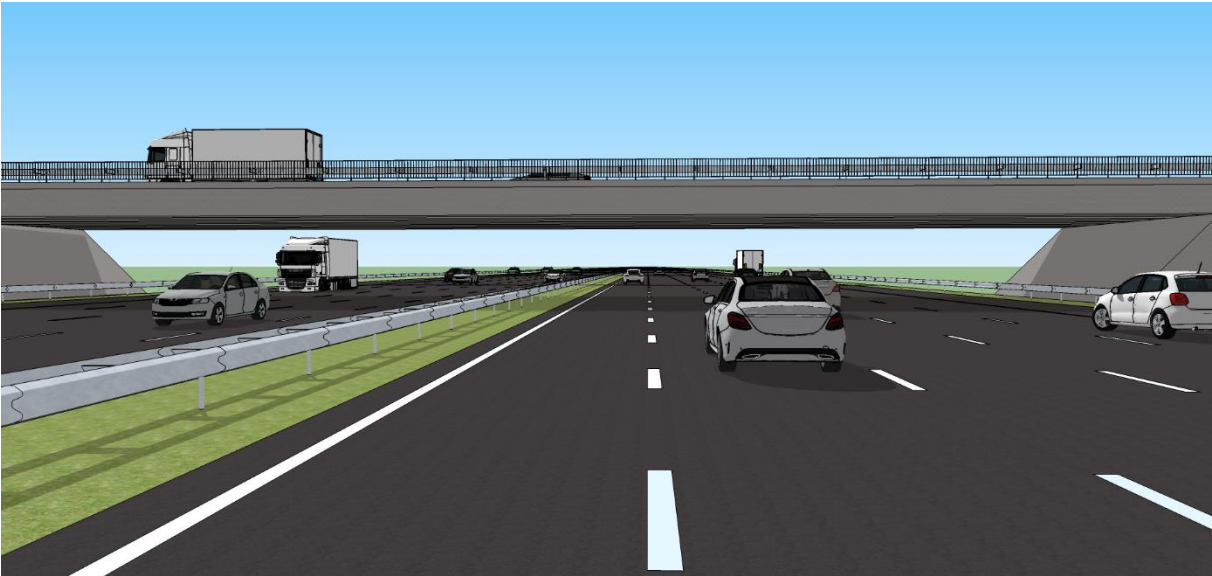


Figure 12-5: Impression of a 60m long UHPC bridge consisting of the SIW-beams showing the crossing of a highway without intermediate piers

12.4 Comparison with Other Box Beam Solutions

In the graphs below the slenderness and weight of SKK-beams and both UHPC variants are shown. The beams with the kinked strands are called KS-beams and the beams with the strands in the web are called SIW-beams. From these graphs the benefits of applying SIW-beams for slenderness and weight can be deducted.

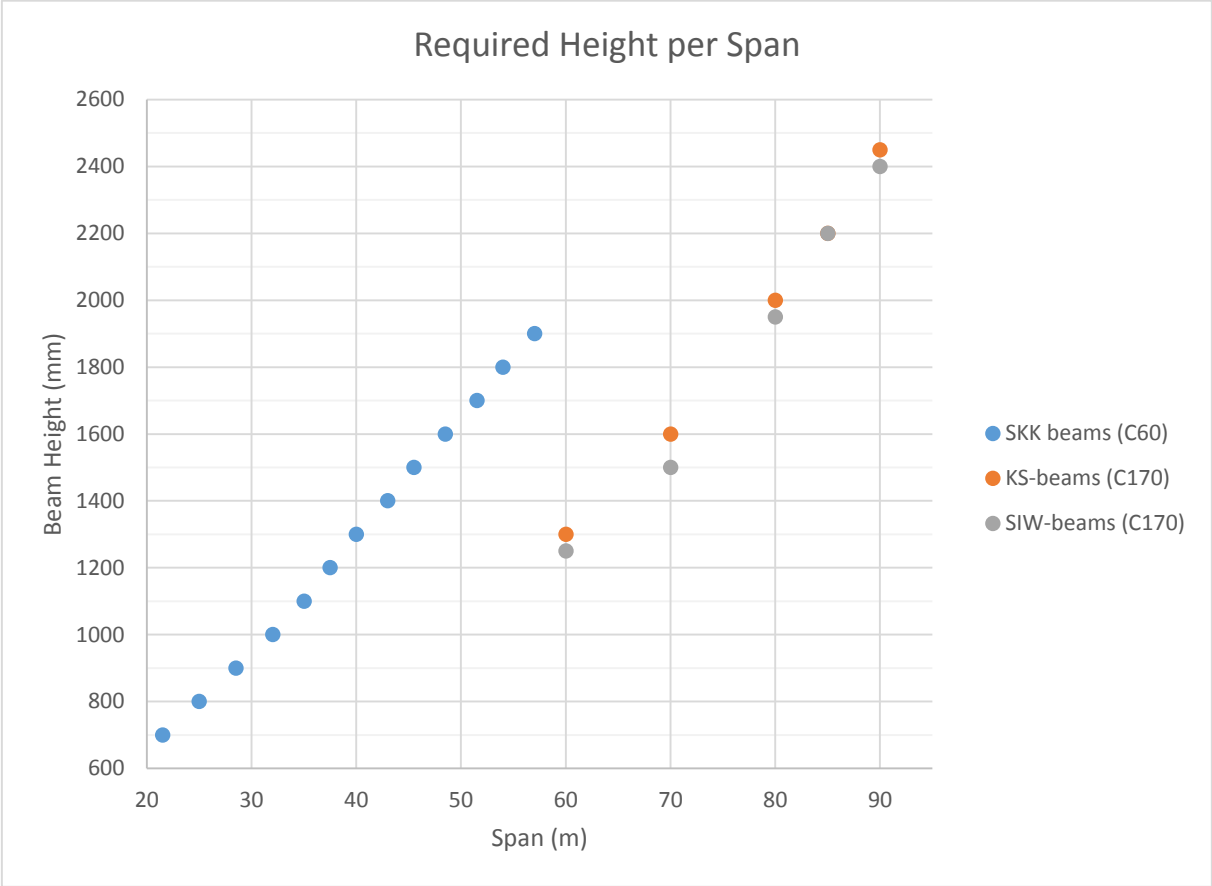


Figure 12-6: Required beam height of several beam types for different spans under traffic loads according to Eurocode

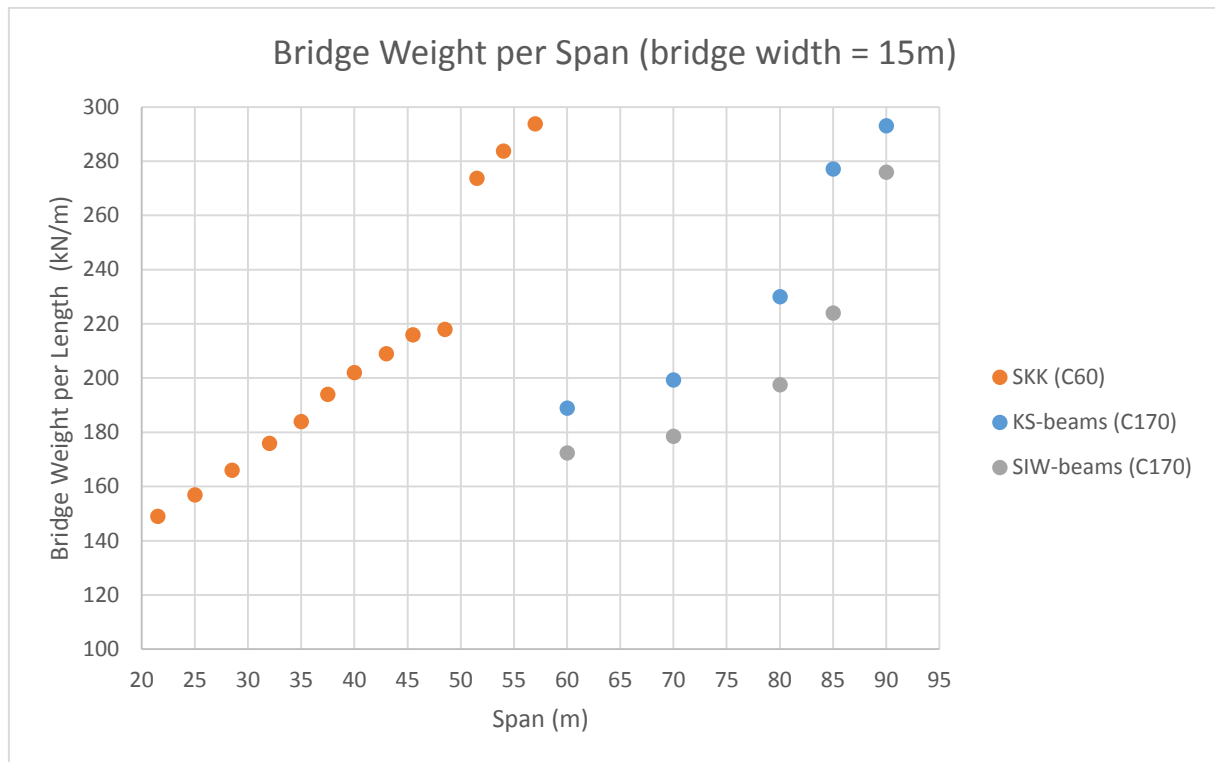


Figure 12-7: Self-weight of UHPC and SKK bridges for different spans under traffic loads according to Eurocode

As expected the SIW-beams can be more slender than KS-beams. However the SIW-beams do not necessarily benefit the slenderness very much. The height can only be reduced up to 10cm and the design for 85m does not have any benefit for the construction height.

The SIW-beams have a more favorable effect on the weight. The designs of the SIW-beams have a decreased height and bottom flange thickness leading to a significant weight reduction. The increased web thickness, due to the fact that there is no more favorable effect from the kinked strands, does not affect the total weight enough to increase to total weight. Instead the decreased height and bottom flange thickness leads to a decrease in total weight. A weight reduction ranging from 6% to 19% can be achieved when applying SIW-beams instead of KS-beams. Note that this weight reduction enables the 90m SIW-beams to be transported by road, since the mass of these beams are 168,8t.

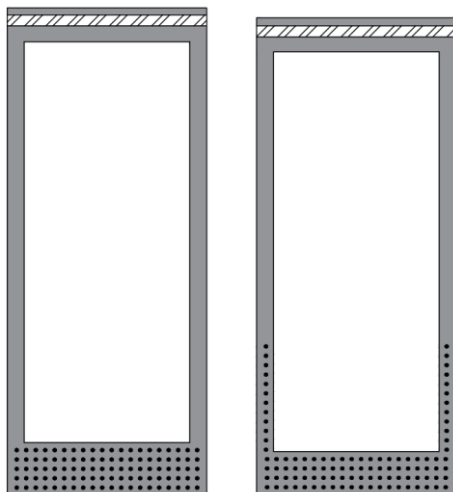


Figure 12-8: A 90m KS-beam (left) compared to a 90m SIW-beam (right)

13 Optimization Variant: Kinked Strands in Web (KSIW)

13.1 Purpose

Although the SIW variant is more optimized than the KS variant, there is still room for more optimization. In the SIW-beams the strands in the web and the strands in the bottom flange positioned below the web can be kinked. This variant will be called KSIW-beams. The strands will be kinked for two reasons. First of all the kink induces a vertical force, which has a favorable effect on the shear capacity. In addition the kink reduces the drape at the supports, which will limit tensile stresses at the top and also spalling stresses. This way the strands do not have to unbonded anymore.

13.2 Overview of the Designs

Beam and Bridge Properties					
Span	60	70	80	85	90
Concrete Class	C170	C170	C170	C170	C170
Slenderness ratio	48,0	46,7	41,0	38,6	37,5
Height	1250	1500	1950	2200	2400
Width	1500	1667	1500	1250	1000
Top flange thickness	170	170	170	170	170
Bottom flange thickness	175	175	175	175	225
Web thickness	85	85	85	85	85
Beam mass	102,7	137,6	161,1	161,7	168,8
Total cross-section area	6,71	6,94	7,90	8,96	11,04
Total amount of p-steel	144000	144450	166500	181800	234000
Unity Checks					
Moment	0,69	0,73	0,67	0,67	0,57
Shear	0,98	0,96	0,78	0,74	0,61
Transverse moment top flange (cracking)	0,45	0,52	0,49	0,41	0,34
Transverse moment web (cracking)	0,83	0,90	0,61	0,42	0,26
Deflection (traffic)	0,40	0,39	0,28	0,26	0,21
Deflection (camber)	0,12	0,17	0,19	0,27	0,32
Cracking	0,48	0,50	0,51	0,54	0,46
Concrete fatigue	0,60	0,24	0,45	0,19	0,27
Steel fatigue	0,12	0,20	0,28	0,28	0,26

Table 13-1: Overview of properties and unity checks of the UHPC box beam designs (KSIW-beams)

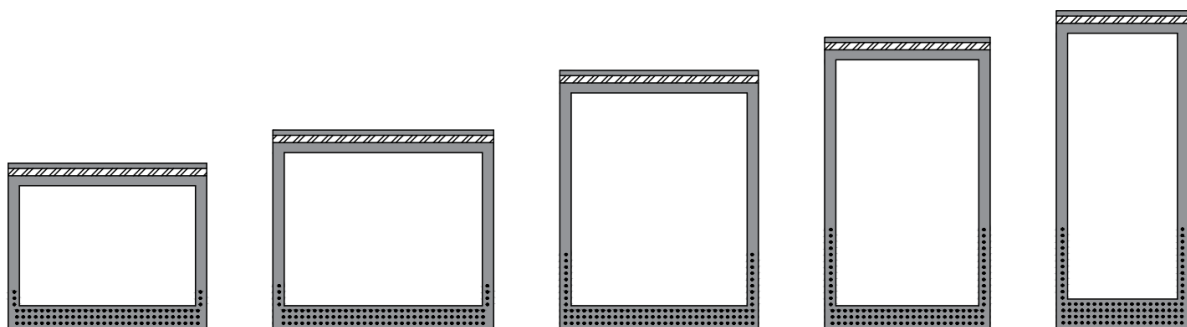


Figure 13-1: Overview of KSIW box beams for 60m, 70m, 80m, 85m and 90m (f.l.t.r)

13.3 Comparison with Other Box Beam Solutions

In the graphs below the slenderness and weight of ZIP(XL)-beams SKK-beams and all the UHPC variants are shown. From these graphs the benefits of applying SIW-beams for slenderness and weight can be deduced.

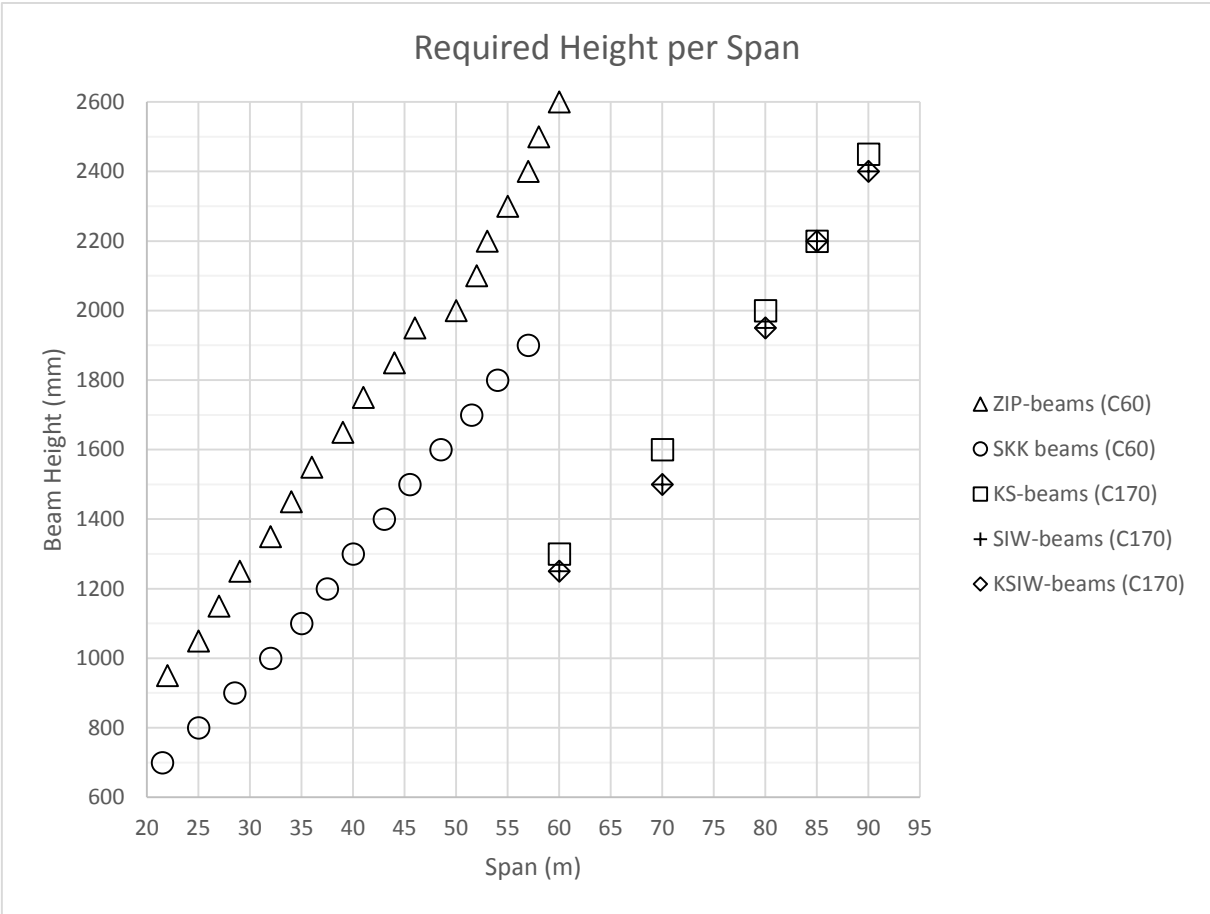


Figure 13-2: Required beam height of several beam types for different spans under traffic loads according to Eurocode

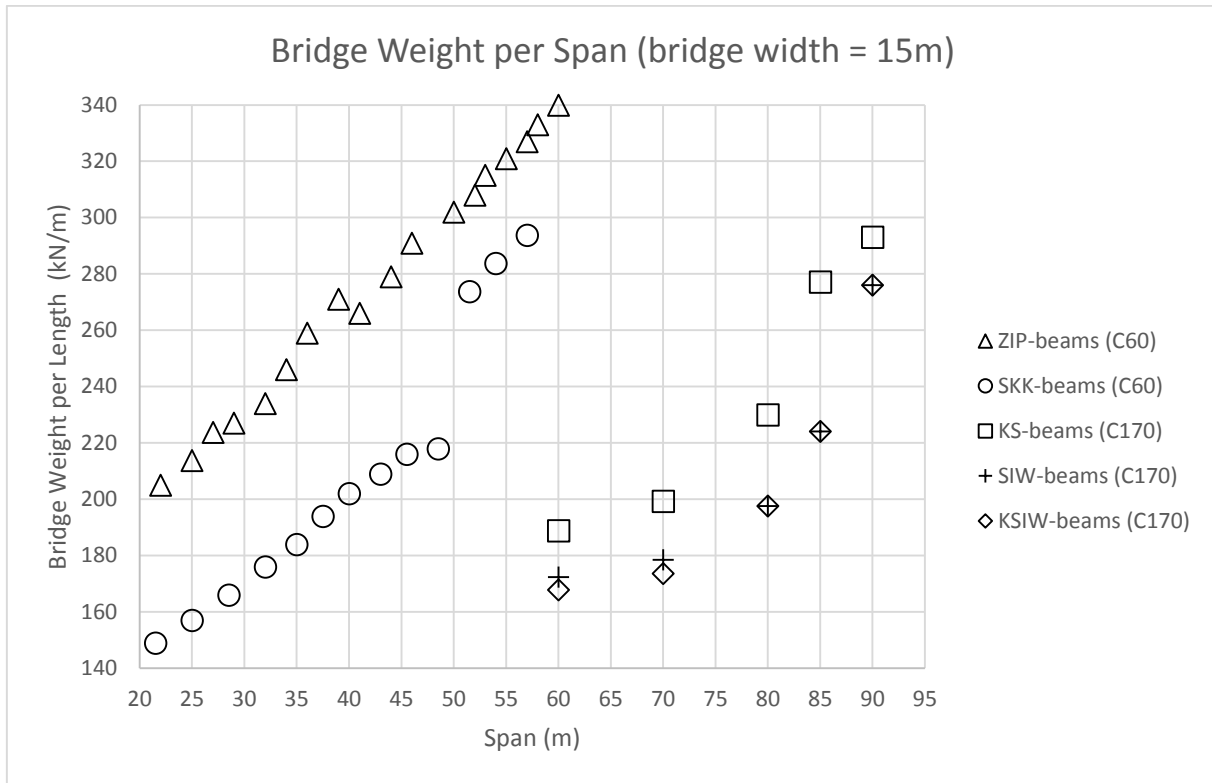


Figure 13-3: Self-weight of UHPC, ZIP(XL) and SKK bridges for different spans under traffic loads according to Eurocode

The plots for the SIW and KSIW-beams overlap almost completely. The beam height cannot be limited, due to fatigue in the compression zone. Only the 60m and 70m KSIW-beams are a bit lighter. This is due to either the thinner webs or the wider beam that can be applied, because the shear capacity is increased by the kinked strands. The larger beams could not become any wider despite the increased shear capacity, because the beam is constrained by the 170t weight limit. Therefore these beams cannot make lighter bridges and the overcapacity in shear increases as the span increases.

14 Application of the Designed UHPC Box Beams

14.1 New Bridges

As shown in the previous chapters UHPC box beams can be very slender and light. Even in case of very long spans the beams remain a high level of slenderness. Moreover the beams can be made very light, allowing them to be transported by road, even for long spans of 90m. Therefore they provide a fit solution for new bridges that require spans that are too long for conventional box beam solutions, without having to build an intermediate pier or switch to segmented or cast in-situ solutions, which causes considerably more traffic hindrance during construction.

14.2 Replacing Old Bridge

14.2.1 Retaining entire substructure

Another useful application for the UHPC box beams is to use it to replace bridges that cannot carry increased traffic intensities. A UHPC box beam bridge with the same construction height has considerably more strength than bridges made out of conventional concrete. In addition this bridge will also be lighter. Therefore an existing bridge can be replaced for a stronger bridge without having to replace or strengthen the substructure.

For example a SKK 1500 bridge can be replaced with a KSIW 1500 bridge. An SKK 1500 bridge is designed to span approximately 45m, while a KSIW 1500 bridge is strong enough to span 70m. Therefore the capacity of the superstructure is increased significantly. However since the old substructure will be saved, the substructure has no increased capacity. This will be accommodated by the decreased self-weight of the superstructure allowing an increased traffic loading on the substructure. The SKK 1500 weighs 21,6 kN/m, which is 14,59 kN/m per meter of width (beam width = 1480mm). The KSIW 1500 weighs 19,29 kN/m, which is 11,57 kN/m per meter of width (beam width = 1667mm). For a bridge with a span of 45m and a width of 15m, the total force on the substructure decreased with approximately 2000kN.

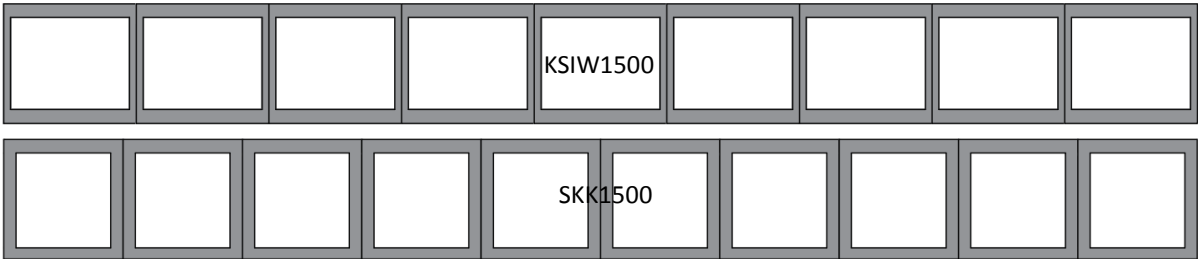


Figure 14-1: A cross-section of a KSIW 1500 bridge (above) compared to a SKK 1500 bridge

In addition to replacing an old bridge with a new UHPC box beam bridge with the same slenderness, it is also possible to replace an old bridge with a more slender one. This way the headroom can be increased, which might be necessary to prevent collision loads. Especially when overlaying of the asphalt layer has taken place.

For example a SKK 1900 bridge can be replaced with a KSIW 1250 bridge. These bridges have the same capacity, but the UHPC bridge will provide an additional headroom of 650mm.

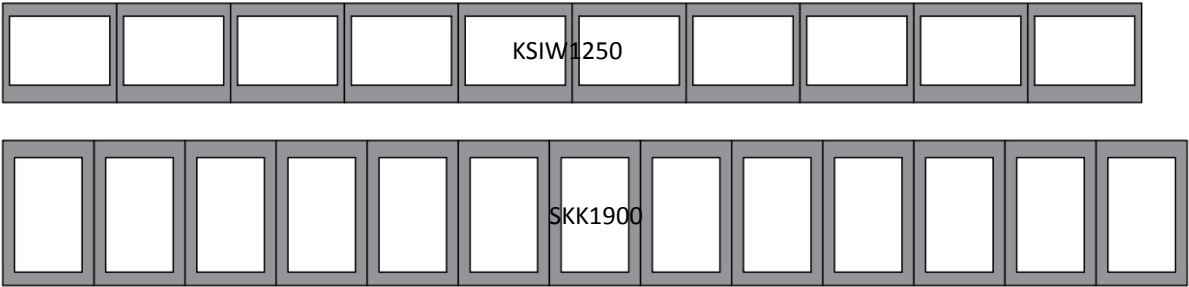


Figure 14-2: A cross-section of a KSIW 1250 bridge (above) compared to a SKK 1900 bridge

In case ZIP-bridges are replaced with KSIW-bridges the increase of headroom is even more. A ZIP-bridge with a height of 2600mm ca be replaced with a KSIW 1250 bridge, which gains 1350mm of additional headroom.

14.2.2 Omitting intermediate pier

In addition the UHPC box beams might be used to replace old bridges, while leaving out the intermediate pier(s) and keeping the rest of the existing substructure and embankments to minimize traffic hindrance. This is only possible if the replacing UHPC box beam can span all the existing spans at once with the same construction height, while also being light enough to remain the same forces on the substructure, despite the absence of the intermediate pier.

To investigate the possibility of such an application an attempt is made to replace a 2x30m span bridge consisting of ZIPXL-beams by “Spanbeton” (C60) with a 1x60m span bridge consisting of KSIW-beams (C170). ZIPXL beams are rather high and heavy so these type of bridges are suitable candidates for this type of replacement operation. According to the slenderness graph provided in the “Spanbeton” brochure for ZIP and ZIPXL-beams a profile height of 1100mm is required to span 30m.

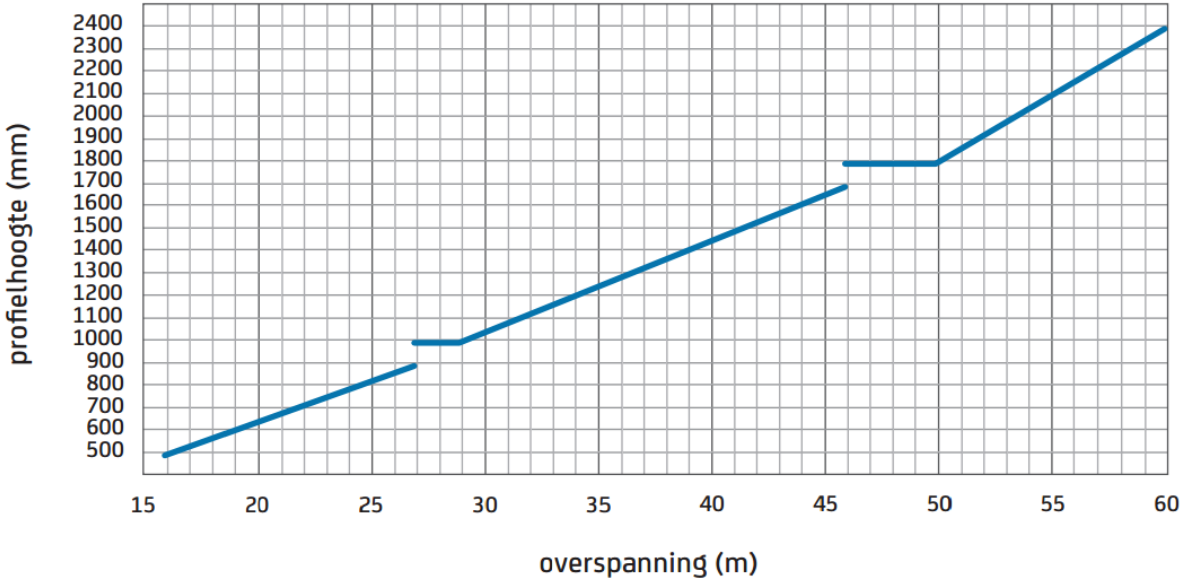
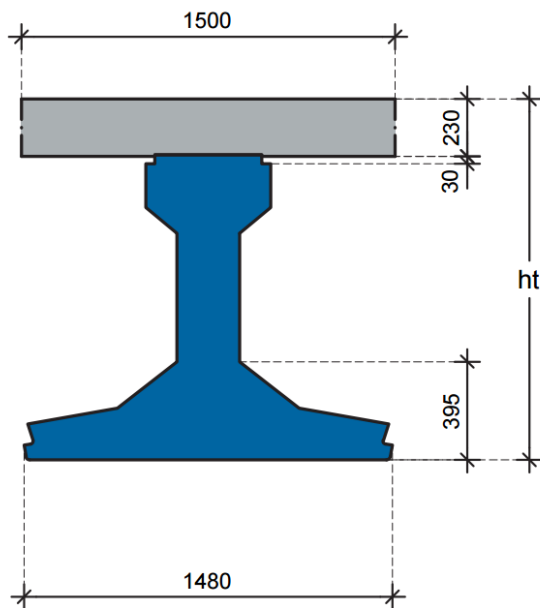


Figure 14-3: Slenderness graph for ZIP and ZIPXL-beams by “Spanbeton” as provided in the brochure

Unlike box beams ZIPXL-beams do not have a top flange that can act as a deck. Therefore a concrete topping with a thickness of 230mm is applied, which adds to the construction height. A ZIPXL 1100 has a total height of 1350mm as shown in the figures below.



ZIPXL 1000 t/m 1700 met druklaag

	Afmetingen (mm)			Eigen gewicht (kN/m ³)		
	h	h1	ht	ZIP	druklaag	Totaal
ZIPXL 1400	1390	375	1650	18.5	8.6	27.1
ZIPXL 1300	1290	275	1550	17.3	8.6	25.9
ZIPXL 1200	1190	175	1450	16.0	8.6	24.6
ZIPXL 1100	1090	75	1350	14.8	8.6	23.4
ZIPXL 1000	990	75	1250	14.1	8.6	22.7
ZIP 900	890	615	1150	11.0	6.9	17.9
ZIP 800	790	515	1050	10.2	6.9	17.1
ZIP 700	690	415	950	9.5	6.9	16.4
ZIP 600	590	315	850	8.7	6.9	15.6
ZIP 500	490	215	750	8.0	6.9	14.9

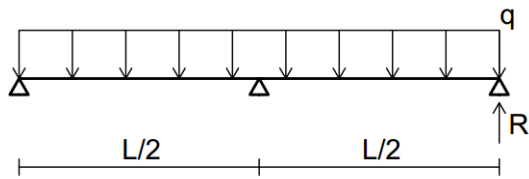
Figure 14-4: Dimensions of ZIPXL-beams by “Spanbeton” as provided in the brochure

The 60m KSIW-beams have a construction height of 1250mm, which is 100mm smaller than the 30m ZIPXL-beams. Therefore it can be concluded that height wise a single span 60m KSIW-beam bridge can replace a 60m ZIPXL-beam bridge with an intermediate pier, without having to replace the existing substructure and embankments.

The same holds for 70m KSIW-beams. Height wise they can replace 2x35m ZIPXL bridges, since a 60m KSIW-beam has a height of 1500mm and a 35m span ZIPXL bridge requires a height of 1550mm. 80m and longer KSIW-beams do not have sufficient slenderness to do the same.

However besides the slenderness the forces on the substructure should also be checked. There is a significant increase of forces that go to the abutments, since the intermediate pier is omitted. The increase of forces should be compensated for by a lighter structure.

ZIP Bridge



KSIW Bridge

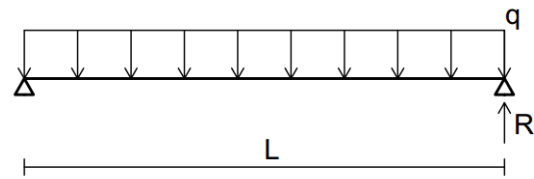


Figure 14-5: Schematization of a bridge with two spans (left) and a single span (right)

The reaction force R as shown in the figure above represents the total force on the abutment. This force can be determined for the ZIP bridge by the following formula:

$$R_{ZIP} = \frac{3}{16} q_{ZIP} L$$

For the KSIW bridge the reaction force R is determined with:

$$R_{KSIW} = \frac{1}{2} q_{KSIW} L$$

Note that this only holds given that all the supports are rigid, which is assumed.

So in order for the KSIW bridge to have the same force on the abutment as the ZIP bridge, the ratio between the self-weight of the beams should be:

$$q_{KSIW} = \frac{3}{8} q_{ZIP} = 0,375 q_{ZIP}$$

However the ZIPXL 1100 has a self-weight of 23,4 kN/m and the KSIW-60 has a self-weight of 16,8, which yields a ratio of approximately 0,7. Therefore the force on the substructure increases significantly despite of the lighter superstructure. So it can be concluded that only if the substructure has sufficient overcapacity or if the substructure is strengthened, UHPC box beams can be applied to replace old ZIPXL bridges, while leaving out intermediate piers.

In order to find the required overcapacity or strengthening the maximum reaction force is calculated for both the 2x30m ZIPXL bridge and the 60m KSIW bridge.

For the ZIPXL bridge:

$$q_{tot} = 10 * 23,4 \frac{kN}{m} + 15m * 3,6 \frac{kN}{m^2} + 2 * 3,65 \frac{kN}{m} + 3m * 10,35 \frac{kN}{m^2} + 9m * 3,5 \frac{kN}{m^2} = 319,21 \frac{kN}{m}$$

$$R_{max} = \frac{3}{16} q_{tot} L + Q = \frac{3}{16} * 319,21 \frac{kN}{m} * 60m + 1200kN = 4791kN$$

For the KSIW bridge:

$$q_{tot} = 10 * 16,8 \frac{kN}{m} + 15m * 3,6 \frac{kN}{m^2} + 2 * 3,65 \frac{kN}{m} + 3m * 10,35 \frac{kN}{m^2} + 9m * 3,5 \frac{kN}{m^2} = 291,65 \frac{kN}{m}$$

$$R_{max} = \frac{1}{2} q_{tot} L + Q = \frac{1}{2} * 291,65 \frac{kN}{m} * 60m + 1200kN = 9949kN$$

So the maximum reaction force increases with the following factor:

$$\frac{9949kN}{4791kN} = 2,08$$

Since the substructure of bridges is often designed with plenty of overcapacity, the required overcapacity is not very high and there is always an option to strengthen the substructure, it is concluded that replacing a ZIPXL deck with a KSIW deck without intermediate pier is a viable application.

15 Conclusions

During this master thesis research was done on the application of UHPC in long span bridges, which was expected to be a viable solution because of the potential to make more slender and lighter bridges. In the preliminary study it was investigated how and to which extent this hypothesis can be supported. This was done by studying the material properties and making simple design calculations for rectangular cross-sections under different types of loading and compare it to normal strength concrete.

The results provided insight on how rectangular cross-sections of UHPC perform under these different types of loading. It showed that the application of UHPC has significant material saving ability compared to C45, especially under shear loading, which is proven by the very low CVE value. UHPC under tension also has a very low CVE value provided that prestressing is applied. UHPC under compression has a slightly higher CVE, but is still considered to be very effective because of the high compression strength in general. Rectangular cross-sections under bending have a very high CVE value and is therefore deemed as inefficient.

A box-shaped cross-section utilizes the strengths of UHPC by having a rectangular cross-section in compression (top flange), a prestressed rectangular cross-section in tension (bottom flange) and two shear members (webs). As a result the precast prestressed box beam is chosen as the most efficient concept.

A total of five designs for UHPC box beam bridges with spans of 60m, 70m, 80m, 85m and 90m were developed to support this hypothesis. The designs are optimized to minimize material use and find the most slender and light bridge possible. This can be done with the following optimization strategies:

- Omit transverse reinforcement as much as possible
- Minimizing beam height until the maximum level of prestress or deformation capacity is reached
- Maximizing beam width and minimizing web thickness until shear capacity is reached
- Minimizing bottom flange thickness by applying as many strands as possible per layer

The designs for spans of 60m and 70m could be optimized with the strategy above. The design for 80m was constrained by the weight limit of 170t for transportation by road. To maintain this limit the beam width is decreased. The width of 1500mm would lead to an exceedance, therefore the 80m design has a width of 1250mm. For the same reason the 85m beam has a decreased width of 1000mm. The design for 90m could not be kept below 170t without decreasing the width to below 1000mm. However a 90m design was still made with 1000mm width to demonstrate the feasibility and efficiency of the UHPC beam.

Ultimately the optimized designs were compared with existing box beam solutions that use more conventional concrete classes such as C60. This comparison study showed that the UHPC beams have the following benefits:

- More slender beams with a slenderness ratio up to 46,2 can be made to meet strict slenderness requirements and to reduce required elevation height of the bridge. SKK-beams have a slenderness ratio ranging from 30 to 32.
- Lighter bridges with weight reductions up to 36% compared to SKK-beam bridges can be made to reduce loading on the bridge and increase the ease of transportation. Moreover longer beams of 85m can be made, while still being able to transport these by road.

- Wider beams of 1500 instead of 1200mm can be made reducing the overall weight of webs and reducing the number of beams that have to be manufactured and transported.
- Beams that do not require transverse reinforcement with the exception of transverse post-tensioning can be made. This can reduce the required amount of steel and labor.

In addition to the UHPC box beams with kinked strands in the webs another variant with straight strands in the webs is developed. This allows a reduction in the number of strands in the bottom flange and more strands in the web. As a result even more slender and lighter beams can be made in comparison to the UHPC box beams with kinked strands. The slenderness of these beams reaches up to 48 and the weight reduction reaches up to 41%. This variant becomes so light that they can be transported by road even for 90m long beams. To further optimize this variant the strands in the web and the strands in the bottom flange positioned below the web can be kinked. As a result the shear capacity increases. This is beneficial for smaller spans, allowing lighter bridges, by increasing either beam width or decreasing web thickness. For larger spans the beams cannot be made any wider due to the 170t weight limit, so this optimization strategy only works for shorter bridges. However if these longer beams can be transported by water, then the weight limit no longer applies. In this case these beams can be made wider and the strategy becomes more interesting.

This last most optimized variant called KSIW-beams (Kinked Strands In Web) offer plenty of possible applications because they are both very light and slender. First of all, they provide a fit solution for new bridges with spans that are too long for conventional box beam solutions, without having to build an intermediate pier or switch to segmented or cast in-situ solutions. Second of all, they allow us to replace old bridges with a stronger one without having to replace the existing substructure. Both these applications have the benefit of reducing traffic hindrance. For the second application it is also investigated whether it is possible to omit the existing intermediate pier. Slenderness wise this is possible, since the KSIW-beams only require very little height for long spans. However, they are not light enough, to prevent the reaction force at the abutment to stay the same without intermediate pier. Therefore the substructure must have sufficient overcapacity or the substructure has to be strengthened to make this possible.

In conclusion UHPC box beams are a fit solution for both new bridges and replacing old bridges, because they have the ability to cause less traffic hindrance, thanks to their excellent slenderness and lightness.

16 Recommendations

Regarding the results of this master thesis the following recommendations are made:

- Because of the iterative nature of the design optimization process it is very time-consuming to fully optimize the designs of the UHPC box beams. Due to the limited amount of time it was chosen to stop further optimization. However there is still some room for optimization:
 - The top flange did not require transverse reinforcement bars, however the thickness is still based on a thickness with transverse reinforcement bars. The top flange thickness can therefore be reduced. The optimization can go even further by placing the transverse prestressing in transverse ribs.
 - For some designs the beam width can be slightly increased since the unity checks for transverse moment capacity are still a bit conservative and the shear force was also determined in a conservative way
- Besides further optimization using the optimization strategy applied during this master thesis, it is also possible to continue the optimization by applying external prestressing, which was mentioned in this report, but was not investigated:
 - External prestressing can be applied to reduce the bottom flange thickness by placing strands in the void of the box beams instead of in the bottom flange.
 - External prestressing can be combined with internal prestressing by applying additional external prestress, when concrete has reached a higher strength.
- UHPC has very favorable post-cracking behavior due to the fibers. The beams from this thesis are designed not to crack in both SLS and ULS and do not utilize this characteristic. Therefore the effects of applying partial prestressing should be investigated. The expectation is that:
 - The amount of prestressing steel will decrease significantly.
 - However, passive reinforcement would come in place. Therefore the bottom flange thickness would only reduce slightly.
 - The camber would reduce due to the low level of prestress, making deflection (minimum camber) governing, and causing beam height to increase.

It might not be favorable at all to apply partial prestress, since the beam height increases and the high compressive strength is not utilized to the fullest extent. However, it could be possible that from an economic point of view it is favorable, due to the decrease in prestressing steel. This should be investigated further.

- An economic alternative for box beams are H-beams. These beams are quite similar to box beams, but are cheaper to produce, because no EPS-filling is required to make the void. The disadvantage is however that, due to lower torsional stiffness, there is decreased load distribution in transverse direction. It is recommended that research is done on whether the UHPC H-beam are a more economical alternative for the UHPC box beam.

17 References

- [1] Resplendino, J. (2002) "AFGC Recommendations on Ultra-High Performance Fibre-Reinforced Concrete (Revised Edition, June 2013)", AFGC
- [2] Ketel, H.; Willemse R.; van Rijen, R.; Koolen E. (2011) "Rekenmodel VVUHSB", Cement Online
- [3] Fehling, E.; Schmidt, M.; Walraven, J.C.; Leutbecher, T.; Fröhlich, S. (2014) "BetonKalender – Ultra-High Performance Concrete UHPC – fundamentals – design – examples", Ernst & Sohn,
- [4] Tadros, M.K.; Morcous, G. (2008) "Application of Ultra-High Performance Concrete to Bridge Girders", University of Nebraska - Lincoln
- [5] Pacheco-Torgal F., Cabeza L. F., Labrincha J., Giuntini de Magalhaes A. (2014) "Eco-efficient Construction and Building Materials: Life Cycle Assessment (LCA), Eco-Labeling and Case Studies", Woodhead Publishing
- [6] Ten Voorde, A.; Barten, P.; Jansen, R.; Laurijssen, H. (2011), "Brugligger zonder druklaag - Nieuwe prefab LOD-H-ligger toegepast in de Ramspolbrug", Cement
- [7] Park, H. (2003), "Model-Based Optimization of Ultra-High Performance Concrete Highway Bridge Girders", Massachusetts Institute of Technology
- [8] Russell, H. G.; Graybeal, B. A. (2013), "Ultra-High Performance Concrete: A State-of-the-Art Report for the Bridge Community", U.S. Department of Transportation

18 Appendix

Appendix A: Architectural Design

1 Introduction

This chapter will investigate new design concepts for a 60m long UHPC footbridge. This chapter will use an “architectural approach’ for concept development by at first regarding solely functional aspects, aesthetics, social/emotional impact and spatial assimilation. No structural solutions and construction methods are taken in consideration yet. The main philosophy during drafting was to push boundaries and coming up with new shapes for bridges.

After concepts are developed, they will be evaluated for their structural behaviour. This evaluation will be carried out using SCIA. Based on the results of this evaluation the application of UHPC is investigated for the members of the structure. The philosophy is *to apply UHPC only when it’s needed to carry the stresses, while maintaining the shape and slenderness of the architectural design*. This means the design is fixed and material will be applied according to the stress distribution in the structure and the strengths of the material.

At the end of this chapter a design concept is presented with recommendations on where UHPC can effectively applied.

As a starting point the following functional requirements are assumed:

1. The bridge has a total span of 60m.
2. No intermediate piers are allowed to prevent traffic hindrance.
3. The bridge has a total width of 5,0m. The 5,0m will facilitate a recommended two-way cycle path of 4,0m [6], while having 0,5m left on each side for additional foot traffic and the placement of parapets.
4. In case of a roofed bridge the headroom will be 3,0m. This height is chosen so that the bridge has nice proportions and doesn’t feel cramped.
5. For the comfort of pedestrians and cyclists the bridge deck should be strictly horizontal (no slope).
6. The bridge shall be made entirely out of concrete, either UHPC or UHPC combined with conventional concrete.
7. In addition the following keywords are provided to match the identity of the bridge: iconic, innovative, aesthetic, slender.

These requirements are considered while drafting design concepts.

2 Design Concepts

The following concepts are developed as candidates for the case study design. They are developed using the design philosophy described in chapter 1 of appendix A. From these concepts three will be investigated further.

2.1 Voided Box Girder

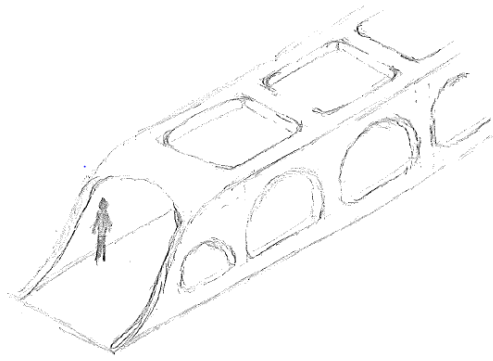


Figure 2-1: Draft Voided Box Girder

This concept is based on the frequently used box girder bridge concept. Normally traffic goes on top of the box girder, but for this concept the traffic goes through the box. This reduces the required height significantly. A large portion of surface area of the box is voided, allowing daylight and wind to go through the box. This makes the experience of passing the bridge more pleasant, than moving through a dark and isolated box. The voids have an organic shape giving the bridge a futuristic feel, while the arches on the sides, resembling ancient Roman aqueducts, also give a classic feel.



Figure 2-2: 3D Render Voided Box Girder

2.2 TopOpt-Inspired Truss

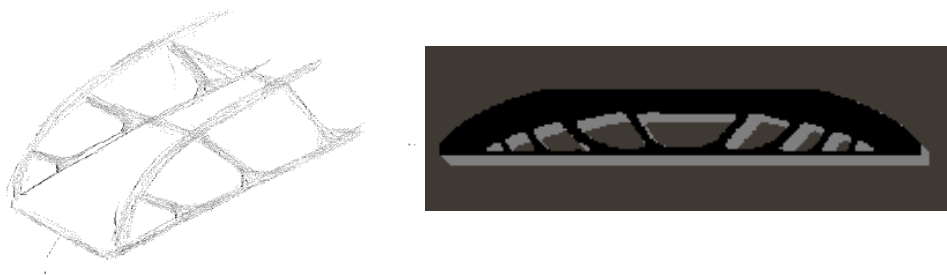


Figure 2-3: Draft TopOpt-Inspired Truss (left) & the TopOpt shape on which the concept was based on (right)

This concept is based on a shape derived from topology optimization (TopOpt). The topology optimization method is based on iteratively removing inefficient elements from an initial design space to achieve an optimized design by finding maximum stiffness with minimized material use. Therefore this design yields great stiffness. This concept is a somewhat streamlined version of the original TopOpt shape to make it more aesthetic. The TopOpt shape is found using the “Interactive 2D TopOpt App” (<http://www.topopt.dtu.dk/>). The input for the ESO is a uniformly distributed load

on a simply supported beam with a restricted height. The braces of the truss don't stand vertically but with a small angle. The braces also increase in thickness as they approach the joints at the deck.

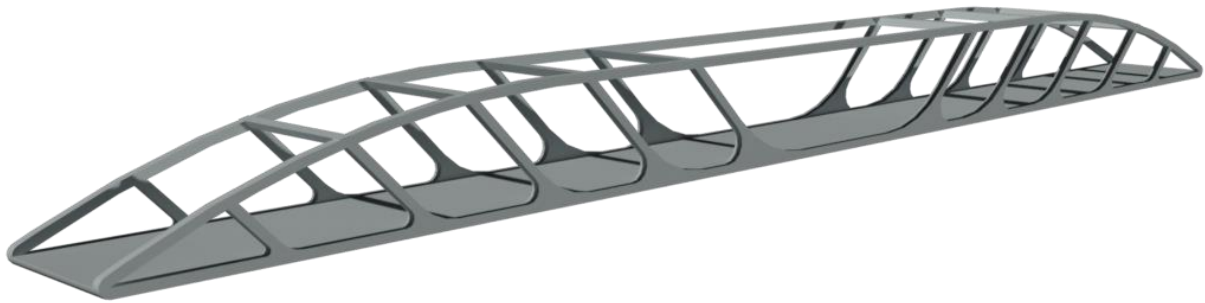


Figure 2-4: 3D Render TopOpt-Inspired Truss

2.3 Π -truss

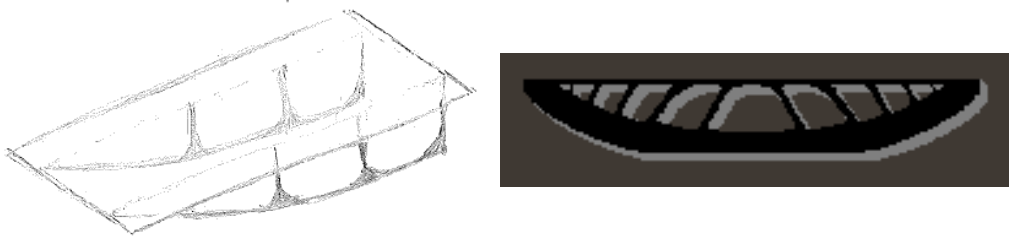


Figure 2-5: Draft Π -Truss (left) and the TopOpt shape it was inspired by (right)

This is another concept based upon an TopOpt shape, somewhat similar to the TopOpt-Inspired Truss described in the previous paragraph. This concept has the truss below the bridge deck instead of above, hiding the structural elements for the traffic on the bridge. For the traffic going under the bridge the truss is very prominent in sight. The braces stand with a small angle and increase in thickness as it approaches the deck. The trusses are not placed at the ends of the deck but slightly to middle, so it resembles



Figure 2-6: 3D Render Π -Truss

2.4 Ellipse Portal

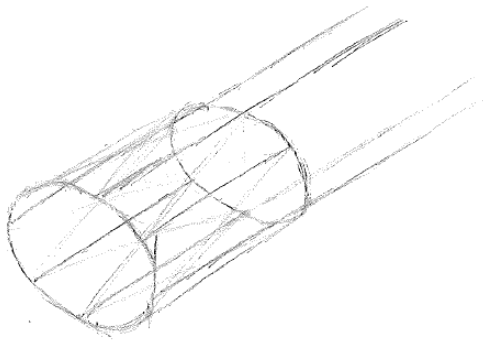


Figure 2-7: Draft Ellipse Portal

Inspired by “De Netkous”, a tram viaduct in The Hague, this concept was developed. The cylindrical shaped bridge with braces has been done a few times before, but exclusively in steel. This concept made entirely out of concrete will have a completely new look and feel because of its concrete appearance.

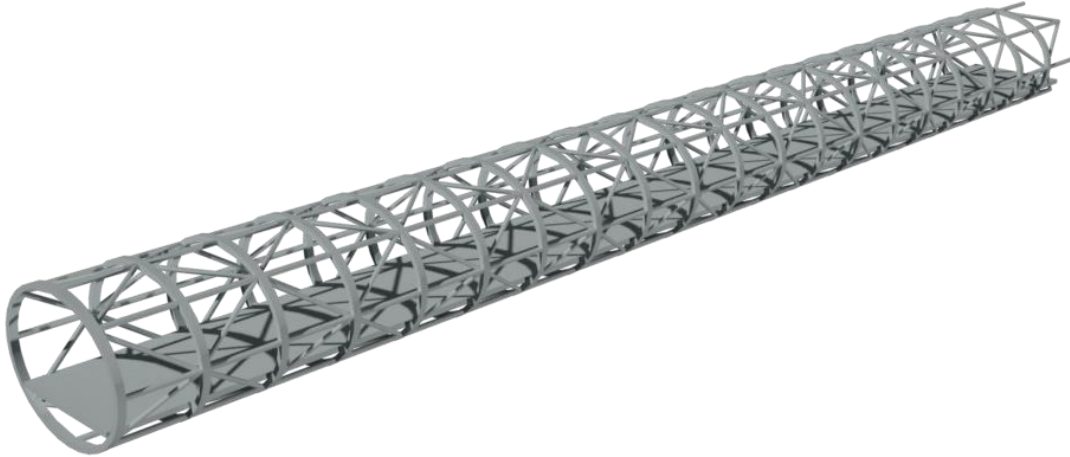


Figure 2-8: 3D Render Ellipse Portal

2.5 Diamond Portal

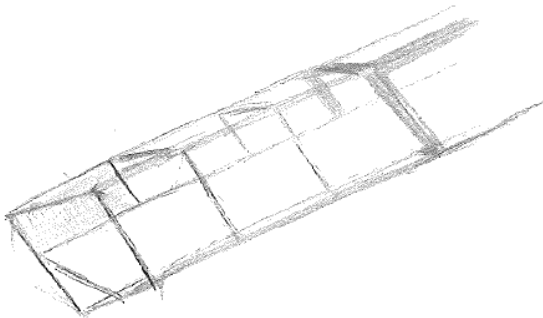


Figure 2-9: Draft Diamond Portal

Building on the “Ellipse Portal” concept from the previous paragraph, this concept was developed. Similar to the Ellipse Portal it has a constant base that connected with braces that resemble a truss.

However in this case the base is not shaped as an ellipse but as a rhombus. Travelling through rhombus-shaped portals will give a unique and futuristic experience,

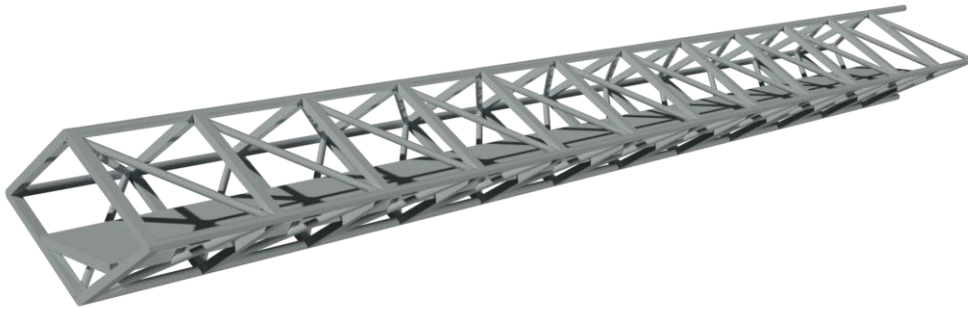


Figure 2-10: 3D Render Diamond Portal

2.6 H-girder (Prestressed Wall/Girder)

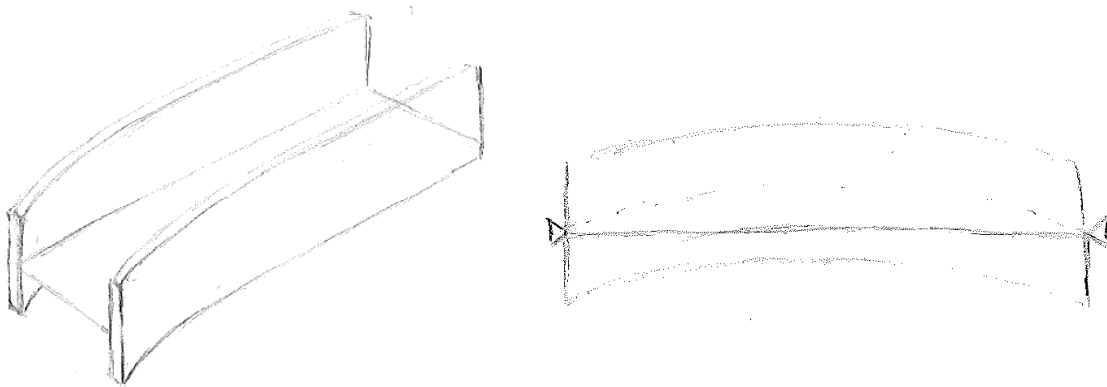


Figure 2-11: Draft H-Girder (left) and the prestressing system it was based on (right)

This concept is based on the parabolic tendon profile typically used in prestressed beams. In this case however the two beams on the sides are curved so that the tendon profile can be straight, following the alignment of the bridge deck. Moreover these beams also function as a railing in addition to being the main load bearing elements.

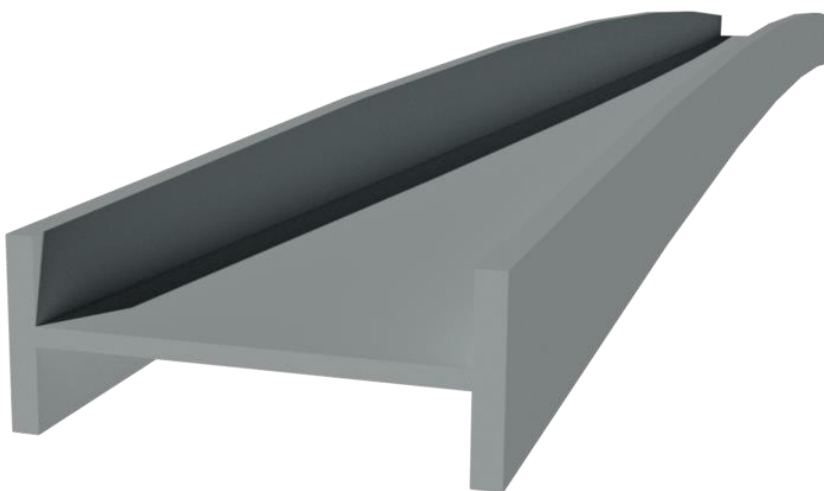


Figure 2-12: 3D Render H-Girder

2.6.1 Organic Arch

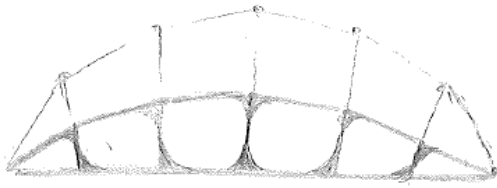


Figure 2-13: Draft Organic Arch

This concept is based on the conventional arch bridge. The ties have an organic shape at the joints with the deck, so the forces are gradually introduced without sharp angles. Moreover these ties stand at varying angles with the deck.



Figure 2-14: 3D Render Organic Arch

The three bridge concepts shown in the following figure are chosen for further investigation. They have in common, that they all have unique and challenging shapes that have not been built before. Moreover they are aesthetic for people going over the bridge as for people going under it.

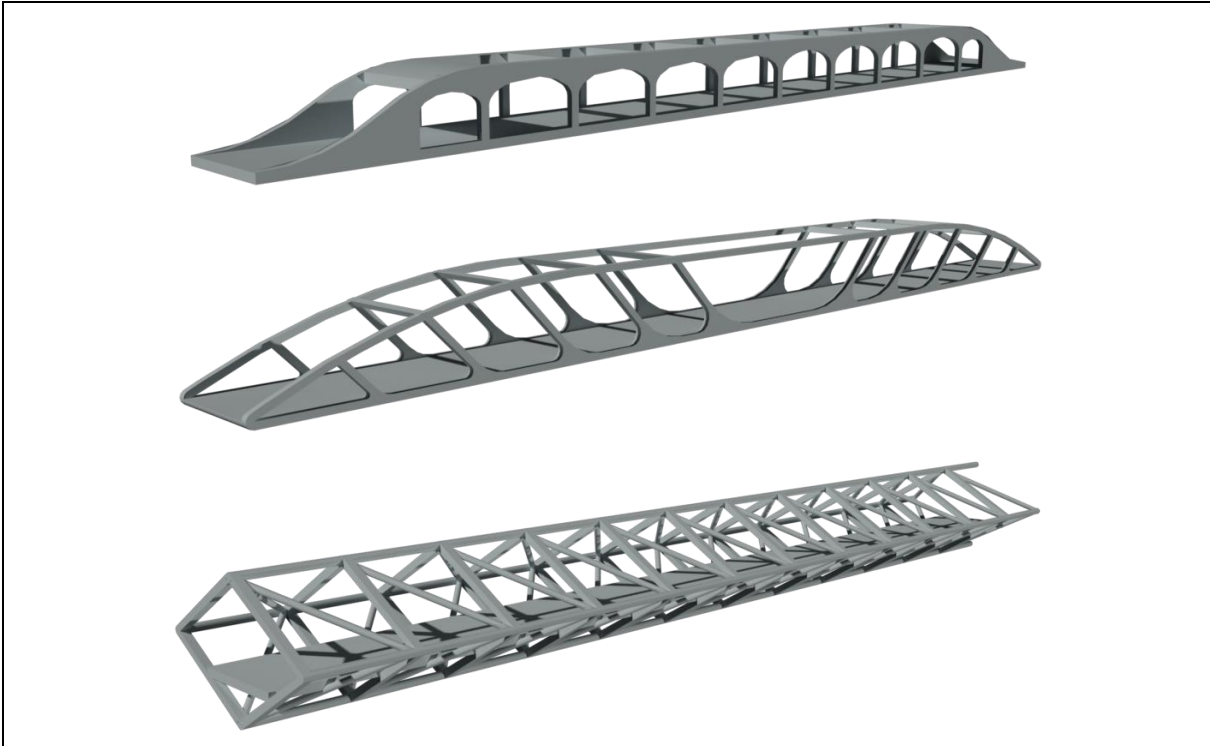


Figure 2-15: Selected Concepts (from top to bottom) "Voided Box Girder", " TopOpt-Inspired Truss" and "Diamond Portal"

The concepts shown in the following figure didn't make the cut.

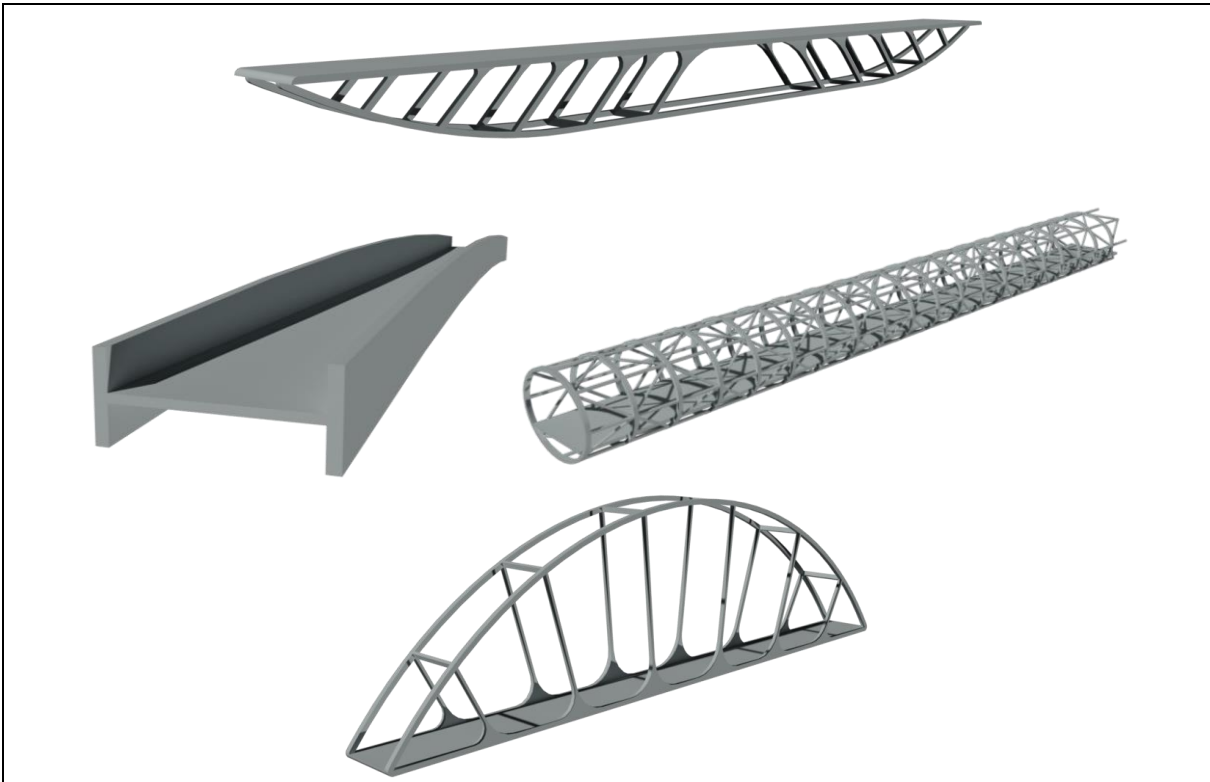


Figure 2-16: Fallen Concepts "Pi-truss" (t.l.), "H-girder" (t.r.), "Ellipse Portal" (b.l.) and "Organic Arch" (b.r.)

3 Structural Analysis

In this chapter each of the selected concepts will be discussed regarding structural behaviour. The structural behaviour will only be evaluated qualitatively, as dimensions and loading are not

determined yet. Structural analysis will be carried out using SCIA. The dimensions and loads of the model are approximated.

3.1 Structural Analysis: Voided Box Girder

Although the concept of this bridge is based on a box girder, the voids affect the structure in such a way that its behaviour is more comparable with either a Vierendeel truss. A Vierendeel truss is a special case of a truss. In contrast to a conventional truss the Vierendeel truss has no triangular member configuration but has rectangular shaped openings. In order to accommodate this shape the truss contains moment resisting joints. The bridge can be modelled to this type of structure. In that case the bridge deck acts as a tensile bottom chord. The sides of the roof, where it is uninterrupted longitudinally, act as compressive top chords. The columns of the portals act as ties.

To describe the structural behaviour the structure will be divided in the member types as described above, which are top chord, bottom chord and ties. Their behaviour is described by determining the three member forces: axial force (tension/compression), shear force and bending moments.

To verify the structural behaviour the concept is modelled as a simply supported 60m long Vierendeel truss in SCIA. The loading is modelled as uniformly distributed load of 4,0kN/m on the bottom chord without any self-weight. For now the behaviour of the structure is determined only qualitatively, so the exact values are not relevant.

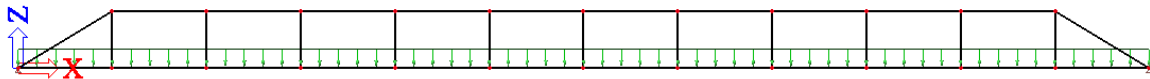


Figure 3-1: SCIA model of the Voided Box Girder with variable loading

Results for axial forces are shown below. Blue lines and numbers represent tensile forces and red represents compression forces. As stated before the top chord takes up compression forces that increase up to midspan. The bottom chord takes up tensile forces that also increase up to midspan. The vertical members only take up relatively small tensile forces.

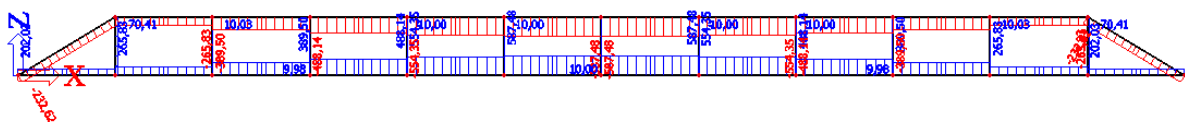


Figure 3-2: Axial forces Voided Box Girder (overview)

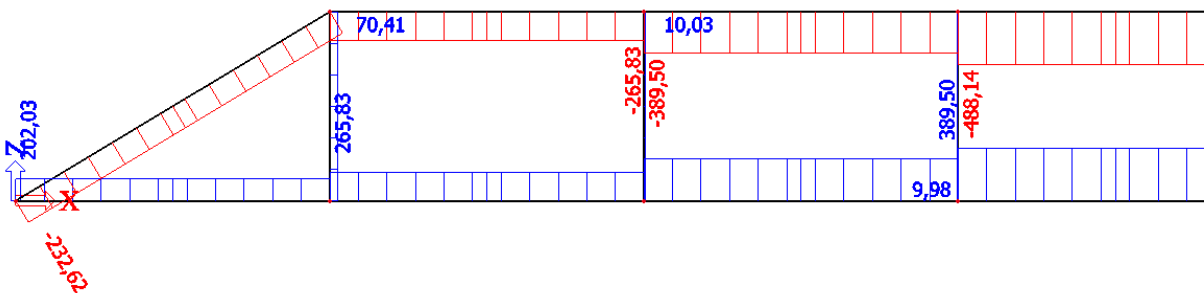


Figure 3-3: Axial forces Voided Box Girder (zoomed in)

the structure takes up higher stresses, is more prone to buckling and the diagonals take up relatively more axial forces and less shear forces and bending moments. A more elaborate description of its behaviour can be found in paragraph **Error! Reference source not found.**

To verify the structural behaviour the concept is modelled as a simply supported 60m long Vierendeel truss in SCIA somewhat similar to the Voided Box Girder. The only difference with the Voided Box Girder is that for the vertical members the bottom joints are slightly shifted to midspan, so the members stand diagonally.

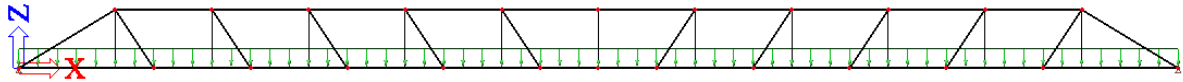


Figure 3-8: SCIA model of the TopOpt-inspired truss with variable loading

The axial forces are shown below. It shows similar behaviour as the Vierendeel truss model for the Voided Box Girder. However the normal tensile forces in the braces are significantly higher because these members are diagonal instead of vertical.

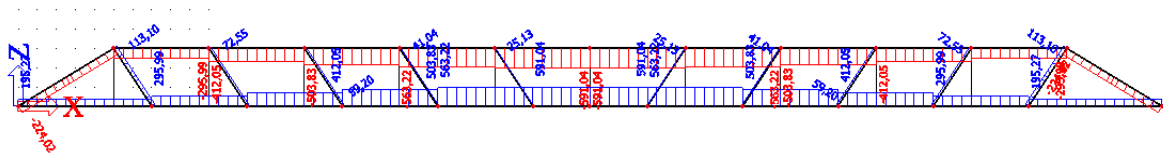


Figure 3-9: Axial forces TopOpt-inspired Truss (overview)

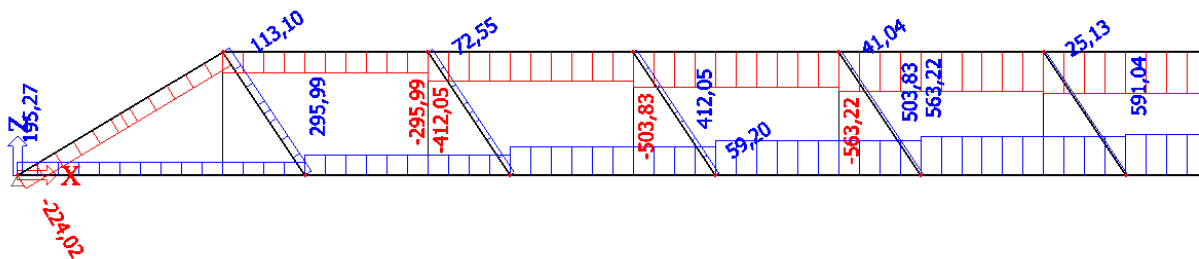


Figure 3-10: Axial forces TopOpt-inspired Truss (zoomed in)

The shear forces decrease as the members are closer to midspan similar to the modelled Voided Box Girder. However the shear forces are smaller for this concept, due to the diagonal members. These diagonal members can avoid shear forces, while attracting more axial forces.

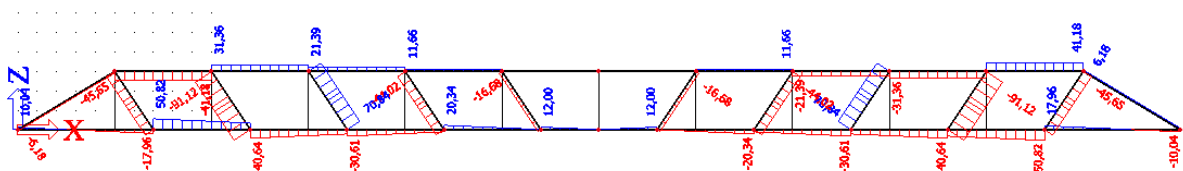
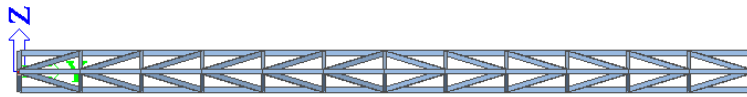


Figure 3-11: Shear forces TopOpt-inspired Truss (overview)



To simplify the model only the self-weight, which is the most significant loading, is taken in consideration. Also a constant cross-section and material is used to model the members. The values are not relevant as this investigation is purely to qualitatively investigate the structural behaviour. The members are divided in three groups: chord members (horizontal longitudinal members), portal members (members in y-plane) and diagonal members. For the members groups the member forces are investigated, namely axial forces (N), shear forces in y- and z-plane (V_y, V_z) and bending moments in x-, y- and z-plane (M_x, M_y, M_z).

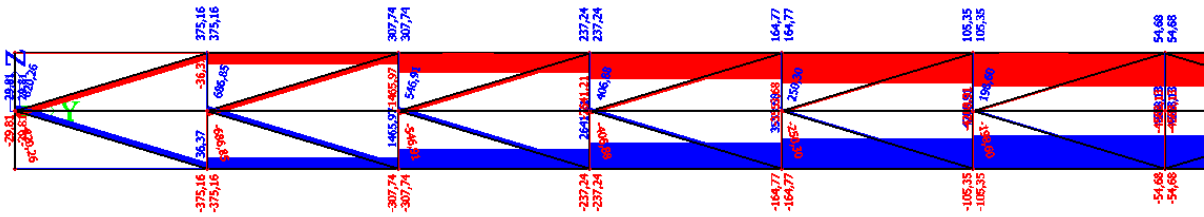


Figure 3-15: Axial forces from self-weight only (side view)

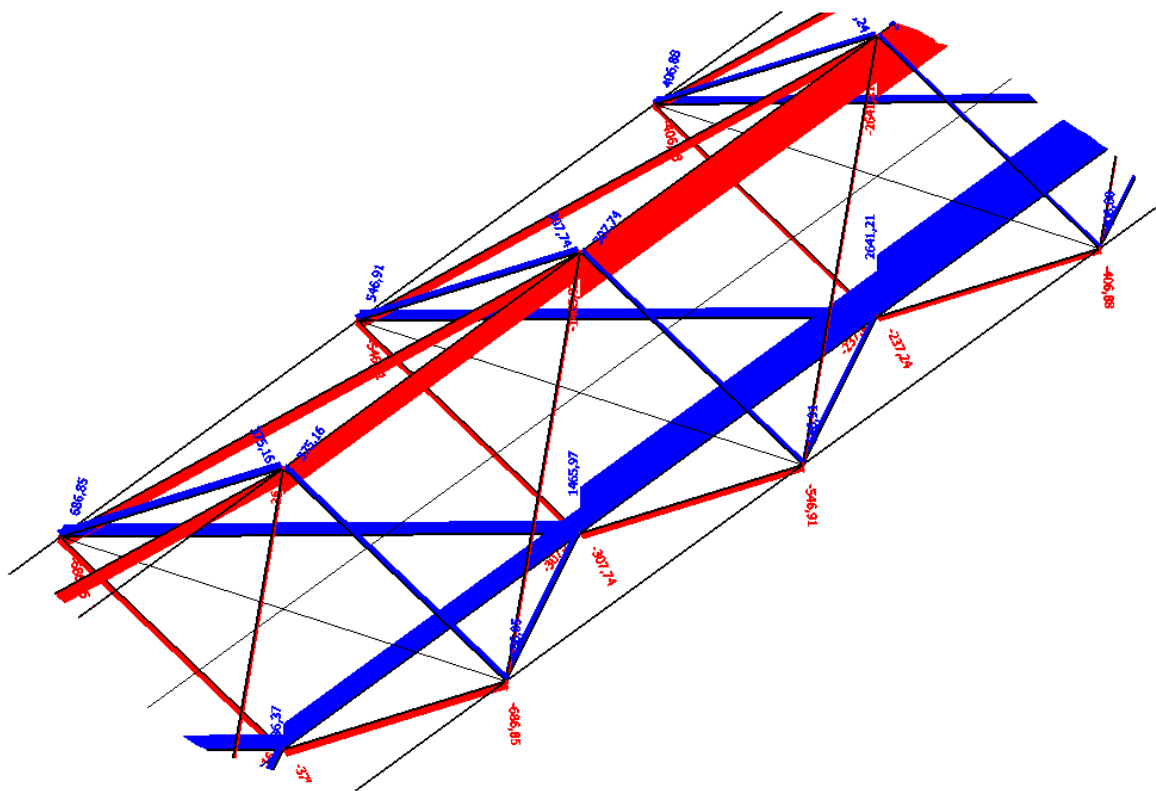


Figure 3-16: Axial forces from self-weight only (isometric partial view)

4 Structural Solutions

The need for application of UHPC in a structure depends on the stresses in the structure and the strength of the material. UHPC specifically excels in compression strength, so naturally it should be applied in members that have to resist very high compressive stress.

However the high compressive strength in combination with the increased tensile capacity can also provide benefits for the bending members. The high compressive strength increases the bending moment capacity in the compression zone and the tensile strength and ductility adds to the tension force that normally is taken up exclusively by the reinforcement bar. So for bending members cross-sections can also be decreased, when UHPC is applied, although this is not very effective compared to pure compressive members as the high compressive strength is only utilized by a small compression zone and reinforcement bars still carry most of the tension, instead of over the whole cross-section.

However UHPC members can be applied very effectively to resist shear force. UHPC has excellent shear capacity and takes away the need for shear reinforcement, which decreases complexity of reinforcement cages and is beneficial for the amount of bar bending labour.

Although UHPC has a low tensile strength. It still has significantly more tensile strength than NSC. So for members under very low tensile stress it can even perform without reinforcement bars, without the need for very large cross-sections. It can also be applied to reduce cross-sectional size of members. But since it is also very expensive, it is advised only to apply it when cross-sections get very large and small cross-sections are required.

4.1 Structural Solutions: Voided Box Girder

Unfortunately a Vierendeel truss does not have members that exclusively or mostly contain compressive stress, unless they are prestressed. Most members will contain high tensile stresses due to bending moments at the joints. So for this type of structure the most obvious and effective possibility of application is ruled out. However the moment resisting joints in a Vierendeel truss can also benefit from UHPC. The higher bending moment capacity can decrease the required volume of concrete. Moreover because all members in a Vierendeel are shear members, applying UHPC can be an effective way to prevent the need for shear reinforcement.

Member	Loading	Solution
Bottom Chord	High compressive stress Even higher tensile stress Especially around joints Small shear stress	UHPC girders, with either passive reinforcement or prestress
Top Chord	High tensile stress Even higher compressive stress Especially around joints High shear stress	UHPC girders, with either passive reinforcement or prestress. Some members around midspan suffice with UHPC without steel reinforcement bars
Ties	Shear member High axial bending stresses Very high shear stress	UHPC column, with either passive reinforcement or prestress
Roof beams	Only loaded, when structure is loaded by horizontal loads, Low stresses	NSC
Deck slab	Low stresses	NSC slab

Table 4-1: Summary member loading and materials for Voided Box Girder

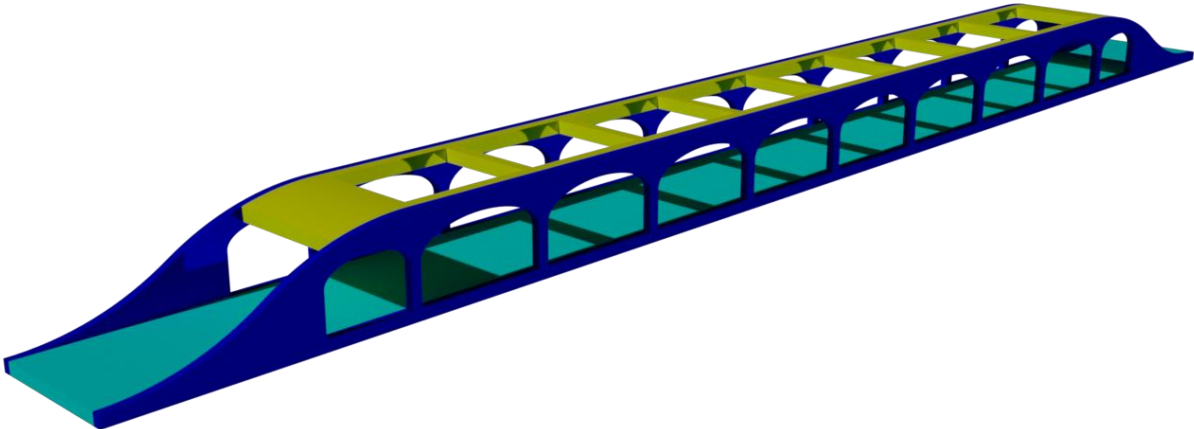


Figure 4-1: Voided Box Girder member materials indicated by colour; yellow for NSC; blue for reinforced UHPC; cyan for NSC voided slab

4.2 Structural Solutions: TopOpt-Inspired Truss

Because of the similarities with the Voided Box Girder reference is made to the structural solution of this concept. However, some differences have to be mentioned. The members are considerably smaller in this concept. For this reason the application of UHPC to decrease cross-section size is of more importance to the TopOpt-inspired truss than to the Voided Box Girder.

Member	Loading	Solution
Bottom Chord	High compressive stress Even higher tensile stress Especially around joints High shear stress	UHPC girder, with either passive reinforcement or prestress
Top Chord	High tensile stress Even higher compressive stress Especially around joints High shear stress	UHPC girders, with either passive reinforcement or prestress. Some members around midspan suffice with UHPC without steel reinforcement bars.
Ties	Shear member High axial bending stresses High shear stress	UHPC column, with either passive reinforcement or prestress
Roof beams	Only loaded, when structure is loaded by horizontal loads, Low stresses	NSC
Deck slab	Low stresses	NSC slab

Table 4-2: Summary member loading and materials for TopOpt-inspired Truss

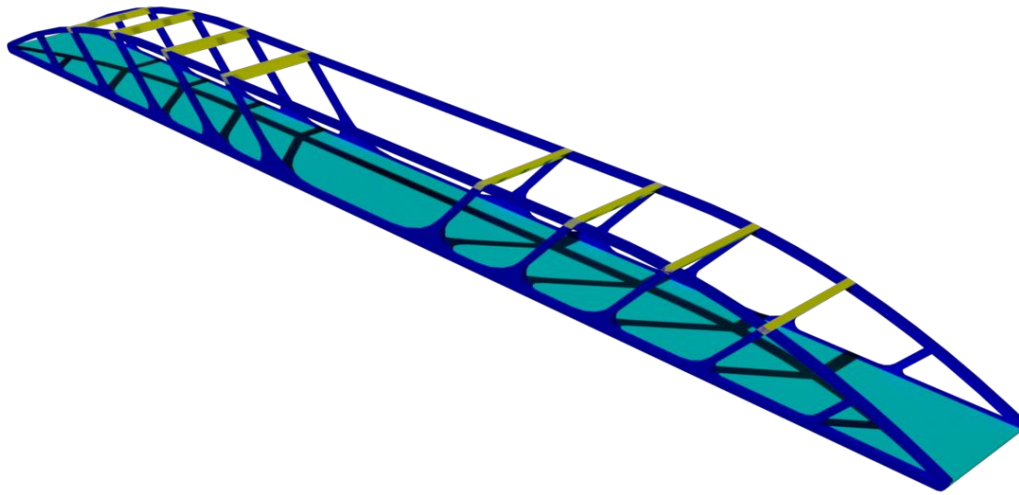


Figure 4-2: TopOpt-inspired Truss member materials indicated by colour; yellow for NSC; blue for reinforced UHPC; cyan for NSC voided slab

4.3 Structural Solutions: Diamond Portal

Because the Diamond portal actually has members that solely have to resist very high compressive stresses, UHPC can be efficiently be applied in these parts of the structure. This holds for the top chord, especially at midspan, where very high compressive stress is expected. Applying UHPC in the bottom chord can also be beneficial. The high tensile strength can decrease the cross-sectional size, which can be necessary due to high tensile stresses that occur in the bottom chord. Furthermore there are members that have to resist high axial bending stresses, such as the portal members. These can also benefit from the application of UHPC, although this is not as effective as for pure compression members. It is however very effective for resisting the shear stresses as it can allow the omitting of shear reinforcement. The diagonals can be executed in NSC, since they carry low stresses.

In conclusion the Diamond Portal allows some elements to be very effective when applied in UHPC, such as the top and bottom chord. Cross-sections can significantly be reduced with this material. However most members like the diagonals don't really need UHPC or don't fully utilize the excellent properties of UHPC like the portals. However the high shear strength allows UHPC members to resist shear stresses without the need for shear reinforcement.

Member		Loading	Solution
Chords	Top	Very high compression Low shear	UHPC
	Bottom	Very high tension Low shear	UHPC with passive reinforcement or prestress
	Side	Some axial force from bending moments Low shear	NSC, possibly UHPC when shear strength doesn't suffice
Portals	Top	Medium tension Low compression Medium shear	UHPC possibly with passive reinforcement or prestress
	Bottom	Medium compression Low tension Medium shear	UHPC possibly with passive reinforcement or prestress
Diagonals	Top	High compression Low tension Low shear	NSC
	Bottom	High tension Low compression Low shear	NSC
Deck slab		Some axial force from bending moments High shear	UHPC

Table 4-3: Summary Member forces and structural solutions

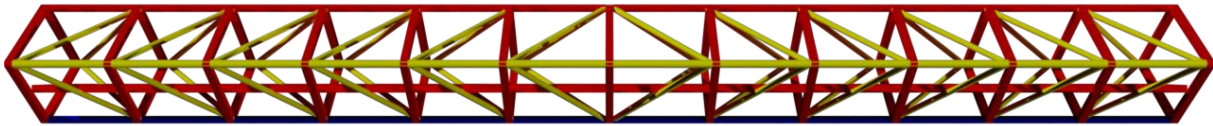


Figure 4-3: Member materials indicated by colour (red for UHPC; yellow for NSC; blue for reinforced UHPC)

Appendix B: Topology Optimization

1 Method

Topology optimization will be executed using Altair OptiStruct. OptiStruct is capable of topology optimization with multiple load cases. Moreover it can run optimizations with a wide range of different types of objectives and constraints.

The student edition is limited to models with 10.000 nodes. This will limit the size of the design space and the number of elements. A small design space limits the free distribution and can be an unwanted constraint, if there is actually a possibility to further optimize the structure outside the design space. A small number of elements leads to a coarser mesh and will result in decreased optimization. To maintain a fine mesh with the limited amount of nodes, the model will be 2D, which is acceptable since the bridge will have a small width in comparison to the length and height.

The following steps are taken to obtain the desired results:

1. Define design space (and non-design space)
2. Specify mesh
3. Specify boundary conditions (load cases and supports)
4. Material Input
5. Define optimization objectives and constraints
6. Run optimization and evaluate results
7. If required: update model and repeat from step 1

1.1 Design space and mesh

Initially the design space will be defined as a 2D rectangle with a length of 60m and a height of 10m. The bottom 0,25m of the design space is the bridge deck, which is fixed. On top of the bridge deck 9,75m of free design space is located.

The mesh should be balanced to remain short calculation time, while also obtaining a detailed optimized structure. Moreover the only 10.000 nodes are allowed. Initially quad elements with a size of 250mm are chosen.

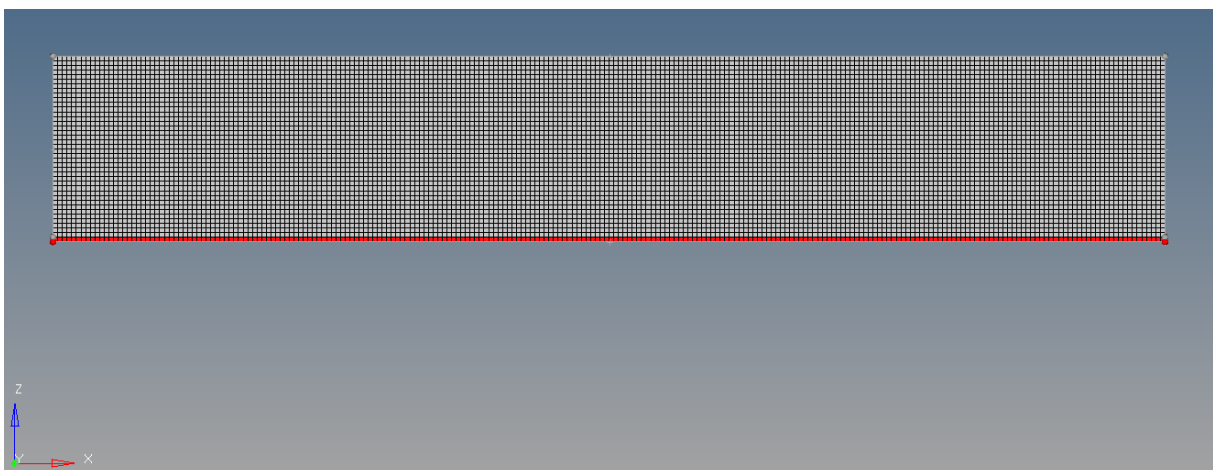


Figure 1-1: Design space and mesh for topology optimization

Note that since the design is chosen as such, the optimization is already limited to material distribution above the deck. No material shall be distributed below. The two main reasons for this choice are:

- Minimum overhead clearance for traffic below the bridge
- Node limitation

1.2 Boundary conditions

A simply supported beam is assumed, so the supports will be defined as hinged supports at each end below the bridge deck. Different load combinations can be taken into account using load steps. The load combinations that will be accounted for are all combinations of either nodal loading or no nodal loading at 5 different nodes. This comes to a total $2^5 = 32$ load combinations.

1.3 Objectives and constraints

Different objectives and constraints can be investigated. However OptiStruct can only handle multiple load cases for certain optimization responses. An available and most relevant optimization method that will be carried out is:

Objective	Constraint
Minimum weighted compliance	Volume fraction

Table 1-1: Objective and constraint for topology optimization

Although constraining the buckling factor is quite relevant, OptiStruct does not allow this for topology optimization. Also dynamic loading/response will not be investigated.

2 Results

First a test model with only 16 load combinations is executed to make sure the load step system works:

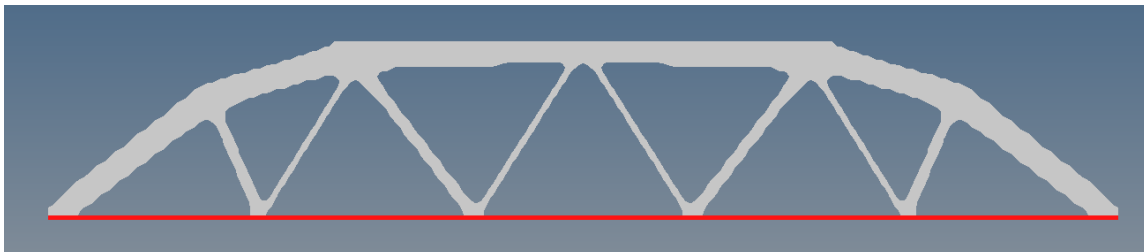


Figure 2-1: Minimum compliance optimization with four points that either carry a downward vertical force or not, leading to an optimization problem with 16 load combinations

Since it seemed to be working correctly the extra load combinations up to 32 are included:

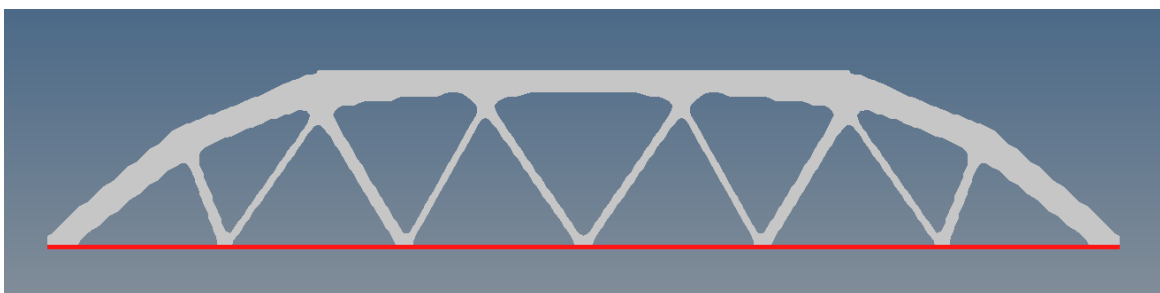


Figure 2-2: Minimum compliance optimization with five points that either carry a downward vertical force or not, leading to an optimization problem with 32 load combinations

Since it seemed that the height is restricting the structure at the top, elements are halved in the x-direction, making the model 30m long. These elements are placed on top of the model doubling the height:

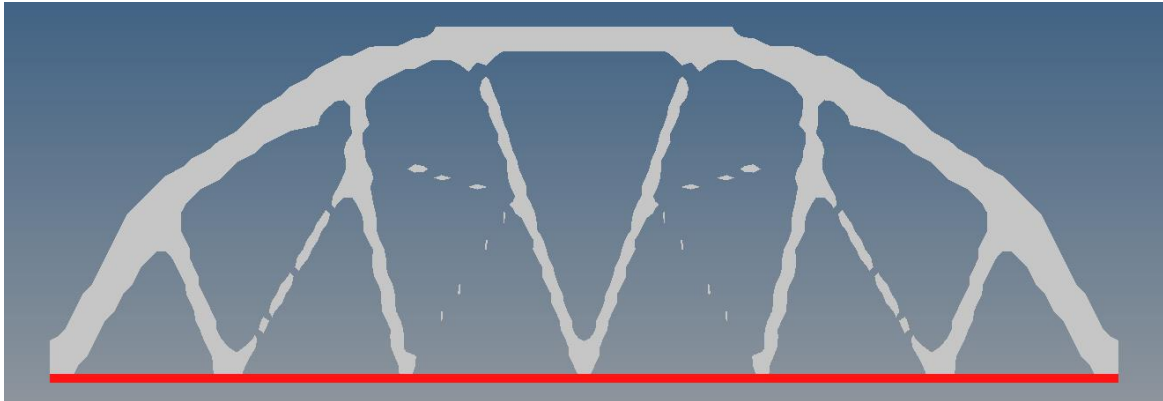


Figure 2-3: Figure 2-4: Minimum compliance optimization without height restriction with five points that either carry a downward vertical force or not, leading to an optimization problem with 32 load combinations

This resulted in an arch bridge with diagonal ties. Clearly the ties follow the positioning of the nodal loads. This is obviously only an optimal solution, if loads only occur at these positions, which is not a realistic assumption. An optimal solution for more realistic loading, of course result in an infinite number of combinations.

3 Other Results

In earlier stages of the topology optimization research other methods were used, which later were deemed incorrect. They are shown in the following paragraphs.

3.1 Method

Topology optimization will be executed using Altair OptiStruct. OptiStruct is capable of topology optimization with multiple load cases. Moreover it can run optimizations with a wide range of different types of objectives and constraints.

The student edition is limited to models with 10.000 nodes. This will limit the size of the design space and the number of elements. A small design space limits the free distribution and can be an unwanted constraint, if there is actually a possibility to further optimize the structure outside the design space. A small number of elements leads to a coarser mesh and will result in decreased optimization. To maintain a fine mesh with the limited amount of nodes, the model will be 2D, which is acceptable since the bridge will have a small width in comparison to the length and height.

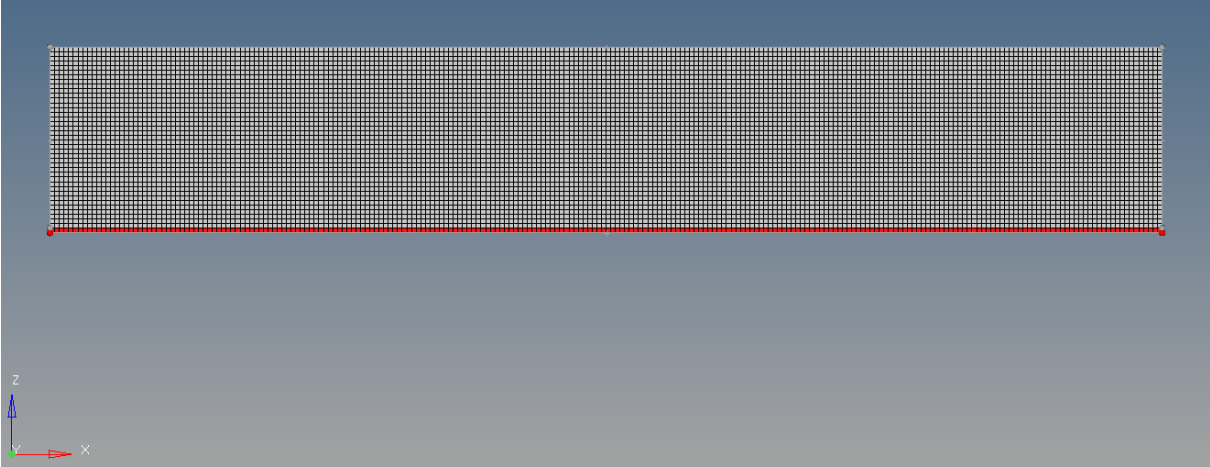
The following steps are taken to obtain the desired results:

8. Define design space (and non-design space)
9. Specify mesh
10. Specify boundary conditions (load cases and supports)
11. Material Input
12. Define optimization objectives and constraints
13. Run optimization and evaluate results
14. If required: update model and repeat from step 1

3.1.1 Design space and mesh

Initially the design space will be defined as a 2D rectangle with a length of 60m and a height of 10m. The bottom 0,25m of the design space is the bridge deck, which is fixed. On top of the bridge deck 9,75m of free design space is located.

The mesh should be balanced to remain short calculation time, while also obtaining a detailed optimized structure. Moreover the only 10.000 nodes are allowed. Initially quad elements with a size of 250mm are chosen.



3.1.2 Boundary conditions

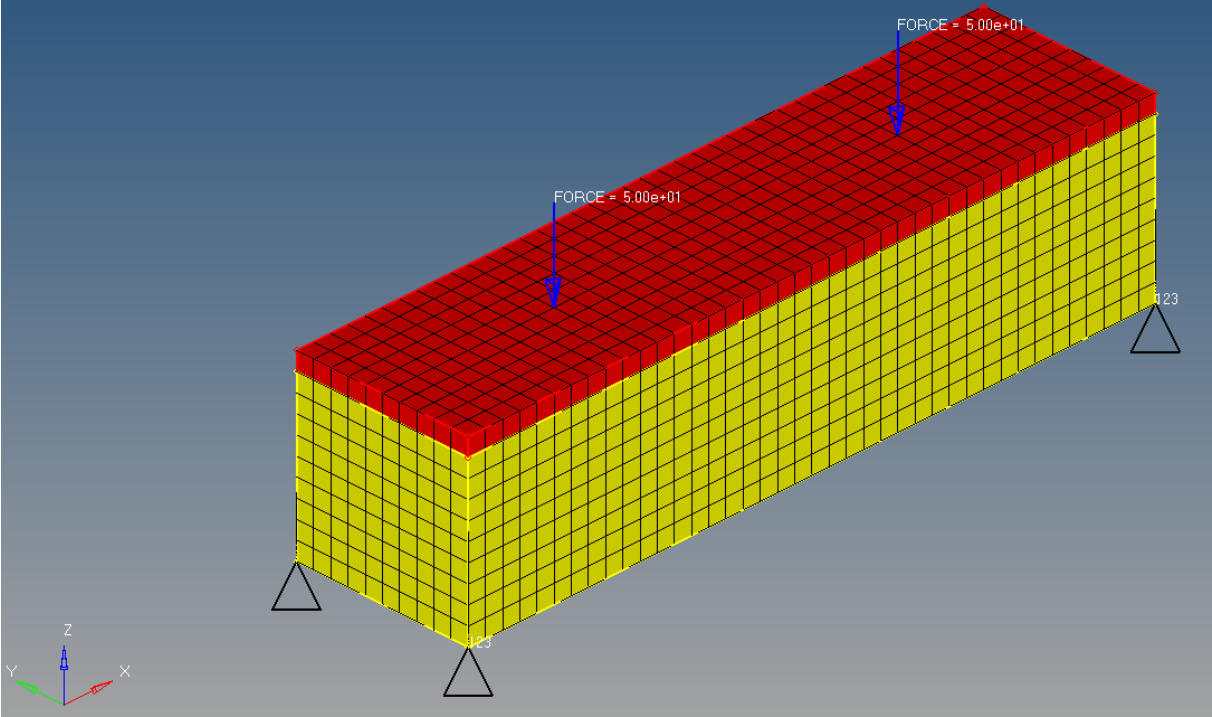
A simply supported beam is assumed, so the supports will be defined as hinged supports at each end below the bridge deck. Different load combinations can be taken into account using load steps. The following load steps will be used in the optimization:

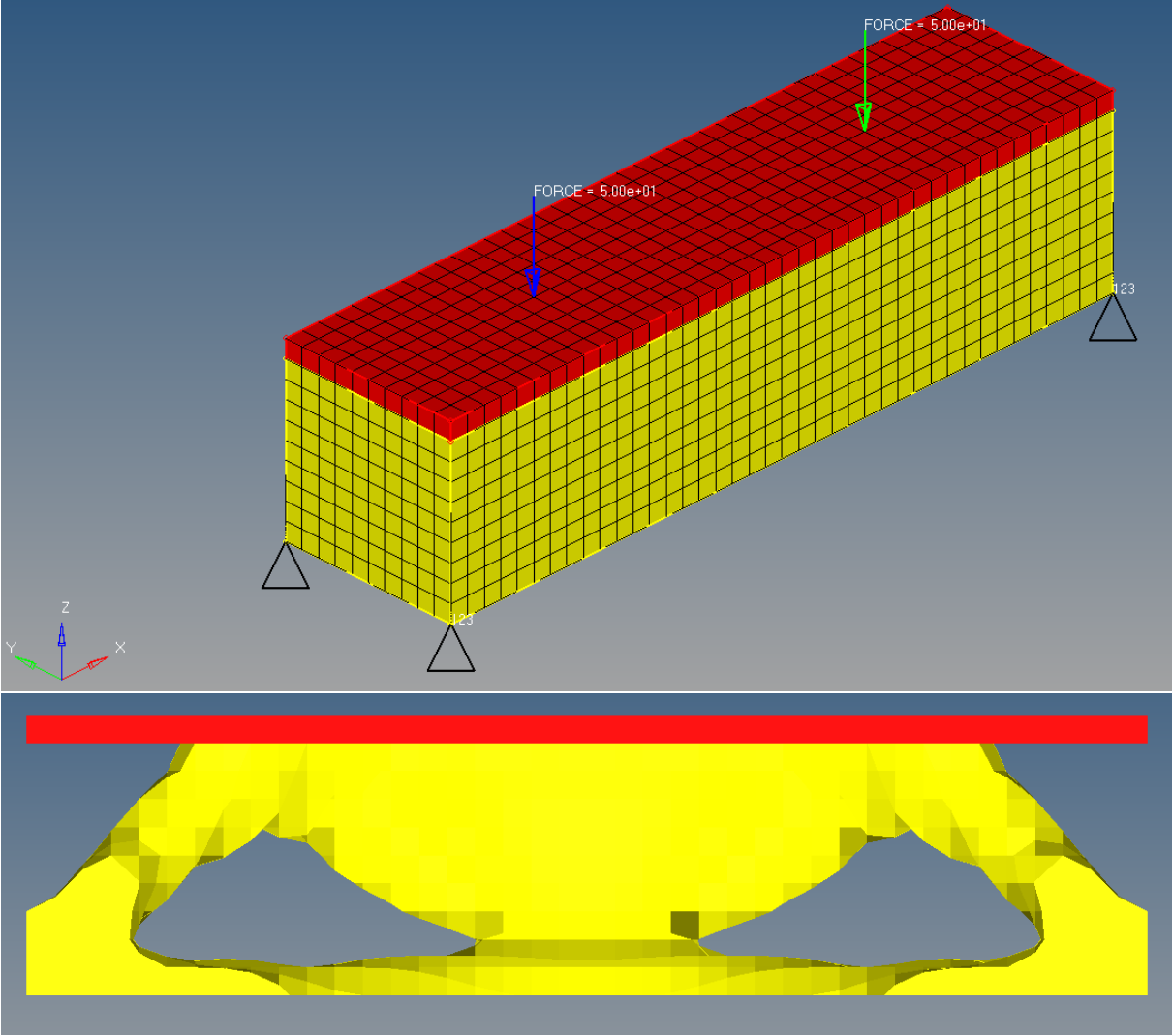
Combination	Loading	Magnitude	Location	# load steps
1	Self-weight	-	Whole span	1
	Full crowd	5 kN/m	Whole span	
2	Self-weight	-	Whole span	5
	Reduced crowd	4 kN/m	Whole span	
	Service vehicle	50 kN	At 5 different locations	
3	Self-weight	-	Whole span	5
	Accidental vehicle	120 kN	At 5 different locations	

Table 3-1: Load combinations that will be investigated

A total of 11 load steps will be set.

Below the difference between one and two load cases are shown for optimization to minimum weighted compliance, proving that OptiStruct works with multiple loadcases.





3.1.3 Material Input

Material properties determined during the literature study of this thesis are used to define the material properties. OptiStruct works with several “material data cards”, representing different types of material behaviour. The material card that matches the constitutive laws of UHPC must be chosen. (The card is not determined yet. There might not be a card available that matches entirely, but there are plenty cards that can model several types of elastic-plastic behaviour.)

3.1.4 Objectives and constraints

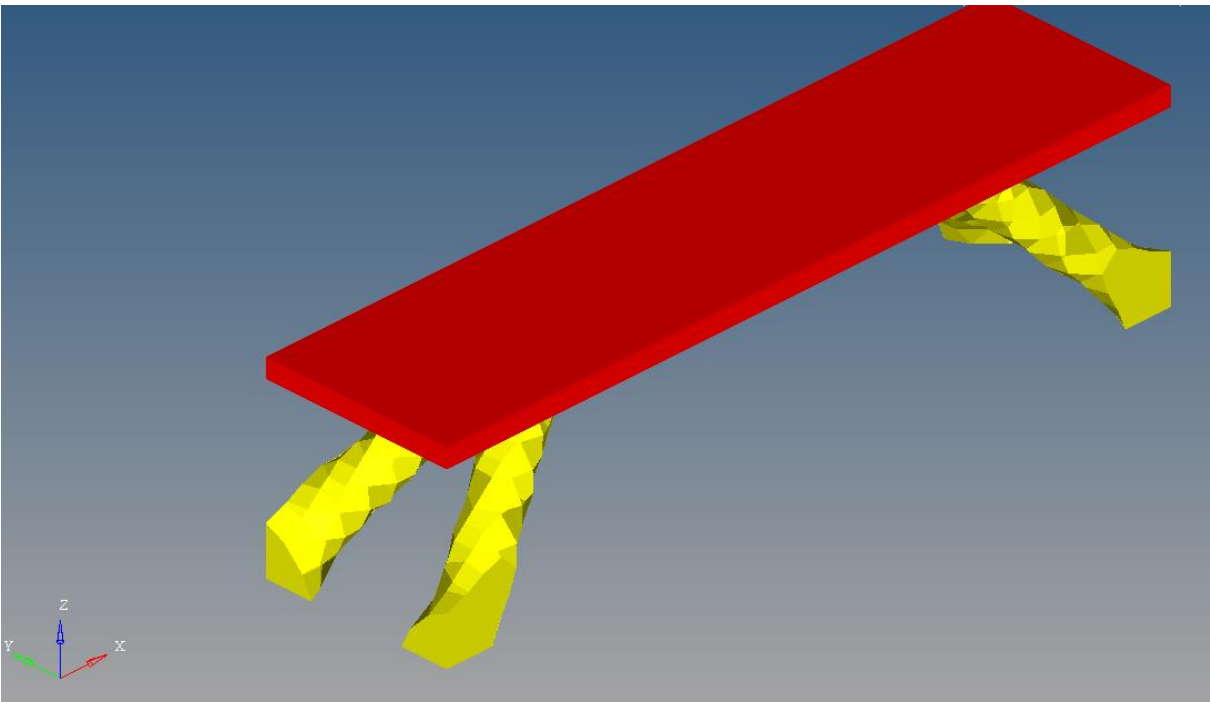
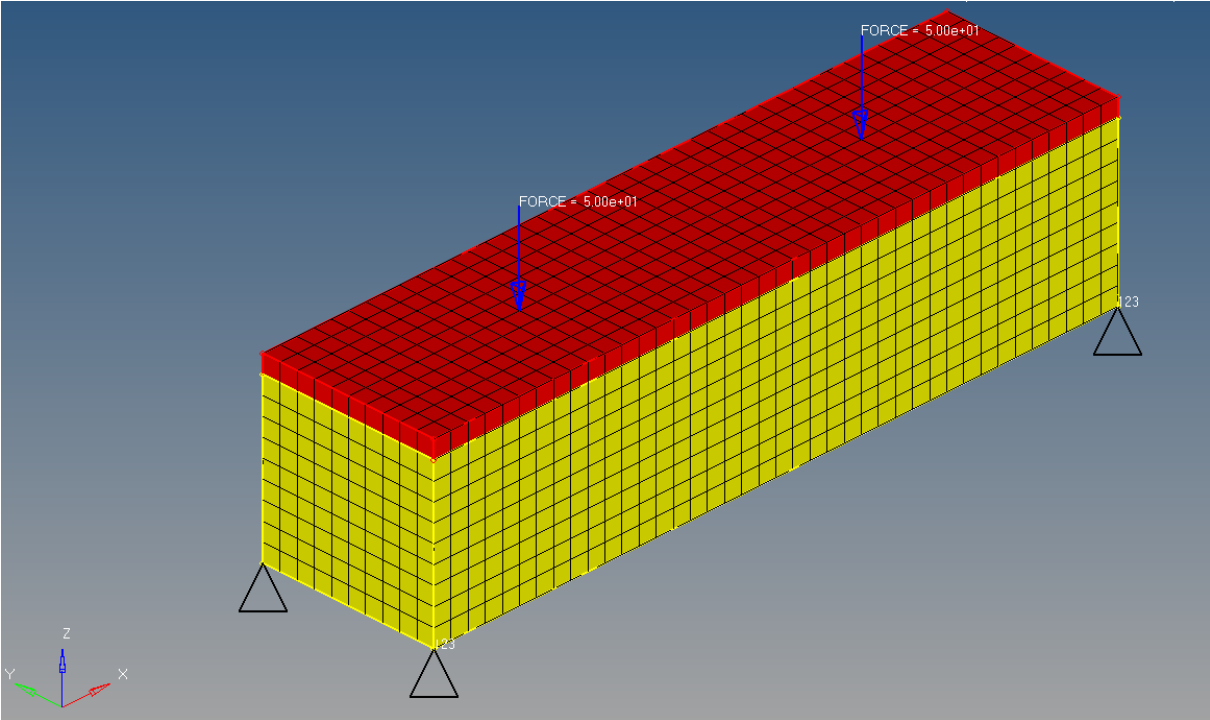
Different objectives and constraints can be investigated. However OptiStruct can only handle multiple loadcases for certain optimization responses. Available and relevant optimization methods that will be carried out include:

Objective	Constraints
Minimum weighted compliance	Volume fraction
Minimum volume	Stress

Table 3-2: Objectives and constraints for topology optimization

Although constraining the buckling factor is quite relevant, OptiStruct does not allow this for topology optimization. Also dynamic loading/response will not be investigated.

Below an example is shown for a topology optimization, with minimizing volume as objective and static stress as constraint.



Literature on two-material topology optimization is available. These consider optimal distribution of both concrete and passive reinforcement/prestressing. OptiStruct cannot do this. However it is possible to apply prestress in the topology optimization as external forces. These will be modelled as two nodal forces on the sides of the design space at the height of the bridge deck pointing inwards.

3.1.5 Evaluation

If the result does not turn out to be as expected, it could be that the method described above is not correct/suitable. In that case the method should be modified. If the results seem to be correct, efforts could be made to optimize the results in case the time allows.

3.2 2D Results

Limitations:

- Only minimum compliance investigated
- Non-linearity of concrete not taken into account

3.2.1 2D shell elements with 5 load combinations

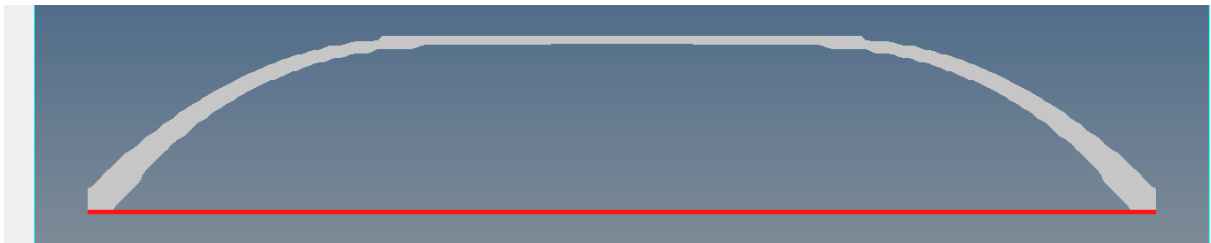
- (Self-weight + Crowd loading + Service Vehicle) x 5



This yields a structure with a compression arch only. The fixed deck elements serve as a tie.

3.2.2 2D shell elements with 1 load combinations

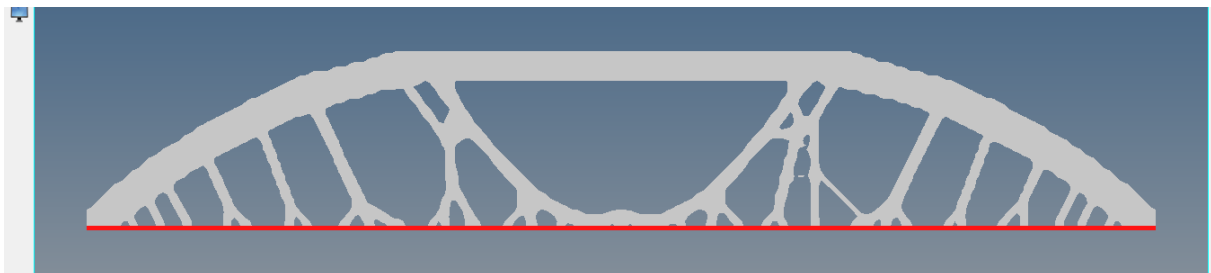
- (Self-weight + Crowd loading)



This optimization yields the same results as the one that includes the vehicle loads. Apparently it is not significant compared to the self-weight and crowd loading.

3.2.3 2D shell elements with 5 load combinations

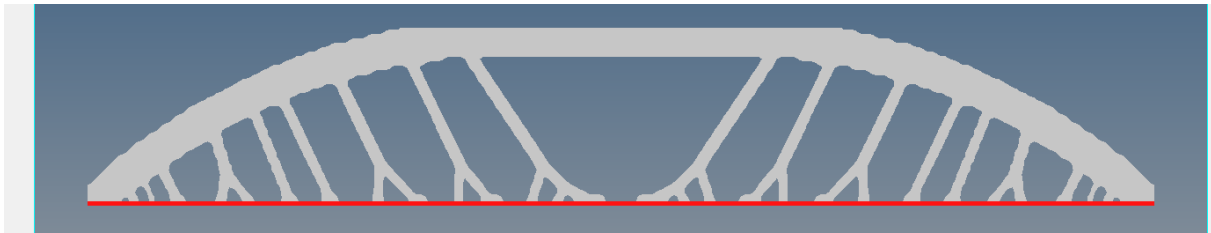
- (Crowd loading + Service Vehicle) x 5



Without the self-weight included diagonal ties are introduced. These increase the shear stiffness.

3.2.4 2D shell elements with 1 load combinations

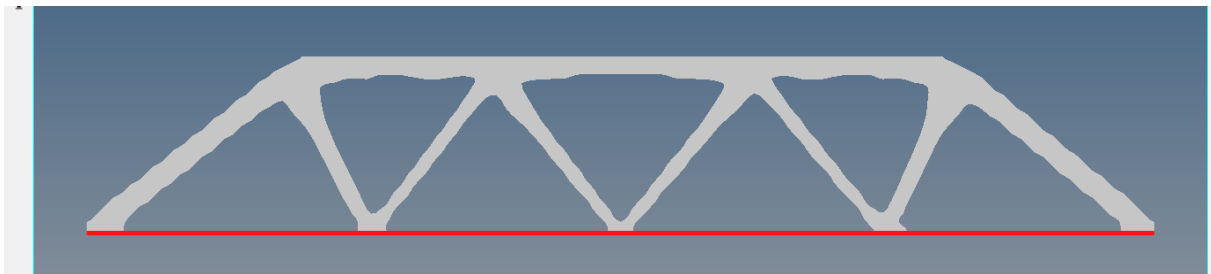
- Crowd loading



Without the vehicle combinations are excluded not much is changed. Only some the material is more evenly distributed, such as less material at midspan and more in the intermediate area between midspan and the supports.

3.2.5 2D shell elements with 5 load combinations

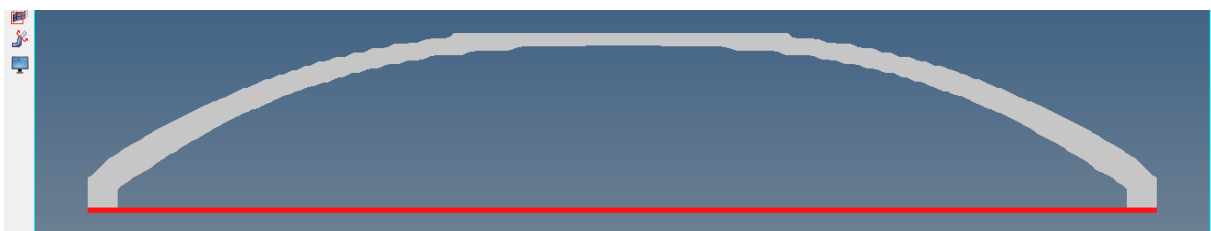
- (Service Vehicle) x 5



When only the vehicle load is applied, a conventional truss is found. It is seen directly where the loads have been modelled, except for the 2 loads close to the supports.

3.2.6 2D shell elements with 5 load combinations

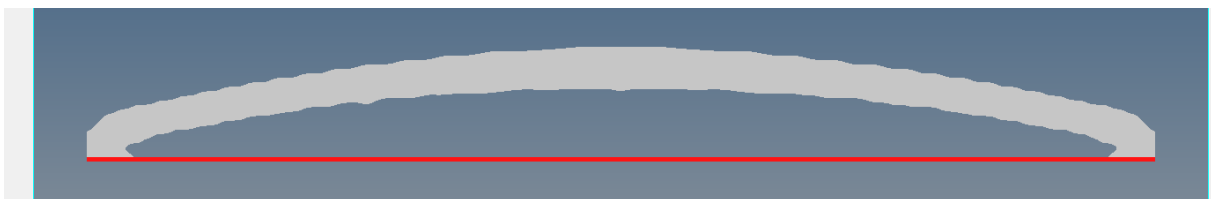
- (Self-weight + Crowdloading + Service Vehicle + Prestress) x 5



When the tie is prestressed to reduce the tensile stress, the compression arch lowers.

3.2.7 2D shell elements with 5 load combinations

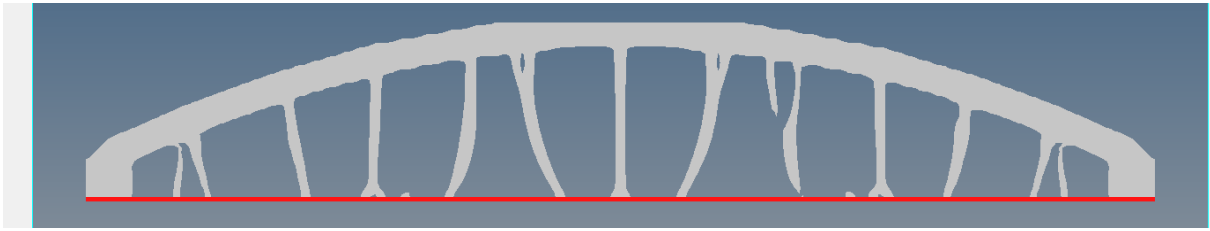
- (Self-weight + Crowdloading + Service Vehicle + Increased Prestress) x 5



When the prestressing force is increased, the arch lowering effect increases as well.

3.2.8 2D shell elements with 5 load combinations

- (Crowdloading + Service Vehicle + Prestress) x 5

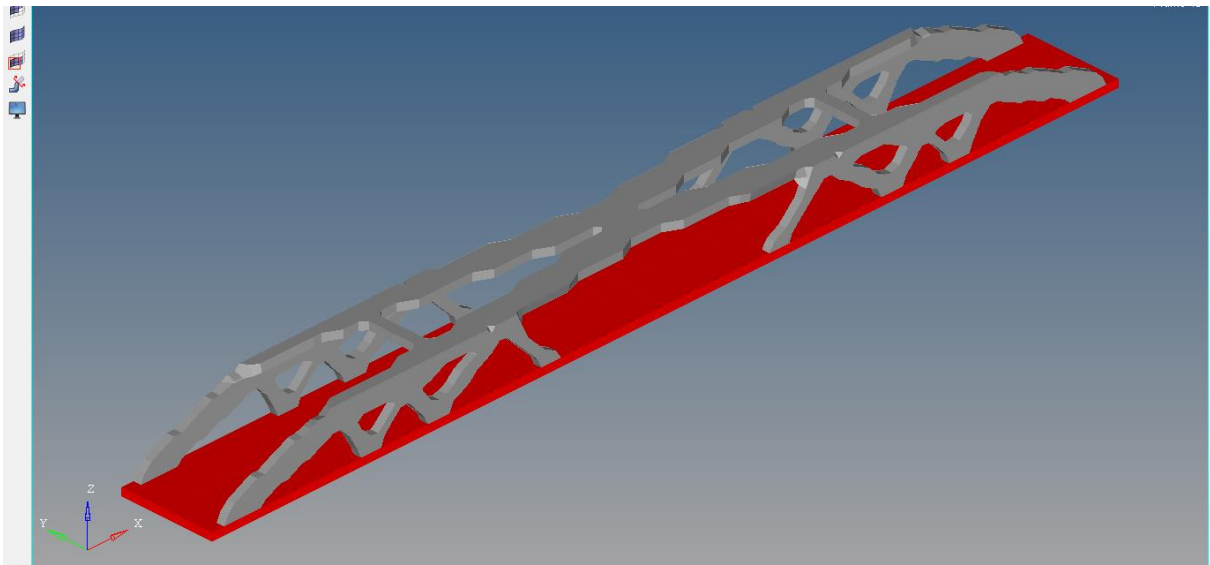


If we look again at the optimization without self-weight, but we apply the prestress, the diagonal ties become vertical.

3.3 3D results

3.3.1 3D solid elements using symmetry in x and y-plane with 1 load combination

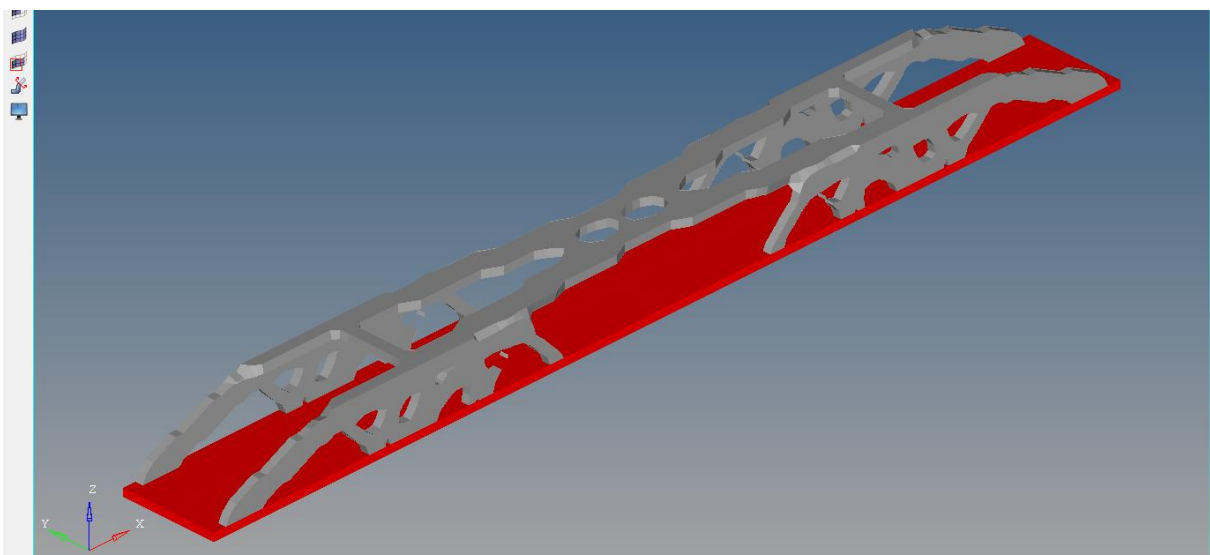
- Crowloading



At midspan axial bending forces are dominant, thus the thick top flange. At the supports shear forces are dominant, so a massive web is found there.

3.3.2 3D solid elements using symmetry in x and y-plane with 1 load combination

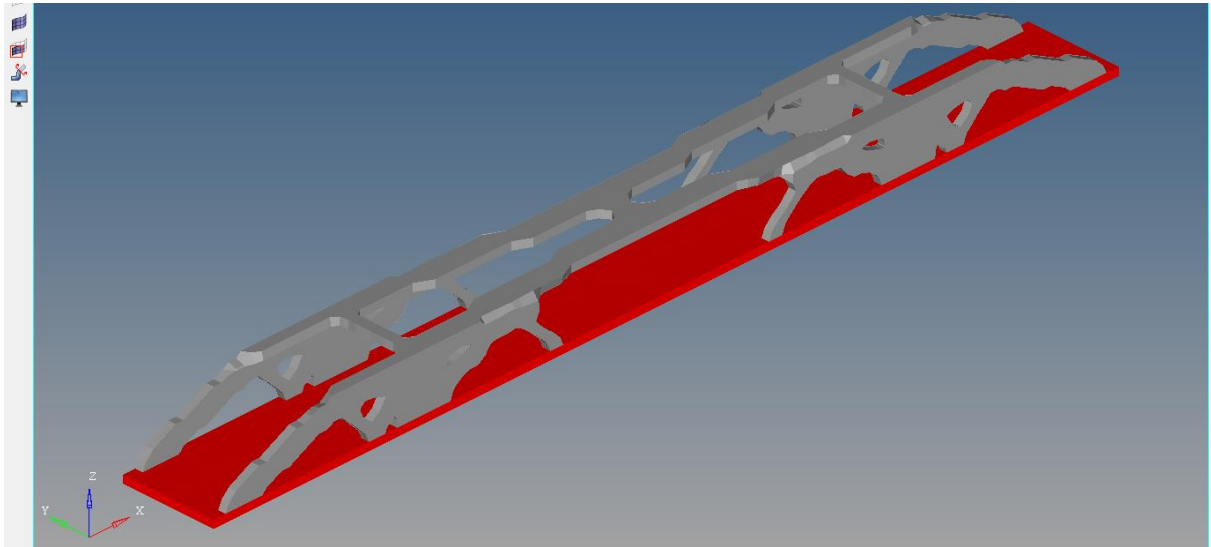
- Crowloading + Self-weight



With self-weight included in the model, the top flange is less massive and material shifts to the intermediate zone, where the diagonal ties are.

3.3.3 3D solid elements using symmetry in x and y-plane with 2 load combinations

- Crowd loading + Self-weight
- Service vehicle at midspan + Self-weight



The extra load combination of a vehicle at midspan does not significantly change the structure.

3.4 Conclusion

When using minimum compliance topology optimization for truss-like concrete bridges with a long span, self-weight plays a very important part. It is the governing loading and will determine the material distribution for the most part. Vehicle loading plays a minor role and does not have much effect on the material distribution regardless of its position on the structure.

Appendix C: SCIA Engineering Reports

1. SCIA Plaatmodel: Bepaling van Maatgevende Moment

1.1. Knopen

Naam	Coördinaat X [m]	Coördinaat Y [m]	Naam	Coördinaat X [m]	Coördinaat Y [m]	Naam	Coördinaat X [m]	Coördinaat Y [m]
K1	0,000	0,000	K41	60,000	8,125	K51	0,000	9,375
K2	60,000	0,000	K42	60,000	9,375	K52	0,000	10,625
K3	60,000	15,000	K43	60,000	10,625	K53	0,000	11,875
K4	0,000	15,000	K44	0,000	0,625	K54	60,000	11,875
K35	60,000	0,625	K45	0,000	1,875	K55	60,000	13,125
K36	60,000	1,875	K46	0,000	3,125	K56	60,000	14,375
K37	60,000	3,125	K47	0,000	4,375	K57	0,000	13,125
K38	60,000	4,375	K48	0,000	5,625	K58	0,000	14,375
K39	60,000	5,625	K49	0,000	6,875			
K40	60,000	6,875	K50	0,000	8,125			

1.2. Knoopondersteuningen

Naam	Knoop	Type	Z	Rx	Ry
Sn1	K35	Standaard	Vast	Vrij	Vrij
Sn2	K36	Standaard	Vast	Vrij	Vrij
Sn3	K37	Standaard	Vast	Vrij	Vrij
Sn4	K38	Standaard	Vast	Vrij	Vrij
Sn5	K39	Standaard	Vast	Vrij	Vrij
Sn6	K40	Standaard	Vast	Vrij	Vrij
Sn7	K41	Standaard	Vast	Vrij	Vrij
Sn8	K42	Standaard	Vast	Vrij	Vrij
Sn9	K43	Standaard	Vast	Vrij	Vrij
Sn10	K44	Standaard	Vast	Vrij	Vrij
Sn11	K45	Standaard	Vast	Vrij	Vrij
Sn12	K46	Standaard	Vast	Vrij	Vrij
Sn13	K47	Standaard	Vast	Vrij	Vrij
Sn14	K48	Standaard	Vast	Vrij	Vrij
Sn15	K49	Standaard	Vast	Vrij	Vrij
Sn16	K50	Standaard	Vast	Vrij	Vrij
Sn17	K51	Standaard	Vast	Vrij	Vrij
Sn18	K52	Standaard	Vast	Vrij	Vrij
Sn19	K54	Standaard	Vast	Vrij	Vrij
Sn20	K53	Standaard	Vast	Vrij	Vrij
Sn21	K55	Standaard	Vast	Vrij	Vrij
Sn22	K56	Standaard	Vast	Vrij	Vrij
Sn23	K57	Standaard	Vast	Vrij	Vrij
Sn24	K58	Standaard	Vast	Vrij	Vrij

1.3. 2D-elementen

Naam	Laag	Type	Rekenmodel	Materiaal	Dikte type	D. [mm]
E1	Laag1	vloer (90)	Standaard	C90/105		200

1.4. Orthotropie

OT1	
Type van orthotropie	Standaard
Dikte van Plaat/Wand [mm]	200
Materiaal	C90/105
D11 [MNm]	6,4600e+06
D22 [MNm]	2,6400e+04
D12 [MNm]	5,2800e+03
D33 [MNm]	3,8500e+06
D44 [MN/m]	2,7100e+07
D55 [MN/m]	6,2500e+06
K xy [MN/m]	2,0000e+00
K yx [MN/m]	2,8379e-05

1.5. Belastingsgevallen

Naam	Omschrijving	Actie type	Lastgroep	Duur	'Master' belastingsgeval
	Spec	Belastingtype			
BG1	Traffic Standaard	Variabel Statisch	LG2	Kort	Geen
BG2	Asphalt	Permanent Standaard	LG1		
BG3	Edge Load	Permanent Standaard	LG1		

1.6. Combinaties

Naam	Omschrijving	Type	Belastingsgevallen	Coëff. [-]
Combi1	Super-Imposed Dead Load	Omhullende - uiterst	BG2 - Asphalt BG3 - Edge Load	1,00 1,00

1.7. Vrije puntlast

Naam	Belastingsgeval	Systeem	Type	Coördinaat X [m]	Coördinaat Y [m]	Coördinaat Z [m]	Waarde - F [kN]
FF1	BG1 - Traffic	GCS	Kracht	30,600	2,000	0,000	-150,00
FF2	BG1 - Traffic	GCS	Kracht	29,400	2,000	0,000	-150,00
FF3	BG1 - Traffic	GCS	Kracht	29,400	4,000	0,000	-150,00
FF4	BG1 - Traffic	GCS	Kracht	30,600	4,000	0,000	-150,00
FF5	BG1 - Traffic	GCS	Kracht	29,400	5,000	0,000	-100,00
FF6	BG1 - Traffic	GCS	Kracht	30,600	5,000	0,000	-100,00
FF7	BG1 - Traffic	GCS	Kracht	29,400	7,000	0,000	-100,00
FF8	BG1 - Traffic	GCS	Kracht	30,600	7,000	0,000	-100,00
FF9	BG1 - Traffic	GCS	Kracht	29,400	8,000	0,000	-50,00
FF10	BG1 - Traffic	GCS	Kracht	30,600	8,000	0,000	-50,00
FF11	BG1 - Traffic	GCS	Kracht	29,400	10,000	0,000	-50,00
FF12	BG1 - Traffic	GCS	Kracht	30,600	10,000	0,000	-50,00

Verklaring van symbolen	
Belastingsgeval	Traffic

1.8. Lijnlast op 2D elementrand

Naam	2D-element	Type	Rich	Waarde - P ₁ [kN/m]	Pos x ₁	Loc	Rand
	Belastingsgeval	Systeem	Verdeling	Waarde - P ₂ [kN/m]	Pos x ₂	Coör	Oors
LFS1	E1	Kracht	Z	-3,65	0.000	Lengte	1
	BG3 - Edge Load	LCS	Gelijkmatig		1.000	Rela	Vanaf begin
LFS2	E1	Kracht	Z	-3,65	0.000	Lengte	3
	BG3 - Edge Load	LCS	Gelijkmatig		1.000	Rela	Vanaf begin

1.9. Vrije oppervlakte last

Naam	Belastingsgeval	Rich	Type	Verdeling	q [kN/m ²]	Geldigheid	Selecteer	Systeem	Locatie
FF1	BG1 - Traffic	Z	Kracht	Gelijkmatig	-10,35	Alle	Auto	GCS	Lengte
FF2	BG1 - Traffic	Z	Kracht	Gelijkmatig	-3,50	Alle	Auto	GCS	Lengte

1.10. Vlaklast

Naam	Rich	Type	Waarde [kN/m ²]	2D-element	Belastingsgeval	Systeem	Loc
SF1	Z	Kracht	-3,60	E1	BG2 - Asphalt	LCS	Lengte

1.11. 2D element - Interne krachten

1.11.1. Traffic

Lineaire berekening, Extreem : Globaal

Selectie : Alle

Belastingsgevallen : BG1

Basis grootheden. In knopen, gem. op elem..

Staafl	elem	BG	mx [kNm/m]	my [kNm/m]	mxy [kNm/m]	vx [kN/m]	vy [kN/m]
E1	301	BG1	-91,82	-118,27	25,78	531,78	323,13
E1	150	BG1	3143,27	10,45	0,00	0,00	-0,94
E1	241	BG1	-91,30	-119,59	16,43	592,92	313,30
E1	301	BG1	86,16	118,09	73,19	-165,80	316,75
E1	357	BG1	484,54	1,37	-242,89	-154,11	-5,58
E1	303	BG1	484,54	1,37	242,89	154,11	-5,58
E1	300	BG1	-91,30	-119,59	-16,43	-592,92	313,30
E1	61	BG1	25,20	77,98	-56,47	-73,87	-136,09

1.11.2. Asphalt

Lineaire berekening, Extreem : Globaal

Selectie : Alle

Belastingsgevallen : BG2

Basis grootheden. In knopen, gem. op elem..

Staaf	elem	BG	mx [kNm/m]	my [kNm/m]	mxy [kNm/m]	vx [kN/m]	vy [kN/m]
E1	120	BG2	-0,35	29,87	-37,24	-20,56	27,06
E1	30	BG2	1620,28	0,00	0,00	0,00	0,27
E1	1	BG2	6,18	-55,31	18,18	250,25	-71,56
E1	61	BG2	-0,35	29,87	37,24	20,56	27,06
E1	660	BG2	7,46	-3,70	-44,96	-94,10	5,11
E1	601	BG2	7,46	-3,70	44,96	94,10	5,11
E1	60	BG2	6,18	-55,31	-18,18	-250,25	-71,56
E1	1	BG2	45,74	-18,05	-36,34	-28,73	-78,75
E1	721	BG2	45,74	-18,05	36,34	-28,73	78,75

1.11.3. Edge Load

Lineaire berekening, Extreem : Globaal

Selectie : Alle

Belastingsgevallen : BG3

Basis grootheden. In knopen, gem. op elem..

Staaf	elem	BG	mx [kNm/m]	my [kNm/m]	mxy [kNm/m]	vx [kN/m]	vy [kN/m]
E1	120	BG3	-39,25	-73,70	-7,64	-315,96	148,62
E1	750	BG3	222,36	0,29	0,00	0,00	3,24
E1	61	BG3	-39,25	-73,70	7,64	315,96	148,62
E1	120	BG3	32,71	81,99	-17,27	265,06	148,17
E1	602	BG3	29,56	2,46	-56,05	-17,69	1,88
E1	62	BG3	29,56	2,46	56,05	-17,69	-1,88
E1	661	BG3	-39,25	-73,70	-7,64	315,96	-148,62

Studentenversie

Studentenversie

1. SCIA Plaatmodel: Bepaling van Maatgevende Moment

1.1. Knopen

Naam	Coördinaat X [m]	Coördinaat Y [m]	Naam	Coördinaat X [m]	Coördinaat Y [m]	Naam	Coördinaat X [m]	Coördinaat Y [m]
K1	0,000	0,000	K41	60,000	8,125	K51	0,000	9,375
K2	60,000	0,000	K42	60,000	9,375	K52	0,000	10,625
K3	60,000	15,000	K43	60,000	10,625	K53	0,000	11,875
K4	0,000	15,000	K44	0,000	0,625	K54	60,000	11,875
K35	60,000	0,625	K45	0,000	1,875	K55	60,000	13,125
K36	60,000	1,875	K46	0,000	3,125	K56	60,000	14,375
K37	60,000	3,125	K47	0,000	4,375	K57	0,000	13,125
K38	60,000	4,375	K48	0,000	5,625	K58	0,000	14,375
K39	60,000	5,625	K49	0,000	6,875			
K40	60,000	6,875	K50	0,000	8,125			

1.2. Knoopondersteuningen

Naam	Knoop	Type	Z	Rx	Ry
Sn1	K35	Standaard	Vast	Vrij	Vrij
Sn2	K36	Standaard	Vast	Vrij	Vrij
Sn3	K37	Standaard	Vast	Vrij	Vrij
Sn4	K38	Standaard	Vast	Vrij	Vrij
Sn5	K39	Standaard	Vast	Vrij	Vrij
Sn6	K40	Standaard	Vast	Vrij	Vrij
Sn7	K41	Standaard	Vast	Vrij	Vrij
Sn8	K42	Standaard	Vast	Vrij	Vrij
Sn9	K43	Standaard	Vast	Vrij	Vrij
Sn10	K44	Standaard	Vast	Vrij	Vrij
Sn11	K45	Standaard	Vast	Vrij	Vrij
Sn12	K46	Standaard	Vast	Vrij	Vrij
Sn13	K47	Standaard	Vast	Vrij	Vrij
Sn14	K48	Standaard	Vast	Vrij	Vrij
Sn15	K49	Standaard	Vast	Vrij	Vrij
Sn16	K50	Standaard	Vast	Vrij	Vrij
Sn17	K51	Standaard	Vast	Vrij	Vrij
Sn18	K52	Standaard	Vast	Vrij	Vrij
Sn19	K54	Standaard	Vast	Vrij	Vrij
Sn20	K53	Standaard	Vast	Vrij	Vrij
Sn21	K55	Standaard	Vast	Vrij	Vrij
Sn22	K56	Standaard	Vast	Vrij	Vrij
Sn23	K57	Standaard	Vast	Vrij	Vrij
Sn24	K58	Standaard	Vast	Vrij	Vrij

1.3. 2D-elementen

Naam	Laag	Type	Rekenmodel	Materiaal	Dikte type	D. [mm]
E1	Laag1	vloer (90)	Standaard	C90/105		200

1.4. Orthotropie

OT1	
Type van orthotropie	Standaard
Dikte van Plaat/Wand [mm]	200
Materiaal	C90/105
D11 [MNm]	6,4600e+06
D22 [MNm]	2,6400e+04
D12 [MNm]	5,2800e+03
D33 [MNm]	3,8500e+06
D44 [MN/m]	2,7100e+07
D55 [MN/m]	6,2500e+06
K xy [MN/m]	2,0000e+00
K yx [MN/m]	2,8379e-05

1.5. Belastingsgevallen

Naam	Omschrijving	Actie type	Lastgroep	Duur	'Master' belastingsgeval
	Spec	Belastingtype			
BG1	Traffic Standaard	Variabel Statisch	LG2	Kort	Geen
BG2	Asphalt	Permanent Standaard	LG1		
BG3	Edge Load	Permanent Standaard	LG1		

1.6. Combinaties

Naam	Omschrijving	Type	Belastingsgevallen	Coëff. [-]
Combi1	Super-Imposed Dead Load	Omhullende - uiterst	BG2 - Asphalt BG3 - Edge Load	1,00 1,00

1.7. Vrije puntlast

Naam	Belastingsgeval	Systeem	Type	Coördinaat X [m]	Coördinaat Y [m]	Coördinaat Z [m]	Waarde - F [kN]
FF1	BG1 - Traffic	GCS	Kracht	30,600	2,000	0,000	-150,00
FF2	BG1 - Traffic	GCS	Kracht	29,400	2,000	0,000	-150,00
FF3	BG1 - Traffic	GCS	Kracht	29,400	4,000	0,000	-150,00
FF4	BG1 - Traffic	GCS	Kracht	30,600	4,000	0,000	-150,00
FF5	BG1 - Traffic	GCS	Kracht	29,400	5,000	0,000	-100,00
FF6	BG1 - Traffic	GCS	Kracht	30,600	5,000	0,000	-100,00
FF7	BG1 - Traffic	GCS	Kracht	29,400	7,000	0,000	-100,00
FF8	BG1 - Traffic	GCS	Kracht	30,600	7,000	0,000	-100,00
FF9	BG1 - Traffic	GCS	Kracht	29,400	8,000	0,000	-50,00
FF10	BG1 - Traffic	GCS	Kracht	30,600	8,000	0,000	-50,00
FF11	BG1 - Traffic	GCS	Kracht	29,400	10,000	0,000	-50,00
FF12	BG1 - Traffic	GCS	Kracht	30,600	10,000	0,000	-50,00

Verklaring van symbolen	
Belastingsgeval	Traffic

1.8. Lijnlast op 2D elementrand

Naam	2D-element	Type	Rich	Waarde - P ₁ [kN/m]	Pos x ₁	Loc	Rand
	Belastingsgeval	Systeem	Verdeling	Waarde - P ₂ [kN/m]	Pos x ₂	Coör	Oors
LFS1	E1	Kracht	Z	-3,65	0.000	Lengte	1
	BG3 - Edge Load	LCS	Gelijkmatig		1.000	Rela	Vanaf begin
LFS2	E1	Kracht	Z	-3,65	0.000	Lengte	3
	BG3 - Edge Load	LCS	Gelijkmatig		1.000	Rela	Vanaf begin

1.9. Vrije oppervlakte last

Naam	Belastingsgeval	Rich	Type	Verdeling	q [kN/m ²]	Geldigheid	Selecteer	Systeem	Locatie
FF1	BG1 - Traffic	Z	Kracht	Gelijkmatig	-10,35	Alle	Auto	GCS	Lengte
FF2	BG1 - Traffic	Z	Kracht	Gelijkmatig	-3,50	Alle	Auto	GCS	Lengte

1.10. Vlaklast

Naam	Rich	Type	Waarde [kN/m ²]	2D-element	Belastingsgeval	Systeem	Loc
SF1	Z	Kracht	-3,60	E1	BG2 - Asphalt	LCS	Lengte

1.11. 2D element - Interne krachten

1.11.1. Traffic

Lineaire berekening, Extreem : Globaal

Selectie : Alle

Belastingsgevallen : BG1

Basis grootheden. In knopen, gem. op elem..

Staafl	elem	BG	mx [kNm/m]	my [kNm/m]	mxy [kNm/m]	vx [kN/m]	vy [kN/m]
E1	301	BG1	-91,82	-118,27	25,78	531,78	323,13
E1	150	BG1	3143,27	10,45	0,00	0,00	-0,94
E1	241	BG1	-91,30	-119,59	16,43	592,92	313,30
E1	301	BG1	86,16	118,09	73,19	-165,80	316,75
E1	357	BG1	484,54	1,37	-242,89	-154,11	-5,58
E1	303	BG1	484,54	1,37	242,89	154,11	-5,58
E1	300	BG1	-91,30	-119,59	-16,43	-592,92	313,30
E1	61	BG1	25,20	77,98	-56,47	-73,87	-136,09

1.11.2. Asphalt

Lineaire berekening, Extreem : Globaal

Selectie : Alle

Belastingsgevallen : BG2

Basis grootheden. In knopen, gem. op elem..

Staaf	elem	BG	mx [kNm/m]	my [kNm/m]	mxy [kNm/m]	vx [kN/m]	vy [kN/m]
E1	120	BG2	-0,35	29,87	-37,24	-20,56	27,06
E1	30	BG2	1620,28	0,00	0,00	0,00	0,27
E1	1	BG2	6,18	-55,31	18,18	250,25	-71,56
E1	61	BG2	-0,35	29,87	37,24	20,56	27,06
E1	660	BG2	7,46	-3,70	-44,96	-94,10	5,11
E1	601	BG2	7,46	-3,70	44,96	94,10	5,11
E1	60	BG2	6,18	-55,31	-18,18	-250,25	-71,56
E1	1	BG2	45,74	-18,05	-36,34	-28,73	-78,75
E1	721	BG2	45,74	-18,05	36,34	-28,73	78,75

1.11.3. Edge Load

Lineaire berekening, Extreem : Globaal

Selectie : Alle

Belastingsgevallen : BG3

Basis grootheden. In knopen, gem. op elem..

Staaf	elem	BG	mx [kNm/m]	my [kNm/m]	mxy [kNm/m]	vx [kN/m]	vy [kN/m]
E1	120	BG3	-39,25	-73,70	-7,64	-315,96	148,62
E1	750	BG3	222,36	0,29	0,00	0,00	3,24
E1	61	BG3	-39,25	-73,70	7,64	315,96	148,62
E1	120	BG3	32,71	81,99	-17,27	265,06	148,17
E1	602	BG3	29,56	2,46	-56,05	-17,69	1,88
E1	62	BG3	29,56	2,46	56,05	-17,69	-1,88
E1	661	BG3	-39,25	-73,70	-7,64	315,96	-148,62

Studentenversie

Studentenversie

1. SCIA Plaatmodel: Bepaling van Maatgevende Moment

1.1. Knopen

Naam	Coördinaat X [m]	Coördinaat Y [m]	Naam	Coördinaat X [m]	Coördinaat Y [m]	Naam	Coördinaat X [m]	Coördinaat Y [m]
K1	0,000	0,000	K41	60,000	8,125	K51	0,000	9,375
K2	60,000	0,000	K42	60,000	9,375	K52	0,000	10,625
K3	60,000	15,000	K43	60,000	10,625	K53	0,000	11,875
K4	0,000	15,000	K44	0,000	0,625	K54	60,000	11,875
K35	60,000	0,625	K45	0,000	1,875	K55	60,000	13,125
K36	60,000	1,875	K46	0,000	3,125	K56	60,000	14,375
K37	60,000	3,125	K47	0,000	4,375	K57	0,000	13,125
K38	60,000	4,375	K48	0,000	5,625	K58	0,000	14,375
K39	60,000	5,625	K49	0,000	6,875			
K40	60,000	6,875	K50	0,000	8,125			

1.2. Knoopondersteuningen

Naam	Knoop	Type	Z	Rx	Ry
Sn1	K35	Standaard	Vast	Vrij	Vrij
Sn2	K36	Standaard	Vast	Vrij	Vrij
Sn3	K37	Standaard	Vast	Vrij	Vrij
Sn4	K38	Standaard	Vast	Vrij	Vrij
Sn5	K39	Standaard	Vast	Vrij	Vrij
Sn6	K40	Standaard	Vast	Vrij	Vrij
Sn7	K41	Standaard	Vast	Vrij	Vrij
Sn8	K42	Standaard	Vast	Vrij	Vrij
Sn9	K43	Standaard	Vast	Vrij	Vrij
Sn10	K44	Standaard	Vast	Vrij	Vrij
Sn11	K45	Standaard	Vast	Vrij	Vrij
Sn12	K46	Standaard	Vast	Vrij	Vrij
Sn13	K47	Standaard	Vast	Vrij	Vrij
Sn14	K48	Standaard	Vast	Vrij	Vrij
Sn15	K49	Standaard	Vast	Vrij	Vrij
Sn16	K50	Standaard	Vast	Vrij	Vrij
Sn17	K51	Standaard	Vast	Vrij	Vrij
Sn18	K52	Standaard	Vast	Vrij	Vrij
Sn19	K54	Standaard	Vast	Vrij	Vrij
Sn20	K53	Standaard	Vast	Vrij	Vrij
Sn21	K55	Standaard	Vast	Vrij	Vrij
Sn22	K56	Standaard	Vast	Vrij	Vrij
Sn23	K57	Standaard	Vast	Vrij	Vrij
Sn24	K58	Standaard	Vast	Vrij	Vrij

1.3. 2D-elementen

Naam	Laag	Type	Rekenmodel	Materiaal	Dikte type	D. [mm]
E1	Laag1	vloer (90)	Standaard	C90/105		200

1.4. Orthotropie

OT1	
Type van orthotropie	Standaard
Dikte van Plaat/Wand [mm]	200
Materiaal	C90/105
D11 [MNm]	6,4600e+06
D22 [MNm]	2,6400e+04
D12 [MNm]	5,2800e+03
D33 [MNm]	3,8500e+06
D44 [MN/m]	2,7100e+07
D55 [MN/m]	6,2500e+06
K xy [MN/m]	2,0000e+00
K yx [MN/m]	2,8379e-05

1.5. Belastingsgevallen

Naam	Omschrijving	Actie type	Lastgroep	Duur	'Master' belastingsgeval
	Spec	Belastingtype			
BG1	Traffic Standaard	Variabel Statisch	LG2	Kort	Geen
BG2	Asphalt	Permanent Standaard	LG1		
BG3	Edge Load	Permanent Standaard	LG1		

1.6. Combinaties

Naam	Omschrijving	Type	Belastingsgevallen	Coëff. [-]
Combi1	Super-Imposed Dead Load	Omhullende - uiterst	BG2 - Asphalt BG3 - Edge Load	1,00 1,00

1.7. Vrije puntlast

Naam	Belastingsgeval	Systeem	Type	Coördinaat X [m]	Coördinaat Y [m]	Coördinaat Z [m]	Waarde - F [kN]
FF1	BG1 - Traffic	GCS	Kracht	30,600	2,000	0,000	-150,00
FF2	BG1 - Traffic	GCS	Kracht	29,400	2,000	0,000	-150,00
FF3	BG1 - Traffic	GCS	Kracht	29,400	4,000	0,000	-150,00
FF4	BG1 - Traffic	GCS	Kracht	30,600	4,000	0,000	-150,00
FF5	BG1 - Traffic	GCS	Kracht	29,400	5,000	0,000	-100,00
FF6	BG1 - Traffic	GCS	Kracht	30,600	5,000	0,000	-100,00
FF7	BG1 - Traffic	GCS	Kracht	29,400	7,000	0,000	-100,00
FF8	BG1 - Traffic	GCS	Kracht	30,600	7,000	0,000	-100,00
FF9	BG1 - Traffic	GCS	Kracht	29,400	8,000	0,000	-50,00
FF10	BG1 - Traffic	GCS	Kracht	30,600	8,000	0,000	-50,00
FF11	BG1 - Traffic	GCS	Kracht	29,400	10,000	0,000	-50,00
FF12	BG1 - Traffic	GCS	Kracht	30,600	10,000	0,000	-50,00

Verklaring van symbolen	
Belastingsgeval	Traffic

1.8. Lijnlast op 2D elementrand

Naam	2D-element	Type	Rich	Waarde - P ₁ [kN/m]	Pos x ₁	Loc	Rand
	Belastingsgeval	Systeem	Verdeling	Waarde - P ₂ [kN/m]	Pos x ₂	Coör	Oors
LFS1	E1	Kracht	Z	-3,65	0.000	Lengte	1
	BG3 - Edge Load	LCS	Gelijkmatig		1.000	Rela	Vanaf begin
LFS2	E1	Kracht	Z	-3,65	0.000	Lengte	3
	BG3 - Edge Load	LCS	Gelijkmatig		1.000	Rela	Vanaf begin

1.9. Vrije oppervlakte last

Naam	Belastingsgeval	Rich	Type	Verdeling	q [kN/m ²]	Geldigheid	Selecteer	Systeem	Locatie
FF1	BG1 - Traffic	Z	Kracht	Gelijkmatig	-10,35	Alle	Auto	GCS	Lengte
FF2	BG1 - Traffic	Z	Kracht	Gelijkmatig	-3,50	Alle	Auto	GCS	Lengte

1.10. Vlaklast

Naam	Rich	Type	Waarde [kN/m ²]	2D-element	Belastingsgeval	Systeem	Loc
SF1	Z	Kracht	-3,60	E1	BG2 - Asphalt	LCS	Lengte

1.11. 2D element - Interne krachten

1.11.1. Traffic

Lineaire berekening, Extreem : Globaal

Selectie : Alle

Belastingsgevallen : BG1

Basis grootheden. In knopen, gem. op elem..

Staafl	elem	BG	mx [kNm/m]	my [kNm/m]	mxy [kNm/m]	vx [kN/m]	vy [kN/m]
E1	301	BG1	-91,82	-118,27	25,78	531,78	323,13
E1	150	BG1	3143,27	10,45	0,00	0,00	-0,94
E1	241	BG1	-91,30	-119,59	16,43	592,92	313,30
E1	301	BG1	86,16	118,09	73,19	-165,80	316,75
E1	357	BG1	484,54	1,37	-242,89	-154,11	-5,58
E1	303	BG1	484,54	1,37	242,89	154,11	-5,58
E1	300	BG1	-91,30	-119,59	-16,43	-592,92	313,30
E1	61	BG1	25,20	77,98	-56,47	-73,87	-136,09

1.11.2. Asphalt

Lineaire berekening, Extreem : Globaal

Selectie : Alle

Belastingsgevallen : BG2

Basis grootheden. In knopen, gem. op elem..

Staaf	elem	BG	mx [kNm/m]	my [kNm/m]	mxy [kNm/m]	vx [kN/m]	vy [kN/m]
E1	120	BG2	-0,35	29,87	-37,24	-20,56	27,06
E1	30	BG2	1620,28	0,00	0,00	0,00	0,27
E1	1	BG2	6,18	-55,31	18,18	250,25	-71,56
E1	61	BG2	-0,35	29,87	37,24	20,56	27,06
E1	660	BG2	7,46	-3,70	-44,96	-94,10	5,11
E1	601	BG2	7,46	-3,70	44,96	94,10	5,11
E1	60	BG2	6,18	-55,31	-18,18	-250,25	-71,56
E1	1	BG2	45,74	-18,05	-36,34	-28,73	-78,75
E1	721	BG2	45,74	-18,05	36,34	-28,73	78,75

1.11.3. Edge Load

Lineaire berekening, Extreem : Globaal

Selectie : Alle

Belastingsgevallen : BG3

Basis grootheden. In knopen, gem. op elem..

Staaf	elem	BG	mx [kNm/m]	my [kNm/m]	mxy [kNm/m]	vx [kN/m]	vy [kN/m]
E1	120	BG3	-39,25	-73,70	-7,64	-315,96	148,62
E1	750	BG3	222,36	0,29	0,00	0,00	3,24
E1	61	BG3	-39,25	-73,70	7,64	315,96	148,62
E1	120	BG3	32,71	81,99	-17,27	265,06	148,17
E1	602	BG3	29,56	2,46	-56,05	-17,69	1,88
E1	62	BG3	29,56	2,46	56,05	-17,69	-1,88
E1	661	BG3	-39,25	-73,70	-7,64	315,96	-148,62

Studentenversie

Studentenversie

1. SCIA Plate Model: Determination of Governing Shear Force

1.1. Knopen

Naam	Coördinaat X [m]	Coördinaat Y [m]
K1	0,000	0,000
K2	60,000	0,000
K3	60,000	15,000
K4	0,000	15,000

1.2. 2D-elementen

Naam	Laag	Type	Rekenmodel	Materiaal	Dikte type	D. [mm]
E1	Laag1	vloer (90)	Standaard	C90/105		200

1.3. Orthotropie

OT1	
Type van orthotropie	Standaard
Dikte van Plaat/Wand [mm]	200
Materiaal	C90/105
D11 [MNm]	6,4600e+06
D22 [MNm]	2,6400e+04
D12 [MNm]	5,2800e+03
D33 [MNm]	3,8500e+06
D44 [MN/m]	2,7100e+07
D55 [MN/m]	6,2500e+06
K xy [MN/m]	2,0000e+00
K yx [MN/m]	2,8379e-05

1.4. Ondersteuningen op 2D elementranden

Naam	2D-element Rand	Oors Coör	Pos x ₁ Pos x ₂	Z	Rx	Ry
Sle1	E1	Vanaf begin	0,000	Vast	Vrij	Vrij
	4	Rela	1,000			
Sle2	E1	Vanaf begin	0,000	Vast	Vrij	Vrij
	2	Rela	1,000			

1.5. Vrije puntlast

Naam	Belastingsgeval	Systeem	Type	Coördinaat X [m]	Coördinaat Y [m]	Coördinaat Z [m]	Waarde - F [kN]
FF1	BG1	GCS	Kracht	56,625	2,000	0,000	-150,00
FF2	BG1	GCS	Kracht	55,425	2,000	0,000	-150,00
FF3	BG1	GCS	Kracht	55,425	4,000	0,000	-150,00
FF4	BG1	GCS	Kracht	56,625	4,000	0,000	-150,00
FF5	BG1	GCS	Kracht	52,425	5,000	0,000	-100,00
FF6	BG1	GCS	Kracht	53,625	5,000	0,000	-100,00
FF7	BG1	GCS	Kracht	52,425	7,000	0,000	-100,00
FF8	BG1	GCS	Kracht	53,625	7,000	0,000	-100,00
FF9	BG1	GCS	Kracht	49,425	8,000	0,000	-50,00
FF10	BG1	GCS	Kracht	50,625	8,000	0,000	-50,00
FF11	BG1	GCS	Kracht	49,425	10,000	0,000	-50,00
FF12	BG1	GCS	Kracht	50,625	10,000	0,000	-50,00

1.6. Vrije oppervlakte last

Naam	Belastingsgeval	Rich	Type	Verdeling	q [kN/m ²]	Geldigheid	Selecteer	Systeem	Locatie
FF1	BG1	Z	Kracht	Gelijkmatig	-10,35	Alle	Auto	GCS	Lengte
FF2	BG1	Z	Kracht	Gelijkmatig	-3,50	Alle	Auto	GCS	Lengte

1.7. 2D element - Interne krachten

1.7.1. Traffic

Lineaire berekening, Extreem : Globaal

Selectie : Alle

Belastingsgevallen : BG1

Hoofd grootheden. In knopen, gem. op elem..

Staafl	elem	BG	m1 [kNm/m]	m2 [kNm/m]	alfa [deg]	mtmax [kNm/m]	qmax-b [kN/m]	beta [deg]
E1	180	BG1	-25,64	-28,68	-35,60	1,52	398,89	175,67
E1	92	BG1	2141,17	4,50	-0,08	1068,34	3,24	127,03
E1	479	BG1	333,63	-144,74	-34,35	239,19	199,02	159,09
E1	60	BG1	51,03	19,28	-84,59	15,88	171,86	-122,14

Staafl	elem	BG	m1 [kNm/m]	m2 [kNm/m]	alfa [deg]	mtmax [kNm/m]	qmax-b [kN/m]	beta [deg]
E1	841	BG1	33,32	5,48	78,35	13,92	62,90	78,96
E1	32	BG1	2139,71	-0,24	-0,03	1069,98	5,87	178,13
E1	873	BG1	2098,37	-0,34	-0,03	1049,35	0,44	110,38
E1	240	BG1	0,20	-66,54	-29,18	33,37	509,85	156,13
E1	48	BG1	1601,96	-0,14	0,22	801,05	45,64	-179,97
E1	47	BG1	1667,03	-0,14	0,18	833,59	43,40	180,00

Studentenversie

Studentenversie

1. SCIA Plate Model: Determination of Fatigue Load

1.1. Knopen

Naam	Coördinaat X [m]	Coördinaat Y [m]
K1	0,000	0,000
K2	60,000	0,000
K3	60,000	15,000
K4	0,000	15,000

1.2. 2D-elementen

Naam	Laag	Type	Rekenmodel	Materiaal	Dikte type	D. [mm]
E1	Laag1	vloer (90)	Standaard	C90/105		200

1.3. Ondersteuningen op 2D elementranden

Naam	2D-element Rand	Oors Coör	Pos x ₁ Pos x ₂	Z	Rx	Ry
Sle1	E1	Vanaf begin	0.000	Vast	Vrij	Vrij
	2	Rela	1.000			
Sle2	E1	Vanaf begin	0.000	Vast	Vrij	Vrij
	4	Rela	1.000			

1.4. Orthotropie

OT1	
Type van orthotropie	Standaard
Dikte van Plaat/Wand [mm]	200
Materiaal	C90/105
D11 [MNm]	6,4600e+06
D22 [MNm]	2,6400e+04
D12 [MNm]	5,2800e+03
D33 [MNm]	3,8500e+06
D44 [MN/m]	2,7100e+07
D55 [MN/m]	6,2500e+06
K xy [MN/m]	2,0000e+00
K yx [MN/m]	2,8379e-05

1.5. Vrije puntlast

Naam	Belastingsgeval	Systeem	Type	Coördinaat X [m]	Coördinaat Y [m]	Coördinaat Z [m]	Waarde - F [kN]
FF1	BG1	GCS	Kracht	30,600	2,000	0,000	-105,00
FF2	BG1	GCS	Kracht	29,400	2,000	0,000	-105,00
FF3	BG1	GCS	Kracht	29,400	4,000	0,000	-105,00
FF4	BG1	GCS	Kracht	30,600	4,000	0,000	-105,00
FF5	BG1	GCS	Kracht	29,400	5,000	0,000	-70,00
FF6	BG1	GCS	Kracht	30,600	5,000	0,000	-70,00
FF7	BG1	GCS	Kracht	29,400	7,000	0,000	-70,00
FF8	BG1	GCS	Kracht	30,600	7,000	0,000	-70,00
FF9	BG1	GCS	Kracht	29,400	8,000	0,000	-35,00
FF10	BG1	GCS	Kracht	30,600	8,000	0,000	-35,00
FF11	BG1	GCS	Kracht	29,400	10,000	0,000	-35,00
FF12	BG1	GCS	Kracht	30,600	10,000	0,000	-35,00

1.6. Vrije oppervlakte last

Naam	Belastingsgeval	Rich	Type	Verdeling	q [kN/m ²]	Geldigheid	Selecteer	Systeem	Locatie
FF1	BG1	Z	Kracht	Gelijkmatig	-3,11	Alle	Auto	GCS	Lengte
FF2	BG1	Z	Kracht	Gelijkmatig	-0,75	Alle	Auto	GCS	Lengte

1.7. 2D element - Interne krachten

1.7.1. Traffic

Lineaire berekening, Extreem : Globaal

Selectie : Alle

Belastingsgevallen : BG1

Basis grootheden. In knopen, gem. op elem..

Staafl	elem	BG	mx [kNm/m]	my [kNm/m]	mxy [kNm/m]	vx [kN/m]	vy [kN/m]
E1	121	BG1	-9,82	-13,59	2,41	150,36	35,83
E1	210	BG1	1362,77	5,91	0,04	0,01	0,03
E1	240	BG1	-0,83	-18,32	-19,19	-132,41	97,80
E1	841	BG1	2,28	16,70	3,57	-2,82	27,77

StAAF	elem	BG	mx [kNm/m]	my [kNm/m]	mxy [kNm/m]	vx [kN/m]	vy [kN/m]
E1	477	BG1	173,30	0,88	-118,47	-54,97	-2,19
E1	363	BG1	178,31	0,59	118,49	58,54	-2,55
E1	180	BG1	-9,42	-13,22	-2,48	-146,95	35,51
E1	60	BG1	5,27	13,19	-4,63	-33,31	-43,08
E1	361	BG1	2,71	-3,07	31,84	62,38	155,83

Studentenversie

Studentenversie